NUREG/CR-0063
LA-7279-MS, Vol. I
Informal Report

27
8-3-78
25 to NTIS

MASTER

TRAC-P1:

An Advanced Best Estimate Computer Program for PWR LOCA Analysis

I. Methods, Models, User Information, and Programming Details

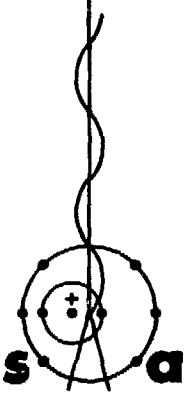

los alamos
scientific laboratory
of the University of California
LOS ALAMOS, NEW MEXICO 87545

UNITED STATES
DEPARTMENT OF ENERGY
CONTRACT W-7405-ENG. 36

NUREG/CR-0063
LA-7279-MS, Vol. I
Informal Report
R-4

TRAC-P1:
An Advanced Best Estimate Computer Program for PWR LOCA Analysis
I. Methods, Models, User Information, and Programming Details

Thermal Reactor Safety Group

Manuscript submitted: May 1978
Date published: June 1978

Prepared for
Office of Nuclear Regulatory Research
US Nuclear Regulatory Commission
Washington, DC 20555

AUTHORSHIP AND ACKNOWLEDGMENTS

A large number of people have contributed to the development of the TRAC-P1 code and to preparation of this report. Since it was a team effort, there was considerable overlap in the areas of responsibility and contribution. The participants are listed below according to their area of primary activity. Those with the prime responsibility for each area are listed first.

FLUID DYNAMICS:	Dennis R. Liles and John H. Mahaffy
HEAT TRANSFER:	Walter L. Kirchner
CODE ARCHITECTURE AND METHODS:	Richard J. Pryor and William H. Reed
COMPONENT MODULES:	Kenneth A. Williams, Richard J. Pryor, Dennis R. Liles, William H. Reed, John W. Bolstad, and John H. Mahaffy
STEADY-STATE CALCULATION:	James M. Sicilian
CODE DEVELOPMENT AND PROGRAMMING:	Richard J. Pryor, James M. Sicilian, James C. Ferguson, Ronald P. Harper, Scott T. Bennion, and Carol A. Greiner
SAMPLE PROBLEM:	Paul B. Bleiweis and John R. Ireland
REPORT COMPILATION:	John C. Vigil, Richard J. Pryor, and James F. Jackson
PROJECT MANAGEMENT:	James F. Jackson, William H. Reed, Kaye D. Lathrop, and John C. Vigil

The developers of TRAC-P1 would also like to acknowledge a number of useful discussions and technical exchanges that have occurred with the following: Louis Shotkin, Novak Zuber, and Stanislav Fabic, USNRC; Tony Hirt, Dan Butler, Frank Harlow, William Rivard, and Burton Wendroff, LASL; John Meyer and Peter Griffith, MIT; George Bankoff, Northwestern University; and Garrett Birkhoff, Harvard University. We would also like to thank Pat Thorn for her lead role in typing this report.

CONTENTS

CONTENTS (cont)

TABLES

FIGURES

CONTENTS (cont)

TABLES

FIGURES

CONTENTS

TABLES

FIGURES

CONTENTS (cont)

TABLES

FIGURES

CONTENTS (cont)

CONTENTS (cont)

STANDARD NOMENCLATURE

Independent Variables

r	Radial coordinate in cylindrical geometry.
t	Time.
θ	Azimuthal coordinate in cylindrical geometry.
x	Coordinate for one-dimensional geometry.
z	Axial coordinate in cylindrical geometry.

Other Variables

A	Area.
c	Shear or friction coefficient in two-fluid equations.
c_p	Specific heat at constant pressure.
c_v	Specific heat at constant volume.
D	Diameter.
e	Specific internal energy.
f	Friction factor in drift-flux equations.
FA	Flow area.
g	Acceleration due to gravity.
G	Mass flux (ρV).
h	Specific enthalpy or heat transfer coefficient.
$h_{\ell g}$	Latent heat of vaporization.
k	Thermal conductivity, form loss coefficient, or pipe roughness.
K	Wall shear coefficient in drift-flux equations.
m	Mass.
Nu	Nusselt number.
p	Pressure.
q	Heat generation rate.
q"	Heat flux.
q"'	Volumetric heat generation rate.
R	Radius.
Re	Reynolds number.
T	Temperature.

Other Variables (cont)

V	Velocity.
vol	Hydrodynamic cell volume.
We	Weber number.
x	Quality.
α	Vapor volume fraction or absorptivity.
Γ	Net volumetric vapor production rate due to phase change.
δ	Mean-fuel surface roughness.
Δ	Increment.
ε	Emissivity.
μ	Viscosity.
ρ	Microscopic density.
σ	Surface tension or Stefan-Boltzmann contant.
τ	Shear stress.
ϕ^2	Two-phase friction factor multiplier.
ω	Angular velocity.

Subscripts

b	Bubble.
c	Cladding.
d	Droplet.
f	Fuel or friction.
g	Vapor (gas) field.
h	Hydraulic.
i	Interface (liquid-vapor) quantity or one-dimensional cell index in heat transfer equations.
j	One-dimensional cell index in hydrodynamics equations.
ℓ	Liquid field.
ℓg	Liquid to vapor.
m	Mixture quantities.
mw	Metal-water reaction.
qf	Quench front.
r	Relative quantities.
r,θ,z	Cylindrical coordinate directions.

Subscripts (cont)

$r \pm \frac{1}{2}$ $\theta \pm \frac{1}{2}$ $z \pm \frac{1}{2}$	Mesh cell boundary indices.
s	Saturation quantities.
sp	Single-phase quantities.
ss	Steady-state quantities.
t	Transient quantities.
tp	Two-phase quantities.
w	Wall quantities.

Superscripts

k	Iteration count index.
n,n+1	Time step boundary indices.

ABSTRACT

The Transient Reactor Analysis Code (TRAC) is being developed at the Los Alamos Scientific Laboratory (LASL) to provide an advanced "best estimate" predictive capability for the analysis of postulated accidents in light water reactors (LWRs). TRAC-P1 provides this analysis capability for pressurized water reactors (PWRs) and for a wide variety of thermal-hydraulic experimental facilities. It features a three-dimensional treatment of the pressure vessel and associated internals; two-phase nonequilibrium hydrodynamics models; flow-regime-dependent constitutive equation treatment; reflood tracking capability for both bottom flood and falling film quench fronts; and consistent treatment of entire accident sequences including the generation of consistent initial conditions.

The TRAC-P1 User's Manual is composed of two separate volumes. Volume I gives a description of the thermal-hydraulic models and numerical solution methods used in the code. Detailed programming and user information is also provided. Volume II presents the results of the developmental verification calculations.

I. COMPUTER PROGRAM OUTLINE

1. Name of Program: TRAC-P1

2. Computer for Which Code is Designed: CDC 7600.

3. Description of Problem or Function: TRAC-P1 performs "best estimate" analyses of loss-of-coolant accidents and other transients in pressurized light water reactors. The code can also be used to model a wide range of thermal-hydraulic experiments in reduced-scale facilities. Models employed include reflood, multidimensional two-phase flow, nonequilibrium thermodynamics, generalized heat transfer, and reactor kinetics. Automatic steady-state and dump/restart capabilities are also provided.

4. Method of Solution: The system of partial differential equations describing the two-phase flow and heat transfer are written in finite difference form. In one-dimensional components the nonlinear difference equations are solved by Newton-Raphson iteration. In the three-dimensional vessel the linearized difference equations are solved by Gauss-Seidel iteration. A Gauss-Seidel iteration procedure is also used to handle coupling between components. The level of implicitness varies from fully implicit to semi-implicit in the fluid dynamics and is semi-implicit in the heat transfer.

5. Restrictions on the Complexity of the Problem: All storage arrays in the code are dynamically allocated so the only limit on the size of a problem is the amount of core memory available. The number of reactor components in the problem and the manner in which they are coupled together are arbitrary. Reactor components available in TRAC-P1 include accumulators, pipes, pressurizers, pumps, steam generators, tees, valves, and vessels with associated internals.

6. Typical Running Time: Running time is highly problem dependent and is a function of the number of total mesh cells and the maximum allowable time step size. Total run time can be estimated from a unit run time of 2-3 ms per mesh cell per time step and an average time step size of 5 ms.

7. Unusual Features of the Program: TRAC-P1 is a highly versatile program which can describe most thermal-hydraulic experiments in addition to the wide variety of reactor system designs. The architecture of the code is completely modular permitting better geometric description of a problem, more detailed models of physical processes, and reduced maintenance cost.

8. Related and Auxiliary Programs: One of the output files written by TRAC contains graphics information which can be used to produce plots and movies. An auxiliary program which reads the file is not provided because of differences in system-dependent features likely to be encountered. The user should develop his own program for this purpose.

9. Status: In use.

10. References: References are provided in the manual.

11. Machine Requirements: CDC 7600 computer with 60 K words of small core memory and 220 K words of large core memory.

12. Programming Languages Used: FORTRAN-IV.

13. Operating System or Monitor Under Which Program is Executed: Standard CDC 7600 operating system with FTN FORTRAN compiler and loader.

14. Other Programming or Operating Information or Restrictions: None.

15. Material Available:
    1. Source listing.
    2. TRAC-P1 manual.
    3. Sample problems.

II. INTRODUCTION

The Transient Reactor Analysis Code (TRAC) is an advanced best-estimate systems code for analyzing accidents in LWRs. It was developed at the Los Alamos Scientific Laboratory under the sponsorship of the Reactor Safety Research Division of the U.S. Nuclear Regulatory Commission. The initial release version, designated as TRAC-P1, is described in this document. A preliminary version consisting of only one-dimensional components was completed in December 1976. This version was not released publically nor formally documented. It was absorbed into the development of TRAC-P1 and formed the basis for the one-dimensional loop component modules.

TRAC-P1 is designed primarily for the analysis of large break loss-of-coolant accidents (LOCAs) in pressurized water reactors (PWRs). Because of its versatility, however, it can be applied directly to a wide variety of analyses ranging from blowdowns in simple pipes to integral LOCA tests in multiloop facilities. Models specifically required to treat boiling water reactors (BWRs) and other accident types, such as anticipated transients without scram (ATWS) and reactivity insertion accidents (RIAs), will be incorporated into future versions of the code.

A. TRAC Characteristics

Some of the distinguishing characteristics of TRAC-P1 are summarized below. All of these characteristics reflect the state of the art in the various areas.

1. Multidimensional Fluid Dynamics

Although the flow within the ex-vessel components is treated in one-dimension, a full three-dimensional (r,θ,z) flow calculation is used within the reactor vessel. This was done to allow an accurate calculation of the complex multidimensional flow patterns inside the reactor vessel that play an important role in determining accident behavior. For example, phenomena such as emergency core cooling (ECC) downcomer penetration during blowdown, multidimensional plenum and core flow effects, and upper plenum de-entrainment and fallback during reflood can be treated directly.

2. Nonhomogeneous, Nonequilibrium Modeling

A full two-fluid (six-equation) hydrodynamics approach is used to describe the steam-water flow within the reactor vessel, thereby allowing such important phenomena as countercurrent flow to be treated explicitly. The flow in the one-dimensional loop components is described using a five-equation drift-flux model, which differs from the standard four-equation drift-flux approach due to the addition of a separate vapor energy equation. This provides a consistent nonequilibrium thermodynamic treatment in both the vessel and loop components, and permits more accurate modeling of the fluid dynamics through a direct treatment of flashing and condensation effects.

3. Flow-Regime-Dependent Constitutive Equation Package

The thermal-hydraulic equations in TRAC describe the transfer of mass, energy, and momentum between the steam-water phases, and the interaction of these phases with the system structure. Since the nature of these interactions is dependent on the flow topology, a sophisticated flow-regime-dependent constitutive equation package has been incorporated into the code. Although this package will undoubtedly be improved in the future, verification calculations performed to date indicate that a broad range of flow conditions can be adequately handled with the current package.

4. Comprehensive Heat Transfer Capability

TRAC-P1 incorporates a detailed heat transfer analysis capability for both the vessel and loop components. Included is a reflood tracking capability for both bottom flood and falling film quench fronts. The heat transfer from the fuel rods and other system structures is calculated using flow-regime-dependent heat transfer coefficients obtained from a generalized boiling curve based on local conditions.

5. Consistent Analysis of Entire Accident Sequences

An important feature of TRAC is the ability to address entire accident sequences, including computation of initial conditions, with a consistent and continuous calculation. For example, the code models the blowdown, refill, and reflood phases of a LOCA. This eliminates the necessity of synthesizing several calculations performed with different codes to complete the analysis of a given accident. In addition, a steady-state solution capability is

provided that can be used to obtain self-consistent initial conditions for subsequent transient calculations. Both a steady-state and a transient calculation can be performed in the same run if desired.

6. Component and Functional Modularity

TRAC is completely modular by component. The component modules are assembled through input data to form virtually any PWR design or experimental configuration. This gives TRAC great versatility in the possible range of applications. It also allows component modules to be improved, modified, or added without disturbing the remainder of the code. Modules are available to model accumulators, pipes, pressurizers, pumps, steam generators, tees, valves, and vessels with associated internals.

TRAC is also modular by function. This means that the major aspects of the calculations are performed in separate modules. For example, the basic one-dimensional hydrodynamics solution algorithm, pipe wall temperature field solution algorithm, heat transfer coefficient selection, and other functions are performed in separate sets of routines that are accessed by all component modules. This type of modularity allows the code to be readily upgraded as improved correlations and experimental information become available.

B. Physical Phenomena Treated

Because of the detailed modeling in TRAC, most of the physical phenomena important in LOCA analysis can be treated. Included are the following:

1. ECC downcomer penetration and bypass, including the effects of countercurrent flow and hot walls.
2. Lower plenum refill with entrainment and phase separation effects.
3. Bottom flood and falling film reflood quench fronts.
4. Multidimensional flow patterns in the core and plenum regions.
5. Pool formation and fallback at the upper core support plate (UCSP) region.
6. De-entrainment and pool formation in the upper plenum.
7. Steam binding.
8. Average-rod and hot-rod cladding temperature histories.
9. Alternate ECC injection systems, including hot-leg and upper-head injection.
10. Direct injection of subcooled ECC water, without the requirement for artificial mixing zones.

11. Critical flow (choking).
12. Liquid carryover during reflood.
13. Metal-water reaction.
14. Water hammer effects.
15. Wall friction losses.

C. Planned Improvements

Despite the advanced modeling capabilities provided in TRAC-P1, there are a number of additions and improvements being planned for future versions of the code. Some of the more important of these are summarized below.

1. Work is under way to provide the capability to explicitly treat countercurrent flow between entrained droplets and falling films. The vessel hydrodynamics treatment has been augmented through the addition of a separate droplet mass equation and the required entrainment models. This will be made available in the next version of the code.
2. The basic flow equations are also being modified to include a noncondensible gas field. This will allow the code to account for the presence of accumulator nitrogen or air ingression from the containment during a LOCA.
3. The necessary components to model BWRs (e.g., jet pumps and steam separators) will be made available in a future version.
4. A fuel-cladding structural dynamics model will be added to provide more accurate gap conductances and cladding deformation effects.
5. Improved models for upper plenum entrainment/de-entrainment and upper core support plate (UCSP) fallback will be developed as better experimental information becomes available.
6. The capability to treat other accident types such as RIAs and ATWS will be added.

One of the important constraints that will be considered in the applications of TRAC will be the computer running time requirements. Although care has been taken to provide efficient computational techniques, the developmental effort to date has emphasized accurate modeling more than short running times. A major effort will be undertaken shortly to develop a faster running version of the code.

Experience to date has shown that significant gains in running time are possible without sacrificing computational accuracy. For example, an optional fully implicit solution strategy was developed for use in pipe components near breaks. This substantially increased the time step sizes during blowdown calculations and consequently reduced the running times. Several other improvements in the solution strategy are currently under development and will be incorporated in future code versions. The fact remains, however, that the calculation of large problems (with several hundred mesh cells) will continue to require the equivalent of at least several hours of CDC 7600 computation time.

D. Scope of TRAC Manual

An important aspect of the TRAC program involves the developmental verification of the code through comparisons with measurements obtained with test facilities. A number of developmental verification calculations have already been performed with TRAC-P1. To present these verification results, the TRAC-P1 manual is organized into two volumes. Volume II summarizes the key developmental verification results.

The present volume (Vol. I) describes the TRAC basic methods and models, and provides user information and programming details. Chapter III describes the basic hydrodynamics and heat transfer methods, and discusses the overall strategies for transient and steady-state solutions. Chapter III is supplemented by Appendices A and B which supply, respectively, the fluid and material properties for the thermal-hydraulic analyses.

A guide to the standard nomenclature used in this report is given at the beginning of this volume. Quantities that are not included in the standard nomenclature list are defined where they are used. All units are SI unless otherwise specified. Component model descriptions are given in Chap. IV. These descriptions should be referenced if questions arise during the preparation of detailed input specifications for a TRAC problem.

Input specifications are provided in Chap. V along with other user information. To provide additional guidance to the user in the area of input preparation, input decks for a four-loop PWR sample problem are provided in Appendix C. Error messages that might occur during the course of a calculation are explained in Appendix D.

The overall code organization, input and output processing, storage re-

quirements, and other programming details associated with both transient and steady-state solutions are discussed in Chap. VI. Other programming details are given in Appendices E, F, and G. These provide a list of TRAC subprograms, a compilation of COMMON arrays, and component data tables, respectively.

III. BASIC METHODS

A. Hydrodynamics

1. One-Dimensional Components

The two-phase, one-dimensional, hydrodynamics formulation used by all of the components except the reactor vessel is a five-equation drift-flux model. We believe that this is the simplest model that adequately describes both the thermal and velocity nonequilibrium which may occur in the reactor loop components for a wide variety of transients. The principal subroutines in TRAC that actually define and solve the field equations are DF1DS for the semi-implicit solution and DF1DI for the fully implicit solution.

a. Field Equations

The differential field equations[1,2] for the two-phase, five-equation drift-flux model are given below.

Mixture Mass Equation

$$\frac{\partial}{\partial t}\rho_m + \frac{\partial}{\partial x}(\rho_m V_m) = 0 \tag{1}$$

Vapor Mass Equation

$$\frac{\partial}{\partial t}(\alpha\rho_g) + \frac{\partial}{\partial x}(\alpha\rho_g V_m) + \frac{\partial}{\partial x}\left[\frac{\alpha\rho_g(1-\alpha)\ \rho_\ell V_r}{\rho_m}\right] = \Gamma \tag{2}$$

Mixture Equation of Motion

$$\frac{\partial}{\partial t}V_m + V_m\frac{\partial}{\partial x}V_m + \frac{1}{\rho_m}\frac{\partial}{\partial x}\left[\frac{\alpha\rho_g(1-\alpha)\ \rho_\ell V_r^2}{\rho_m}\right] = -\frac{1}{\rho_m}\frac{\partial p}{\partial x} - K V_m|V_m| + g \tag{3}$$

Vapor Thermal Energy Equation

$$\frac{\partial}{\partial t}(\alpha\rho_g e_g) + \frac{\partial}{\partial x}(\alpha\rho_g V_m e_g) + \frac{\partial}{\partial x}\left[\frac{\alpha\rho_g(1-\alpha)\ \rho_\ell V_r e_g}{\rho_m}\right] + p\frac{\partial}{\partial x}(\alpha V_m)$$

$$+ p\frac{\partial}{\partial x}\left[\frac{\alpha(1-\alpha)\ \rho_\ell}{\rho_m}V_r\right] = q_{wg} + q_{ig} - p\frac{\partial\alpha}{\partial t} + \Gamma h_{sg} \tag{4}$$

Mixture Thermal Energy Equation

$$\frac{\partial}{\partial t}(\rho_m e_m) + \frac{\partial}{\partial x}(\rho_m e_m V_m) + \frac{\partial}{\partial x}\left[\frac{(1-\alpha)\ \rho_\ell\ \alpha\rho_g (e_g - e_\ell)}{\rho_m} V_r\right] + p\frac{\partial V_m}{\partial x}$$

$$+ p\frac{\partial}{\partial x}\left[\frac{\alpha(1-\alpha)(\rho_\ell - \rho_g)}{\rho_m} V_r\right] = q_{wg} + q_{w\ell}\,, \tag{5}$$

where

$$\rho_m = \alpha\rho_g + (1-\alpha)\rho_\ell \tag{6}$$

$$V_m = \frac{\alpha\rho_g V_g + (1-\alpha)\ \rho_\ell\ V_\ell}{\rho_m} \tag{7}$$

and

$$V_r = V_g - V_\ell\ . \tag{8}$$

The expression for e_m is the same as Eq. (7) with V replaced by e.

In addition to the thermodynamic relations that are required for closure, specifications for the relative velocity (V_r), the interfacial heat transfer (q_{ig}), the phase change rate (Γ), the wall shear coefficient (K), and the wall heat transfers (q_{wg} and $q_{w\ell}$) are required. The relative velocity V_r is calculated in subroutine SLIP while the wall shear coefficient K is calculated in FWALL. The correlations used for these quantities are discussed in subsequent sections. Gamma is evaluated from a simple thermal energy jump relation

$$\Gamma = \frac{-q_{ig} - q_{i\ell}}{h_{sg} - h_{s\ell}}\,, \tag{9}$$

where

$$q_{ig} = h_{ig} A_i\ (T_s - T_g)/\text{vol} \tag{10}$$

and

$$q_{i\ell} = h_{i\ell} A_i (T_s - T_\ell)/\text{vol.} \tag{11}$$

The quantities h_{ig}, $h_{i\ell}$, and A_i are evaluated in DF1DS and DF1DI under a section delineated as a constitutive package. The evaluation of these three terms is performed in a manner analogous to the three-dimensional interfacial heat transfers (see Sec. III.A.2).

Wall heat transfer terms assume the form:

$$q_{wg} = h_{wg} A_{wg} (T_w - T_g)/\text{vol} \tag{12}$$

and

$$q_{w\ell} = h_{w\ell} A_{w\ell} (T_w - T_\ell)/\text{vol.} \tag{13}$$

The wall heat transfer coefficients are evaluated in subroutine HTCOR, which is discussed in Sec. III.B. The areas are the actual heated surface areas of the cell, except during reflood when the average heat transfer coefficients reflect the fraction of the heated surface area which is quenched.

b. Finite Difference Equations

The one-dimensional flow equations have been written in two separate sets of finite difference equations for TRAC. The first form of the difference equations is semi-implicit and has a time step size stability limit of the form

$$\Delta t < \left|\frac{\Delta x}{V}\right| ,$$

where Δx is the mesh spacing and V the fluid velocity. In blowdown problems this time step is usually prohibitively small due to the high velocities near the break. To alleviate this problem a set of unconditionally stable, fully implicit difference equations was written for use in pipes where the fluid velocities are expected to be high.

The equations are solved for one-dimensional pipes using a staggered difference scheme on the Eulerian mesh. State variables such as pressure, internal energy, and void fraction are obtained at the center of the mesh cells which have length Δx_j, and the mean and relative velocities are obtained at the cell boundaries. Because of this staggered difference scheme, it is necessary to form spatial averages of various quantities to obtain the

finite difference form of the divergence operators. To produce stability in the partially implicit method, a donor-cell average is used of the form,

$$\langle YV\rangle_{j+\frac{1}{2}} = Y_j V_{j+\frac{1}{2}} \qquad \text{for } V_{j+\frac{1}{2}} \geq 0$$

$$= Y_{j+1} V_{j+\frac{1}{2}} \qquad \text{for } V_{j+\frac{1}{2}} < 0 \ , \tag{14}$$

where Y is any state variable or combination of state variables. An integer subscript indicates that a quantity is evaluated at a mesh cell center and a half integer denotes that it is obtained at a cell boundary. With this notation the finite difference divergence operator is

$$\nabla_j(YV) = \{A_{j+\frac{1}{2}}\langle YV\rangle_{j+\frac{1}{2}} - A_{j-\frac{1}{2}}\langle YV\rangle_{j-\frac{1}{2}}\}/\mathrm{vol}_j \ , \tag{15}$$

where A is the cross-sectional area, and vol_j is the volume of the j^{th} cell. Slight variations of these donor cell terms appear in the velocity equation of motion. Donor-cell averages are of the form

$$\langle YV_r^2\rangle_j = Y_j V_{r,j-\frac{1}{2}}^2 \qquad \text{for } V_{r,j-\frac{1}{2}} \geq 0$$

$$= Y_j V_{r,j+\frac{1}{2}}^2 \qquad \text{for } V_{r,j+\frac{1}{2}} < 0 \tag{16}$$

and the donor-cell form of the term $V_m \nabla V_m$ is

$$V_{m,j+\frac{1}{2}} \nabla_{j+\frac{1}{2}} V_m = V_{m,j+\frac{1}{2}}(V_{m,j+\frac{1}{2}} - V_{m,j-\frac{1}{2}})/\Delta x_j \qquad \text{for } V_{m,j+\frac{1}{2}} \geq 0$$

$$= V_{m,j+\frac{1}{2}}(V_{m,j+3/2} - V_{m,j+\frac{1}{2}})/\Delta x_{j+1} \qquad \text{for } V_{m,j+\frac{1}{2}} < 0 \ . \tag{17}$$

Given the preceding notation, the finite difference equations for the partially implicit method are:

Mixture Mass Equation

$$(\rho_m^{n+1} - \rho_m^n)_j/\Delta t + \nabla_j(\rho_m^n V_m^{n+1}) = 0 \ , \tag{18}$$

Vapor Mass Equation

$$(\alpha^{n+1}\rho_g^{n+1} - \alpha^n\rho_g^n)_j/\Delta t + \nabla_j(\alpha^n\rho_g^n V_m^{n+1}) + \nabla_j(\rho_f^n V_r^n) = \Gamma^{n+1} \ , \tag{19}$$

Mixture Energy Equation

$$(\rho_m^{n+1}e_m^{n+1} - \rho_m^n e_m^n)_j/\Delta t + \nabla_j(\rho_m^n e_m^n V_m^{n+1}) + \nabla_j\left|\rho_f^n(e_g^n - e_\ell^n)V_r^n\right|$$

$$= -p_j^{n+1}\nabla_j\left|V_m^{n+1} + \left|\rho_f^n\left(\frac{1}{\rho_g^n} - \frac{1}{\rho_\ell^n}\right)V_r^n\right|\right| + q_{j,wg} + q_{j,w\ell} \quad , \tag{20}$$

Vapor Energy Equation

$$[(\alpha\rho_g e_g)^{n+1} - (\alpha\rho_g e_g)^n]_j/\Delta t + \nabla_j(\alpha^n\rho_g^n e_g^n V_m^{n+1}) + \nabla_j(\rho_f^n e_g^n V_r^n) + p^{n+1}\nabla_j(\alpha^n V_m^{n+1})$$

$$+ p\nabla_j(\rho_f^n V_r^n/\rho_g^n) = -p_j^{n+1}(\alpha_j^{n+1} - \alpha_j^n)/\Delta t + (q_{wg} + q_{ig} + \Gamma h_{sg}^{n+1})_j \quad , \tag{21}$$

Mixture Equation of Motion

$$(V_m^{n+1} - V_m^n)_{j+\frac{1}{2}}/\Delta t + V_{m,j+\frac{1}{2}}^n \nabla_{j+\frac{1}{2}} V_m^n$$

$$= -\left|(p_{j+1}^{n+1} - p_j^{n+1})/\overline{\overline{\Delta x}}_{j+\frac{1}{2}} + \nabla_{j+\frac{1}{2}}(\rho_f V_r^2)^n\right| / \bar{\rho}_{m,j+\frac{1}{2}}^n + g^n - K^n V_m^{n+1}|V_m^n| \quad , \tag{22}$$

where

$$\overline{\overline{\Delta x}}_{j+\frac{1}{2}} = (\Delta x_j + \Delta x_{j+1})/2 \quad , \tag{23}$$

$$\rho_f^n = \frac{\alpha^n(1-\alpha^n)\ \rho_g^n\ \rho_\ell^n}{\rho_m^n} \quad , \tag{24}$$

and

$$\bar{\rho}_{m,j+\frac{1}{2}}^n = \rho_{m,j}^n \qquad \text{for } V_{j+\frac{1}{2}} \geq 0$$

$$= \rho_{m,j+1}^n \qquad \text{for } V_{j+\frac{1}{2}} < 0 \quad . \tag{25}$$

The superscript n indicates that the quantity is evaluated at the "current" time and thus is known, while the superscript n+1 indicates that the variable is evaluated at the new time and hence is an unknown for which the equations must be solved. These equations are equivalent to those given in Ref. 3 in

the full donor cell limit.

Time levels were not assigned to the heat transfer and phase-change terms because they involve a mixture of old and new time quantities. For the interfacial heat transfer, only the potential $(T_s - T_g)$ is calculated at the new time level. For the phase-change rate, the quantities $(T_s - T_g)$, $(T_s - T_\ell)$, and $(h_{sg} - h_{s\ell})$ are all evaluated at the new time level. The remaining interfacial terms are explicit. In the case of the wall heat transfers, only the fluid temperatures T_g and T_ℓ are evaluated at the new time.

Equations (18-22) produce excellent results over a wide range of physical conditions. However, when highly subcooled water flows through a one-dimensional component which was initially filled with steam, pressure spikes can be produced when a computational cell first completely fills with water. When this occurs, Eq. (22) is replaced with the equation

$$p_j^{n+1} = p_j^n \tag{26}$$

and the downstream (with respect to the liquid flow) velocity normally computed from the equation of motion is replaced with a velocity determined from continuity considerations. This logic is incorporated only in the semi-implicit hydrodynamics package.

The fully implicit finite difference equations also use a donor-cell averaging. Therefore, they are very similar in form to the partially implicit equations. Using previous notation, these difference equations are,

Mixture Mass Equation

$$(\rho_m^{n+1} - \rho_m^n)_j/\Delta t + \nabla_j(\rho_m^{n+1} V_m^{n+1}) = 0 \ , \tag{27}$$

Vapor Mass Equation

$$(\alpha^{n+1}\ \rho_g^{n+1} - \alpha^n \rho_g^n)_j/\Delta t + \nabla_j(\alpha^{n+1}\ \rho_g^{n+1}\ V_m^{n+1}) + \nabla_j(\rho_f^{n+1} V_r^n) = \Gamma^{n+1} \ , \tag{28}$$

Mixture Energy Equation

$$(\rho_m^{n+1}e_m^{n+1} - \rho_m^n e_m^n)_j/\Delta t + \nabla_j(\rho_m^{n+1}e_m^{n+1}V_m^{n+1}) + \nabla_j\left|\rho_f^{n+1}(e_g^{n+1} - e_\ell^{n+1})V_r^n\right|$$

$$= - p_j^{n+1}\nabla_j\left|V_m^{n+1} + \left|\rho_f^{n+1}\left(\frac{1}{\rho_g^{n+1}} - \frac{1}{\rho_\ell^{n+1}}\right)V_r^n\right|\right| + q_{j,wg} + q_{j,w\ell} , \qquad (29)$$

Vapor Energy Equation

$$\left|(\alpha\rho_g e_g)^{n+1} - (\alpha\rho_g e_g)^n\right|_j/\Delta t + \nabla_j(\alpha^{n+1}\rho_g^{n+1}e_g^{n+1}V_m^{n+1}) + \nabla_j(\rho_f^{n+1}e_g^{n+1}V_r^n)$$

$$+ p^{n+1}\nabla_j(\alpha^{n+1}V_m^{n+1}) + p\nabla_j\left(\frac{\rho_f^{n+1}}{\rho_g^{n+1}}V_r^n\right)$$

$$= - p_j^{n+1}(\alpha_j^{n+1} - \alpha_j^n)/\Delta t + (q_{wg} + q_{ig} + \Gamma h_{sg}^{n+1})_j , \qquad (30)$$

Mixture Equation of Motion

$$(V_m^{n+1} - V_m^n)_{j+\frac{1}{2}}/\Delta t + V_{m,j+\frac{1}{2}}^{n+1}(V_{m,j+3/2}^{n+1} - V_{m,j-\frac{1}{2}}^{n+1})/(\Delta x_j + \Delta x_{j+1})$$

$$= - \left|(p_{j+1}^{n+1} - p_j^{n+1})/\overline{\Delta x}_{j+\frac{1}{2}} + \nabla_{j+\frac{1}{2}}\rho_f^{n+1}(V_r^2)^n\right|/\overline{\rho}_{m,j+\frac{1}{2}}^{n+1} + g^n - K^n V_m^{n+1}|V_m^{n+1}| . \qquad (31)$$

The major difference between these equations and those for the partially implicit scheme is in the differencing for the V ∇ V term in the momentum equation. The central difference form was found to be superior for calculations of choking but is not stable with the partially implicit method. Presently, the relative velocity is evaluated as an old time quantity, because it does not appear to affect the stability but does save computation time.

In a one-cell transition zone between a region which is solved partially implicitly and another region solved fully implicitly, the finite difference equations must be altered to maintain conservation of mass and energy. In such a zone the fully implicit formulation is used, except that the divergence

terms are altered to the form,

$$\nabla_j(YV_m) = \left\{ A_{j+\frac{1}{2}} \langle Y^{n+1} V_m^{n+1} \rangle_{j+\frac{1}{2}} - A_{j-\frac{1}{2}} \langle Y^{n} V_m^{n+1} \rangle_{j-\frac{1}{2}} \right\} / \mathrm{vol}_j \quad , \tag{32}$$

where it has been assumed that the fully implicit region is at the higher value of j. The velocity at the junction between the two difference schemes is calculated with the semi-implicit difference equation.

The fully implicit package is currently written only to connect with semi-implicit components, breaks, and fills. At a junction with a break, the fully implicit velocity equation is maintained, but the $V \nabla V$ term is donor-celled.

c. Slip Correlations

For a one-dimensional component using the drift-flux model, it is necessary to specify the relative velocity between the vapor and liquid phases, $V_r = V_g - V_\ell$. Relative velocities are calculated in an explicit manner, i.e., they are updated only once at the beginning of each time step. Since the relative velocities are defined at each mesh cell edge, a component having NCELL number of cells requires NCELL+1 values for V_r.

Subroutine SLIP calculates the relative velocities for the one-dimensional components. The procedure for determining the relative velocities is formulated on the basis of a flow regime map. This map is two-dimensional in that the flow regime is a function of both vapor fraction and mass flux, $G = \rho_m V_m$, as shown in Fig. 1. It is very similar to the map used in the three-dimensional vessel hydrodynamics (see Sec. A.2.c below).

Subroutine SLIP is divided into two parts. The first part determines which flow regime exists at each cell edge; the second part performs the actual calculation of the relative velocity based on averaged local properties and/or the mixture velocity. This approach makes it straightforward to change either the flow regime map or the particular correlation in a regime, or both. In addition, a more accurate determination of the relative velocity can be obtained by using a correlation developed for a particular flow regime than by applying a single correlation in all flow topologies.

Because the values of vapor fraction, liquid/vapor densities, and surface tension are defined at mesh cell centers, it is necessary to compute the cell edge values by some averaging procedure. The procedure is to

donor-cell upstream values of these cell-centered variables. This value is then used in both the determination of flow regime and the relative velocity correlation.

For the flow regime map shown in Fig. 1, the following relative velocity correlations are used for nonhorizontal flow. These correlations have been shown to be in satisfactory agreement with experimentally measured relative velocities in steam/water flows for each particular flow regime.[4,5]

Bubbly Regime

$$V_r = \frac{1.41}{(1-\alpha)} \left[\frac{\sigma g(\rho_\ell - \rho_g)}{\rho_\ell^2} \right]^{\frac{1}{4}}, \tag{33}$$

Slug Regime

$$V_r = \frac{0.345}{(1-\alpha)} \left[\frac{g D_h(\rho_\ell - \rho_g)}{\rho_\ell} \right]^{\frac{1}{2}}, \tag{34}$$

Churn-Turbulent Regime

$$V_r = \frac{V_m}{\frac{1-c\alpha}{c-1} + \frac{\alpha\rho_g}{\rho_m}}, \tag{35}$$

where $c = 1.1$ and α is restricted to a maximum value of 0.8, and

Annular Regime

$$V_r = \frac{V_m}{\left[\frac{\rho_g(76-75\alpha)}{\rho_\ell\sqrt{\alpha}} \right]^{\frac{1}{2}} + \frac{\alpha\rho_g}{\rho_m}}. \tag{36}$$

The dashed lines in Fig. 1 are transition regions between flow regimes. In these transition regions, the relative velocity is linearly interpolated between values for the two adjacent flow regimes. The linear coefficient is determined by the vapor fraction if $G < 2000$ kg/m^2 s and also by the mass flux if $2000 \leq G \leq 3000$ kg/m^2 s. For example, if $G < 2000$ and $\alpha = 0.18$, then V_r = 0.2 times Eq. (33) evaluated at $\alpha = 0.10$ plus 0.8 times Eq. (34) evaluated at $\alpha = 0.20$. In the transition region between the annular flow

regime and 100% vapor fraction, V_r is linearly interpolated between the annular flow value and zero.

For horizontal flow the relative velocity is determined from Eq. (35) independent of flow regime.

d. Wall Friction and Form Losses

The total pressure gradient calculated in the mixture momentum equation is expressed as the sum of the frictional dissipation, acceleration head, and potential head terms. Subroutine FWALL calculates a coefficient for the frictional dissipation term and a coefficient for losses associated with abrupt area changes. Under single-phase flow conditions, pressure drops associated with frictional losses are correlated as functions of fluid velocity, fluid density, fluid viscosity, channel hydraulic diameter, and surface roughness of the channel wall. When a two phase mixture is flowing in a channel, a correction to the single phase frictional losses is necessary to account for added dissipation between phases and interactions with the channel walls. This correction factor is referred to as the two-phase flow multiplier and is a feature of four of the five friction factor options available in TWINC.

The friction factor returned to the fluid dynamics solution section is defined as follows:

$$f = (\Delta p/\Delta z)_f \Big/ \frac{2 \rho_m V_m |V_m|}{D_h} , \qquad (37)$$

where $(\Delta p/\Delta z)_f$ is the pressure drop associated with frictional losses. The options available for calculating f are:

NFF = 0 = constant value (user input),

NFF = 1 = homogeneous model,

NFF = 2 = Armand correlation,

NFF = 3 = CISE correlation,

NFF = 4 = modified annular flow model, and

NFF = 5 = Chisholm correlation,

where NFF is the user-supplied index. Using a negative value of the index will result in an automatic calculation of an appropriate form loss coefficient in addition to the selected two-phase flow friction factor. Recommendations for selection of NFF for each component are given in Chap. IV.

Homogeneous Model

The homogeneous friction factor model alters the single-phase value by using a two-phase viscosity (μ) defined in terms of the quality (x) as follows:[6]

$$\frac{1}{\mu} = \frac{x}{\mu_g} + \frac{(1-x)}{\mu_f} \quad . \tag{38}$$

The homogeneous friction factor[7] is then given by

$$f = 0.046\ [G D_h/\mu]^{-0.2} \quad , \tag{39}$$

where $G = \rho_m V_m$.

Armand Model

The Armand correlation applies a vapor fraction dependent multiplier (Φ^2) to the single-phase friction factor. The single-phase friction factor is defined as in Eq. (39) and the two-phase multipliers are[8]

$$\Phi^2 = 1.0 \qquad \text{for } \alpha = 0, \tag{40}$$

$$\Phi^2 = \frac{(1-x)}{(1-\alpha)^{1.42}} \qquad \text{for } 0.39 \le (1-\alpha) \le 1.0 \ , \tag{41}$$

$$\Phi^2 = \frac{0.478\ (1-x)^2}{(1-\alpha)^{2.2}} \qquad \text{for } 0.1 \le (1-\alpha) \le 0.39 \ , \tag{42}$$

and

$$\Phi^2 = \frac{1.730\ (1-x)^2}{(1-\alpha)^{1.64}} \qquad \text{for } 0.0 \le (1-\alpha) \le 0.1 \ . \tag{43}$$

The Armand correlation for the friction factor is then

$$f = 0.046\ [G D_h/\mu]^{-0.2}\ \Phi^2 \quad . \tag{44}$$

CISE Model

The CISE correlation[9] substitutes a more empirical method for the two-phase multiplier concept used by the other options:

$$f = 0.8\ \rho_m^{-0.46}\ V_m^{0.6}\ \alpha^{0.4}\ D_h^{-0.2} \quad . \tag{45}$$

Annular Flow Model

The annular flow friction factor method of Ref. 10 is adopted in the NFF=4 option, with a modification at high vapor fractions. The single-phase friction factor (f_{sp}) is taken from Ref. 11:

$$f_{sp} = a + b\, Re^{-c}, \tag{46}$$

where

$$a = 0.026\left(\frac{k}{D}\right)^{0.225} + 0.133\left(\frac{k}{D}\right), \tag{47}$$

$$b = 22.0\left(\frac{k}{D}\right)^{0.44}, \tag{48}$$

$$c = 1.62\left(\frac{k}{D}\right), \tag{49}$$

and k/D is the relative pipe wall roughness. A value of $k = 5.0 \times 10^{-6}$ m, corresponding to drawn tubing, is currently used for the absolute pipe roughness. The annular flow friction factor is then

$$f = f_{sp}\, \phi^2, \tag{50}$$

where

$$\phi^2 = \frac{\rho_m V_\ell^2}{\rho_\ell V_m^2}. \tag{51}$$

At vapor fractions above 0.90, the homogeneous friction factor is faired into the annular flow model.

Chisholm Model

The Chisholm correlation[12] is based on a transformation of the graphical procedure of Baroczy for predicting pressure gradients for turbulent flow of two-phase mixtures in smooth pipes. The single-phase friction factor component is evaluated by the method of the preceding section. The Chisholm two-phase multiplier is:

$$\phi^2 = 1 + (R^2 - 1)[B \times (1 - x) + x^2], \tag{52}$$

where

$$R = (\rho_\ell/\rho_g)^{0.5}. \tag{53}$$

The value of B depends on both R and G. For $R \leq 9.5$,

$$\left.\begin{aligned} B &= 4.8 \text{ for } G \leq 500, \\ B &= 2400/G \text{ for } 500 < G < 1900, \\ B &= 55/G^{0.5} \text{ for } G \geq 1900. \end{aligned}\right\} \quad (54)$$

For $9.5 < R < 28$,

$$\left.\begin{aligned} B &= 520/(R\, G^{0.5}) \text{ for } G \leq 600, \\ B &= 21/R \text{ for } G > 600. \end{aligned}\right\} \quad (55)$$

Finally for $R > 28$,

$$B = 15000/(R^2\, G^{0.5}). \quad (56)$$

Form Losses

The semi-implicit finite difference equations yield the correct pressure loss for an abrupt expansion. However, this is not true for an abrupt contraction or for an orifice. The fully implicit difference equations provide a good representation of Bernoulli flow but require pressure-loss corrections for all abrupt area changes.

Form loss corrections can be included in a calculation in two ways. The simplest method is to use a negative value for the input friction option variable NFF (see Sec. V.D) at the location of any abrupt area change. This triggers logic in the code which examines the local pipe geometry, flow direction, and level of implicitness of the difference equations to determine an appropriate loss correction. These corrections are accounted for by an extra term in the Bernoulli equation of the form:

$$\Delta p = \frac{k\rho v^2}{2}, \quad (57)$$

where k is a form loss coefficient. The values available for k are

$$k = \left(1 - \frac{A_1}{A_2}\right)^2 \quad (58)$$

for an abrupt expansion or zero length orifice, and

$$k = 0.5 - 0.7\ \frac{A_1}{A_2} + \ 0.2 \left(\frac{A_1}{A_2}\right)^2 \quad (59)$$

for an abrupt contraction where A_1 and A_2 are, respectively, the smaller and larger flow areas. Equation (59) is a curve fit to the values reported in Ref. 13.

Another way to account for form losses is through use of the FRIC input array. Losses computed using this array are in addition to those specified with the NFF option. The pressure loss which results from the use of FRIC is

$$\Delta p = \frac{(\Delta x_j + \Delta x_{j-1})}{2 D_{h,j}} \text{FRIC}_j \rho_m V_m |V_m| ,$$

where j is the mesh cell index.

2. Three-Dimensional Vessel Hydrodynamics

The field equations, finite difference scheme, solution procedure, and constitutive relations for the three-dimensional, two-fluid, hydrodynamics package are discussed in this section. Subroutines TF3D (Two-Fluid 3-Dimensional), ITR1 (an iteration subroutine), and FF3D (a subroutine that provides a final back-substitution) are the main subroutines of this package.

TF3D includes a constitutive package to provide wall and interfacial shears and the interfacial heat transfer. The wall heat transfer coefficients and temperatures are provided by HTCOR which is discussed in Sec. III.B. TF3D also sets up the basic staggered finite difference scheme for the three-dimensional representation of the core, linearizes the algebraic equations, and provides a forward elimination. This information is then used in the iteration routine ITR1 and finally new pressures, void fractions, velocities (both vapor and liquid), and fluid temperatures (liquid and vapor) are computed in FF3D.

a. Differential Equations

The field equations[1,2] describing the two-phase, two-fluid flow are given below.

Mixture Mass Equation

$$\frac{\partial \rho_m}{\partial t} + \nabla \cdot [\alpha \rho_g \vec{V}_g + (1-\alpha) \rho_\ell \vec{V}_\ell] = 0 , \tag{60}$$

Vapor Mass Equation

$$\frac{\partial (\alpha \rho_g)}{\partial t} + \nabla \cdot (\alpha \rho_g \vec{V}_g) = \Gamma , \tag{61}$$

Vapor Equation of Motion

$$\frac{\partial \vec{V}_g}{\partial t} + \vec{V}_g \cdot \nabla \vec{V}_g = - \frac{C_i}{\alpha \rho_g} \vec{V}_r |\vec{V}_r| - \frac{1}{\rho_g} \nabla p - \frac{\Gamma}{\alpha \rho_g} (\vec{V}_g - \vec{V}_{ig})$$

$$- \frac{C_{wg}}{\alpha \rho_g} \vec{V}_g |\vec{V}_g| + \vec{g} , \tag{62}$$

Liquid Equation of Motion

$$\frac{\partial \vec{V}_\ell}{\partial t} + \vec{V}_\ell \cdot \nabla \vec{V}_\ell = \frac{C_i}{(1-\alpha)\rho_\ell} \vec{V}_r |\vec{V}_r| - \frac{1}{\rho_\ell} \nabla p + \frac{\Gamma}{(1-\alpha)\rho_\ell} (\vec{V}_\ell - \vec{V}_{i\ell})$$

$$- \frac{C_{w\ell} \vec{V}_\ell |\vec{V}_\ell|}{(1-\alpha)\rho_\ell} + \vec{g} , \tag{63}$$

Mixture Thermal Energy Equation

$$\frac{\partial [(1-\alpha)\rho_\ell e_\ell + \alpha \rho_g e_g]}{\partial t} + \nabla \cdot [(1-\alpha)\rho_\ell e_\ell V_\ell + \alpha \rho_g e_g V_g]$$

$$= - p \nabla \cdot [(1-\alpha)V_\ell + \alpha V_g] + q_{wg} + q_{w\ell} , \tag{64}$$

Vapor Thermal Energy Equation

$$\frac{\partial (\alpha \rho_g e_g)}{\partial t} + \nabla \cdot (\alpha \rho_g V_g e_g) = - p \frac{\partial \alpha}{\partial t} - p \nabla \cdot (\alpha V_g) + q_{wg} + q_{ig} + \Gamma h_{sg} , \tag{65}$$

where ρ_m and V_r are identical to the definitions used in the drift-flux model [see Eqs. (6) and (8)].

It is well known that the set of field equations described above have complex characteristics which represent a partially elliptic system. This system can be solved numerically with the present interfacial shear relations as long as the mesh size is not too small. It is recommended that nothing smaller than one centimeter (preferably larger) be used as a length scale for the mesh. This will normally be sufficient to keep the solution from

developing instabilities. Mesh sizes smaller than one centimeter may be used singly (for example, to represent radial downcomer gaps) as long as adjacent mesh cells are larger. The larger mesh cells will damp out any exponential growth in the adjoining smaller cells. Semiscale, LOFT, and full-size PWRs have been modeled and run for thousands of cycles with no apparent difficulties which could be traced to unbounded growth of any of the variables. The mesh spacings used in these calculations are described in Vol. II of this manual.

b. Finite Difference Equations

The momentum equations are separated into the three coordinate components. Only the vapor equation will be discussed with the understanding that the liquid momentum equation is treated in an analogous manner. The three components of the vapor-momentum differential equation are:

Axial (z) Component

$$\frac{\partial V_{gz}}{\partial t} = -\left(V_{gr}\frac{\partial V_{gz}}{\partial r} + \frac{V_{g\theta}}{r}\frac{\partial V_{gz}}{\partial \theta} + V_{gz}\frac{\partial V_{gz}}{\partial z}\right) - \frac{1}{\rho_g}\frac{\partial p}{\partial z}$$

$$- \frac{C_{iz}}{\alpha\rho_g}(V_{gz} - V_{\ell z})\left|\vec{V}_g - \vec{V}_\ell\right| - \frac{\Gamma}{\alpha\rho_g}(V_{gz} - V_{igz}) - \frac{C_{wgz}}{\alpha\rho_g}V_{gz}\left|\vec{V}_g\right| + g \tag{66}$$

Radial (r) Component

$$\frac{\partial V_{gr}}{\partial t} = -\left(V_{gr}\frac{\partial V_{gr}}{\partial r} + \frac{V_{g\theta}}{r}\frac{\partial V_{gr}}{\partial \theta} - \frac{V_{g\theta}^2}{r} + V_{gz}\frac{\partial V_{gr}}{\partial z}\right) - \frac{1}{\rho_g}\frac{\partial p}{\partial r}$$

$$- \frac{C_{ir}}{\alpha\rho_g}(V_{gr} - V_{\ell r})\left|\vec{V}_g - \vec{V}_\ell\right| - \frac{\Gamma}{\alpha\rho_g}(V_{gr} - V_{igr}) - \frac{C_{wgr}}{\alpha\rho_g}V_{gr}\left|\vec{V}_g\right| \tag{67}$$

Azimuthal (θ) Component

$$\frac{\partial V_{g\theta}}{\partial t} = -\left(V_{gr}\frac{\partial V_{g\theta}}{\partial r} + \frac{V_{g\theta}}{r}\frac{\partial V_{g\theta}}{\partial \theta} + \frac{V_{gr}V_{g\theta}}{r} + V_{gz}\frac{\partial V_{g\theta}}{\partial z}\right) - \frac{1}{\rho_g r}\frac{\partial p}{\partial \theta}$$

$$- \frac{C_{i\theta}}{\alpha\rho_g}(V_{g\theta} - V_{\ell\theta})\left|\vec{V}_g - \vec{V}_\ell\right| - \frac{\Gamma}{\alpha\rho_g}(V_{g\theta} - V_{ig\theta}) - \frac{C_{wg\theta}}{\alpha\rho_g}V_{g\theta}\left|\vec{V}_g\right| . \tag{68}$$

Velocities are defined on the mesh-cell surfaces as shown in Fig. 2 where subscript "a" stands for either ℓ or g.

In the staggered scheme[14,15] used in TRAC, the velocities are located on the mesh cell surfaces at the locations shown in Fig. 2 while the volume properties, p, α, T, e, ρ, etc., are located at the mesh-cell centers. The scalar field equations are written over a given mesh cell while the momentum equations are staggered between mesh cells in the three component directions.

To write out the difference scheme for each of the momentum equations is a rather lengthy process due to the cross-derivative terms. Therefore, only the vapor z-direction finite difference equations for a typical mesh cell are given to illustrate the procedure used. The time levels are indicated by the superscript n (old time) or n+1 (new time). The subscript g (for vapor) will be dropped except where it is needed for clarity of the presentation. Using these conventions, the finite difference vapor momentum equation in the z-direction is:

$$V_z^{n+1}(r,\theta,z+\tfrac{1}{2}) = V_z^{n}(r,\theta,z+\tfrac{1}{2}) - \Delta t \left\{ \frac{V_r(r,\theta,z+\frac{1}{2})}{\Delta r}\left[V_z(r+\tfrac{1}{2},\theta,z+\tfrac{1}{2}) - V_z(r-\tfrac{1}{2},\theta,z+\tfrac{1}{2})\right]^n \right.$$

$$+ \frac{V_\theta(r,\theta,z+\frac{1}{2})}{r\Delta\theta}\left[V_z(r,\theta+\tfrac{1}{2},z+\tfrac{1}{2}) - V_z(r,\theta-\tfrac{1}{2},z+\tfrac{1}{2})\right]^n$$

$$+ \frac{V_z(r,\theta,z+\frac{1}{2})}{\Delta z}\left[V_z(r,\theta,z+1) - V_z(r,\theta,z)\right]^n$$

$$- \frac{\left[p(r,\theta,z+1) - p(r,\theta,z)\right]^{n+1}}{\rho^n(r,\theta,z+\frac{1}{2})\Delta z}$$

$$- \frac{c_{iz}^n(r,\theta,z+\frac{1}{2})\left|V_{gz}(r,\theta,z+\frac{1}{2}) - V_{\ell z}(r,\theta,z+\frac{1}{2})\right|^{n+1}}{\alpha^n(r,\theta,z+\frac{1}{2})\ \rho^n(r,\theta,z+\frac{1}{2})}$$

$$\left. \cdot\ \left|V_{gz}(r,\theta,z+\tfrac{1}{2}) - V_{\ell z}(r,\theta,z+\tfrac{1}{2})\right|^n \right.$$

$$- \frac{\Gamma^n(r,\theta,z+\frac{1}{2}) \left| V_z(r,\theta,z+\frac{1}{2}) - V_{iz}(r,\theta,z+\frac{1}{2}) \right|^{n+1}}{\alpha^n(r,\theta,z+\frac{1}{2})\ \rho^n(r,\theta,z+\frac{1}{2})}$$

$$\left. - \frac{c^n_{wz}(r,\theta,z+\frac{1}{2})\ V_z^{n+1}(r,\theta,z+\frac{1}{2}) \left| V_z^n(r,\theta,z+\frac{1}{2}) \right|}{\alpha^n(r,\theta,z+\frac{1}{2})\ \rho^n(r,\theta,z+\frac{1}{2})} \right\} , \qquad (69)$$

where Δt is the time-step size.

As with any finite difference scheme, certain quantities are required at locations where they are not formally defined so that additional relations are required. The volume properties Γ, α, and ρ_g are donor-celled depending on the direction of $V_z(r,\theta,z+\frac{1}{2})$. For example,

$$\begin{aligned} \alpha(r,\theta,z+\tfrac{1}{2}) &= \alpha(r,\theta,z) && \text{if } V_z(r,\theta,z+\tfrac{1}{2}) \geq 0 \\ &= \alpha(r,\theta,z+1) && \text{if } V_z(r,\theta,z+\tfrac{1}{2}) < 0 . \end{aligned} \qquad (70)$$

The radial component of velocity at axial location $z+\frac{1}{2}$ is obtained from

$$V_r(r,\theta,z+\tfrac{1}{2}) = \tfrac{1}{4}[V_r(r+\tfrac{1}{2},\theta,z) + V_r(r-\tfrac{1}{2},\theta,z) + V_r(r+\tfrac{1}{2},\theta,z+1)$$

$$+ V_r(r-\tfrac{1}{2},\theta,z+1)] \qquad (71)$$

with a similar expression applying to $V_\theta(r,\theta,z+\frac{1}{2})$. The spatial differences for V_z are, in the r-direction,

$$V_z(r+\tfrac{1}{2},\theta,z+\tfrac{1}{2}) - V_z(r-\tfrac{1}{2},\theta,z+\tfrac{1}{2}) = V_z(r,\theta,z+\tfrac{1}{2}) - V_z(r-1,\theta,z+\tfrac{1}{2})$$

if $V_r(r,\theta,z+\frac{1}{2}) \geq 0$, or

$$= V_z(r+1,\theta,z+\tfrac{1}{2}) - V_z(r,\theta,z+\tfrac{1}{2})$$

if $V_r(r,\theta,z+\frac{1}{2}) < 0$. (72)

In the θ direction,

$$V_z(r,\theta+\tfrac{1}{2},z+\tfrac{1}{2}) - V_z(r,\theta-\tfrac{1}{2},z+\tfrac{1}{2}) = V_z(r,\theta,z+\tfrac{1}{2}) - V_z(r,\theta-1,z+\tfrac{1}{2})$$

if $V_\theta(r,\theta,z+\tfrac{1}{2}) \geq 0$, or

$$= V_z(r,\theta+1,z+\tfrac{1}{2}) - V_z(r,\theta,z+\tfrac{1}{2})$$

if $V_\theta(r,\theta,z+\tfrac{1}{2}) < 0$. (73)

In the z-direction,

$$V_z(r,\theta,z+1) - V_z(r,\theta,z) = V_z(r,\theta,z+\tfrac{1}{2}) - V_z(r,\theta,z-\tfrac{1}{2})$$

if $V_z(r,\theta,z+\tfrac{1}{2}) \geq 0$, or

$$= V_z(r,\theta,z+3/2) - V_z(r,\theta,z+\tfrac{1}{2})$$

if $V_z(r,\theta,z+\tfrac{1}{2}) < 0$. (74)

The convective terms in the finite difference relations for the scalar field equations are written in conservation form. The finite difference form of the overall mixture mass equation is

$$\rho_m^{n+1} = \rho_m^n + (\Delta t/\mathrm{vol}) \Bigg\{ FA_{z-\frac{1}{2}} \left[\left((1-\alpha)\rho_\ell\right)^n V_\ell^{n+1} + (\alpha\rho_g)^n V_g^{n+1} \right]_{z-\frac{1}{2}}$$

$$- FA_{z+\frac{1}{2}} \left[\left((1-\alpha)\rho_\ell\right)^n V_\ell^{n+1} + (\alpha\rho_g)^n V_g^{n+1} \right]_{z+\frac{1}{2}} + FA_{r-\frac{1}{2}} \left[\left((1-\alpha)\rho_\ell\right)^n V_\ell^{n+1} \right.$$

$$\left. + (\alpha\rho_g)^n V_g^{n+1} \right]_{r-\frac{1}{2}} - FA_{r+\frac{1}{2}} \left[\left((1-\alpha)\rho_\ell\right)^n V_\ell^{n+1} + (\alpha\rho_g)^n V_g^{n+1} \right]_{r+\frac{1}{2}}$$

$$+ FA_{\theta-\frac{1}{2}} \left[\left((1-\alpha)\rho_\ell\right)^n V_\ell^{n+1} + (\alpha\rho_g)^n V_g^{n+1} \right]_{\theta-\frac{1}{2}}$$

$$\left. - FA_{\theta+\frac{1}{2}} \left[\left((1-\alpha)\rho_\ell\right)^n V_\ell^{n+1} - (\alpha\rho_g)^n V_g^{n+1} \right]_{\theta+\frac{1}{2}} \right\} , \quad (75)$$

where vol is the hydrodynamic cell volume and FA is the flow area at the mesh cell edge. The other scalar equations are differenced similarly.

All of the field equations (60-65) have additional source terms to allow piping to be connected anywhere in the mesh. These sources in the scalar equations contain both an explicit and an implicit term. The implicit term is iterated with the rest of the new time variables in order to provide a consistent (in terms of time differencing) procedure for providing one-dimensional connections to the vessel. The source terms appearing in the mass and energy equations are given below. Subscripts p and v refer to pipe and vessel quantities, respectively.

Overall Mass Continuity Source Term

$$(\rho_m^n \, FA \, V_m^{n+1})_p$$

Vapor Mass Continuity Source Term

$$[(\alpha\rho_g)^n \, FA \, V_m^{n+1}]_p + [\alpha(1-\alpha) \frac{\rho_g \rho_\ell}{\rho_m} FA \; V_r]_p^n$$

Overall Energy Source Term

$$[(\rho_m \, e_m)^n \, FA \, V_m^{n+1}]_p + [\alpha(1-\alpha) \frac{\rho_\ell \rho_g}{\rho_m} (e_g - e_\ell) \, FA \, V_r]_p^n$$
$$+ p_v(V_m^{n+1} \, FA)_p + p_v[\alpha(1-\alpha) \frac{(\rho_\ell - \rho_g)}{\rho_m} FA \, V_r]_p^n$$

Vapor Energy Source Term

$$[(\alpha\rho_g \, e_g)^n \, FA \, V_m^{n+1}]_p + [\alpha(1-\alpha) \frac{\rho_\ell \rho_g}{\rho_m} e_g \, FA \, V_r]_p^n$$
$$+ p_v(\alpha^n \, FA \, V_m^{n+1})_p + p_v[\alpha(1-\alpha) \frac{\rho_\ell}{\rho_m} FA \, V_r]_p^n$$

The momentum source terms are complicated due to the staggered differencing and the fact that pipes may enter at an arbitrary angle. For the present

version, we have assumed that the pipe enters normal to the vessel mesh cell face. The basic forms for the liquid and vapor momentum source terms are:

Liquid Momentum Source Term

$$(V_\ell^2 \frac{FA}{\Delta x})^n_p / FA_v \quad ,$$

Vapor Momentum Source Term

$$(V_g^2 \frac{FA}{\Delta x})^n_p / FA_v \quad ,$$

where

$$V_\ell = V_m - \frac{\alpha \rho_g}{\rho_m} V_r \tag{76}$$

and

$$V_g = V_m + (1-\alpha) \frac{\rho_\ell}{\rho_m} V_r \quad . \tag{77}$$

If structure exists in the mesh cell, the hydrodynamic flow areas (FA) and volumes (vol) are reduced from their geometric mesh cell values. Thus, FA may be less than or equal to the geometric mesh cell area and vol may be less than or equal to the geometric mesh cell volume. Flow areas may also be set identically equal to zero. If this is the case, all fluxes across that plane are suppressed along with the individual velocities of each phase. This procedure allows large obstables such as the downcomer walls to be properly modeled. The user is allowed complete freedom to specify the flow and volume restrictions except that a zero hydrodynamic volume is not allowed.

The finite difference equations thus formed are semi-implicit, since the pressure gradient terms in the vapor and liquid momentum equations are treated at the new time. A Courant stability criterion of the form

$$\frac{|V|}{L} = \max \left(\frac{V_{gz}}{\Delta z}, \frac{V_{g\theta}}{\Delta \theta}, \frac{V_{gr}}{\Delta r}, \frac{V_{\ell z}}{\Delta z}, \frac{V_{\ell \theta}}{\Delta \theta}, \frac{V_{\ell r}}{\Delta r} \right)$$

is necessary where

$$\frac{|V| \Delta t}{L} < 1 \quad .$$

In order to solve the system of finite difference equations, a linearization procedure is carried out. All of the scalar equations are reduced to a linear system in V_ℓ, V_g, T_ℓ, T_g, α, and p. This is accomplished by using the thermal equations of state:

$$\rho_\ell = \rho_\ell(p,T_\ell)$$

$$\rho_g = \rho_g(p,T_g) \ ,$$

the caloric equations of state:

$$e_\ell = e_\ell(p,T_\ell)$$

$$e_g = e_g(p,T_g) \ ,$$

and the definitions for ρ_m and e_m.

A further reduction in the system is accomplished by observing that the finite difference vapor and liquid momentum equations yield equations of the form

$$V^{n+1} = V^n + [conv^n + \frac{1}{\rho_\ell} \nabla p^{n+1} + FRIC] \ \Delta t \ , \tag{78}$$

where conv designates the explicit convection terms and FRIC includes both the wall and interfacial shears. Equation (78) indicates that changes in V are linearly dependent (after an explicit pass on the explicit parts of the momentum equations) on changes in pressure. The system of variables may therefore be further reduced to T_ℓ, T_g, p, and α and solved by a Block Gauss-Seidel method. Reference 3 provides a much more detailed description of the basic Newton Block Gauss-Seidel numerical technique.

One improvement to the method proposed in Ref. 3 has been implemented to reduce the computing cost. The linear system that results from this method is a block seven-stripe matrix. In performing the Gauss-Seidel operation, if the nonlinear terms are not updated, the matrix coefficients remain constant for the time step. In this case a Gauss elimination technique can be applied once at each time step to the seven-stripe block array which allows its reduction to a seven-stripe single-element array. This results in a much faster

iteration (after the first iteration) for the pressure. The actual iteration is performed in subroutine ITR1. When the vessel pressures are obtained to a specified convergence criterion, a back-substitution in subroutine FF3D is performed to unfold T_ℓ, T_g, and α and the velocities for each phase. A call to THERMO in FF3D then updates all of the thermodynamic properties and their derivatives in preparation for the next time step.

c. Constitutive Equations

The field equations (60-65) require certain auxiliary or constitutive equations to effect closure. It has already been mentioned that thermal and caloric equations of state for each phase are required. These are discussed in Sec. III.A.3. In addition, the liquid and vapor wall shear, interfacial drag, wall heat transfer, interfacial heat transfer, the net vaporization rate, and a specification for the interfacial velocities are necessary.

In the present version of the code, the vaporization thrust terms in the momentum equations are neglected. Future versions of the vessel module will specify an interfacial velocity in the three coordinate directions and these terms, which are not always second order (in the core region for example), will then be taken into account. The wall heat transfers q_{wg} and $q_{w\ell}$ are accounted for in the standard way [see Eqs. (12) - (13)]. The surface areas represent an actual estimate of the total wall surface area wetted by each phase, while $h_{w\ell}$ and h_{wg} are based on heat transfer correlations from the literature. In many two-phase flow situations the walls are totally wetted by the liquid phase, in which case wall heat transfer to the vapor is zero.

The wall shear coefficients c_{wg} and $c_{w\ell}$ are defined as

$$c_{wg} = \alpha\rho_g \frac{c_{fg}}{2D_h} \tag{79}$$

$$c_{w\ell} = (1-\alpha)\rho_\ell \frac{c_{f\ell}}{2D_h} , \tag{80}$$

where c_{fg} and $c_{f\ell}$ are, respectively, the vapor and liquid wall friction factors and D_h is the hydraulic diameter. The standard Harwell correlation[6] is employed to provide the wall friction factors for two-phase flow. These factors go to the appropriate single-phase values for $\alpha = 0$ and $\alpha = 1$. The average cell vector velocity is used to define the mesh cell Reynolds number, and the two-phase multiplier is calculated using cell-centered

quantities. A total friction factor is calculated from the information above and is ascribed completely to the liquid momentum equation until a vapor fraction of 0.9 is reached. From α of 0.9 to 0.9999, the shear is assigned with linear weighting to both the liquid and vapor. Beyond a vapor fraction of 0.9999, a pure vapor drag coefficient is calculated (laminar or Blausius) and assigned totally to the vapor momentum equation. If the vapor fraction is less than 0.0001, a single-phase liquid correlation (laminar or Blausius) is used.

A single friction coefficient is generated for both the outer radial and upper axial cell face from this procedure. However, the hydraulic diameter used in the radial and axial directions will, in general, vary depending on the geometry. These hydraulic diameters are calculated from

$$D_h = 4FA_i/P_i, \text{ where } i = 0,z,r$$

and where the wetted perimeter (P_i) normal to direction i includes the surface area of any rods, wall heat slabs, or flow boundaries. If there is no solid material in a mesh cell, the wall shear is zero. A similar procedure is used to arrive at a wall shear in the theta direction. In this case, however, vector velocities and properties on the appropriate theta face (rather than the cell-centered averages) are used in order to achieve theta symmetry where such symmetry should exist.

The basic finite difference scheme will properly calculate classical Borda losses at an expansion but overpredicts the losses at a contraction (see discussion in Sec. A.1.d above). Provisions have been made for the user to specify an additional constant hydraulic loss factor in any of the coordinate directions and at any mesh face, but this feature has not yet been implemented.

The flashing rate Γ is determined from a simplified thermal energy jump condition identical to that used in the one-dimensional drift-flux hydrodynamics [see Eqs. (9-11)]. In both the vapor continuity equation and the vapor thermal energy equation, the potentials $T_s - T_g$ and $T_s - T_\ell$ are evaluated at the new time level while $h_{ig} A_i$ and $h_{i\ell} A_i$ are evaluated at the old time.

The interfacial heat transfers during boiling and the interfacial shear are calculated in conjunction with a simple flow regime map.[16] This flow regime map, while originally developed for vertical pipe flow, is the simplest prescription that provides a rational means for defining the constitutive equations.[54] Figure 3 illustrates the manner in which the flow map is implemented in the code.

If the void fraction is less than or equal to 0.25, a bubbly flow is assumed. The interfacial surface area in this regime is calculated in conjunction with a critical bubble Weber number We_b. A value of $We_b = 25$ is used in the present code version. This value was chosen on the basis of comparisons between TRAC predictions and experimental results for low subcooling (i.e., shear dominated) Creare downcomer tests. TRAC results for these tests are not very sensitive to the Weber number in the range $25 \leq We_b \leq 100$. The expression relating interfacial surface area with We_b is:

$$\frac{\rho_\ell V_r^2 D_b}{\sigma} = We_b$$

or

$$D_b = \frac{We_b \sigma}{\rho_\ell V_r^2} , \tag{81}$$

where D_b is the bubble diameter. For this diameter, and assuming a uniform bubble distribution within the mesh cell volume (vol), the number of bubbles is

$$CNB = \frac{6 \alpha \, vol}{\pi D_b^3} \tag{82}$$

and the interfacial area is

$$A_i = 6 \alpha \, vol \, \rho_\ell V_r^2 / We_b \sigma . \tag{83}$$

The liquid side interfacial heat transfer coefficient is taken as the larger of an approximate formulation of the Plesset-Zwick bubble growth model[6,17]

$$Nu = 0.95493 (T_\ell - T_s) \rho_\ell \frac{\partial e_\ell}{\partial T_\ell} / [\rho_g (h_{s\,g} - h_{s\,\ell})] \tag{84}$$

and a sphere convection coefficient[18]

$$Nu = 2.0 + 0.74\ Re_b^{0.5}, \tag{85}$$

where

$$Re_b = \rho_\ell\ V_r\ D_b/\mu_\ell\ .$$

The interfacial shear coefficient is provided by a rather standard set of formulas for a sphere:[11]

$$c_i = \frac{c_b\ \alpha\ \rho_\ell}{2\ D_b}\ , \tag{86}$$

where

$$c_b = 240 \text{ for } Re_b < 0.1,$$

$$= 24/Re_b \text{ for } 0.1 \leq Re_b \leq 2,$$

$$= 9.35/Re_b^{0.68} \text{ for } Re_b > 2.$$

If the cell-average mass flux is less than 2 000 kg/m^2·s and the vapor fraction is between 0.25 and 0.5, the flow enters the slug regime. At the maximum α of 0.5, 40% of the vapor is assumed to exist in the form of trailing bubbles with the remainder contained in the slug. These bubbles probably contribute the majority of the interfacial heat transfer and the liquid side coefficient is calculated from the relations for the entrained bubbles. If the mass flux is greater than 2 700, all of the vapor is assumed to exist in bubbly form. Linear interpolation in mass flux is used in the range 2 000 to 2 700. In the slug regime the interfacial drag is volume averaged between the slug and the trailing bubbles with a constant drag coefficient of 0.44 used for the slug.

In the vapor fraction range of 0.75 to 1.0, an annular or annular mist regime is employed. An approximation to the Wallis entrainment correlation[19] is used to estimate the fraction of liquid that is in droplet form:

$$E = 1 - \exp[-\ 0.125(J_g' - 2.1)]\ , \tag{87}$$

where

$$J_g' = 10^4\ \alpha\ \frac{V_g\ \mu_g}{\sigma}\ \left(\frac{\rho_g}{\rho_\ell}\right)^{\frac{1}{2}}\ .$$

The remainder of the liquid is in a film or sheet. The interfacial shear and

heat transfer are volume averages of the film and droplet relations in the annular mist regime. The wetted surface area of the mesh cell is determined from the rod or slab heat transfer area in the cell and that portion of the geometric flow area which is blocked off. If the cell is in a region devoid of any structure, the geometric surface area is employed as a scaling factor. This is, of course, artificial but in a realistic PWR simulation very few, if any, of the mesh cells are completely free of metal structure. The total interfacial surface area is determined by the sum of the areas contained in the wetted film and the droplets. A critical Weber number equal to 5 for the drops is used with a calculation procedure that is similar to that for bubbly flow. This value of the Weber number is appropriate for accelerating drops. For those cases where sensitivity to We_d was tested, the results were not strongly influenced by We_d in the range $2 \leq We_d \leq 12$. The liquid side heat transfer coefficient is simply

$$h_{i\ell} = c\, k_\ell / D_d \ , \tag{88}$$

where c, a constant, has been adjusted to drive the drops to equilibrium under a variety of flow conditions. In the present code, c = 15 000, which implies a thermal boundary layer in the drops that is about a thousandth of the drop diameter. In the film a correlation

$$Nu = 0.0073\ Re \tag{89}$$

is employed to predict $h_{i\ell}$. The Wallis annular flow model[19] determines the shear for a wavy film while the same drag correlations used for a bubble are employed if droplets exist. The droplet Reynolds number is defined as

$$Re_d = \frac{\rho_g V_{rd} D_d}{\mu_g} \ . \tag{90}$$

Since the actual relative velocity calculated is based on a shear that has been averaged between the film and drop correlations, a separate function[20] is used for V_{rd}:

$$V_{rd} = 1.4\ \alpha[9.8\ \sigma(\rho_\ell - \rho_g)/\rho_g^2]^{\frac{1}{4}} \ . \tag{91}$$

In the interpolated regime defined in Fig. 3, a linear interpolation in vapor fraction is made between the conditions that would exist if the vapor fraction were at 0.75 in the annular or annular-mist topology, and the conditions that would exist if the flow were in the bubbly or bubbly-slug regime at a void fraction of 0.5. This makes the correlation for the interfacial shear, interfacial heat transfer, and surface area a continuous function of vapor fraction, relative velocity, mass flux, and the various fluid thermodynamic and transport properties.

We now discuss the vapor side heat transfer coefficient and the liquid heat transfer coefficient during condensation. The vapor heat transfer coefficient is the simple function $h_{ig} = c$, where $c = 1 \times 10^4$. This implies that the rate for boiling or condensation is determined mainly by the liquid side coefficient with a vapor coefficient designed to drive the vapor toward the saturation temperature. The formulation Eqs. (10 and 11) for the total liquid heat transfer coefficient $h_{i\ell} A_i$ used for boiling seems to provide too high a coefficient during condensation. It is anticipated that a condensation rate based on a film model might be more appropriate. Therefore, for condensation the interfacial area is calculated from

$$A_i = (\text{vol}/\Delta z)c,$$

where the coefficient c accounts for a rough interface and is equal to 10. The specific heat transfer coefficient is the same as the film coefficient used in the annular boiling regime. This model has performed well for the subcooled Creare downcomer tests; it is admittedly simple and may be improved in future versions of the code if additional testing indicates that this is desirable.

B. Heat Transfer

Heat transfer analysis in the TRAC code consists of two essentially separate sections: conduction methods associated with calculation of the temperature fields in structural materials and fuel rods and convection methods which provide the interfacial boundary condition for heat transfer between structure and coolants. For simplicity and code efficiency, the conduction methods are separated by function: cylindrical geometries, slab geometries, and core fuel rod geometries. This is particularly useful for the fuel rod analysis, which is considerably more complex due to possible fuel-clad gap

changes, metal-water reaction, and quenching phenomena. The convective methods are contained in a single heat transfer correlation package which is available to all conduction modules.

1. Wall Heat Transfer

a. Cylindrical Geometry Heat Conduction

Subroutine CYLHT solves for the temperature field in ex-vessel components based on a one-dimensional radial finite difference approximation to the general conduction equation:

$$\frac{1}{r}\left[\frac{\partial}{\partial r}\left(r\,k\,\frac{\partial T}{\partial r}\right)\right] + q''' = \rho\, c_p \frac{\partial T}{\partial t} . \tag{92}$$

The finite difference equations are solved in a conservative manner, sequencing from left to right, where the left boundary corresponds to the smallest radius. Nodal points are positioned on material interfaces and material properties are evaluated between nodes. The finite difference equations are given below.

For the left or innermost (i=1) node,

$$-\left[\frac{r_{3/2}\,k_1}{\Delta r_1} + \frac{1}{2}\left(r_i\,\Delta r_i + \frac{\Delta r_1^2}{4}\right)\frac{(\rho\, c_p)_1}{\Delta t} + f_{ss}\, r_1 (h_\ell + h_g)\right] T_1^{n+1}$$

$$+ \frac{r_{3/2}\,k_1}{\Delta r_1} T_2^{n+1} = -\frac{1}{2}(r_1\,\Delta r_1 + \frac{\Delta r_1^2}{4})\left[\frac{(\rho c_p)_1}{\Delta t} T_1^n + q'''\right]$$

$$+ r_1\left[h_\ell (f_t\, T_1^n - T_\ell^{n+1}) + h_g (f_t\, T_1^n - T_g^{n+1})\right] , \tag{93}$$

where

f_{ss} = steady-state flag (1 for steady-state calculation, 0 otherwise),

f_t = transient flag (1 for transient calculation, 0 otherwise),

Δr_i = $r_{i+1} - r_i$,

Δt = time step size, and

n = time step level.

The boundary condition at the leftmost surface is:

$$-\,k \left.\frac{dT}{dr}\right|_{i=1} = h_\ell (T_\ell - T_1) + h_g (T_g - T_1) . \tag{94}$$

Note that for a steady-state calculation ($f_{ss} = 1$ and $f_t = 0$) a fully implicit form is used. Under transient conditions ($f_{ss} = 0$ and $f_t = 1$) a semi-implicit form is obtained. The semi-implicit scheme ensures conservation of energy between conduction and fluid dynamics solutions by forcing both methods to use identical surface heat fluxes as boundary conditions.

The finite difference equations for all interior nodes ($1 < i < N$) are:

$$\frac{r_{i-\frac{1}{2}}\, k_{i-1}}{\Delta r_{i-1}}\, T_{i-1}^{n+1} - \left\{ \frac{r_{i-\frac{1}{2}}\, k_{i-1}}{\Delta r_{i-1}} + \frac{r_{i+\frac{1}{2}}\, k_i}{\Delta r_i} + \frac{1}{2\Delta t} \left[(r_i\, \Delta r_{i-1} - \frac{\Delta r_{i-1}^2}{4})\, (\rho c_p)_{i-1} \right.\right.$$

$$\left.\left. + (r_i\, \Delta r_i + \frac{\Delta r_i^2}{4})\, (\rho c_p)_i \right] \right\} T_i^{n+1} + \frac{\Delta r_{i+\frac{1}{2}}\, k_i}{\Delta r_i}\, T_{i+1}^{n+1} = -\frac{1}{2}(r_i\, \Delta r_{i-1} - \frac{\Delta r_{i-1}^2}{4})$$

$$\cdot \left[\frac{(\rho c_p)_{i-1}}{\Delta t}\, T_i^n + q''' \right] - \frac{1}{2}(r_i\, \Delta r_i + \frac{\Delta r_i^2}{4}) \left[\frac{(\rho c_p)_i}{\Delta t}\, T_i^n + q''' \right] . \qquad (95)$$

For the right or outermost node ($i = N$),

$$\frac{r_{N-\frac{1}{2}}\, k_{N-1}}{\Delta r_{N-1}}\, T_{N-1}^{n+1} - \left[\frac{r_{N-\frac{1}{2}}\, k_{N-1}}{\Delta r_{N-1}} + \frac{1}{2}(r_N\, \Delta r_{N-1} - \frac{\Delta r_{n-1}^2}{4})\, \frac{(\rho c_p)_{N-1}}{\Delta t} \right.$$

$$\left. + f_{ss}\, r_N (h_\ell + h_g) \right] T_N^{n+1} = -\frac{1}{2}(r_N\, \Delta r_{N-1} - \frac{\Delta r_{N-1}^2}{4}) \left[\frac{(\rho c_p)_{N-1}}{\Delta t}\, T_N^n + q''' \right]$$

$$+ r_N \left[h_\ell (f_t\, T_N^n - T_\ell^{n+1}) + h_g (f_t\, T_N^n - T_g^{n+1}) \right] , \qquad (96)$$

where the boundary condition at the outermost surface is:

$$-k \left.\frac{dT}{dr}\right|_{i=N} = h_\ell (T_N - T_\ell) + h_g (T_N - T_g) . \qquad (97)$$

The equations above result in a three-stripe diagonal matrix, which is solved by using a Gaussian elimination method.

The user may choose a lumped parameter solution in place of the multinode

method outlined above by setting input parameter NODES=1. The finite difference equation for this option is:

$$T^{n+1} = \left\{ \frac{1}{2}\left(2\Delta r + \frac{\Delta r^2}{R_i}\right)\left(\frac{\rho c_p}{\Delta t} T^n + q'''\right) + h_{\ell i}\left(T_{\ell i}^{n+1} - f_t\, T^n\right) + h_{gi}\left(T_{gi}^{n+1} - f_t\, T^n\right) \right.$$

$$\left. - \left(1 + \frac{\Delta r}{R_i}\right)\left[h_{\ell o}\left(f_t\, T^n - T_{\ell o}^{n+1}\right) + h_{go}\left(f_t\, T^n - T_{go}^{n+1}\right)\right] \right\}$$

$$\Bigg/ \left\{ \frac{1}{2}\left(2\Delta r + \frac{\Delta r^2}{R_i}\right)\left(\frac{\rho c_p}{\Delta t}\right) + f_{ss}\left[h_{\ell i} + h_{gi} + \left(1 + \frac{\Delta r}{R_i}\right)\left(h_{\ell o} + h_{go}\right)\right] \right\} \qquad (98)$$

where the subscripts i and o refer to inner and outer radius quantities, respectively, and $\Delta r = R_o - R_i$.

b. Slab Geometry Heat Conduction

Subroutine SLABHT solves for the lumped parameter temperature of a slab of arbitrary configuration. For a given user-supplied mass (m) and surface area (A), an effective thickness ($\bar{x}$) is calculated for use in the conduction solution:

$$\bar{x} = \frac{m}{\rho A} . \qquad (99)$$

The temperature solution is:

$$T^{n+1} = \left[\frac{\rho c_p}{\Delta t}\bar{x}\, T^n - h_\ell\left(f_t\, T^n - T_\ell^{n+1}\right) - h_g\left(f_t\, T^n - T_g^{n+1}\right)\right]$$

$$\Bigg/ \left[\frac{\rho c_p}{\Delta t}\bar{x} + f_{ss}\left(h_\ell + h_g\right)\right] . \qquad (100)$$

The slab heat transfer solution is available to the vessel component only.

2. Core Heat Transfer

The core heat transfer package analyzes, on a rod by rod basis, four important processes which contribute to the resultant predictions of cladding temperature versus time: 1) thermal conduction (including axial conduction, decay energy, and metal-water reaction heat sources), 2) dynamic fuel-clad gap conductance, 3) metal-water reaction rates, and 4) reflood heat transfer effects. Figure 4 illustrates schematically the calculational strategy used in

the code for the core heat transfer analysis. For each core fluid computational cell there is an associated average fuel rod, a hot rod (which does not feed back to the fluid solution), and provision for a user-defined heat slab.

a. Fuel Rod Model

The fuel rod conduction solution method is similar to that described in the cylindrical geometry section. The major differences pertain to treatment of boundary conditions, user selection of composite material structure, and provision for spatial and time-dependent internal heat generation. Finite difference fuel rod conduction equations are given below.

For the innermost fuel pellet node (i=1), the finite difference equation is

$$-\left[\frac{r_{3/2}\,k_1}{\Delta r_1}+\frac{1}{2}\left(r_1\,\Delta r_1+\frac{\Delta r_1^2}{4}\right)\frac{(\rho c_p)_1}{\Delta t}\right]T_1^{n+1}+\frac{r_{3/2}\,k_1}{\Delta r_1}\,T_2^{n+1}$$

$$=-\frac{1}{2}\left(r_1\,\Delta r_1+\frac{\Delta r_1^2}{4}\right)\left[\frac{(\rho c_p)_1}{\Delta t}\,T_1^n+q_1'''^{,n+1}\right] \tag{101}$$

with the boundary condition

$$-rk\left.\frac{dT}{dr}\right|_{i=1}=0 \tag{102}$$

at the inner surface. For interior nodes ($1 < i < NF$) in the fuel pellet,

$$\frac{r_{i-\frac{1}{2}}\,k_{i-1}}{\Delta r_{i-1}}\,T_{i-1}^{n+1}-\left\{\frac{r_{i-\frac{1}{2}}\,k_{i-1}}{\Delta r_{i-1}}+\frac{r_{i+\frac{1}{2}}\,k_i}{\Delta r_i}+\frac{1}{2\Delta t}\left[\left(r_i\,\Delta r_{i-1}-\frac{\Delta r_{i-1}^2}{4}\,(\rho c_p)_{i-1}\right)\right.\right.$$

$$\left.\left.+\left(r_i\,\Delta r_i+\frac{\Delta r_i^2}{4}\right)(\rho c_p)_i\right]\right\}T_i^{n+1}+\frac{r_{i+\frac{1}{2}}\,k_i}{\Delta r_i}\,T_{i+1}^{n+1}$$

$$=-\frac{1}{2}\left\{\left(r_i\,\Delta r_{i-1}-\frac{\Delta r_{i-1}^2}{4}\right)\left[\frac{(\rho c_p)_{i-1}}{\Delta t}\,T_i^n+q_{i-1}'''^{,n+1}\right]\right.$$

$$\left.+\left(r_i\,\Delta r_i+\frac{\Delta r_i^2}{4}\right)\left[\frac{(\rho c_p)_i}{\Delta t}\,T_i^n+q_i'''^{,n+1}\right]\right\}, \tag{103}$$

where NF is the number of nodes in the fuel.

The gap that exists between the fuel and the cladding in fuel rods is treated by explicit noding on fuel and clad surfaces and a dynamic heat transfer coefficient between these nodes. Stored energy and internal heat generation in the gap region is neglected. The finite difference equation for the outermost fuel pellet node (i=NF) is:

$$\frac{r_{NF-\frac{1}{2}}\, k_{NF-1}}{\Delta r_{NF-1}}\, T^{n+1}_{NF-1} - \left[\frac{r_{NF-\frac{1}{2}}\, k_{NF-1}}{\Delta r_{NF-1}} + r_{NF}\, h_{gap} + \frac{1}{2}\left(r_{NF}\, \Delta r_{NF-1} - \frac{\Delta r^2_{NF-1}}{4}\right) \frac{\left(\rho c_p\right)_{NF-1}}{\Delta t} \right] T^{n+1}_{NF} + r_{NF}\, h_{gap}\, T^{n+1}_{NF+1}$$

$$= -\frac{1}{2}\left(r_{NF}\, \Delta r_{NF-1} - \frac{\Delta r^2_{NF-1}}{4}\right) \left[\frac{\left(\rho c_p\right)_{NF-1}}{\Delta t}\, T^{n}_{NF} + q'''^{\,n+1}_{NF-1} \right] \qquad (104)$$

and the boundary condition at the outer pellet surface is

$$-k \left.\frac{dT}{dr}\right|_{i=NF} = h_{gap}\left(T_{NF} - T_{NF+1}\right) . \qquad (105)$$

In the cladding region, the internal heat generation rate is redefined to include metal-water reaction and axial conduction heat sources when appropriate. These additional heat source terms are computed by assuming that the cladding is one region. A more detailed discussion of these heat source terms is given in subsequent sections.

For the innermost cladding node (i=NF+1), the finite difference equation is

$$r_{NF+1}\, h_{gap}\, T^{n+1}_{NF} - \left[r_{NF+1}\, h_{gap} + \frac{r_{NF+3/2}\, k_{NF+1}}{\Delta r_{NF+1}} + \frac{1}{2}\left(r_{NF+1}\, \Delta r_{NF+1} + \frac{r^2_{NF+1}}{4}\right) \frac{\left(\rho c_p\right)_{NF+1}}{\Delta t} \right] T^{n+1}_{NF+1} + \frac{r_{NF+3/2}\, k_{NF+1}}{\Delta r_{NF+1}}\, T^{n+1}_{NF+2}$$

$$= -\frac{1}{2}\left(r_{NF+1}\, \Delta r_{NF+1} + \frac{\Delta r^2_{NF+1}}{4}\right) \left[\frac{\left(\rho c_p\right)_{NF+1}}{\Delta t}\, T^{n}_{NF+1} + q'''^{\,n+1}_{NF+1} \right] . \qquad (106)$$

The boundary condition at the cladding inner surface is identical to Eq. (105) and the finite difference equation for interior cladding nodes [(NF+1)< i < N] is identical to Eq. (103). For the outermost cladding node (i=N), the finite difference equation is

$$\frac{r_{N-\frac{1}{2}}\, k_{N-1}}{\Delta r_{N-1}}\, T_{N-1}^{n+1} - \left[\frac{r_{N-\frac{1}{2}}\, k_{N-1}}{\Delta r_{N-1}} + \frac{1}{2}\left(r_N\, \Delta r_{N-1} - \frac{\Delta r_{N-1}^2}{4}\right) \frac{(\rho c_p)_{N-1}}{\Delta t} + f_{ss}\, r_N (h_\ell + h_g) \right] T_N^{n+1}$$

$$= -\frac{1}{2}\left(r_N\, \Delta r_{N-1} - \frac{\Delta r_{N-1}^2}{4}\right)\left[\frac{(\rho c_p)_{N-1}}{\Delta t}\, T_N^n + q'''^{\,n+1}_{N-1} \right]$$

$$+ r_N \left[h_\ell (f_t\, T_N^n - T_\ell^{n+1}) + h_g (f_t\, T_N^n - T_g^{n+1}) \right] \qquad (107)$$

with the boundary condition at the outer surface given by

$$-k \left.\frac{dT}{dr}\right|_{i=N} = h_\ell (T_N - T_\ell) + h_g (T_N - T_g) \ . \qquad (108)$$

b. Dynamic Gap Conductance

This model is currently under development and exists in this initial version of the code in a very rudimentary form. Subroutine GAPHT calculates the gap heat transfer coefficient (h_{gap}) as a function of three components including gap gas conductance, fuel-clad interfacial contact, and fuel-clad thermal radiation:

$$h_{gap} = h_{gas} + h_{contact} + h_{radiation} \ , \qquad (109)$$

where

$$h_{gas} = \frac{k_{gas}}{\Delta r_{gap} + \delta} \ , \qquad (110)$$

$$h_{radiation} = \sigma\, F (T_f^4 - T_c^4)/(T_f - T_c) \ , \qquad (111)$$

and

$$F = \frac{1}{\frac{1}{\varepsilon_f} + \frac{R_f}{R_c}\left(\frac{1}{\varepsilon_c} - 1\right)} \quad . \tag{112}$$

In the present context, subscripts f and c refer to fuel and clad, respectively, and σ is the Stefan-Boltzman constant. A value of 4.4×10^{-6}m is used for δ, the mean fuel surface roughness.[21]

The gap gas conductivity evaluation methods are outlined in the material properties section. Presently, the interfacial contact component is set to zero. The developmental effort in this area will draw upon the modeling experience of the MATPRO, FRAP-S, FRAP-T, and GAPCON codes.[21-24]

c. Metal-Water Reaction

When sufficiently high temperatures are reached by Zircaloy in a steam environment, an exothermic reaction may occur which will influence the peak cladding temperatures attained. The zirconium-steam reaction equation is:

$$Z_r + 2H_2O \rightarrow ZrO_2 + 2H_2 + \text{Heat.} \tag{113}$$

In the presence of sufficient steam, the reaction rate equation of Ref. 25 is assumed to be valid:

$$-\frac{dr}{dt} = \frac{1.126 \times 10^{-6}}{(R_o - r)} \exp\left(-\frac{18\,062}{T}\right) \tag{114}$$

where

r = reacting surface radius (m) and

R_o = clad outer radius (m).

The method outlined in Ref. 26 is used to calculate the zirconium-oxide penetration depth and associated heat source. The mass of zirconium (m_{Zr}) consumed by the reaction in one time step is:

$$m_{Zr} = \pi \rho_{Zr} \left[(r^n)^2 - (r^{n+1})^2 \right] \quad . \tag{115}$$

Equation (114) is used to calculate r^{n+1}, yielding:

$$r^{n+1} = R_o - \left[(r^n)^2 + 2.252 \times 10^{-6} \Delta t \exp(-1.8062 \times 10^4/T) \right]^{\frac{1}{2}} \quad . \tag{116}$$

The heat source (q'''_{mw}) added to the conduction equations, assuming a one-

region clad, is:

$$q'''_{mw} = 6.513 \times 10^6 \, m_{Zr} \left| \Delta t (R_0^2 - R_i^2) \right|^{-1} , \tag{117}$$

where R_i is the inner clad radius, and 6.513×10^6 J/kg corresponds to the energy release per kilogram of zirconium oxidized.

d. Reflood Heat Transfer

Experimental studies simulating the reflood stage of a postulated loss-of-coolant accident in an LWR indicate that detailed modeling methods are necessary to successfully predict cladding temperature-time histories. To achieve that objective, a synthesized reflood heat transfer methodology is available as a user option in the code. The methodology treats quench front initialization, quench front propagation, and heat transfer by conduction and convection in a consistent, integral package.

Limitations on computer running times require TRAC fluid cells in the core region to be on the order of a half meter in length in the axial direction. However, under reflood conditions, signficiant variations in transport processes may take place in a much shorter axial length. To allow improved modeling of these processes, without incurring prohibitive computer costs, a renodalization of the fuel rod conduction calculation is available. Based on user-supplied input, the coarse axial mesh corresponding to the fluid cell is subdivided into an arbitrary number of fine-mesh intervals. The radial conduction solution is then applied in each fine-mesh interval.

Material properties and gap heat transfer coefficient continue to be based on coarse-mesh values, but heat transfer coefficients are now evaluated for each fine mesh. To better approximate actual temperature profiles, a temperature interpolation scheme is used to initially fill the fine-mesh temperature fields. A Lagrangian interpolation scheme[27] is used:

$$T(z) = \sum_{i=0}^{n} \ell_i \, T_i , \tag{118}$$

where

$$\ell_i = \frac{(z-z_o) \ \ldots \ (z-z_{i-1})(z-z_{i+1}) \ \ldots \ (z-z_n)}{(z_i-z_o) \ \ldots \ (z_i-z_{i-1})(z_i-z_{i+1}) \ \ldots \ (z_i-z_n)} \tag{119}$$

and T_i are the coarse-mesh temperatures. The quadratic equation obtained by fitting three coarse-mesh temperatures at a time yields the fine-mesh profile.

To ensure conservation of energy, and taking advantage of constant properties within a coarse mesh, the fine-mesh temperatures (T_j) are normalized as follows:

$$T_j = N_f T_i \bar{T}_j \Big/ \sum_{j=1}^{N_f} \bar{T}_j \quad , \tag{120}$$

where

N_f = number of axial fine meshes in coarse mesh i,

$\bar{T}_j = az_j^2 + bz_j + c$,

and a, b, and c are obtained from Eq. (119).

The second procedure used in the reflood initialization is a search to locate quench fronts. Rather than assume the core is dry at the beginning of reflood, which may not be the case, a pattern search of each average rod is made for the combined condition of clad surface temperature less than the Leidenfrost temperature and sufficient liquid available to form a film on the rod. Only two quench fronts per rod are accounted for: a falling film from the top and a bottom quench front.

The motion of a quench front on a hot surface is a complex function of axial conduction, radial convection both ahead and behind the front, internal heat generation, and heat transfer to the material. Since axial conduction of heat from ahead of the front to the quenched side occurs on a length scale of a centimeter or less, and typical fuel rods are several meters long, analytical methods have been developed to approximate quench front motion without resorting to costly two-dimensional conduction solutions.[28,29] A correlation which approximates the one- and two-dimensional solutions of Refs. 28 and 29 is used for the quench front velocity V_{qf}:[30]

$$V_{qf} = \frac{k}{\rho c_p \delta} \left[\bar{B}(1 + 0.40\ \bar{B}) \right]^{1/2} , \tag{121}$$

where

$$\bar{B} = B/\bar{T}^2$$

$$B = h\delta/k$$

$$\bar{T} = \theta_o^{\frac{1}{2}}/(1-\theta_o)$$

$$\theta_o = (T_w - T_o)/(T_w - T_s)$$

and

h = film heat transfer coefficient,

T_o = Leidenfrost temperature,

T_w = wall temperature an infinite distance ahead of the quench front, and

δ = mean fuel surface roughness.

There is considerable ambiguity as to the proper definition of the Leidenfrost temperature.[28] The value currently used in TRAC is:

$$T_o = T_s + 100 \text{ (K)},$$

which is in general agreement with values used in most quench front propagation models. For most cases the fine-mesh axial spacing will be much greater than the few millimeters over which axial conduction is important. Therefore, the T_w used in calculating the quench velocity is that of the fine-mesh interval ahead of the quench front. Since a detailed radial conduction solution, including convective heat transfer at the clad surface, is calculated for all fine mesh intervals, precursory cooling is reflected in the lower wall temperature ahead of the quench front, resulting in a higher value of the quench velocity. When the temperature ahead of the quench front is less than the Leidenfrost temperature, and liquid is present, the front position is automatically advanced. This ensures compatibility with the radial conduction calculation, which for this case would indicate a strong convective precooling process characteristic of high flooding rates and subcooling. The method outlined above is used for bottom flooding and falling film, which is in agreement with the observation that the physics of both quenching processes are identical, differing only with respect to boundary conditions.[29]

The reflood stage of an accident sequence may not be a steady fill process. Experiments indicate that bottom flooding by gravity fill of the

downcomer region is accompanied by flow oscillations similar to those in a manometer. Under these conditions, liquid may withdraw from the core region, resulting in quench fronts also retreating from previous positions. The case wherein the quench front retreats probably corresponds to high local void fraction, independent of average liquid velocity direction. At low void fractions, corresponding to an inverted annular flow pattern, sufficient liquid is available to allow continued quench front motion upward into the core, even if the liquid velocity is down out of the core.

If the liquid velocity is down in the core region and the void fraction is greater than 0.95, the following analysis is used to diminish the quench front position. The flow regime is considered to be annular and deposition and entrainment are neglected. Applying a heat and mass balance to the film, assuming constant film thickness, yields:

$$F = \frac{q'' \, \Delta t}{h_{\ell g} \, \delta \rho_{\ell}} \quad , \tag{122}$$

where

F = fractional decrease in quench front position per fine-mesh cell,

q'' = heat flux behind quench front, and

δ = film thickness = $D(1-\alpha)/4$.

The rationale for using a cutoff value of 0.95 in the vapor fraction is that if a greater quantity of liquid is present, then the quench front may progress independent of the liquid flow direction. For a falling film quench front, progress is assumed to always be downward into the core, unless the void fraction equals unity, whereupon it is stopped. An explicit momentum and mass balance is not included in the falling film analysis.

To ensure consistency beween the normal conduction and convection methods and the imposed quench front position, the axial conduction associated with propagating a quench front a certain distance per time step is treated as a source term in the fine-mesh radial conduction solution. Figure 5 illustrates the method used. The clad is assumed to be insulated from the fuel only in computing the axial heat transfer. Fuel-to-clad heat transfer ahead of the quench front affects the clad temperature, which determines the quench front velocity.

The volumetric heat source terms for the node ahead (i+1) and behind (i) the quench front are:

$$q'''_{i+1} = -\rho c_p \Delta T V_{qf} \quad (123)$$

and

$$q'''_i = \rho c_p \Delta T V_{qf} f , \quad (124)$$

where

$$f = \frac{\Delta z_{i+1}}{\Delta z_i} \left[\frac{(R_o^2 - R_i^2)_{i+1}}{(R_o^2 - R_i^2)_i} \right] , \text{ and}$$

$$\Delta T = T_{i+1} - T_s .$$

The correction factor, f, is unity except when variable axial mesh spacing is chosen or cladding radial deformation is calculated.

The liquid heat transfer coefficient (h_ℓ) is modified to reflect the partial quenching of a cell:

$$h_\ell = F_q \frac{(T_{i-1} - T_s)}{(T_i - T_s)} h_{film} + (1 - F_q) \frac{(T_{i+1} - T_s)}{(T_i - T_s)} h_{i+1} , \quad (125)$$

where

F_q = fraction of cell quenched and

h_{film} = maximum (h_{i-1}, 10,000).

The value of the heat transfer coefficient behind the quench front, h_{film}, is the maximum of either the radial heat transfer coefficient h_{i-1} (one cell behind the quench front) or 10,000 W/m^2 K. The latter value is based on an order of magnitude analysis of the FLECHT results.[31]

3. Heat Transfer Correlations

Subroutine HTCOR contains a library of heat transfer correlations that are accessible by all code component modules which perform heat transfer analyses. Based on local surface temperature, surface properties, and fluid conditions, a generalized boiling curve is constructed from the correlation library. The curve is then referenced to obtain values for liquid and vapor heat transfer coefficients, wall temperature at the critical heat flux point, and heat transfer regime identification flag. Figure 6 illustrates schematically the boiling curve that is obtained. As local conditions change

the shape and slopes of the segments comprising the curve may change, but continuity of the curve is always maintained. This procedure ensures numerical stability as transitions in heat transfer regimes occur. Figure 7 illustrates, by use of a flow chart, the manner in which the heat transfer regimes are identified. The heat transfer regimes and correlations used are summarized in Table I.

a. Critical Heat Flux

The key points which anchor the boiling curve are the critical heat flux (CHF) and the minimum stable film boiling temperature. For ex-vessel components the user may select from three correlation options for the critical heat flux:

ICHF	Correlation
1	Zuber pool boiling/Biasi dryout correlations
2	Biasi dryout correlation only
3	Bowring correlation

Option ICHF=1 is recommended and is used in all vessel calculations.

During postulated loss-of-coolant accidents, an extremely wide range of flow conditions is encountered. At low flow rates, CHF is probably a pool boiling-type phenomenon, whereas at high flow rates, a dryout of the liquid film on the wall is probably the CHF mechanism. Since no single CHF model has been shown to accurately predict this range of conditions, a combination of models is necessary. At low flow rates (e.g., flow stagnation and reflood) the Zuber pool boiling correlation[32] is used:

$$q''_{CHF} = (1-\alpha)\ 0.131\ \rho_g\ h_{\ell g} \left[\frac{\sigma\, g(\rho_\ell - \rho_g)}{\rho_g^2} \right]^{1/4}, \tag{126}$$

where the factor $(1-\alpha)$ was recommended by Griffith[33] for low flow and countercurrent flow conditions. For high flow rates, the Biasi correlation[34] is used:

$$q''_{CHF} = \frac{1.883 \times 10^7}{D^n\, G^{1/6}} \left[\frac{f_p}{G^{1/6}} - x \right] \tag{127}$$

for low quality and

$$q''_{CHF} = \frac{3.78 \times 10^7}{D^n G^{0.6}} h_p (1-x) \qquad (128)$$

for high quality, where

$n = 0.4$ for $D \geq 1$ cm,

$n = 0.6$ for $D < 1$ cm

and

$$f_p = 0.724\ 9 + 0.099\ p \exp(-0.032p),$$

$$h_p = -1.159 + 0.149\ p \exp(-0.019p) + \frac{8.99p}{10+p^2},$$

D = rod diameter (cm),

G = mass flux ($g/cm^2 \cdot s$), and

p = pressure (bars).

As recommended by Collier,[6] Eq. (128) is used for mass fluxes less than 300 $kg/m^2 \cdot s$; otherwise the maximum of Eqs. (127) and (128) is used.

A criterion is necessary to distinguish between high and low flow conditions for both up and down flow. Following the recommendations of Bjornard and Griffith,[35] the Biasi correlation is used for mass fluxes greater than 100 $kg/m^2 \cdot s$ in up flow and greater than 600 $kg/m^2 \cdot s$ in down flow. The difference in mass flux values reflects the observed reduction in CHF in down flow, attributed to higher local void fraction for a given set of flow conditions.

The Bowring correlation,[36] available to ex-vessel components, is a dryout correlation similar to the Biasi correlation:

$$q''_{CHF} = (A - B\, h_{\ell g}\, x)/C, \qquad (129)$$

where

$$A = 2.317(0.25\, h_{\ell g}\, DG)F_1/(1 + 0.0143\ F_2\, D^{\frac{1}{2}}\, G)$$

$$B = 0.25\, D\, G$$

$$C = 0.077\, F_3\, D\, G/[1 + 0.347\, F_4 (G/1356)^n]$$

$$n = 2.0 - 0.5\, p_R$$

$$p_R = 0.145\, p/10^5$$

and for

$\underline{p_R < 1}$,

$$F_1 = [p_R^{18.942} e^{20.890(1-p_R)} + 0.917]/1.917$$

$$F_1/F_2 = [p_R^{1.316} e^{2.444(1-p_R)} + 0.309]/1.309$$

$$F_3 = [p_R^{17.023} e^{16.658(1-p_R)} + 0.667]/1.667$$

$$F_4/F_3 = p_R^{1.649}$$

while for

$\underline{p_R > 1}$,

$$F_1 = p_R^{-0.368} e^{0.648(1-p_R)}$$

$$F_1/F_2 = p_R^{-0.448} e^{0.245(1-p_R)}$$

$$F_3 = p_R^{0.219}$$

$$F_4/F_3 = p_R^{1.649} \quad .$$

For most cases of interest, the Biasi and Bowring correlations give comparable results. The Biasi correlation is normally chosen as it is computationally more efficient.

The heat transfer selection logic is based on local wall surface temperature, hence the critical heat flux is converted to a CHF wall temperature:

$$T_{CHF} = T_s + q''_{CHF}/h_{NB} \quad , \tag{130}$$

where

h_{NB} = nucleate boiling heat transfer coefficient.

The value used for the nucleate boiling heat transfer coefficient is outlined in a following section.

b. Minimum Film Boiling Temperature

The minimum stable film boiling temperature is that value at which contact between liquid and a hot surface is prevented by vapor generation processes. For low pressures, the classic film boiling instability analysis has been successfully used by Berenson[37] to predict this temperature. Henry[38] modified that analysis to account for surface effects:

$$T_{MINHB} = T_{MINB} + 0.42(T_{MINB} - T_\ell)\left[\frac{h_{\ell g}}{c_{p\,w} DT_{MINB}}\left(\frac{k_\ell \rho_\ell c_{p\ell}}{k_w \rho_w c_{p\,w}}\right)^{1/2}\right]^{0.6}, \quad (131)$$

where Berenson's formula is:

$$T_{MINB} = T_s + 0.127 \frac{\rho_\ell h_{\ell g}}{k_g}\left[\frac{g(\rho_\ell-\rho_g)}{\rho_\ell + \rho_g}\right]^{2/3}\left[\frac{\sigma}{g(\rho_\ell-\rho_g)}\right]^{1/2}\left[\frac{\mu_g}{g(\rho_\ell-\rho_g)}\right]^{1/3}. \quad (132)$$

At higher pressures, the homogeneous nucleation mechanism[39] appears to dominate. Bjornard and Griffith[35] recommend Henry's modification to the Berenson formula be adopted also for the homogeneous nucleation phenomena:

$$T_{MINHN} = T_{HN} + (T_{HN} - T_\ell)\left[\frac{k_\ell \rho_\ell c_{p\,\ell}}{k_w \rho_w c_{p\,w}}\right]^{1/2}, \quad (133)$$

where T_{HN} is the homogenous nucleation temperature. T_{HN} is a weak function of pressure and varies from 580 K at atmospheric pressure to the critical temperature at the critical pressure. The minimum of Eqs. (131) and (133) is chosen as the minimum stable film boiling temperature. The corresponding minimum film boiling heat flux is:

$$q''_{MIN} = h_{FB}(T_{MIN} - T_s), \quad (134)$$

where the film boiling heat transfer coefficient h_{FB} is defined in a later section.

c. Heat Transfer Coefficients

Heat transfer coefficients are given below for the regimes identified

in Fig. 7. In the regime identified as forced or natural convection to single-phase liquid (i=1), the maximum of either a laminar correlation,[7]

$$h_\ell = 4.0\ k/D \tag{135}$$

or a turbulent (Dittus-Boelter) correlation,[40]

$$h_\ell = 0.023 \frac{k_\ell}{D} \left(\frac{\rho_\ell V_\ell D}{\mu_\ell} \right)^{0.8} \left(\frac{\mu_\ell c_{p\ell}}{k_\ell} \right)^{0.4} \tag{136}$$

is used.

For nucleate boiling or forced convection vaporization (i=2), the Chen correlation[41] is used:

$$h = 0.023 \frac{k}{D} \left(\frac{\rho_\ell V_\ell D}{\mu_\ell} \right)^{0.8} \left(\frac{\mu_\ell c_{p\ell}}{k_\ell} \right)^{0.4} F$$

$$+ 0.00122 \frac{k_\ell^{0.79}\ c_{p\ell}^{0.45}\ \rho_\ell^{0.49}}{\sigma^{0.5}\ \mu_\ell^{0.29}\ h_{\ell g}^{0.24}\ \rho_g^{0.24}} (T_w - T_s)^{0.24} (p_w - p)^{0.75} S , \tag{137}$$

where P_w is the saturation pressure corresponding to the wall temperature, and F and S are functions which are given in graphical form by Chen. The Reynolds number factor, F, and the suppression factor, S, can be expressed as:[35]

$$F = 1.0 \qquad \text{for } \chi_{TT}^{-1} \leq 0.10 ,$$

$$F = 2.35(\chi_{TT}^{-1} + 0.213)^{0.736} \qquad \text{for } \chi_{TT}^{-1} > 0.10 ,$$

where χ_{TT}^{-1}, the Lockhart-Martinelli factor, is

$$\chi_{TT}^{-1} = \left(\frac{x}{1-x}\right)^{0.9} \left(\frac{\rho_\ell}{\rho_g}\right)^{0.5} \left(\frac{\mu_g}{\mu_\ell}\right)^{0.1}$$

and

$$S = [1 + 0.12(Re_{tp})^{1.14}]^{-1} \qquad \text{for } Re_{tp} < 32.5 ,$$

$$S = [1 + 0.42(Re_{tp})^{0.78}]^{-1} \qquad \text{for } 32.5 \leq Re_{tp} < 70.0 ,$$

$$S = 0.1 \qquad \text{for } Re_{tp} \geq 70 ,$$

where

$$Re_{tp} = \frac{10^{-4}\, G(1-x)D}{\mu_\ell}\, F^{1.25} .$$

The correlation may be extended to subcooled liquid cases. Collier[6] recommends that F be set to unity and the single-phase Reynolds number be used in place of the two-phase value for those cases.

The main component of the transition boiling regime (i=3 in Fig. 7) heat transfer coefficient is determined by constructing a log-log interpolation of the boiling curve between the critical heat flux and minimum film boiling points:[42]

$$h_{TB} = \frac{q''_{CHF}}{(T_w - T_s)} \left(\frac{T_w}{T_{CHF}}\right)^{XPNT} , \tag{138}$$

where

$$XPNT = \frac{\log q''_{CHF} - \log q''_{MIN}}{\log T_{CHF} - \log T_{MIN}} .$$

To maintain continuity, the film boiling and radiation components are included in the final form used by the code:

$$h_\ell = (1-\alpha)\,(h_{TB} + h_{RAD}) \tag{139}$$

and

$$h_g = \frac{(T_w - T_{CHF})}{(T_w - T_{MIN})} \left[(1-\alpha)\, h_{FB} + \alpha h_{FC}\right] , \tag{140}$$

where h_{RAD}, h_{FB}, and h_{FC} are defined below.

For film boiling (i=4), the liquid and vapor heat transfer coefficients are given by,

$$h_\ell = (1-\alpha)\,(h_{TB} + h_{RAD}) \tag{141}$$

and

$$h_g = (1-\alpha)\, h_{FB} + \alpha h_{FC} . \tag{142}$$

The radiation heat transfer coefficient is based on Bromley's[43] analysis:

$$h_{RAD} = \sigma F(T_w^4 - T_\ell^4)/(T_w - T_\ell), \tag{143}$$

where

$$F = \frac{1}{\frac{1}{\varepsilon} + \frac{1}{\alpha} - 1},$$

ε = emissivity of the wall, and

α = absorptivity of the fluid.

For cases where liquid is present, radiation-to-liquid is the dominant mode and radiation-to-vapor is neglected.

Based on experiments investigating film boiling on vertical cylinders, Bailey[44] recommended Bromley's[43] film boiling analysis, which was originally obtained from horizontal cylinders:

$$h_{FB} = 0.62 \left[\frac{k_g^3 (\rho_\ell - \rho_g) g \, h'_{\ell g}}{\mu_g (T_w - T_s) \lambda} \right]^{1/4}, \tag{144}$$

where

$$\lambda = 2\pi \left[\frac{\sigma}{g(\rho_\ell - \rho_g)} \right]^{1/2}$$

and the latent heat of vaporization is modified as suggested by Kutateladze:[45]

$$h'_{\ell g} = h_{\ell g} + 0.5 \, c_{p,g} (T_w - T_s) .$$

The forced convection component is based on Dougall and Rohsenow's[46] modification to the Dittus-Boelter equation:

$$h_{FC} = 0.023 \frac{k_g}{D} \left\{ \frac{\rho_g [\alpha V_g + (1-\alpha) V_\ell] D}{\mu_g} \right\}^{0.8} \left[\frac{\mu_g \, c_{p,g}}{k_g} \right]^{0.4}, \tag{145}$$

where the Reynolds number is modified to reflect the volumetric flow rate of the two-phase mixture.

For the regime identified as forced or free convection to single-phase vapor (i=6 in Fig. 7), the maximum of either the McAdams free convection correlation,[47]

$$h_g = 0.13 \frac{k_g}{D} \left[\frac{D^3 \rho_g^2 g \beta (T_w - T_g)}{\mu_g^2} \right]^{1/3} \left[\frac{\mu_g c_{p,g}}{k_g} \right]^{1/3}, \tag{146}$$

where, assuming a perfect gas,

$$\beta = 1/T_g,$$

or a turbulent flow (Dittus-Boelter) correlation,[40]

$$h_g = 0.023 \frac{k_g}{D} \left(\frac{\rho_g V_g D}{\mu_g} \right)^{0.8} \left(\frac{\mu_g c_{p,g}}{k_g} \right)^{0.4}, \tag{147}$$

is used.

For forced convection to two-phase mixtures (regime i=7), the maximum of a laminar flow correlation and a turbulent flow correlation is used. The laminar flow correlation[7] is

$$h_\ell = 4.0 \frac{k_{tp}}{D}, \tag{148}$$

and the turbulent flow correlation[40] is

$$h_\ell = 0.023 \frac{k_{tp}}{D} Re_{tp}^{0.8} \left(\frac{\mu_\ell c_{p,\ell}}{k_\ell} \right)^{0.4}. \tag{149}$$

The two-phase mixture properties are defined by

$$y_{tp} = \frac{1}{\frac{x}{y_g} + \frac{1-x}{y_\ell}},$$

and the two-phase Reynolds number is

$$Re_{tp} = \frac{G D}{\mu_{tp}}.$$

For low flow rates a stratified flow regime exists, which is identified as the horizontal film condensation regime (i=11) in Fig. 7. The Chato[48]

modification of the Nusselt theory of film condensation, as reported by Collier,[36]

$$h_\ell = 0.296 \left[\frac{\rho_\ell (\rho_\ell - \rho_g) g \, h_{\ell g} \, k_\ell^3}{D \, \mu_\ell (T_s - T_w)} \right]^{1/4} , \tag{150}$$

or Eq. (152) is used in this regime. The correlation chosen is that which yields the larger value for h_ℓ.

For the vertical film condensation regime (i=12), the modification to the Nusselt theory of film condensation suggested by Collier[6] is used:

$$h_\ell = 1.132 \left[\frac{\rho_\ell (\rho_\ell - \rho_g) g \cos\theta \, h_{\ell g} \, k_\ell^3}{D \, \mu_\ell (T_s - T_w)} \right]^{1/4} , \tag{151}$$

where θ is the angle of inclination from the vertical direction. If Eq. (152) yields a larger value, it is used instead of Eq. (151).

The correlation of Carpenter and Colburn,[49] which accounts for interfacial shear effects of the vapor stream, is used in the turbulent film condensation regime (i=13):

$$h_\ell = 0.065 \frac{k_\ell \rho_\ell^{\frac{1}{2}}}{\mu_\ell} \left[\frac{\mu_\ell c_{p_\ell}}{k_\ell} \right]^{1/2} \tau_i^{\frac{1}{2}} , \tag{152}$$

where the interfacial shear, τ_i, is

$$\tau_i = \frac{0.046}{\left(\frac{\rho_g V_g D}{\mu_g} \right)} \left(\frac{\rho_g V_g^2}{2} \right) .$$

C. Reactor Kinetics

Power generation in the reactor core during the course of a problem is calculated by the RKIN subroutine. Two options are provided by specifying the method of calculation. The first method is simply a table lookup of power using the power versus time table supplied as input. Linear interpolation is used to extract values lying between entries in the table. In the second method, the power is determined from the solution of the point-reactor kinetics equations. These equations describe the time behavior of the core power level with the total reactivity acting as the controlling parameter.

The point-reactor kinetics equations include effects arising from the direct fission power and the decay of fission products. These equations are:

$$\frac{dP}{dt} = \frac{\beta}{\Lambda}(R - 1)P + \sum_{i=1}^{n} \lambda_i C_i \tag{153}$$

$$\frac{dC_i}{dt} = -\lambda_i C_i + \frac{\beta_i}{\Lambda} P \qquad (i = 1, 2, \ldots, n) \tag{154}$$

$$\frac{dH_j}{dt} = -\lambda_j^H H_j + E_j P \qquad (j = 1, 2, \ldots, m), \tag{155}$$

where

P = instantaneous total fission power,

β = total effective delayed neutron fraction,

Λ = prompt neutron generation time,

n = number of delayed neutron groups,

m = number of decay heat groups,

R = total reactivity in dollars,

λ_i = decay constant of delayed neutron group i,

β_i = effective delayed neutron fraction of delayed group i,

C_i = fission power of delayed neutron group i,

H_j = decay power of decay heat group j,

λ_j^H = decay constant of decay heat group j, and

E_j = effective energy fraction of decay heat group j.

Of interest is effective power generation rate or the heat actually deposited in the core. This is given by the expression,

$$P_{eff} = P\left(1 - \sum_{j=1}^{m} E_j\right) + \sum_{j=1}^{m} \lambda_j^H H_j \,. \tag{156}$$

Currently, the number of delayed neutron groups (n) and the number of decay heat groups (m) are fixed at 6 and 11, respectively. The constants appearing in the above equations are built into the code and are given in Tables II and III. These constants are identical to those used in the RELAP and RETRAN computer codes[26,50] and have been shown to produce results which closely follow the standard ANS decay heat curve.[50]

The point-reactor kinetics equations (153-155) are solved by numerical integration using a fourth-order accurate Runge-Kutta technique as modified by

Gill.[51,52] This technique is fast, highly accurate, and has excellent round-off error-limiting characteristics. However, because this is an explicit technique, the maximum time step size is governed by a stability condition,

$$\Delta t_{max} < 0.8 \frac{\Lambda}{\beta}/(|R| + 1), \tag{157}$$

which could limit the problem time step size, Δt_p. To prevent this from occurring in cases where $\Delta t_{max} < \Delta t_p$, the kinetics equations are integrated over k equal subintervals Δt_{rk}, where

$$k = INT[\Delta t_p/\Delta t_{max}] + 1 \tag{158}$$

and

$$\Delta t_{rk} = \Delta t_p/k \ . \tag{159}$$

In cases where Δt_{max} exceeds Δt_p, only one integration is performed using Δt_p.

A steady-state condition is assumed to exist at the beginning of a problem. Initial values for the delayed neutron and decay group contributions are given by

$$C_i(0) = \frac{\beta_i \ P(0)}{\lambda_i \Lambda} \tag{160}$$

and

$$H_j(0) = \frac{E_j \ P(0)}{\lambda_j^H} \ , \tag{161}$$

where P(0) is the initial specified power.

Parameters needed for the reactor kinetics option are P(0) and a table of reactivity versus time. A complete discussion of the input is given in the VESSEL module input specifications.

D. Overall Solution Strategy

Overall solution strategies for both transient and steady-state calculations are described in this section. Each time step in the transient calculation consists of several sweeps through all the components in the system. These sweeps, whose purpose is to converge the boundary data between com-

ponents, are called outer iterations. For each outer iteration, the thermal-hydraulic dynamic equations for the mesh cells within each component are solved by a sequence of inner iterations. Two types of steady-state calculations are available in TRAC. The first type has general applicability while the second type is used to obtain initial steady-state conditions for a PWR. Both steady-state calculations utilize the transient fluid dynamics and heat transfer routines.

1. Transient Solutions

a. Outer Iteration Strategy

Solution of the thermal-hydraulic flow equations for all components is controlled by subroutines TRANS and OUTER. TRANS controls the overall strategy while OUTER calls each component in turn.

At least three passes are made through each component. A prepass is made to update certain explicit information which must be available before any calls to DF1DS, DF1DI, or TF3D. The heat transfer coefficients and relative velocities are examples of information calculated on the prepass. The next pass or series of passes calls the basic hydrodynamic routines until the convergence criterion is met or the maximum number of iterations is exceeded. The recommended convergence criterion (EPSO) is between 10^{-3} and 10^{-4}, and the maximum outer iteration count (OUTMAX) should generally range between 10 and 20. The order in which OUTER calls the given components is determined by the IORDER input array. The only constraint on the order of iteration is that all of the one-dimensional components in the problem must be called before the three-dimensional vessel.

If the OUTER iteration process converges, a final pass is made to update the wall, slab, or rod heat conduction and to generate information required to begin the next time step. If the OUTER iteration fails to converge, the time step size is reduced by an order of magnitude (subject to the constraint that t must be greater than or equal to the minimum time step size indicated in the input) and another attempt to converge the OUTER iteration cycle is begun. After three unsuccessful attempts, the code shuts down after producing a dump and edit.

Programming details of the iteration procedure for transient solutions are given in Chap. VI, Sec. D. A flow schematic for the TRANS routine is given in Fig. 5 of that chapter.

b. One-Dimensional Inner Iteration Strategy

For a given call to a one-dimensional numerical hydrodynamics subroutine (DF1DS or DF1DI), the boundary conditions are treated as fixed and solutions for the new time flow variables within the component are updated by a standard Newton-Raphson procedure.

For the semi-implicit finite difference equations, the unknown variables are the new time values of pressure, void fraction, liquid temperature, and vapor temperature. Velocities are eliminated as unknowns by using the momentum equation to relate them to pressures. After substituting in these equations for velocities, along with the necessary thermodynamic relations, the remaining four equations per cell for mass and energy have the functional form:

$$f_j(p_{j-1}^{n+1}, p_j^{n+1}, p_{j+1}^{n+1}, \alpha_j^{n+1}, T_{g,j}^{n+1}, T_{\ell,j}^{n+1}) = 0, \tag{162}$$

where n is the time step index and j is the mesh cell index. The functions represented by f always have a nonlinear dependence on the variables p_j^{n+1}, $T_{g,j}^{n+1}$, $T_{\ell,j}^{n+1}$, and α_j^{n+1}; and a linear dependence on p_{j-1}^{n+1} and p_{j+1}^{n+1}. If successive approximations to the independent variables are generated by equations such as

$$(p_j^{n+1})^{k+1} = (p_j^{n+1})^k + \delta p_j^{k+1} , \tag{163}$$

where k is the inner iteration index, then the linearized approximation to Eq. (162) is

$$\frac{\partial f_j^k}{\partial p_{j-1}^{n+1}} \delta p_{j-1}^{k+1} + \frac{\partial f_j^k}{\partial p_j^{n+1}} \delta p_j^{k+1} + \frac{\partial f_j^k}{\partial p_{j+1}^{n+1}} \delta p_{j+1}^{k+1} + \frac{\partial f_j^k}{\partial \alpha_j^{n+1}} \delta \alpha_j^{k+1}$$
$$+ \frac{\partial f_j^k}{\partial T_{g,j}^{n+1}} \delta T_{g,j}^{k+1} + \frac{\partial f_j^k}{\partial T_{\ell,j}^{n+1}} \delta T_{\ell,j}^{k+1} = - f_j^k . \tag{164}$$

The collection of all such equations for all the mesh cells in the component forms a block tridiagonal linear system, which is inverted directly to obtain the corrections (δp, $\delta \alpha$, δT_g and δT_ℓ) for the new time variables.

The inner iteration procedure for the fully implicit method is similar to

the one just described. However, it is necessary to also treat the new time velocities as unknown variables.

c. Three-Dimensional Inner Iteration Strategy

Subroutine TF3D sets up the algebraic field equations and inverts each center matrix block in preparation for the iteration. In subroutine ITR1, the iteration for the pressure proceeds using a Gauss-Seidel iteration if the total number of mesh cells per level ($r-\theta$ plane) is greater than 8. If the number is less than 8, then a direct inversion for that level is performed with the z-direction elements handled in a Gauss-Seidel fashion. Any pipe source terms are treated using Gauss-Seidel for a given mesh cell.

The iteration in ITR1 is inexpensive and additional inner iterations (up to 10) are performed for each outer iteration until a tighter convergence tolerance than EPSO is reached (usually 10^{-6}). On the final pass, FF3D is called by VSSL3 to unfold the separate phase temperatures, the void fraction, and the velocities. THERMO is called by FF3D to update the densities, energies, and the various thermodynamic derivatives.

2. Steady-State Solutions

The TRAC steady-state capability is designed to provide time-independent solutions which may be of interest in their own right or as initial conditions for transient calculations. Two distinct calculations are available within the steady-state capability: the Generalized Steady-State calculation and the PWR Initialization calculation. The first is utilized to find the time-independent conditions of a system for arbitrary but fixed geometry and parameters. The second is utilized to adjust certain loop parameters to match a set of user-specified flow conditions but only for the fixed geometry typical of current PWR systems.

Both calculations utilize the transient fluid dynamics and heat transfer routines to search for time-independent conditions. The search is terminated when the normalized rates of change of fluid and thermal variables (described below) are reduced below a user-specified criterion throughout the system.

Although the same subroutines are used in the transient and steady-state calculations, there are important ways in which their behavior differs between the two calculations. The most crucial differences are:

1. The time step size used by the heat transfer and fluid flow calculations may not be equal during a steady-state calculation. The ratio of these time step sizes is fixed through user-specified input. This permits compensation for the difference in natural time scales of the two processes.

2. The occurrence of CHF is inhibited during the steady-state calculation. This results in a heat transfer coefficient which cannot undergo a rapid reduction due to burnout.

3. Pressurizers are modeled as pressure boundary conditions during steady-state calculations. Therefore, each pressurizer's energy and mass inventory, as well as pressure, will remain constant regardless of the flow rate between it and the remainder of the system.

4. Trips are inhibited during steady-state calculations. Thus, even though conditions may exist which would cause a trip during a transient, the trip will not be activated during the steady-state calculation.

5. The reactor power is set to zero for a period at the beginning of the steady-state calculation. It is increased to its nominal value once the fluid velocity has approached its equilibrium value.

a. Generalized Steady-State Calculations

This calculation is utilized to find the time-independent temperatures and fluid flow conditions for a system of arbitrary geometry. The major advantage gained over the direct use of the transient capability is automatic evaluation of the approach to time-independent conditions.

Reduced to their simplest form, the equations solved by the TRAC transient routines are a set of coupled, ordinary differential equations in time. (The dependence upon spatial variables is eliminated by the introduction of fluid flow cells and heat transfer nodes as described above.) These equations may be written as:

$$\frac{dX_i}{dt} = \sum_{j=1}^{N_i} F_{ij} \ ,$$

where the X_i are the dependent variables (fluid velocities, temperatures, etc.) and the F_{ij} are generalized "forces" acting on these variables. A steady-state situation generally represents a balancing of the various forces on each variable, rather than the simultaneous reduction of all the individual

forces, so that

$$\sum_{j=1}^{N_i} F_{ij} \to 0$$

without the F_{ij} themselves vanishing. This suggests that the proper measure of time independence is the degree to which the F_{ij} terms balance one another, rather than an absolute measure of the rates of change of the dependent variables.

TRAC therefore utilizes the normalized rates of change of the dependent variables, defined as

$$c_i = \frac{\left|\frac{dX_i}{dt}\right|}{\underset{j}{\text{Max}} \left\{ \left| F_{ij} \right| \right\}}$$

to measure the approach of the transient to a time-independent condition.

The dependent variables examined by the current version of TRAC in evaluating the approach to steady state are listed in Table IV, together with the physical interpretation of the generalized forces acting on them. A separate value of c_i is evaluated for each of the appropriate variables at each mesh cell of the system. (In the case of wall and rod temperatures c_i is evaluated for every node.) TRAC catalogs the maximum value of the normalized rate of change for each variable as well as the point at which the maximum was found, and compares that maximum to a user-specified convergence criterion. Some mesh cells are excluded from this comparison for certain variables because the maximum of the generalized forces acting on that variable at that mesh cell is below a threshold value.

b. PWR Initialization Calculation

The PWR Initialization calculation provides a convenient way for the user to match important operating conditions of a PWR system by adjusting certain operating parameters. The conditions which this calculation attempts to match are reactor power, pressurizer pressure, primary loop flow rates, and vessel inlet temperatures. This is accomplished by adjusting the pump speed and steam generator fouling factor in each loop of the reactor system. This

idea was first developed by Sharp,[53] although the method of implementation in TRAC is somewhat different.

As implied by its name, the PWR Initialization calculation is limited to systems whose geometry is characteristic of a PWR. The system must have one and only one VESSEL component. Although the number of primary coolant flow loops is arbitrary, each loop must satisfy the following criteria:

1. There must be a single STGEN component in each loop. This component must be located between the VESSEL hot-leg junction for that loop and the loop pump or pumps.

2. There must be either one or two pumps in each loop. These pumps must be between the STGEN and the VESSEL cold-leg junctions. If there are two pumps they must operate in parallel and each must be connected to the VESSEL through a distinct junction.

3. The secondary side of the steam generator must currently be connected to a BREAK on one side and a FILL on the other. Only pipes may be located between the STGEN and the FILL or BREAK.

4. The primary coolant flow loops must not connect directly to one another, except in that they are all connected to the VESSEL.

The values of operating parameters are determined by an iterative process. Each iteration begins with the execution of a sequence of transient time steps. These should bring the system state close to a steady state for the current value of the operating parameters. The VESSEL inlet temperatures and loop flow rates are compared to their desired values for each primary loop. Once these agree within a user-specified criterion the calculation is complete. Utilizing the state of the system at the conclusion of this sequence, new values of operating parameters are then evaluated.

In the evaluation of operating parameters, each primary coolant flow loop is treated independently. The coupling between loops is treated implicitly by the method used to evaluate VESSEL characteristics for each loop. Because the transient routines force the pressurizer pressure and the vessel power to their prescribed values, only variations in the loop flow rates and VESSEL inlet temperatures need to be considered. TRAC uses only information from the current state of the system (as derived from the transient calculation) in evaluating a new set of operating parameters; no information is stored from previous iterations.

Neglecting components not in the primarily coolant flow path (such as pressurizers and accumulators), each loop can be depicted schematically as shown in Fig. 8. Loops with only one pump are treated in a similar manner. The evaluation of new operating parameters for this primary coolant flow loop is based on the solucion of the pressure and energy balance equations written around this loop. Mass balance is automatically satisfied as a result of the transient calculation. The steady-state pressure and energy balance equations may be written:

$$\Delta P_{v1} + \Delta P_s = \Delta P_{p1}, \tag{165}$$

$$\Delta P_{v2} + \Delta P_s = \Delta P_{p2}, \tag{166}$$

$$\Delta H_s + \Delta H_{p1} + \Delta H_{p2} = \Delta H_{v1} + \Delta H_{v2}, \tag{167}$$

where the subscripts s, p, and v refer to the steam generator, pumps, and vessel, respectively, ΔP stands for a pressure difference, and ΔH stands for a change in the flow rate of enthalpy. Referring to Fig. 8, the pressure and enthalpy flow rate differences may be written:

$$\left.\begin{aligned}
\Delta P_{v1} &= P(C) - P(A) \\
\Delta P_{v2} &= P(D) - P(A) \\
\Delta P_s &= P(A) - P(B) \\
\Delta P_{p1} &= P(C) - P(B) \\
\Delta P_{p2} &= P(D) - P(B) \\
\Delta H_{r1} &= (W_1/W)H(A) - H(C) \\
\Delta H_{v2} &= (W_2/W)H(A) - H(D) \\
\Delta H_s &= H(A) - H(B) \\
\Delta H_{p1} &= (W_1/W)H(B) - H(C) \\
\Delta H_{p2} &= (W_2/W)H(B) - H(D)
\end{aligned}\right\} \tag{168}$$

where the W's are mass flow rates as indicated in Fig. 8.

To solve these equations for new pump speeds and steam generator fouling factors, these variables must be related to the pressure and enthalpy flow rate differences, and to the desired mass flow rates and vessel inlet temperatures. This is accomplished by assuming specific forms for the pressure rise across each pump, the enthalpy difference across each pump, and the enthalpy loss across the steam generator. The pressure rise across each pump is composed of two components: a pump head (PH), which depends on the pump speed, fluid density, and mass flow rate; and a flow resistance (R)

pressure loss which is proportional to the square of the mass flow rate. This results in the expressions,

$$\left.\begin{aligned} \Delta P_{p1} &= PH_1 - W^2 R_{p1} \\ \Delta P_{p2} &= PH_2 - W_2^2 R_{p2} \end{aligned}\right\} \quad (169)$$

The enthalpy difference across the pump is similarly composed of two components: one due to the pump head and a second, which is proportional to the mass flow rate, resulting in the expressions:

$$\left.\begin{aligned} \Delta H_{p1} &= W_1 \delta h_{p1} - \frac{PH_1}{\rho_{p1}} \\ \Delta H_{p2} &= W_2 \delta h_{p2} - \frac{PH_2}{\rho_{p2}} \end{aligned}\right\} \quad (170)$$

The enthalpy change across the steam generator is expressed in terms of the overall heat transfer coefficient, U, the mean-temperature difference, $\Delta\overline{T}$, and the heat transfer area, A; plus a residual loss term due to the mass flow rate:

$$\Delta H_s = W\delta h_s + WAU\overline{\Delta T} \quad . \quad (171)$$

Using the definitions of Eq. (168) and the state of the system at the conclusion of the transient calculation, Eqs. (169) through (171) are solved for the flow resistances, R_{p1} and R_{p2}; the specific enthalpy differentials, δh_{p1}, δh_{p2}, and δh_s; and the overall heat transfer coefficient U. These characteristics are assumed to be independent of the loop operating parameters, which are to be adjusted.

To fully characterize the response of the loop to changes in the operating parameters, we must be able to evaluate the remaining terms in Eqs. (165-167). These may be written in terms of the steam generator flow resistance,

$$\Delta P_s = W^2 R_s \quad (172)$$

and the vessel flow resistances and specific enthalpy differentials:

$$\left.\begin{aligned} \Delta P_{v1} &= W_1^2 R_{v1} \\ \Delta P_{v2} &= W_2^2 R_{v2} \\ \Delta H_{v1} &= W_1 \delta h_{v1} \\ \Delta H_{v2} &= W_2 \delta h_{v2} \end{aligned}\right\} \quad (173)$$

The steam generator flow resistance may be evaluated by using Eq. (172) directly; however, the vessel characteristics are defined somewhat differently to account for the effects of other loops and the possibility of nonequilibrium of the thermal conditions in that component. Therefore, we use the definitions:

$$R_{v1} = WR^2 \frac{P(C) - P(A)}{W_1^2}, \quad (174)$$

$$R_{v2} = WR^2 \frac{P(D) - P(A)}{W_2^2}, \quad (175)$$

$$\delta h_{v1} = QR/WR \left(\frac{H(A)}{W} - \frac{H(C)}{W_1} \right), \quad (176)$$

$$\delta h_{v2} = QR/WR \left(\frac{H(A)}{W} - \frac{H(D)}{W_1} \right), \quad (177)$$

where WR is the ratio of the desired total mass flow rate through the vessel to the current total mass flow rate through the vessel, and QR is the ratio of the desired total energy transfer rate in the vessel to the current total energy transer rate in the vessel. Notice that as the problem converges to the desired solution, Eqs. (174-177) reduce to the solutions of Eq. (173), since both QR and WR approach unity in that situation.

Given the values of flow resistances as calculated above, we can immediately solve Eqs. (165) and (166) for the new pump heads in the loop under consideration. Using the pump curves, the fluid densities in the pumps, and the desired mass flow rates, we can iteratively determine new pump speeds

which should produce the desired pump heads. Once the pump heads have been determined, we can use Eq. (167) to estimate a new value of the steam generator area. All terms of Eq. (167) are known except the steam generator area and the mean-temperature difference between the steam generator primary and secondary sides, $\overline{\Delta T}$. We attempt to match the desired vessel inlet temperature by modifying $\overline{\Delta T}$ by the difference between the desired and current values of the vessel inlet temperature. Solving the resulting equation for the steam generator area drives the ensuing steady state to the desired condition.

REFERENCES

1. G. Kocomustafaogullari, "Thermo-Fluid Dynamics of Separated Two-Phase Flow," Ph.D. Thesis, School of Mechanical Engineering, Georgia Institute of Technology, Atlanta, Georgia (December, 1971).

2. M. Ishii, Thermo-Fluid Dynamic Theory of Two-Phase Flow, Collection de la Direction des Etudes et Recherches D'Electricite de France (Eyrolles, Paris, 1975).

3. D. R. Liles and W. H. Reed, "A Semi-Implicit Method for Two-Phase Fluid Dynamics," Accepted for Publication in J. of Comp. Physics.

4. N. Zuber and J. A. Findlay, "Average Volumetric Concentrations in Two-phase Flow Systems," J. Heat Trans. 87, 453 (1965).

5. M. Ishii, "Light-Water-Reactor Research Program," Argonne National Laboratory report ANL-77-10 (Oct.-Dec. 1976).

6. J. G. Collier, Convective Boiling and Condensation (McGraw-Hill Co., New York, 1972).

7. W. M. Rohsenow and H. Y. Choi, Heat, Mass, and Momentum Transfer (Prentice-Hall Inc., Englewood Cliffs, NJ, 1961).

8. D. S. Rowe, "COBRA IIIC: A Digital Computer Program for Steady-State and Transient Thermal-Hydraulic Analysis of Rod Bundle Nuclear Fuel Elements," Battelle Northwest Laboratories report BNWL-1695 (1973).

9. C. Lombardi and E. Pedrocchi, "A Pressure Drop Correlation In Two-Phase Flow," Energia Nucleare 19, 91-99 (1972).

10. C. W. Hirt and N. C. Romero, "Application of a Drift-Flux Model To Flashing In Straight Pipes," Los Alamos Scientific Laboratory report LA-6005-MS (1975).

11. G. W. Govier and A. Aziz, The Flow Of Complex Mixtures In Pipes (Van Nostrand-Reinhold Co., New York, 1972).

12. D. Chisholm, "Pressure Gradients Due To Friction During The Flow Of Evaporating Two-Phase Mixtures In Smooth Tubes and Channels," Int. J. Heat Mass Transfer 16, 347-358 (1973).

13. B. S. Massey, Mechanics of Fluids (D. Van Nostrand Co., New York, 1968).

14. F. H. Harlow and A. A. Amsdem, "A Numerical Fluid Dynamics Calculation Method for All Flow Speeds," J. Comp. Physics 8, 197 (1971).

15. F. H. Harlow and A. R. Amsdem, "KACHINA: An Eularian Computer Program for Multifield Fluid Flows," Los Alamos Scientific Laboratory report LA-5680 (1975).

16. S. Lekach, "Development of a Computer Code for Thermal Hydraulics of Reactors (THOR)," Brookhaven National Laboratory Quarterly Progress report BNL-19978 (1975).

17. W. C. Rivard and M. D. Torrey, "Numerical Calculation of Flashing from Long Pipes Using a Two-Field Model," Los Alamos Scientific Laboratory report LA-6104-MS (1975).

18. K. Lee and D. J. Ryley, "The Evaporation of Water Droplets in Superheated Steam," ASME paper 68-HT-11 (1968).

19. G. B. Wallis, One-Dimensional Two-Phase Flow (McGraw-Hill, New York, 1969).

20. V. G. Levich, Physicochemical Hydrodynamics (Prentice-Hall, New York, 1962), pp. 430-432.

21. "MATPRO - Version 09: A Handbook of Materials Properties for Use in the Analysis of Light Water Reactor Fuel Rod Behavior," Idaho National Engineering Laboratory report TREE-NUREG-1005 (December 1976).

22. "FRAP-S2: A Computer Code for the Steady-State Analysis of Oxide Fuel Rods," Idaho National Engineering Laboratory report TREE-NUREG-1107 (July 1977).

23. "FRAP-T2: A Computer Code for the Transient Analysis of Oxide Fuel Rods," Idaho National Engineering Laboratory report TREE-NUREG-1040 (March 1977).

24. "CAPCON-THERMAL-2: A Computer Program for Calculating the Thermal Behavior of an Oxide Fuel Rod," Battelle Pacific Northwest Laboratories report BNWL-1898 (November 1975).

25. J. V. Cathcart, "Quarterly Progress Report on the Zirconium Metal-Water Oxidation Kinetics Program," Oak Ridge National Laboratory report ORNL/NUREG/TM-41 (August 1976).

26. "RELAP4/MOD5: A Computer Program for Transient Thermal-Hydraulic Analysis of Nuclear Reactors and Related Systems," Vol. 1, Idaho National Engineering Laboratory report ANCR-NUREG-1335 (September 1976).

27. M. Abramowitz and I. A. Stegun, eds., Handbook of Mathematical Functions, National Bureau of Standards Applied Mathematics Series Vol. 55 (May 1968).

28. R. Semeria and B. Martinet, "Calefaction Spots on a Heating Wall: Temperature Distribution and Resorption," Proceedings of the Institution of Mechanical Engineers 180, 192-205 (1966).

29. R. B. Duffey and D. T. C. Porthouse, "The Physics of Rewetting in Water Reactor Emergency Core Cooling," Nuclear Engineering and Design 25, 379-394 (1973).

30. S. S. Dua and C. L. Tien, "A Generalized Two-Parameter Relation for Conduction-Controlled Rewetting of a Hot Vertical Surface," Int. J. Heat Mass Transfer, 20, pp. 174-176 (1977).

31. J. O. Cermak, A. S. Kitzes, F. F. Cadek, R. H. Leyse, and D. P. Dominicis, "PWR Full Length Emergency Cooling Heat Transfer (FLECHT) Group I Test Report," Westinghouse Electric Co. report WCAP-7435 (January 1970).

32. N. Zuber, M. Tribus, and J. W. Westwater, "The Hydrodynamic Crisis in Pool Boiling of Saturated and Subcooled Liquids," International Developments in Heat Transfer, Part II, 230-236 (1961).

33. P. Griffith, C. T. Avedisian and J. F. Walkush, "Countercurrent Flow Critical Heat Flux," presented at National Heat Transfer Conference, San Francisco (August 1975).

34. L. Biasi, G. C. Clerici, S. Garribba, R. Sala, and A. Tozzi, "Studies on Burnout: Part 3," Energia Nucleare 14, 530-536 (1967).

35. T. A. Bjornard and P. Griffith, "PWR Blowdown Heat Transfer," in Thermal and Hydraulic Aspects of Nuclear Reactor Safety, Vol. 1 (American Society of Mechanical Engineers, New York 1977), pp. 17-41.

36. R. W. Bowring, "A Simple But Accurate Round Tube, Uniform Heat Flux Dryout Correlation over the Pressure Range 0.7-17 MN/m^2 (100-2 500 psia)," Atomic Energy Establishment report AEEW-R789 (1972).

37. P. J. Berenson, "Film Boiling Heat Transfer From A Horizontal Surface," ASME paper 60-WA-147 (1960).

38. R. E. Henry, "A Correlation for the Minimum Film Boiling Temperature," AIChE Symposium Series 138, 81-90 (1974).

39. H. K. Fauske, "Some Aspects of Liquid-Liquid Heat Transfer and Explosive Boiling," Proceedings of Fast Reactor Safety Meeting, Vol. 2, (Beverly Hills, CA, 1974), pp. 992-1005.

40. F. W. Dittus and L. M. K. Boelter, University of California Publ. Eng. 2, 443 (1930).

41. J. C. Chen, "A Correlation for Boiling Heat Transfer of Saturated Fluids in Convective Flow," ASME paper 63-HT-34 (1963).

42. W. L. Kirchner, "Reflood Heat Transfer In A Light Water Reactor," U.S. Nuclear Regulatory Commission report NUREG-0106 (1976).

43. L. A. Bromley, "Heat Transfer In Stable Film Boiling," Chemical Engineering Progress 46, 221-227 (May 1950).

44. N. A. Bailey, "Film Boiling on Submerged Vertical Cylinders," Atomic Energy Establishment report AEEW-M1051 (1971).

45. S. S. Kutateladze, "Heat Transfer During Film Boiling," in Heat Transfer In Condensation and Boiling, AEC-TR-3770 (1952).

46. R. S. Dougall and W. M. Rohsenow, "Film Boiling on the Inside of Vertical Tubes with Upward Flow of the Fluid at Low Qualities," MIT Mechanical Engineering report 9079-26 (1963).

47. W. H. McAdams, Heat Transmission (McGraw-Hill Co., New York, 1954) 3rd ed.

48. J. C. Chato, "Laminar Condensation Inside Horizontal and Inclined Tubes," A.S.H.R.A.E. Journal 4, 52-60 (1962).

49. E. F. Carpenter and A. P. Colburn, "The Effect of Vapor Velocity On Laminar and Turbulent Film Condensation," Transactions ASME 78, 1637-1643 (1956).

50. "RETRAN - A Program for One-Dimensional Transient Thermal-Hydraulic Analyses of Complex Fluid Flow Systems," Electric Power Research Institute report EPRI-NP-408 (January 1977).

51. S. Gill, "A Process for the Step-by-Step Integration of Differential Equations in an Automatic Digital Computing Machine," Proc. Cambridge Philos. Soc. 47, 96-108 (1951).

52. Robert J. Thompson, "Improving Roundoff in Runge-Kutta Computations with Gill's Method," Communication of the ACM 13, No. 12 (December 1970).

53. D. A. Sharp, "The PWR Steady-State Capability of WRAP - A Water Reactor Analysis Package," Savannah River Laboratory report DPST-NUREG-77-3 (June 1977).

54. N. Zuber, Nuclear Regulatory Commission, personal communication, 1977.

TABLE I

HEAT TRANSFER CORRELATIONS

Regime	Flag	Correlation	Eqs.	Ref.
Forced convection to single-phase liquid	1	laminar flow : constant Nusselt number turbulent flow : Dittus-Boelter	135 136	7 40
Nucleate boiling and forced convection vaporization	2	Chen	137	6,35,41
Critical heat flux	-	low flow : Zuber pool boiling high flow : Biasi	126 127,128	32 33,34,6
Transition boiling	3	log-log interpolation	138,139,140	42
Minimum stable film boiling	-	low pressure : Henry-Berenson high pressure : homogeneous nucleation	131,132 133	37,38 35,39
Film boiling	4	modified Bromley Dougall-Rohsenow	141,142,143 144,145	43,44,45 46
Forced convection to single-phase vapor	6	free convection : McAdams turbulent flow : Dittus-Boelter	146 147	47 40
Forced convection to two-phase mixture	7	laminar flow : constant Nusselt number turbulent flow : Dittus-Boelter	148 149	7 40
Horizontal film condensation	11	Chato	150	6,48
Vertical film condensation	12	Nusselt theory	151	6
Turbulent film condensation	13	Carpenter and Colburn	152	49

TABLE II

DELAYED NEUTRON CONSTANTS

Group i	β_i/β	λ_i
1	0.038	0.012 7
2	0.213	0.031 7
3	0.188	0.115
4	0.407	0.311
5	0.128	1.40
6	0.026	3.87

TABLE III

DECAY HEAT CONSTANTS

Group j	E_j	λ_j^H
1	0.002 99	1.772×10^{-0}
2	0.008 25	5.774×10^{-1}
3	0.015 50	6.743×10^{-2}
4	0.019 35	6.214×10^{-3}
5	0.011 65	4.739×10^{-4}
6	0.006 45	4.810×10^{-5}
7	0.002 31	5.344×10^{-6}
8	0.001 64	5.726×10^{-7}
9	0.000 85	1.036×10^{-7}
10	0.000 43	2.959×10^{-8}
11	0.000 57	7.585×10^{-10}

TABLE IV

VARIABLES CONSIDERED IN EVALUATING THE APPROACH TO STEADY STATE

One-Dimensional Fluid Flow Variables

Dependent Variable	Generalized Forces
Mixture Velocity	Wall Friction Pressure Gradients Gravity Momentum Fluxes
Mixture Mass	Sources Mass Fluxes
Mixture Energy	Sources Energy Fluxes
Vapor Mass	Sources Phase Exchange Mass Fluxes
Vapor Energy	Sources Phase Exchange Energy Fluxes

Three-Dimensional Fluid Flow Variables

Dependent Variable	Generalized Forces
Vapor Velocity	Wall Friction Interphase Friction Pressure Gradients Gravity Momentum Fluxes
Liquid Velocity	Wall Friction Interphase Friction Pressure Gradients Gravity Momentum Fluxes
Mixture Mass	Sources Mass Fluxes
Mixture Energy	Sources Energy Fluxes

TABLE IV (cont)

Vapor Mass	Sources Phase Exchange Mass Fluxes
Vapor Energy	Sources Phase Exchange Mass Fluxes
Heat Transfer Variables	
Temperature	Energy Sources Heat Fluxes

TABLE IV (cont)

Vapor Mass	Sources Phase Exchange Mass Fluxes
Vapor Energy	Sources Phase Exchange Mass Fluxes
Heat Transfer Variables	
Temperature	Energy Sources Heat Fluxes

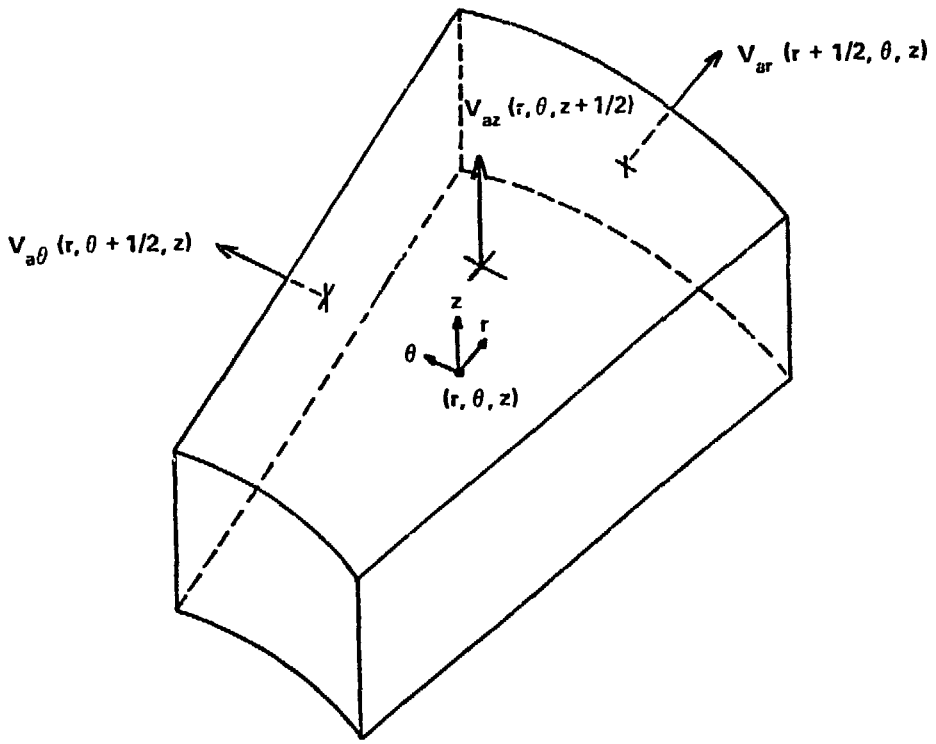

Fig. 2.
Three-dimensional mesh cell velocities.

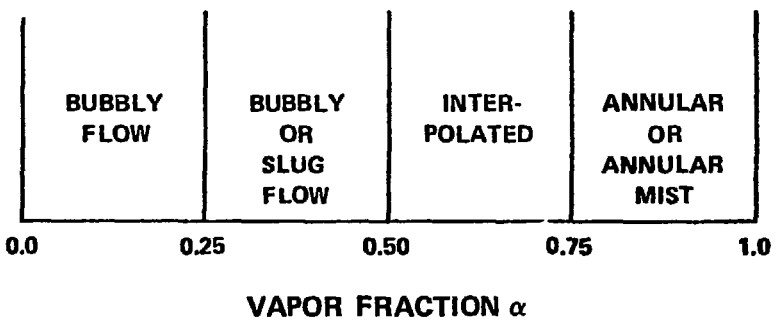

Fig. 3.
Flow regime map for three-dimensional hydrodynamics.

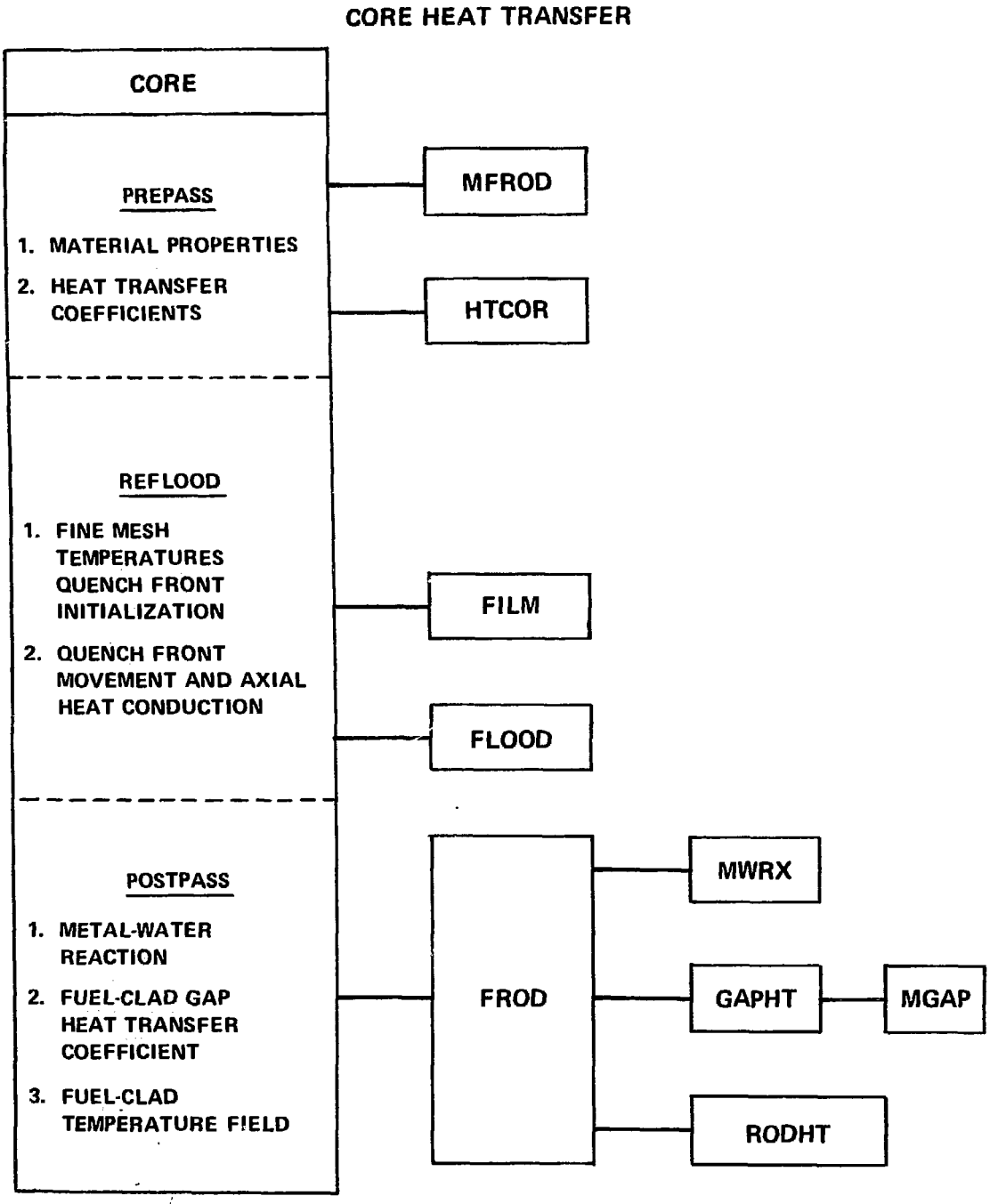

Fig. 4.
Calculational strategy for core heat transfer analysis.

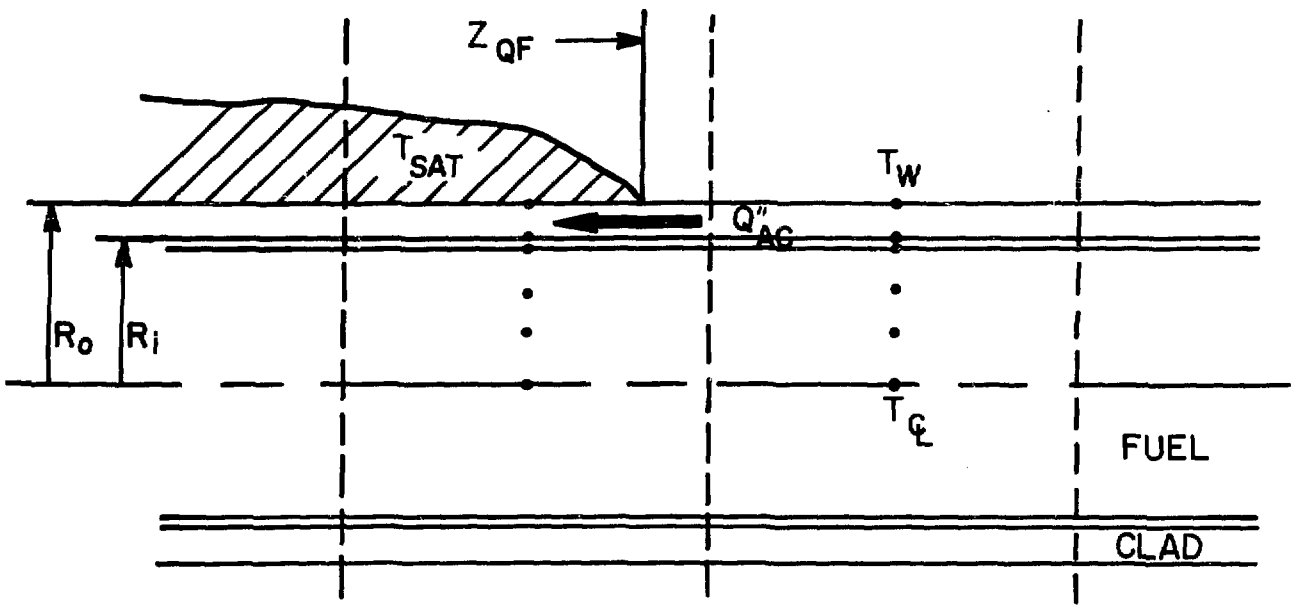

Fig. 5.
Axial conduction heat source due to quench front propagation.

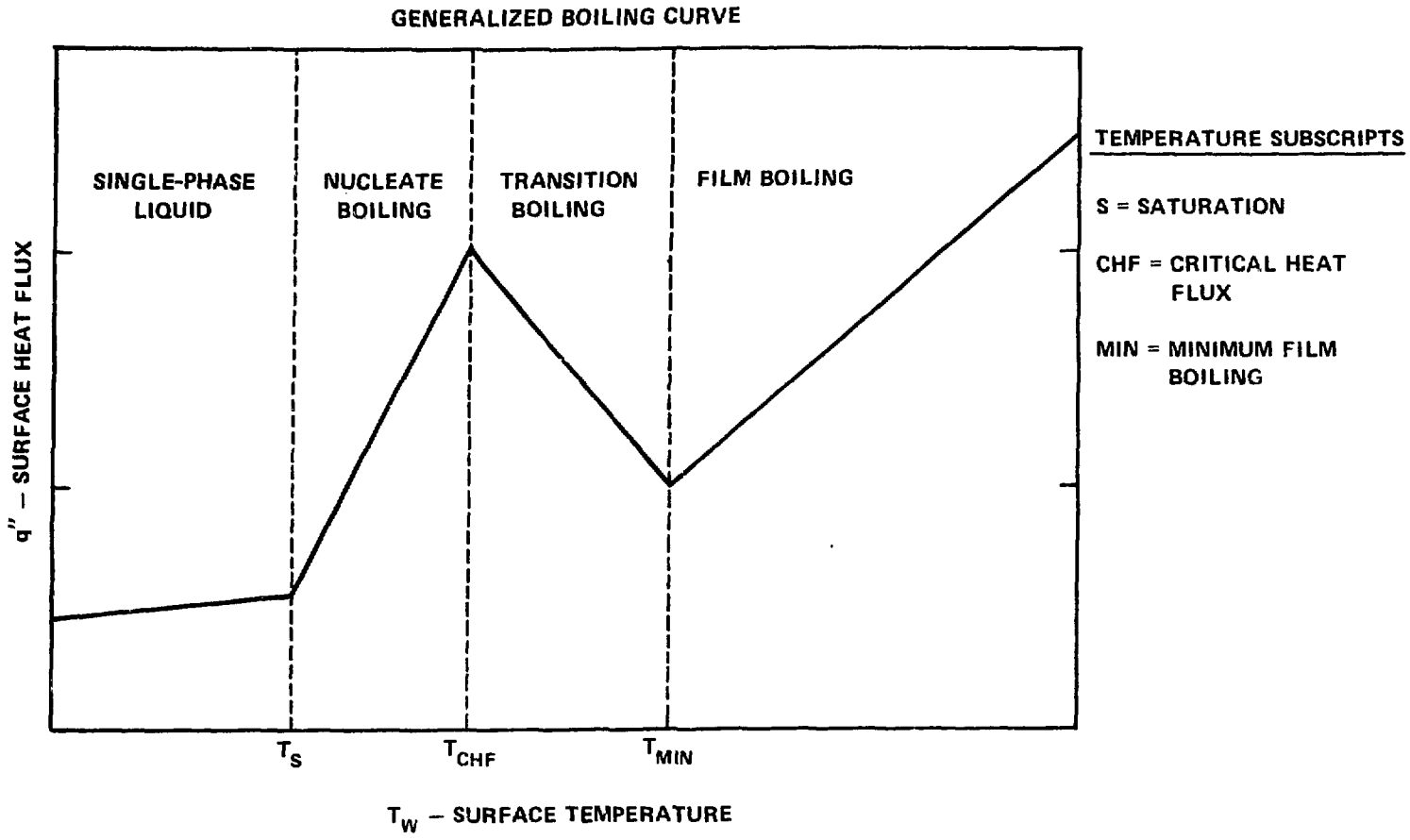

Fig. 6.
Generalized boiling curve.

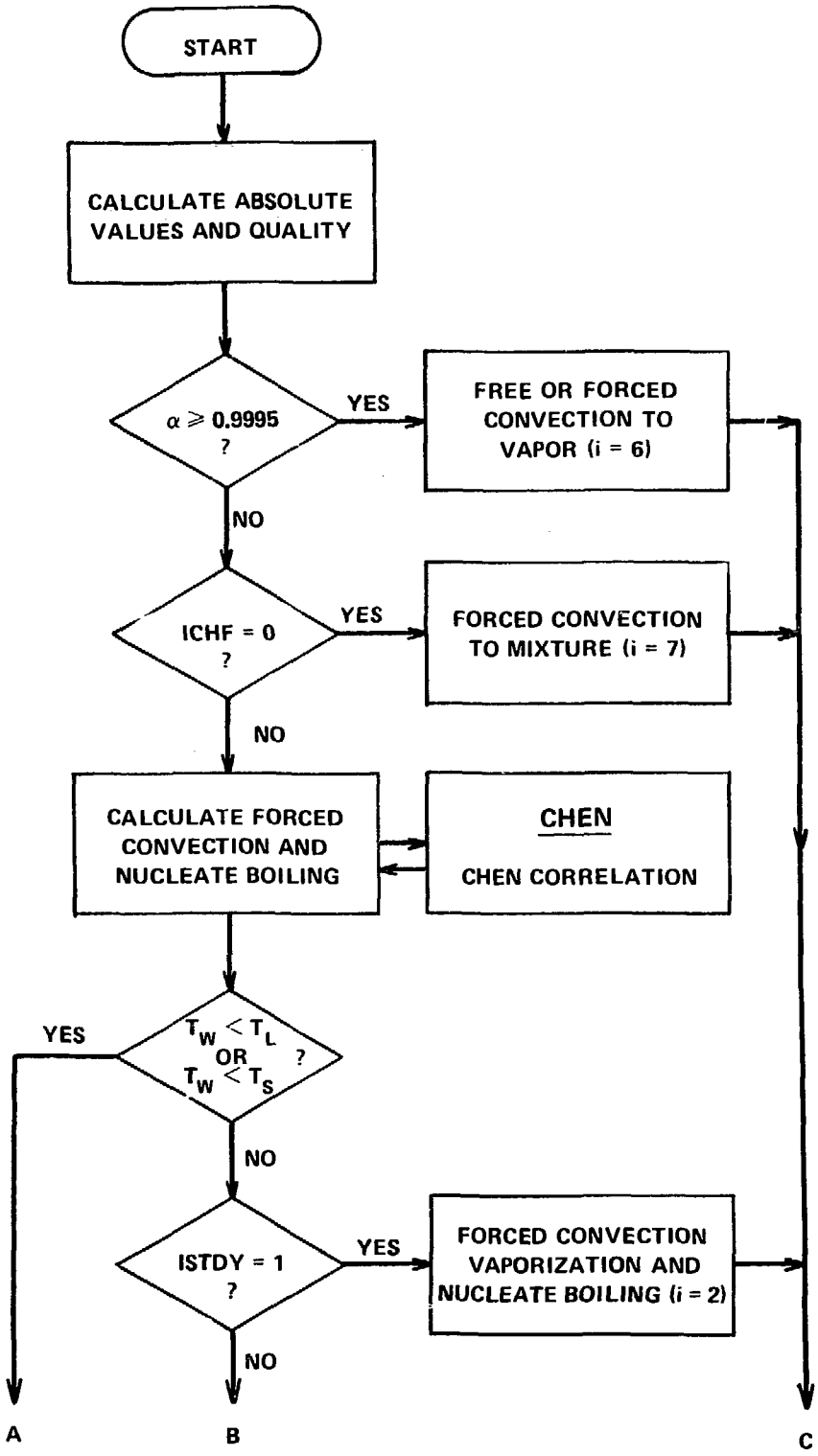

Fig. 7.
Heat transfer regime and correlation selection logic.

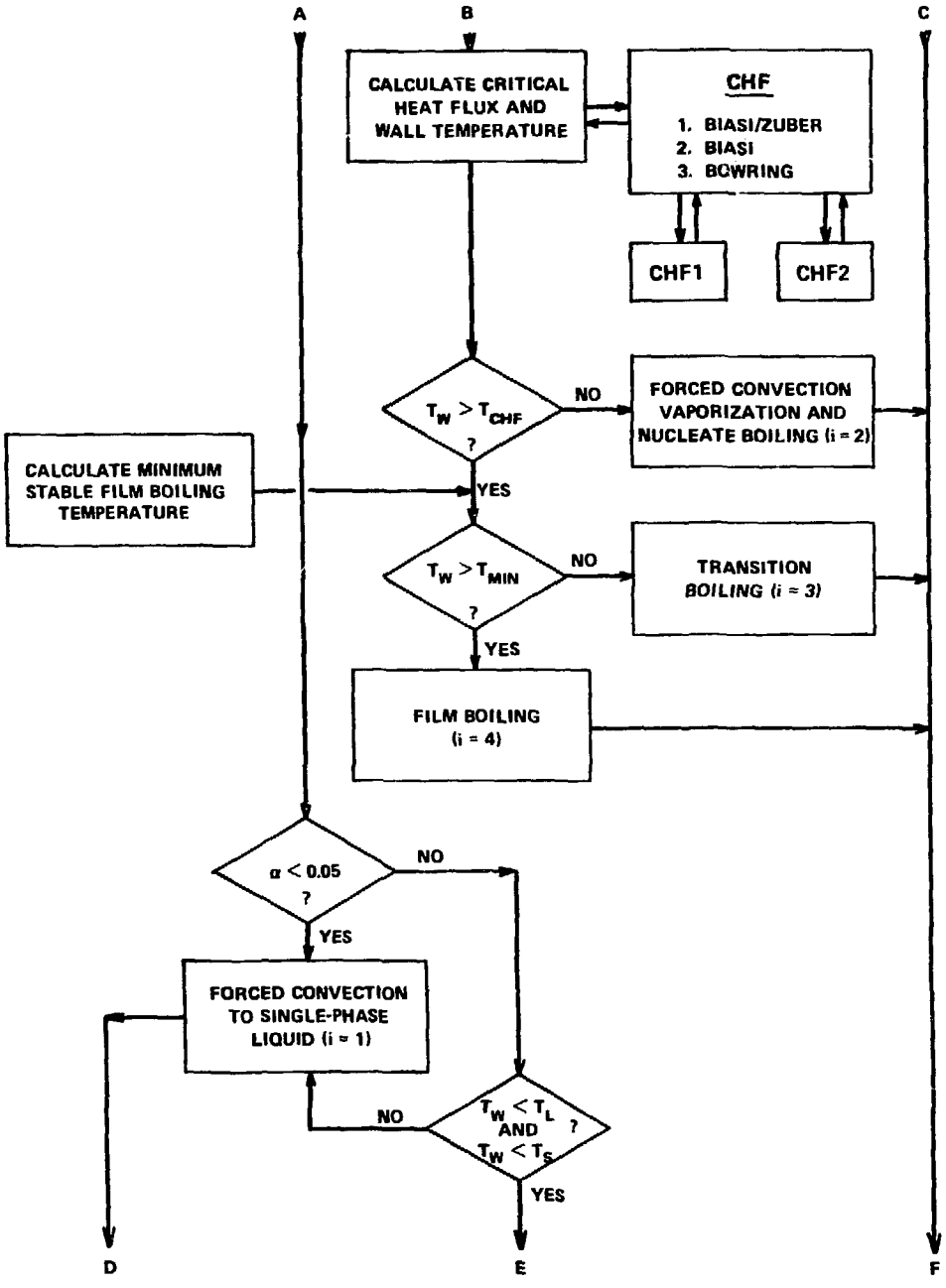

Fig. 7.
Continued

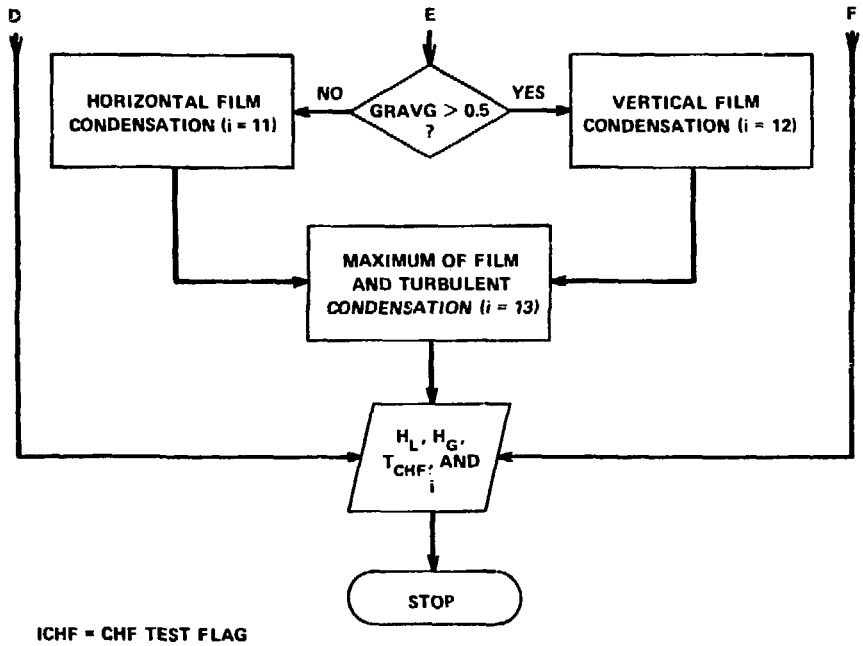

Fig. 7.
Continued

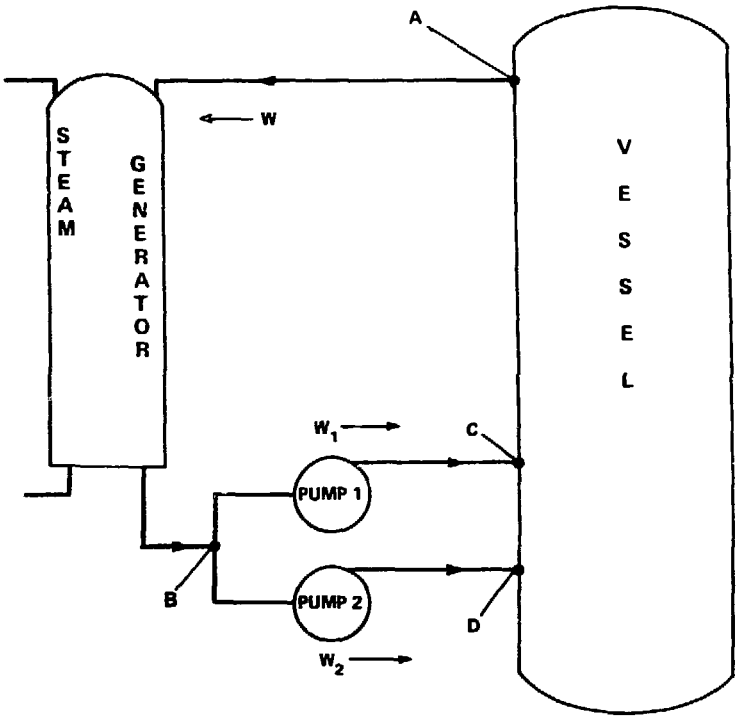

Fig. 8.
Primary loop schematic for a PWR initialization calculation.

IV. COMPONENT MODELS

Descriptions of the various component models that are included in the present version of the TRAC code are given in this chapter. A physical description of each component is presented along with a typical TRAC noding diagram showing the conventions that are used to model the component. Mathematical models including finite difference approximations are given only for those aspects of the component that are not already covered in the basic hydrodynamics and heat transfer descriptions (Chap. III). Options available to the user, restrictions on the use of the component, subroutines used by the component, and input/output information are also given.

A. Accumulator

An accumulator is a pressure vessel filled with Emergency Core Cooling (ECC) water and pressurized with nitrogen gas. During normal operation each accumulator is isolated from the reactor primary coolant system by check valves. Should the reactor coolant system pressure fall below the accumulator pressure, the check valves open and ECC water is forced into the reactor coolant system.

An accumulator component is simulated by the ACCUM module in TRAC. This module can only be connected at one junction to other TRAC components. This connection is at the highest numbered cell, with Cell 1 assumed to be closed off as shown in the typical noding diagram in Fig. 1. It is assumed that the accumulator is not connected to a nitrogen pressure source. Therefore, the nitrogen pressure is that resulting from the expansion of the initial gas volume.

A flow diagram for the subroutines called by ACCUM is given in Fig. 2. Brief descriptions of all the subroutines in the TRAC code are given in Appendix E. The procedures for data input, initialization of arrays, advancement of time-dependent variables, and editing are similar to that given for a PIPE component (see Sec. C below). However, in an accumulator the vapor-phase properties are those for nitrogen gas. The hydrodynamics are treated using the one-dimensional, drift-flux routine DF1D. However, drift velocities are not obtained from the SLIP routine as is the case in PIPE, but are specified in subroutine ACCUM to produce a sharp liquid/vapor interface during accumulator discharge. Additionally, the properties at the accumulator

discharge are controlled such that pure liquid is discharged until the calculated collapsed water level reaches 90% of the height of the last mesh cell. When this occurs, that accumulator is modified such that the last cell has a zero flow area at its upper surface and the void fraction in the cell is set to 0.1. After this time the discharge properties are not controlled and vapor-phase properties are those for steam.

The wall friction coefficients in an accumulator component are set equal to 0.005; however, the additive friction factor, FRIC, at each cell edge can be specified by the user. The walls of an accumulator are assumed to be adiabatic.

The output edit is similar to the PIPE one-dimensional component with the addition of a few variables specific to an accumulator. These are: (1) the discharge volumetric flow rate, (2) total liquid volume discharge, and (3) collapsed liquid level.

B. BREAK and FILL Modules

These modules differ from the other component modules in that they do not model any system component per se and no calculations are performed by them. Otherwise, they are treated as any other component with respect to input, initialization, and identification procedures. The BREAK and FILL modules are used to impose certain boundary conditions at the ends of pipes or at any one-dimensional component terminal junction.

The BREAK module imposes a fixed pressure boundary condition one cell away from its adjacent component, as shown in Fig. 3. This module is commonly used to model the containment system in LOCA calculations. In later versions of the code, this approach will be replaced with a more sophisticated containment module.

The FILL module imposes a fixed or variable velocity boundary condition at the junction between the fill and its adjacent component, as shown in Fig. 4. Fills may be used to fix the mass flow of either vapor or liquid at a junction. ECCS injection may be modeled with a fill. The fill velocity may be a function of time or pressure with or without trip control. Five control options are provided for specifying the type of fill.

The parameters needed for specifying a FILL or a BREAK are described in the input section of this manual. It is suggested that the cell volume and length in FILL and BREAK be the same as those for the neighboring cell in the

adjacent component. The temperature and vapor fraction specified in FILL and BREAK are used to determine the properties of fluid convected into the adjacent component if an inflow condition should occur.

C. PIPE Module

The PIPE module is used to model thermal-hydraulic flow in a one-dimensional duct or pipe. A pipe can be used alone in a problem or can be used to connect other components together to model a reactor system. The capability is provided to model area changes, wall heat sources, and heat transfer across the inner and outer wall surfaces. A wide selection of pipe materials is available for representing the wall material in the wall conduction calculation.

Figure 5 shows a typical noding diagram for a pipe containing a venturi and an abrupt area change. The numbers within the pipe indicate cell numbers and those above it are cell boundary numbers. The geometry is specified by providing a volume and length for each cell and a flow area and hydraulic diameter at each cell boundary. The junction variables JUN1 and JUN2 provide reference numbers for connecting this pipe to other components. The numerical methods used to treat the thermal-hydraulics in PIPE are described in Chap. III.

Input options are available for selecting the degree of implicitness in the numerical hydrodynamics solution method, allowing for wall heat transfer, and selecting correlations to be used for CHF and wall friction factors. Most pipes should be treated with the faster partially implicit numerical hydrodynamics option (IHYDRO=0). However, when very high flow velocities are expected, as in a pipe adjacent to a break, the fully implicit hydrodynamics option (IHYDRO=1) should be used. Wall heat transfer can be omitted by setting the number of heat transfer nodes (NODES) to zero. The user can choose one of three methods of calculating CHF, or this calculation can be bypassed by setting the input parameter ICHF to zero. Wall friction and losses due to abrupt area changes are chosen by setting values of the input arrays NFF and FRIC at each cell interface. The choices for these arrays are described in the input specifications in Chap. V.

PIPE can be connected to any other component but no two components connected together can both use the fully implicit option. The user is cautioned

that TRAC functions best with a minimum number of components. Therefore, joining two pipes, when a single pipe could have been created with the input deck, is not recommended.

Detailed input for the PIPE module, described in Chap. V, is processed by subroutines RPIPE and REPIPE. RPIPE reads input data from the card input file and REPIPE reads the corresponding data from the restart file. Initialization of the remaining necessary variables is performed with subroutines CIPIPE and IPIPE. CIPIPE handles the data transfer between large core memory (LCM) and small core memory (SCM) for this process and calls IPIPE. IPIPE establishes the noding for wall heat transfer, sets the remaining fluid properties with calls to THERMO and FPROP, and initializes boundary data with a call to J1D.

During the execution of a problem, the solution procedure is controlled by routines CPIPE and PIPE. CPIPE handles data transfer and calls PIPE. A flow diagram for the subroutines called by PIPE is given in Fig. 6. The user is referred to Appendix E for a brief description of all subroutines in TRAC. At the beginning of each time step, PIPE calls SLIP to obtain relative velocities, FWALL for wall friction and orifice loss coefficients, MPROP for wall metal properties, and HTPIPE to obtain wall heat transfer coefficients. During the iterations for a time step, PIPE calls DF1D for the numerical hydrodynamics solution (see Chap. III) and J1D to update boundary arrays. After a time step is successfully completed, PIPE updates the wall temperatures with a call to CYLHT, computes new fluid properties (viscosity, heat capacity, and surface tension) with a call to FPROP, and resets the boundary arrays with J1D. If the time step fails to converge, THERMO is called to restore variables to their old values.

Output for a pipe is managed by subroutines CWPIPE and WPIPE. CWPIPE transfers data from LCM to SCM and calls WPIPE. WPIPE prints out the component number, junction numbers, iteration count, pressures, vapor fractions, saturation temperatures, liquid and vapor temperatures, liquid and vapor densities, mixture velocity, slip ratio, and wall friction factor. If wall heat transfer is included (NODES=0), then information on the heat transfer regime, liquid and vapor wall heat transfer coefficients, interfacial heat transfer coefficient, heat transfer rate from the wall, wall temperature for critical heat flux, and wall temperature profiles are also printed.

D. Pressurizer

The pressurizer in a PWR is a large fluid reservoir that maintains the pressure within the reactor primary coolant system by compensating for changes in the coolant volume due to system transients. During normal operation this reservoir contains the highest energy fluid in the primary system. It is usually maintained about 50 - 60% full of saturated liquid pressurized by the saturated steam above it. The pressurizer pressure is the controlling source of the primary coolant loop pressure and is transmitted by a long "surge line" connected to one of the hot legs.

A pressurizer component is simulated by the PRIZER module. This module is normally used to model the pressurizer itself with the surge line being represented by a PIPE component. As shown in a typical noding diagram in Fig. 7, a PRIZER component can be connected only at one junction to other TRAC components. The convention used is that the connection is at the highest numbered cell, with Cell 1 assumed to be the closed-off end.

A flow diagram for the subroutines called by PRIZER is given in Fig. 8. A brief description of TRAC subroutines is given in Appendix E. The procedures for data input, initialization of arrays, advancement of time-dependent variables, and editing are similar to those given for a PIPE component (see Sec. C). The hydrodynamics are treated using the one-dimensional, drift-flux routine DF1D. However, drift velocities are not obtained from the SLIP routine as is the case in PIPE but are specified in subroutine PRIZER to produce a sharp liquid/vapor interface during pressurizer discharge.

In a PRIZER component the walls are adiabatic but energy transfer from a heater/sprayer can be simulated. The primary purpose of this heater/sprayer logic is not to account for the added energy, but rather to serve as a system pressure controller. The user specifies a desired pressure setpoint, PSET, and the pressure deviation, DPMAX, at which the heaters input their maximum power of QHEAT. The power that is input to the pressurizer fluid is directly proportional to the difference between PSET and P(1), the pressure in Cell 1. That is,

$$Q_{input} = QHEAT \quad \frac{PSET - P(1)}{DPMAX}$$

with the maximum value limited to $\pm$ QHEAT. This power is distributed over all fluid cells in the pressurizer with the fraction of power input to each cell

being equal to the fraction of total liquid mass in that cell. Power is not added if the collapsed liquid level is less than the input parameter ZHTR. If pressure control is not desired, it is only necessary to equate QHEAT to zero.

Wall friction coefficients are calculated in routine FWALL by specifying a friction correlation option, NFF, along with additive friction factors, FRIC, for each cell edge. The homogeneous flow friction factor option (NFF=1) is suggested for a pressurizer.

The output edit for a PRIZER component is similar to the PIPE one-dimensional component with the addition of a few variables specific to the pressurizer. These are: (1) the discharge volumetric flow rate, (2) total liquid volume discharged, (3) collapsed liquid level, and (4) heater/sprayer power input to the pressurizer fluid.

E. PUMP Module

The pump module employed in TRAC describes the interaction of the system fluid with a centrifugal pump. The model calculates the pressure differential across the pump and its angular velocity as a function of the fluid flow rate and the fluid properites. The model is designed to treat any centrifugal pump and allows for the inclusion of two-phase effects.

The pump model is represented by a one-dimensional component with N cells where $N > 1$. A typical noding diagram for the pump component is shown in Fig. 9. The pump momentum is modeled as a source (SMOM), which is included between Cells 1 and 2. The source is positive for normal operation so that a pressure rise occurs in going from Cell 1 to Cell 2. Therefore, it is necessary to construct the cell noding such that the cell number increases in the normal flow direction.

The following considerations were felt to be important in creating the pump module:

1. compatibility with adjacent components should be maximized,
2. choking at the pump inlet or outlet should be automatically predicted, and
3. the calculated pressure rise across the pump should agree with that measured at steady-state conditions.

The first two criteria eliminated the use of a lumped-parameter model. Since the adjacent components are usually described by pipe modules, which are based on a one-dimensional drift-flux approximation, the pump is treated likewise.

The resulting PUMP module therefore combines the PIPE module with pump correlations.

The pump model is identical to the one-dimensional pipe model except that a momentum source is included in the mixture momentum equation written between Cells 1 and 2:

$$\frac{V_{1\frac{1}{2}}^{n+1} - V_{1\frac{1}{2}}^{n}}{\Delta t} = \frac{(p_1^{n+1} - p_2^{n+1})}{\rho_{1\frac{1}{2}}^{n} \Delta x} - C^n - g_z$$

$$- \frac{f V_{1\frac{1}{2}}^{n} |V_{1\frac{1}{2}}^{n}|}{D_h} + SMOM, \qquad (1)$$

where C^n represents the convective terms evaluated at time n. The source term, SMOM, is taken to be

$$SMOM = \frac{\Delta P}{\rho_{1\frac{1}{2}}^{n} \Delta x} + C^n - g_z + \frac{f}{D_h} V_{1\frac{1}{2}}^{n} |V_{1\frac{1}{2}}^{n}|, \qquad (2)$$

where ΔP is the pressure rise through the pump evaluated from the pump correlation at the flow velocity $V_{1\frac{1}{2}}^{n}$ and density $\rho_{1\frac{1}{2}}^{n}$. With this definition of the momentum source, the steady-state solution of Eq. (1) is

$$P_2 - P_1 = \Delta P,$$

which is the desired result.

It is only necessary to evaluate the momentum source for one pump cell once each time step, and the source is only needed during the explicit pass in DF1D, which calculates the temporary velocity $\tilde{V}$. Numerical results indicate that evaluating the pump source at the old time (n) is adequate and that it is not necessary to re-evaluate the source during the implicit iteration phase of DF1D. A simplified flow diagram for the PUMP module is shown in Fig. 10 (a brief description of the subroutines in TRAC is given in Appendix E).

The pump characteristic curves describe the pump head and torque response as a function of fluid volumetric flow rate and pump speed. Homologous curves (one curve segment represents a family of curves) are used for this description due to their simplicity. These curves describe, in a compact manner, all operating states of the pump obtained by combining positive or negative impeller velocities with positive or negative flow rates.

In order to take into account two-phase effects on pump performance, the pump curves are divided into two separate regimes. Data indicate that two-phase pump performance in the vapor fraction range of 20-80% is significantly degraded in comparison to its performance at vapor fractions outside of this range. One set of curves describes the pump performance for single-phase fluid (0 or 100% vapor fraction) and another set describes it for two-phase fluid. The pump head at any vapor fraction is calculated from the relationship

$$H = H_1 - M(\alpha)(H_1 - H_2), \tag{3}$$

where

H = total pump head,

H_1 = pump head from single-phase homologous curves,

H_2 = pump head from the fully degraded homologous curves,

M = pump degradation multiplier, and

α = vapor fraction.

The two-phase hydraulic torque is treated similarly. The following definitions are employed in the subsequent development:

H = pump head = $\frac{\Delta P}{\rho}$

Q = pump volumetric flow rate, and

Ω = pump impeller angular velocity,

where

Δp = pump differential pressure and

ρ = pump inlet density.

In order to allow one set of curves to be used for a variety of pumps, the following normalized quantities are used:

$$h = \frac{H}{H_R}$$

$$q = \frac{Q}{Q_R} \quad , \text{ and}$$

$$\omega = \frac{\Omega}{\Omega_R} \quad ,$$

where the subscript R denotes the rated condition. Use of the pump similarity relations[1] shows that

$$\frac{h}{\omega^2} = f\left(\frac{q}{\omega}\right) .$$

For small ω, this correlation is not satisfactory and the following combination of variables is used:

$$\frac{h}{q^2} = f\left(\frac{\omega}{q}\right) .$$

The first correlation is used in the range $0 < \left|\frac{q}{\omega}\right| \leq 1$ and the second is used in the range $0 \leq \left|\frac{\omega}{q}\right| < 1$. The four resulting curve segments, as well as the curve selection logic used in TRAC, are shown in Table I.

The dimensionless hydraulic torque is defined by

$$\beta = \frac{T_{hy}}{T_R} ,$$

where T_{hy} = hydraulic torque and
T_R = rated torque.

The single-phase torque, T, is dependent upon the fluid density and is calculated from

$$T = \beta T_R \frac{\rho}{\rho_R} , \qquad (4)$$

where ρ is the pump inlet density and ρ_R is its rated density. The density ratio multiplier is needed to correct for the density difference between the pumped fluid and the rated condition. For two-phase conditions the impeller torque is calculated from

$$T = T_1 - N(\alpha)(T_1 - T_2),$$

where

T = total impeller torque,
T_1 = impeller torque from single-phase homologous curves,
T_2 = impeller torque from fully degraded homologous curves, and
$N(\alpha)$ = torque degradation multiplier.

The homologous, normalized, torque curve segments are correlated in the same manner as the head curve segments shown in Table I.

In addition to the homologous head and torque curves, the head degradation multiplier and torque degradation multiplier defined in Eqs. (3) and (5) are needed. These functions are usually nonzero only in the vapor-fraction range, where the pump head and torque are either partially or fully degraded.

The pump module treats the pump angular velocity as a constant (input) while its motor is energized. After a drive motor trip, the time rate of change of the pump motor assembly is proportional to the sum of the moments acting on it and is calculated from the equation

$$I \frac{d\Omega}{dt} = \sum_i T_i = (T + T_f + T_b), \tag{6}$$

where

I = pump motor assembly moment of inertia,

T = impeller torque,

T_f = torque due to friction (constant), and

T_b = bearing and windage torque.

T_b is assumed to be of the form

$$T_b = C \frac{\Omega|\Omega|}{\Omega_R^2}, \tag{7}$$

where C is an input constant and Ω_R is the related impeller angular velocity. The impeller torque is evaluated from the homologous torque curves and Eq. (5); it is a function of the fluid density and flow rate as well as pump angular velocity. For time step n+1, Eq. (6) is evaluated explicitly

$$\Omega^{n+1} = \Omega^n + \frac{1}{I} \sum_i T_i \, (\Omega, \rho, Q)^n \, \Delta t^{n+1}. \tag{8}$$

Pump Option

The wall heat transfer, wall friction, CHF calculation, and implicit hydrodynamics options are the same for the pump module as for the pipe module. In addition the following options are specified: pump type, motor action, reverse speed option, two-phase option, and pump curve option.

If the pump motor is energized, its angular velocity is assumed to be the constant value specified. If the motor is not energized, a pump coastdown calculation is performed using the specified initial pump speed.

There are two pump options available (IPMPTY = 1 or 2). For pump option 1 (IPMPTY = 1) the pump speed variation is specified by input. The pump is initially energized at a constant speed specified by input (OMEGA). The pump motor may be tripped by a TRIP signal. If a pump trip has occurred, the pump speed is taken from a pump speed versus time table (array SPTBL).

Pump option 2 (IPMPTY = 2) is similar to option 1 except that a speed table is not input. Instead, the pump speed is calculated from Eq. (8) after a trip has occurred. The relationship between the various pump input parameters and the algorithm for the pump speed calculation are shown in Table II. Note that IPMPTR is the TRIP ID for pump trip initiation and NPMPTX is the number of pairs of points in the pump speed table (SPTBL). If IPMPTR = 0, no pump trip action will occur (constant speed pump).

If the reverse speed option is specified (IRP = 1), the pump can rotate in both the forward and reverse directions. If reverse speed is not allowed (IRP = 0), the pump will rotate in the forward direction only. For this case, if negative rotation is calculated (after trip with option 2 pump) its speed will be set to zero.

If the two-phase option is turned on (IPM = 1), the degraded pump head and torque will be calculated from Eq. (3) and (5). If the two-phase option is turned off (IPM = 0), only the single-phase head and torque homologous curves will be used.

The user may specify pump homologous curves in the input, or may alternatively use the built-in pump curves. The built-in pump curves are for the MOD-1 semiscale system pump and are based on the data in Refs. 2-4. These curves, as well as the head and torque degradation multipliers, are shown in Figs. 11-16. Since these homologous curves are dimensionless, they can be used to describe a variety of pumps by specifying as input the desired rated density, head, torque, flow, and angular velocity.

There are several restrictions and limitations in the current version of the pump module. Since there is no pump motor torque versus speed model, the pump speed is assumed to be input if the motor is energized. Pump noding is restricted such that the pump momentum source is located between cells 1 and 2 of the pump model. Finally, the head degradation multiplier, $M(\alpha)$, and the torque degradation multiplier, $N(\alpha)$, are assumed to apply to all operating states of the pump.

The pump module input consists of the same geometric and hydrodynamic data and initial conditions that are required for the pipe module. In addition, information specific to the pump is required as described in the input specifications. The speed table (SPTBL) as well as the homologous pump curve arrays must be input in the following order:

x(1),y(1),x(2),Y(2), ... x(n),y(n).

Here, x is the independent variable and y is the dependent variable. Furthermore, the independent variables must be input in a monotone increasing order, i.e.,

$x(n) > x(n-1) > \ldots x(2) > x(1)$.

Linear interpolation is used within the arrays.

F. Steam Generator

In a pressurized water reactor the steam generators serve to transfer energy from the primary coolant loop to the secondary coolant to produce steam. The STGEN module can be used to model both a "U-tube" or a "once-through" type steam generator. The user specifies the type of generator through input variable KIND: 1 = U-tube, 2 = once-through. Although there are two different steam generator designs, the basic operation is similar for both types. That is, primary coolant enters an inlet plenum, flows through a tube bank during which the primary coolant exchanges heat with a secondary coolant which flows over the exterior of the tube bank, and finally is discharged into an outlet plenum. A typical noding diagram for a STGEN component is given in Fig. 17. This figure illustrates that there is an inlet plenum (Cell 1) and an outlet plenum (last cell) on the primary side; these two cells are adiabatic. The tube bank, however, is represented by a single "effective" tube that has heat transfer characteristics such that it is representative of the entire tube bank. This is explained in detail below.

In the STGEN module the primary side and the secondary side hydrodynamics are treated separately, with the only coupling of the two sides being through wall heat transfer. The hydrodynamics of the primary side are solved by calling the one-dimensional, drift-flux routine DF1D. The tube wall temperature for each mesh cell is held constant over the time step, but the vapor and liquid temperatures are treated implicitly. This partially implicit heat transfer is discussed further in Chap. III. Next, the hydrodynamics for the secondary side are solved in the same manner. Once convergence has been

reached for all system components, a final pass is made and tube wall temperatures are updated for the current time step.

The procedures for reading input, initialization of arrays, advancement of the time step, and editing are similar to those described for the PIPE module (see Sec. D). The flow diagram for the subroutines called by the STGEN module is identical to that for PIPE except that the sequence of calls is performed twice: once for the primary side and once for the secondary side..

Although the procedure for reading input data is similar to a PIPE module, there are some differences. The most obvious difference is the necessity to specify four junction numbers (see Fig. 17): two for the primary side connections and two for the secondary side. Although it is possible to connect the secondary side junctions to any TRAC component, the most common arrangement is to connect the inlet to a FILL specifying the secondary side fluid inlet conditions and flow rate, and a BREAK at the discharge specifying the steam generator secondary discharge pressure. Since there is currently no provision for modeling the downcomer on the steam generator secondary, the fluid conditions for this FILL should be those for the water entering the tube bank and not those of the feedwater itself.

The number of fluid mesh cells on the primary side is specified as NCELL1 and that on the secondary side is NCELL2. There are some constraints imposed on the possible values for NCELL1, NCELL2 combinations. For a "once-through" type (KIND=2), it is required that NCELL2=NCELL1-2. For a "U-tube" type (KIND=1), it is assumed that there is a one-to-one correspondence between two active primary cells and one active secondary cell (see Fig. 17). Thus, for the fluid cells on the secondary side to reach the U-tube bundle top, it is required that NCELL2 $\geq$ (NCELL1-2)/2. The secondary side cells that are greater than (NCELL1-2)/2 are treated as adiabatic and are used to model possible area changes and volumes above the tube bank. In Fig. 17 these are Cells 6-8 on the secondary side.

The number of wall temperature nodes (NODES) must be specified equal to or greater than one. Three are suggested because this places one node at each tube surface and one at the tube wall center. The tube material is specified with the variable MAT; available material options are given in the input specifications (Chap. V). There are two flags, ICHF1 and ICHF2, that are used to determine if a CHF calculation is to be performed on the primary and

secondary sides, respectively. If CHF calculations are desired, these flags are set equal to 1; otherwise they are set equal to 0. It should be noted that if a CHF calculation is not done, boiling heat transfer calculations are not performed either. Thus, stagnant fluid on the secondary side would have a low heat transfer coefficient typical of natural convection. It is therefore suggested that the combination
ICHF1 = 0 and ICHF2 = 1 be used.

Geometrical input data for the tubes must be determined with caution. As stated earlier, it is necessary to model the heat transfer characteristics of the entire tube bundle with a single "effective" tube. This can best be achieved as follows. The inner tube radius, RADIN, and tube wall thickness, TH, should be those of an actual single tube in the bundle. The user specifies the heat transfer surface area in each cell for both the primary and secondary sides. In most cases, this will be the effective heat transfer surface area for all the tubes in each mesh cell and can be used to account for tube fouling factors or enhanced heat transfer from fins. The steam generator can be made adiabatic by specifying zero heat transfer areas.

Specifying the heat transfer area for a "once-through" generator is straightforward; it is the total effective heat transfer area for the steam generator multiplied by the fraction of total tube length in each mesh cell. For a "U-tube" generator, however, caution must be used. On the primary side the heat transfer area (WA1) is the effective interior area for all the tubes in each mesh cell. The total heat transfer to a secondary side fluid cell is the sum of that transfer from the up tubes and the down tubes in the cell. In the TRAC calculation, the effective heat transfer areas for the up tubes and down tubes are assumed to be equal. Therefore, the user should input an effective area (WA2) that is equal to one-half the effective surface area on the tube exteriors of both the up and the down tubes in that fluid cell.

The volumes and flow areas on the primary side (VOL1, FA1) are those determined by considering all the tubes in the bank. However, the hydraulic diameter (HD1) is that for a single tube. The volumes and flow areas on the secondary side (VOL2, FA2) are the actual geometric values for each mesh cell. The hydraulic diameter (HD2) is determined by standard methods used in heat transfer over tube bundles.

Tube wall initial temperatures must also be specified; the required number is NCELL1*NODES. Thus, even though Cell 1 and Cell NCELL1 are adiabatic, tube wall temperatures must be given for both of these cells. They are only defined to simplify indexing. The numbering convention used is that temperatures begin with Cell 1 and are specified from interior (primary side) to exterior (secondary side) for each mesh cell.

Friction factor correlation options (NFF) and additive friction losses (FRIC) are given separately for the two sides. The possible options for NFF are described in Chap. III. The homogeneous option (NFF=1) is suggested for both the primary and secondary sides.

The output edit for a steam generator component is similar to that given for a one-dimensional pipe component, with primary side variables given first and then secondary side variables. Also, heat transfer variables are always given. Tube wall temperatures are printed for each active mesh cell on a nodal basis.

G. TEE Module

The TEE module is designed to model the thermal-hydraulics of three piping branches; two of which lie along a common line with the third entering at some angle β from the main axis of the other two (see Fig. 18). From the standpoint of the code, the tee is treated as two pipes, as indicated in Fig. 18. Beta is defined as the angle from the low-numbered end of Pipe 1 to Pipe 2. The low-numbered end of Pipe 2 always connects to Pipe 1. The first pipe increments from Cell 1 to NCELL1 with the connection to Pipe 2 at Cell MSC. Pipe 2 begins at Cell 1 and ends at Cell NCELL2.

The connection to Pipe 1 from Pipe 2 is handled as mass, momentum, and energy source terms while Pipe 2 sees boundary conditions from Cell MSC in Pipe 1. The time differencing and iteration procedure are such that conservation of the scalar quantities is preserved (within a convergence tolerance) and the level of implicitness at the connection ensures that no additional stability limitations apply at a tee. At present, only the semi-implicit solution option is available for use at tees and the model does not treat phase separation at the junction.

Since the tee is modeled as essentially two interconnected pipes, the PIPE model description in Sec. C should be referenced for additional information on the calculational sequence. The subroutines called by the TEE module are

identical to those in PIPE. In TEE, however, the sequence of subroutine calls is performed for each of the two pipe branches.

Detailed input specifications for a tee component are given in Chap. V. Input and output information is very similar to that for a pipe component except that two pipes are involved in a tee component.

H. VALVE Module

The VALVE module is used to model the thermal-hydraulic flow in a valve. A valve is modeled as a one-dimensional component with two fluid cells as shown in Fig. 19. The treatment of heat transfer and fluid dynamics in a valve is identical with that of a pipe. The reader should acquaint himself with the description of a pipe (see Sec. C) in this chapter before proceeding.

Modeling the valve action is done by controlling the flow area and hydraulic diameter between the two fluid cells. The following expressions are used for this purpose:

$$\text{Flow Area} = \text{AVLVE}*\text{FRACT} \tag{9}$$

$$\text{Hydraulic Diameter} = \text{HVLVE}*\text{FRACT}\,, \tag{10}$$

where AVLVE and HVLVE are the fully open valve flow area and hydraulic diameter, respectively, and FRACT is the fraction of the valve that is open.

Five user options are provided for controlling the valve action. Options 1 through 4 allow trip control, with the valve opening or closing instantly or as a function of time. Option 5 models a check valve; an open or closed condition is determined by a pressure differential between the cells and a setpoint. The valve option is specified by the value of the input parameter IVTY. The possible value of IVTY and corresponding options are:

IVTY	Option
1	Valve is normally open and is closed instantly on a trip signal
2	Valve is normally closed and is opened instantly on a trip signal
3	Valve is normally open and is closed on a trip signal according to a time-dependent valve table

IVTY	Option
4	Valve is normally closed and is opened on a trip signal according to a time-dependent valve table
5	Check valve is controlled by a static pressure gradient. If IVPG=1, then DP=P(1)-P(2); if IVPG=2, then DP=P(2)-P(1). IF DP+PVC $\geq$ 0, valve opens instantly. If DP+PVC $<$ 0, valve closes instantly.

Table III summarizes the input parameters needed for the five valve options.

I. VESSEL Module

The VESSEL module models a PWR vessel and associated internals. This is a three-dimensional component employing a six-equation, two-fluid model to evaluate the transient thermal-hydraulic flow through and around all internals of a PWR vessel including the downcomer, core, and upper and lower plenums. Models incorporated into the VESSEL module are designed mainly for LOCA analysis, but the VESSEL module can be applied to other types of transient analyses as well. A reflood model with a treatment of bottom flooding and a falling film is included for LOCA transients. Included also is a point reactor kinetics model. Most of the detailed discussion of the fluid dynamics, heat transfer, and reactor kinetics equations and solution methods for the three-dimensional VESSEL module can be found in Chap. III of this manual. In this section, we will discuss the vessel geometry and other important considerations.

A three-dimensional, two-fluid, thermal-hydraulics model in cylindrical coordinates is used to describe the vessel flow. A regular cylindrical mesh, with variable mesh spacings in all three directions, encompasses the downcomer, core, and upper and lower plenums of the vessel as illustrated in Fig. 20. The code user describes the mesh by specifying the radial, angular, and axial coordinates of mesh cell boundaries:

R_i $\quad i = 1,$ NRSX
θ_j $\quad j = 1,$ NTSX
z_k $\quad k = 1,$ NASX ,

where NRSX is the number of rings, NTSX is the number of angular segments, and NASX is the number of axial levels. The point (r_i,θ_j,z_k) is a vertex in the coordinate mesh. Figure 21 illustrates the mesh construction. Mesh cells are formed as shown in Fig. 22 and identified by an axial level number and a cell number. For each axial level, the cell number is determined by counting the cells radially outward starting with the first angular segment and the innermost ring of cells as shown in Fig. 21. Figure 22 also shows the relative face numbering convention which will be used later in connecting other components to the vessel. Note that only three faces need to be identified per mesh cell since the other faces will be defined by neighboring cells.

All fluid flow areas (on cell faces) and all fluid volumes are dimensioned so that internal structure within the vessel can be modeled. Flow areas and fluid volumes are computed based on the geometric mesh spacings and scaled according to factors supplied as input. The scaled volumes and flow areas are then used in the fluid dynamics and heat transfer calculations. Flow restrictions and volume occupied by structure within each mesh cell are modeled through the use of these scale factors. For example, the downcomer walls are modeled by setting the appropriate flow area scale factors to zero. A feature is provided to do this automatically in the code if the downcomer position parameters IDCU, IDCL, and IDCR are specified as described in the input section (Chap. V, Sec. D). Flow restrictions such as the top and bottom core support plates require scale factors between zero and one. Figure 23 illustrates which cell faces are scaled to model the downcomer and core support plate flow restrictions.

Plumbing connections by other components to the vessel are made on faces of mesh cells. Any number of connections may be made to the vessel. In fact, any mesh cell in the vessel can have a component connected to it. Four input parameters are used to describe a connection: ISRL, ISRC, ISRF, and JUNS. The parameter ISRL defines the axial level in which the connection is made. ISRC is the mesh cell number, as defined above. ISRF is the face number, as defined in Fig. 22. If ISRF is positive, the connection is made on the face shown in the figure with the direction of positive flow inward into the cell. If ISRF is negative, the connection is made on the opposite face shown in the figure with the direction of positive flow also inward into the cell. JUNS is the system junction number used to identify this junction. Figure 24 shows

two pipe connections to the vessel. Note that internal as well as external connections are allowed. In making the connections to the vessel, the user is cautioned against connecting any component to the vessel which has a flow area that differs greatly from the flow area of the mesh cell face it is connected to, as this can cause anomalous pressure spikes. Such a situation can be avoided by proper adjustment of the vessel geometry coordinate spacings.

The reactor core region in the vessel is specified by the core positional parameters ICRU, ICRL, and ICRR. These parameters define, respectively, the upper, lower, and radial boundaries of the cylindrical core region. Figure 25 shows a possible configuration in which ICRU=4, ICRL=2, and ICRR=2. Each mesh cell in the core region can contain an arbitrary number of fuel rods. However, heat transfer calculations are only performed on one average fuel rod and one hot fuel rod in each core mesh cell. The average rod represents the average of the ensemble of rods in the mesh cell and its thermal calculation couples directly to the fluid dynamics. The hot fuel rod calculation does not feed back or couple directly to the fluid dynamics analyses. However, the local fluid conditions in the mesh cell are used to calculate a hot fuel rod temperature history. A fuel-clad interaction treatment and a reflood treatment are available for these calculations and are described in Chap. III.

Heat slabs of arbitrary masses and volumes can be defined in any mesh cell (including core regions) to model the heat capacity of structure within the vessel. A heat transfer coefficient is computed for each slab using the local fluid conditions, and the temperature calculation is based on a lumped parameter model (see Chap. III, Sec. B.1.b).

The total power level in the core is determined from either a table lookup or from the solution of the point-reactor kinetics equations, as described in Chap. III. The spatial power distribution in the core is specified by separate axial and radial power shapes, plus a power distribution across the fuel rods. These spatial distributions are specified in relative units at input and are held constant throughout a problem. The power density in fuel rod node i in cell j on core level k is given by the expression:

$$P(i,j,k) = S \cdot P_{tot} \cdot RDPWR(i) \cdot CPOWR(j) \cdot ZPOWR(k), \qquad (11)$$

where P_{tot} is the total core power level, RDPWR(i) is the relative power in fuel node i, CPOWR(j) is the relative power in cell j, ZPOWR(k) is the

relative power at core elevation k, and S is the scale factor used to normalize the three input relative power distributions. The scale factor S is given by the expression:

$$S = \left[\sum_{i,j,k} \left(\text{AREA}(i) \cdot \text{RDPWR}(i) \cdot \text{NRDX}(j) \cdot \text{CPOWR}(j) \cdot \Delta z(k) \cdot \text{ZPOWR}(k) \right) \right]^{-1}, \tag{12}$$

where AREA(i) is the cross-sectional area of fuel rod node i, NRDX(j) is the number of fuel rods in cell j, and $\Delta z(k)$ is the height of core axial level k. For the hot fuel rod analyses, the power density in Eq. (20) is multiplied by an input peaking factor RPKF(j) to obtain the power density for the hot fuel rod. If a peaking factor is set equal to one, a hot fuel rod analysis is not performed.

REFERENCES

1. V. L. Streeter and E. B. Wylie, Hydraulic Transients (McGraw-Hill, New York, 1967), pp. 151-160.

2. D. J. Olsen, "Experiment Data Report for Single- and Two-Phase Steady-State Tests of the 1 -Loop MOD-1 Semiscale System Pump," Aerojet Nuclear Company report ANCR-1150 (May 1974).

3. G. G. Loomis, "Intact Loop Pump Performance During the Semiscale MOD-1 Isothermal Test Series," Aerojet Nuclear Company report ANCR-1240 (October 1975).

4. D. J. Olson, "Single- and Two-Phase Performance Characteristics of the MOD-1 Semiscale Pump Under Steady-State and Transient Fluid Conditions," Aerojet Nuclear Company report ANCR-1165 (October 1974).

TABLE I

DEFINITION OF THE FOUR CURVE SEGMENTS USED TO DESCRIBE HOMOLOGOUS PUMP CURVES

Curve Segment	$\left\|\frac{q}{\omega}\right\|$	ω	q	Correlation
1	≤ 1	> 0		$\left[\frac{h}{\omega^2} = f\left(\frac{q}{\omega}\right)\right]$
4	≤ 1	< 0		
3	> 1		< 0	$\left[\frac{h}{q^2} = f\left(\frac{\omega}{q}\right)\right]$
2	> 1		≥ 0	

q = normalized flow

ω = normalized angular velocity

h = normalized head

TABLE II

PUMP CONTROL INPUT PARAMETERS

IPMPTY Pump Option	IPMPTR Pump trip I.D.	NPMPTX Pairs of Points	SPTBL Speed Table	Pump Speed Algorithm
1	x = Pump trip desired	x	x	OMEGA before trip
	0 = No pump trip	0		SPTBL after trip
2	x = Pump trip desired	x		OMEGA before trip
	0 = No pump trip	0		Code calculated after trip

TABLE III

VALVE CONTROL INPUT PARAMETERS

IVTY: Valve Option Number	IVTR: Valve TRIP ID Number	NVTX: No. of Valve Table Entries	IVPG: Pressure Gradient Option	PVC: Check Valve Setpoint	VLTB: Valve Table (fraction open)	AVLVE: Valve Open Area	HVLVE: Valve Open Hydraulic Diameter
1	X					X	X
2	X					X	X
3	X	X			X	X	X
4	X	X			X	X	X
5			X	X		X	X

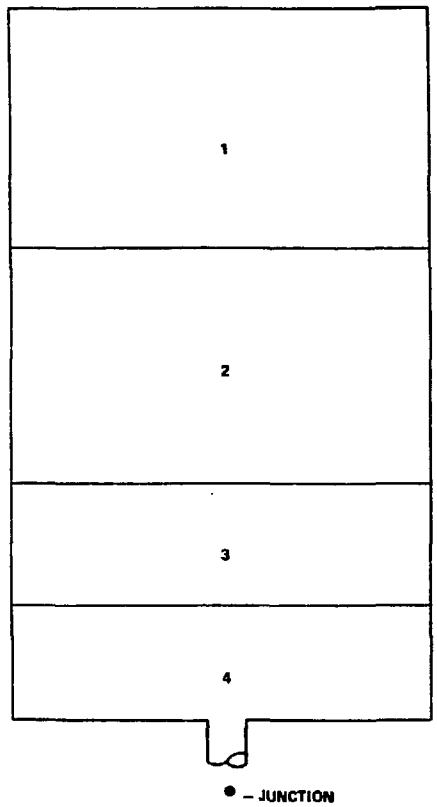

Fig. 1.
Accumulator noding diagram.

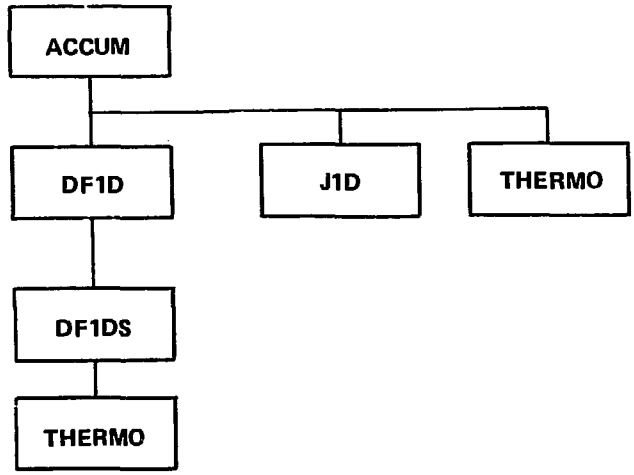

Fig. 2.
Accumulator module calling tree.

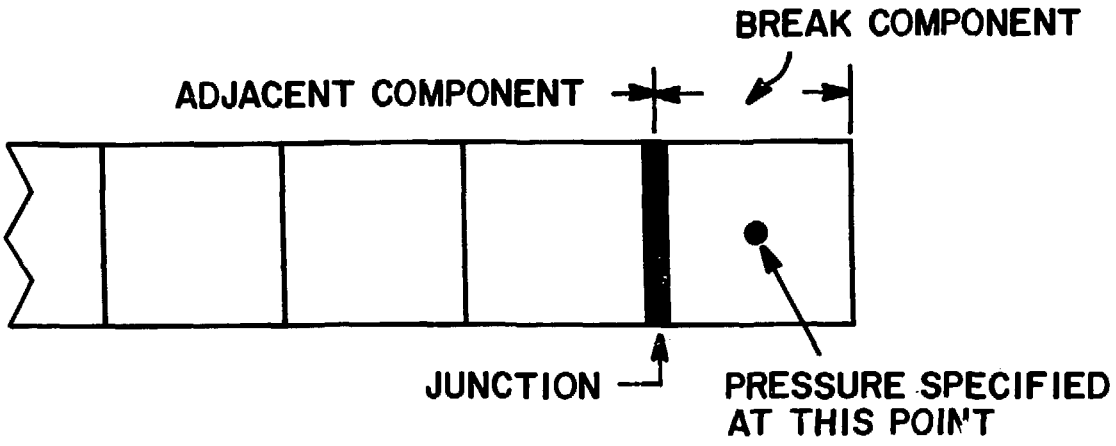

Fig. 3.
Break noding diagram

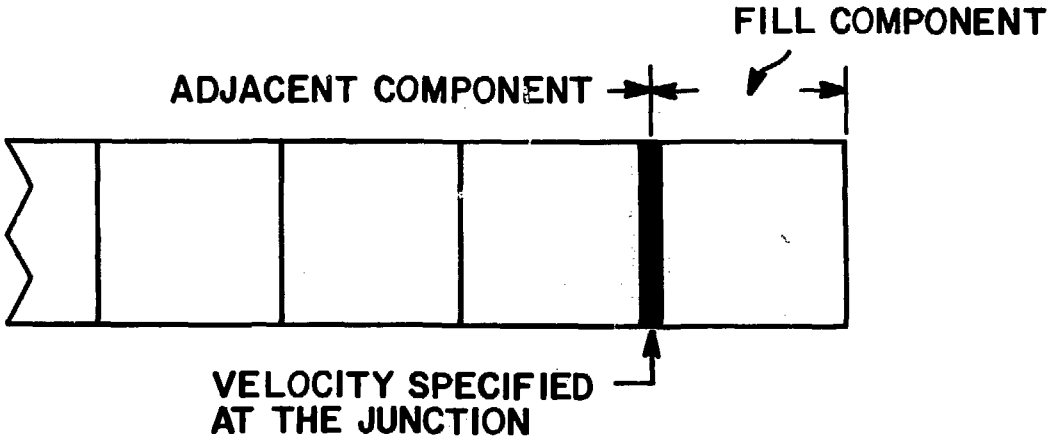

Fig. 4.
Fill noding diagram.

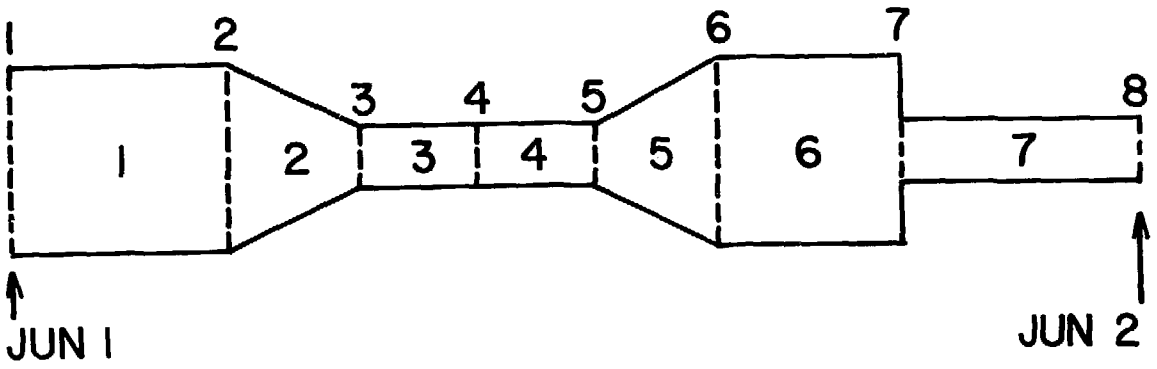

Fig. 5.
Pipe noding diagram.

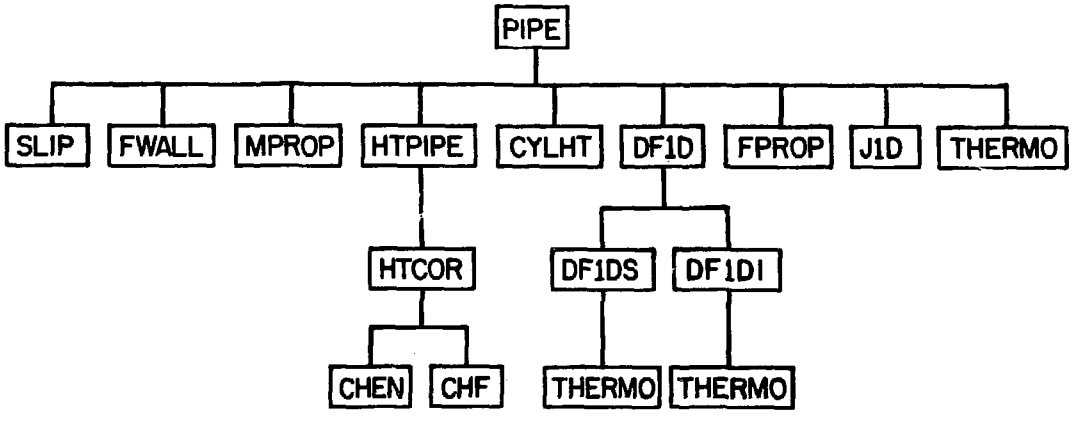

Fig. 6.
Pipe module calling tree.

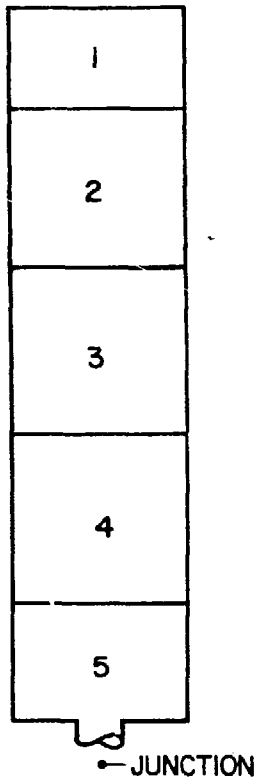

Fig. 7.
Pressurizer noding diagram.

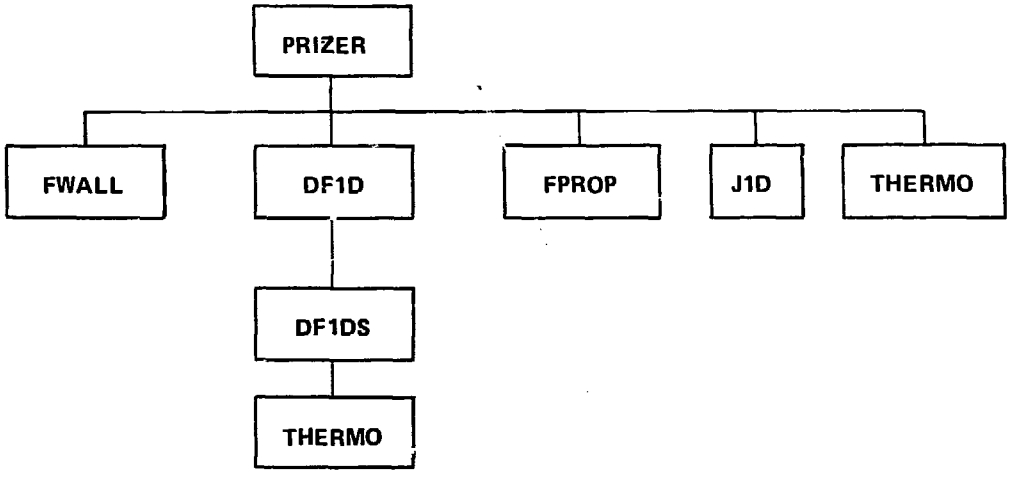

Fig. 8.
Pressurizer module calling tree.

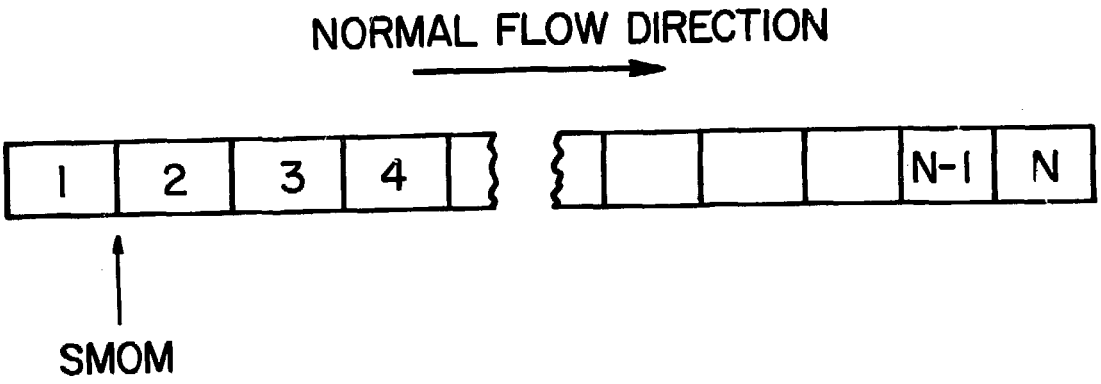

Fig. 9.
Pump noding diagram.

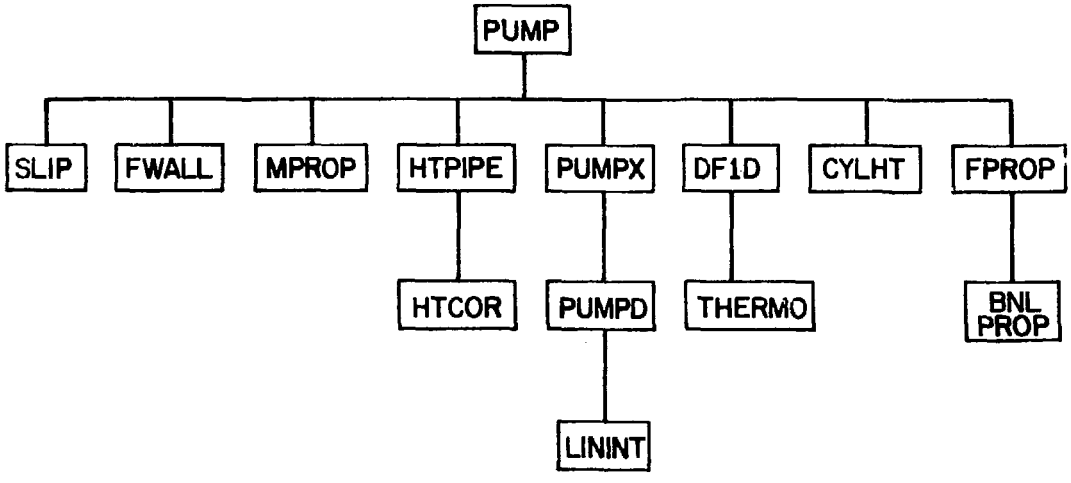

Fig. 10.
Pump module calling tree.

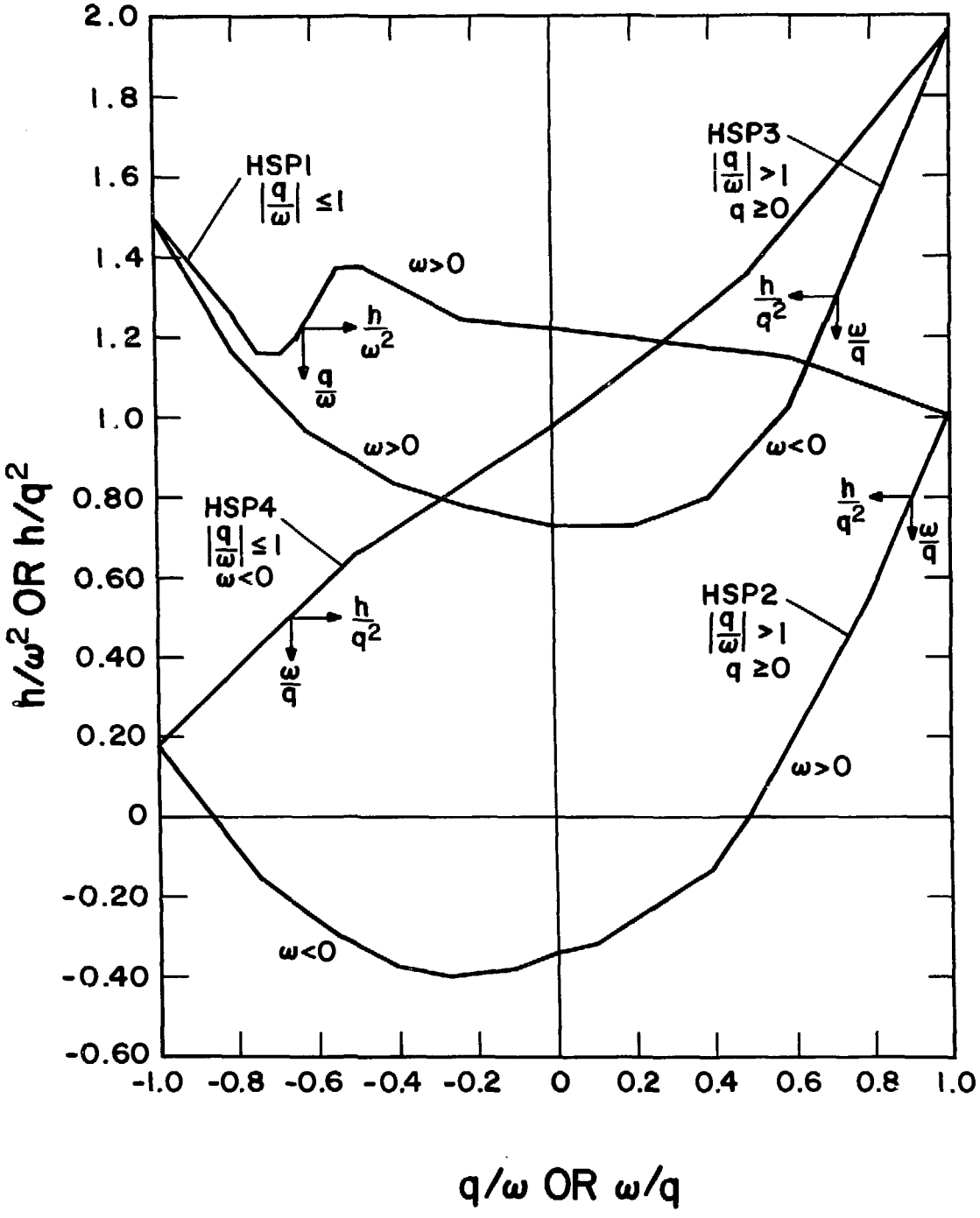

Fig. 11.
Single-phase homologous head curves.

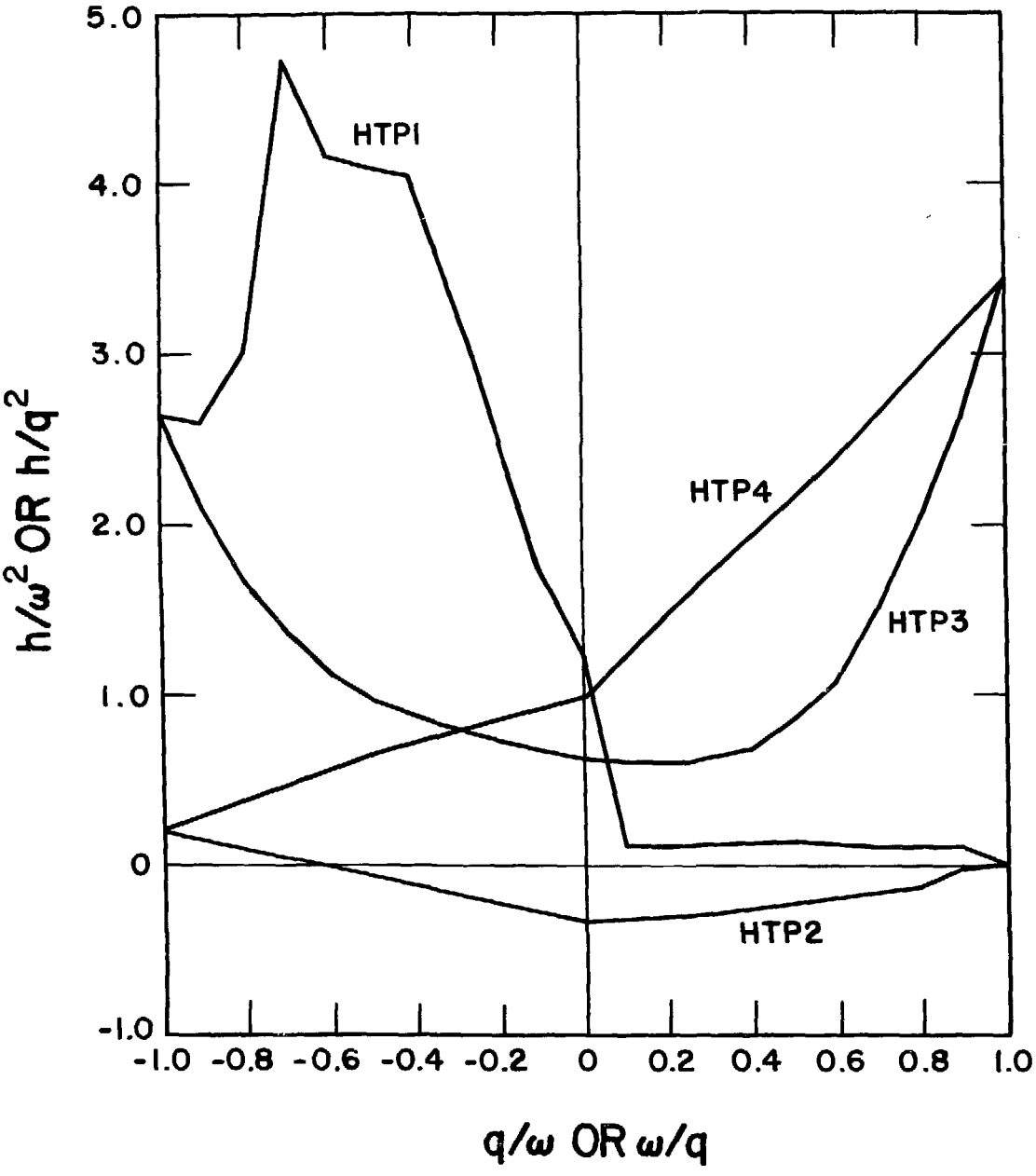

Fig. 12.
Fully degraded homologous head curves.

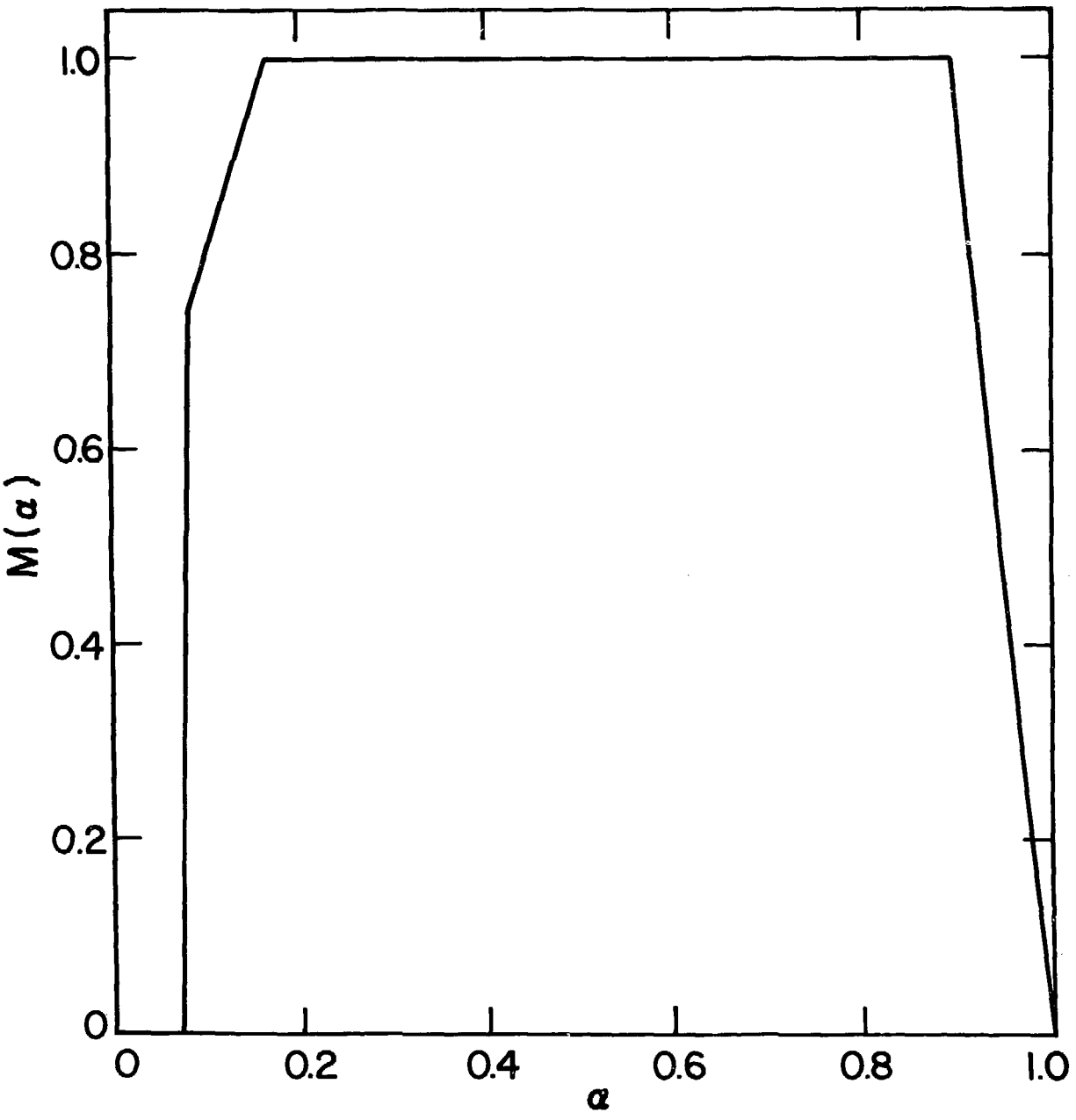

Fig. 13.
Head degradation multiplier.

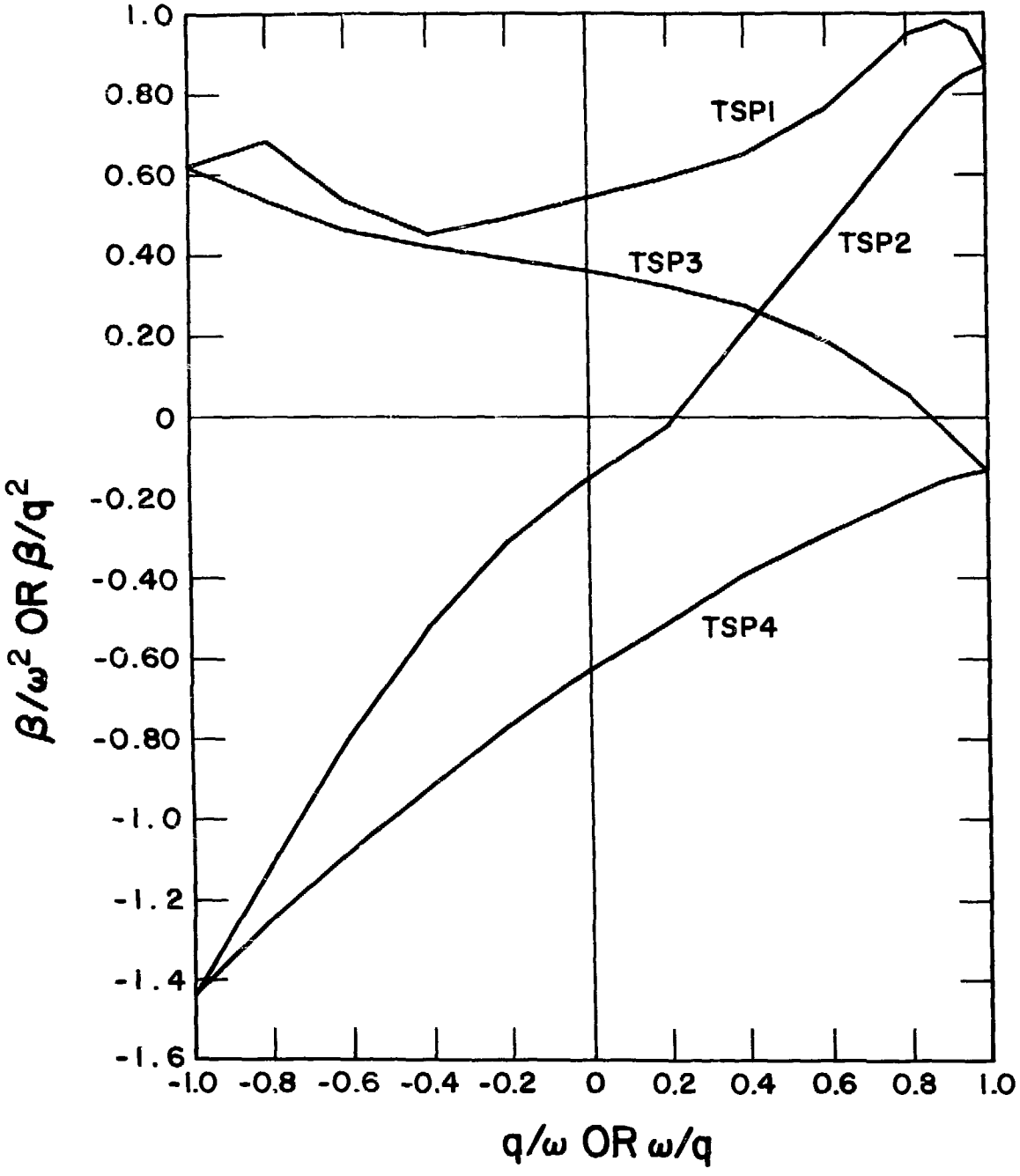

Fig. 14.
Single-phase homologous torque curves.

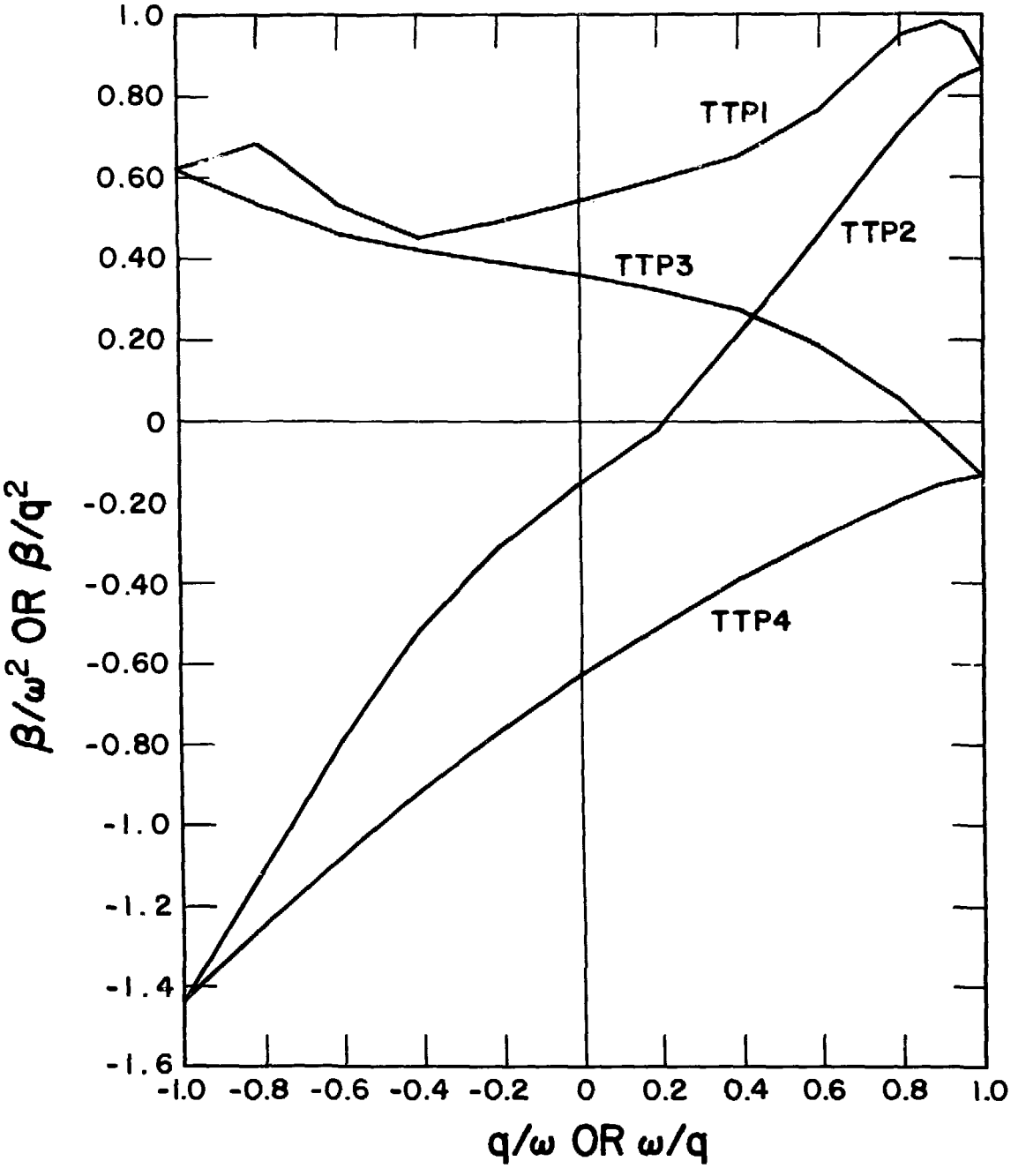

Fig. 15.
Fully degraded homologous torque curves.

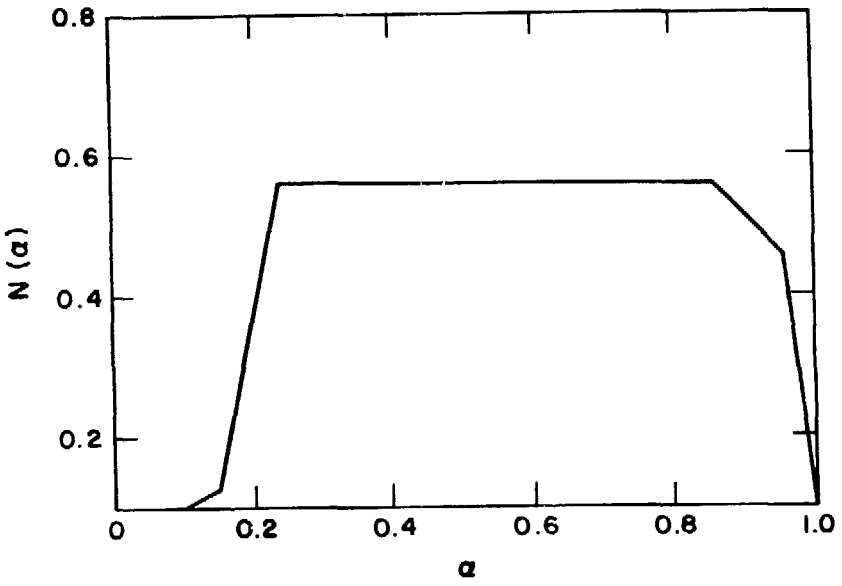

Fig. 16.
Torque degradation multiplier.

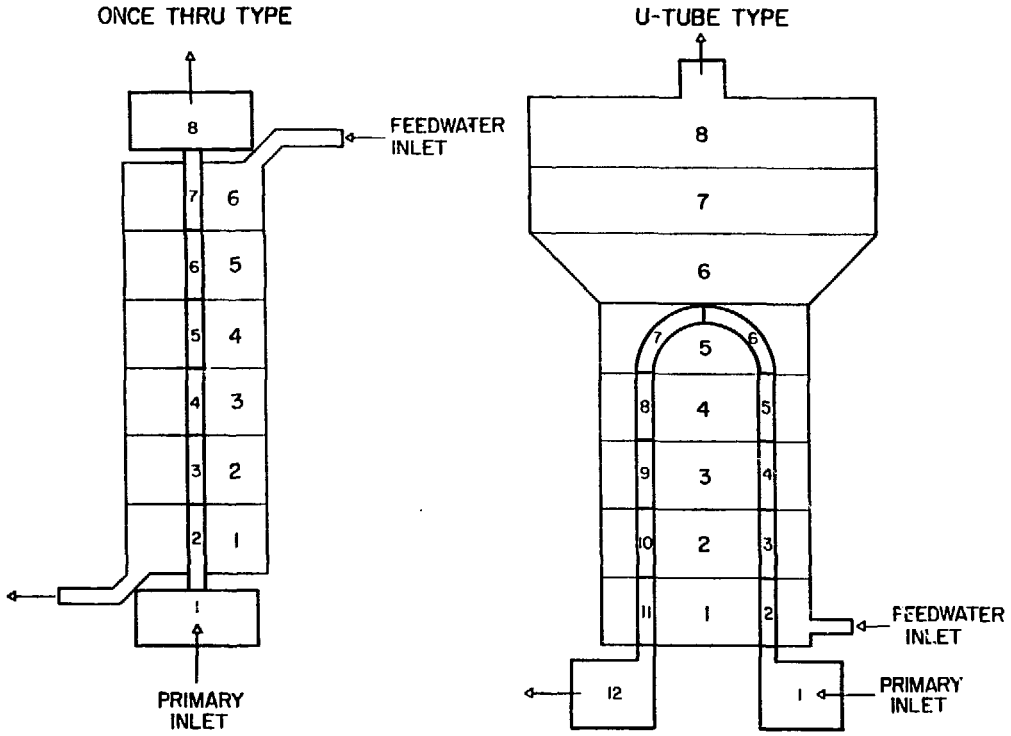

STEAM GENERATOR GEOMETRY

Fig. 17.
Steam generator noding diagram.

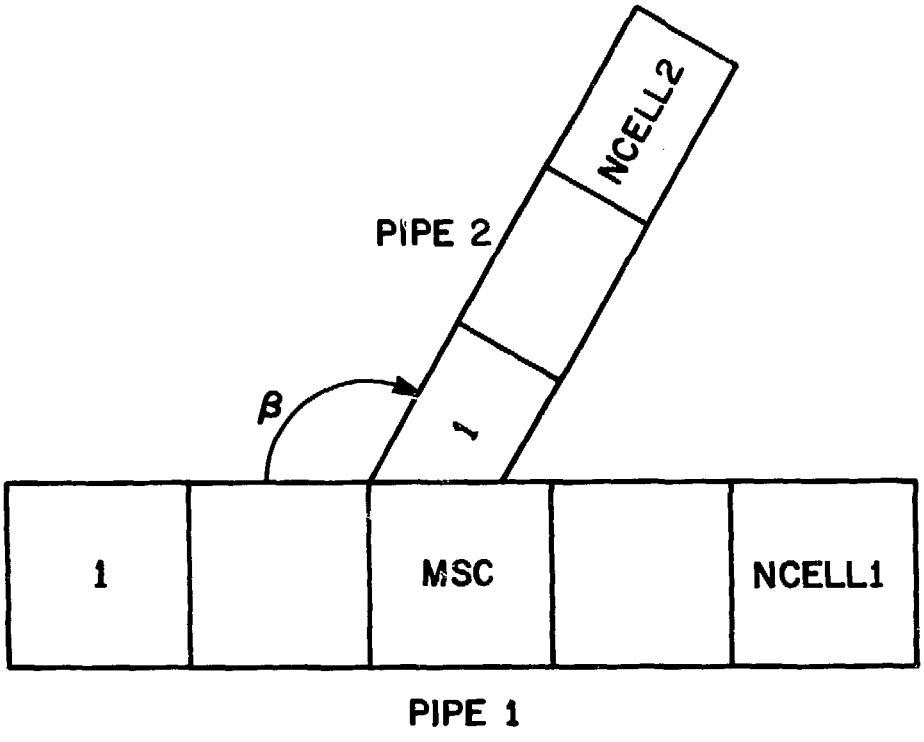

Fig. 18.
Tee noding diagram.

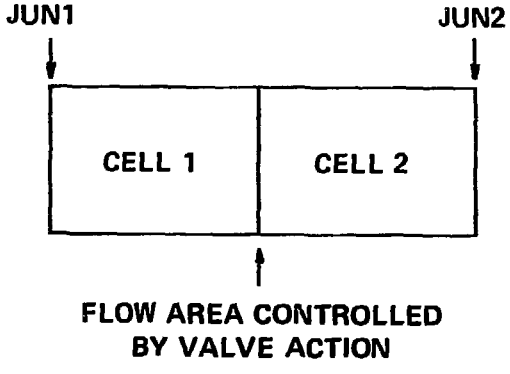

Fig. 19.
Valve noding diagram.

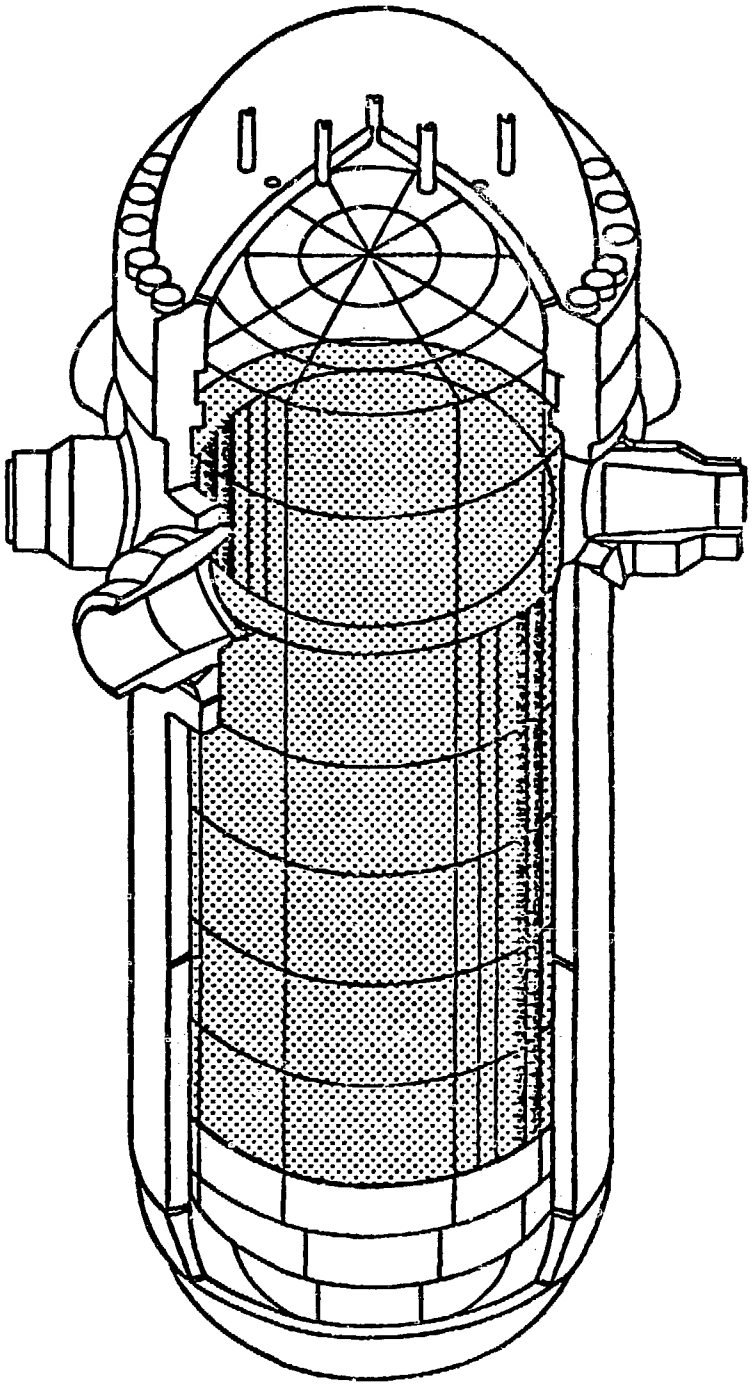

Fig. 20.
Cell noding diagram for a typical PWR vessel.

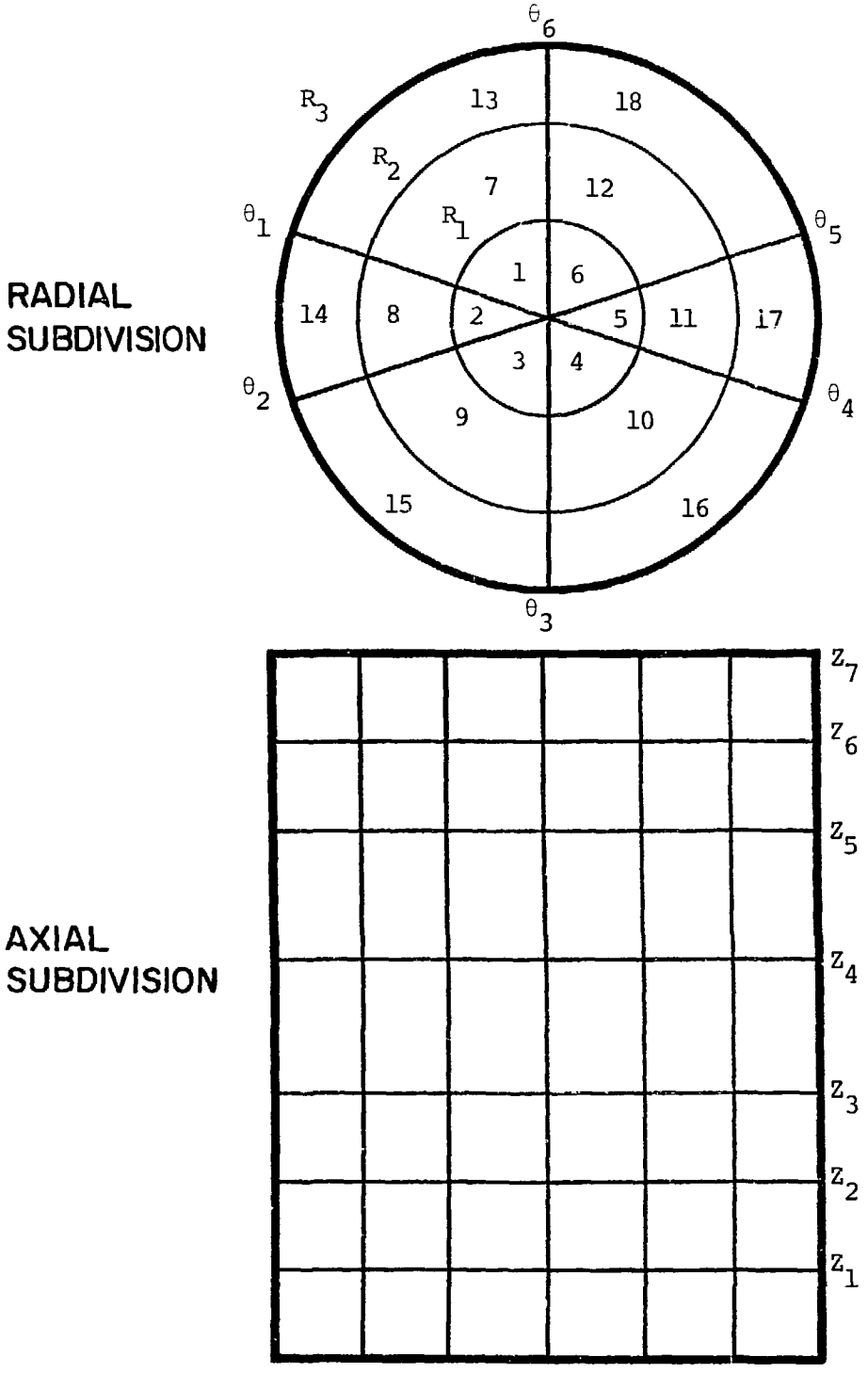

Fig. 21.
3-D mesh construction with 3 rings,
6 angular segments, and 7 axial intervals.

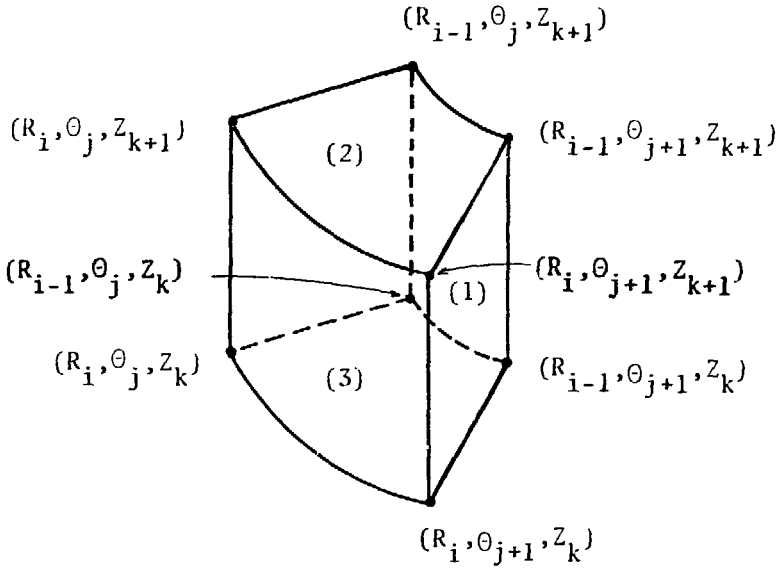

Fig. 22.
Boundaries of a 3-D mesh cell. The face numbering convention is also shown. Faces 1, 2, and 3 are in the θ, z, and r directions, respectively.

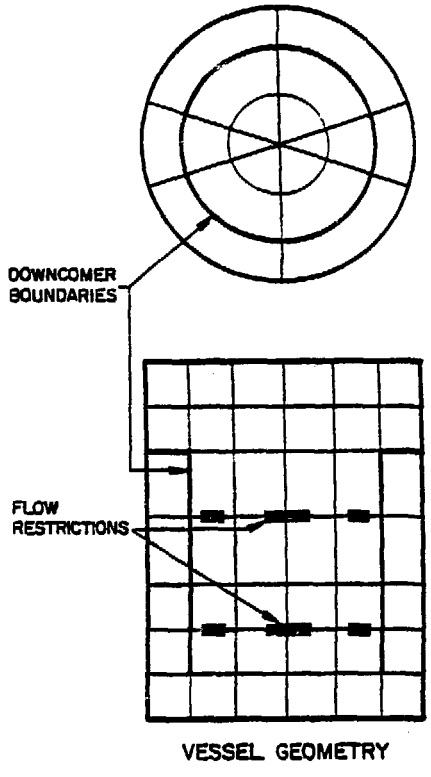

Fig. 23.
Flow restrictions and downcomer modeling.

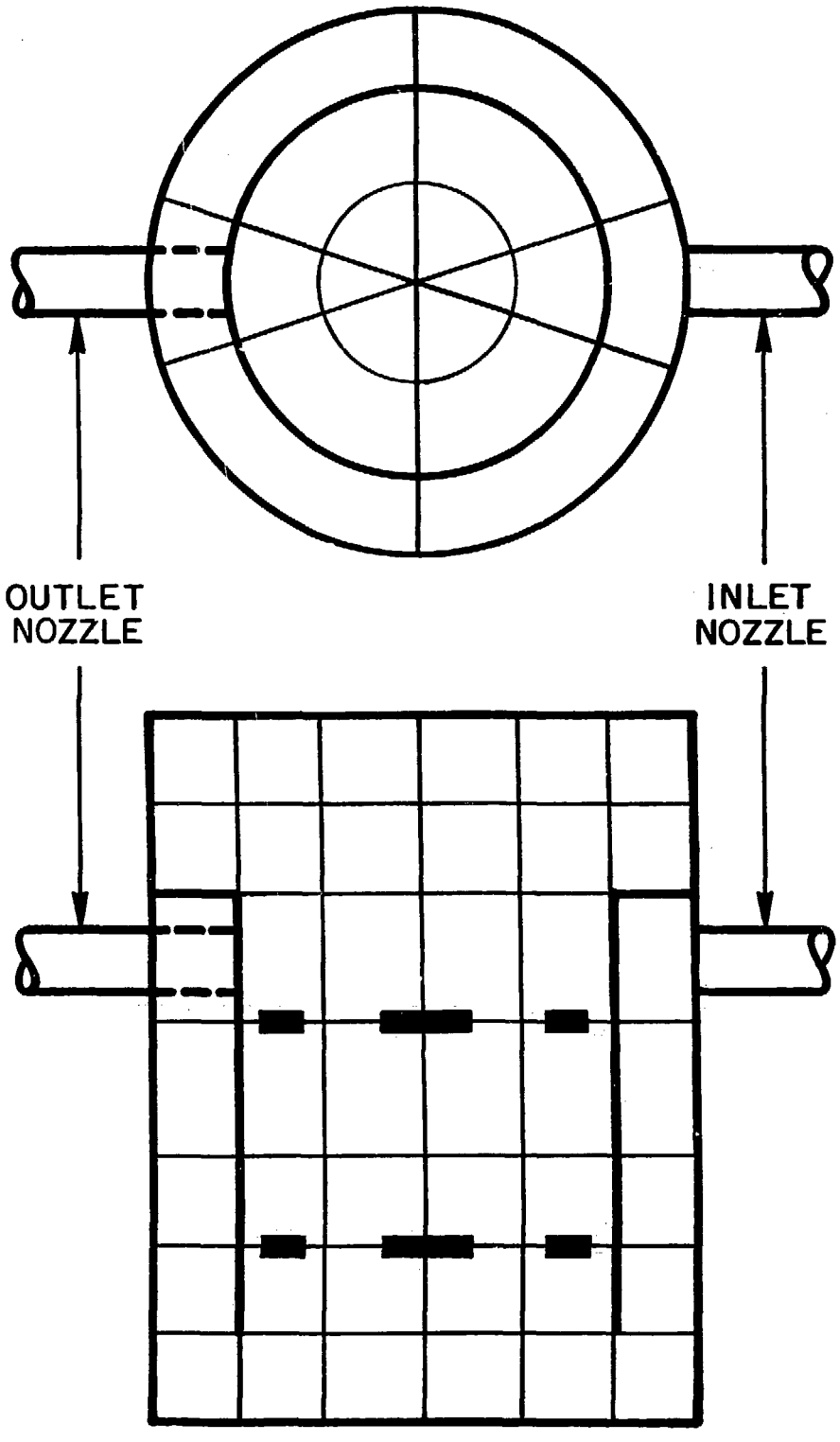

Fig. 24.
Illustration of pipe connections to the vessel.

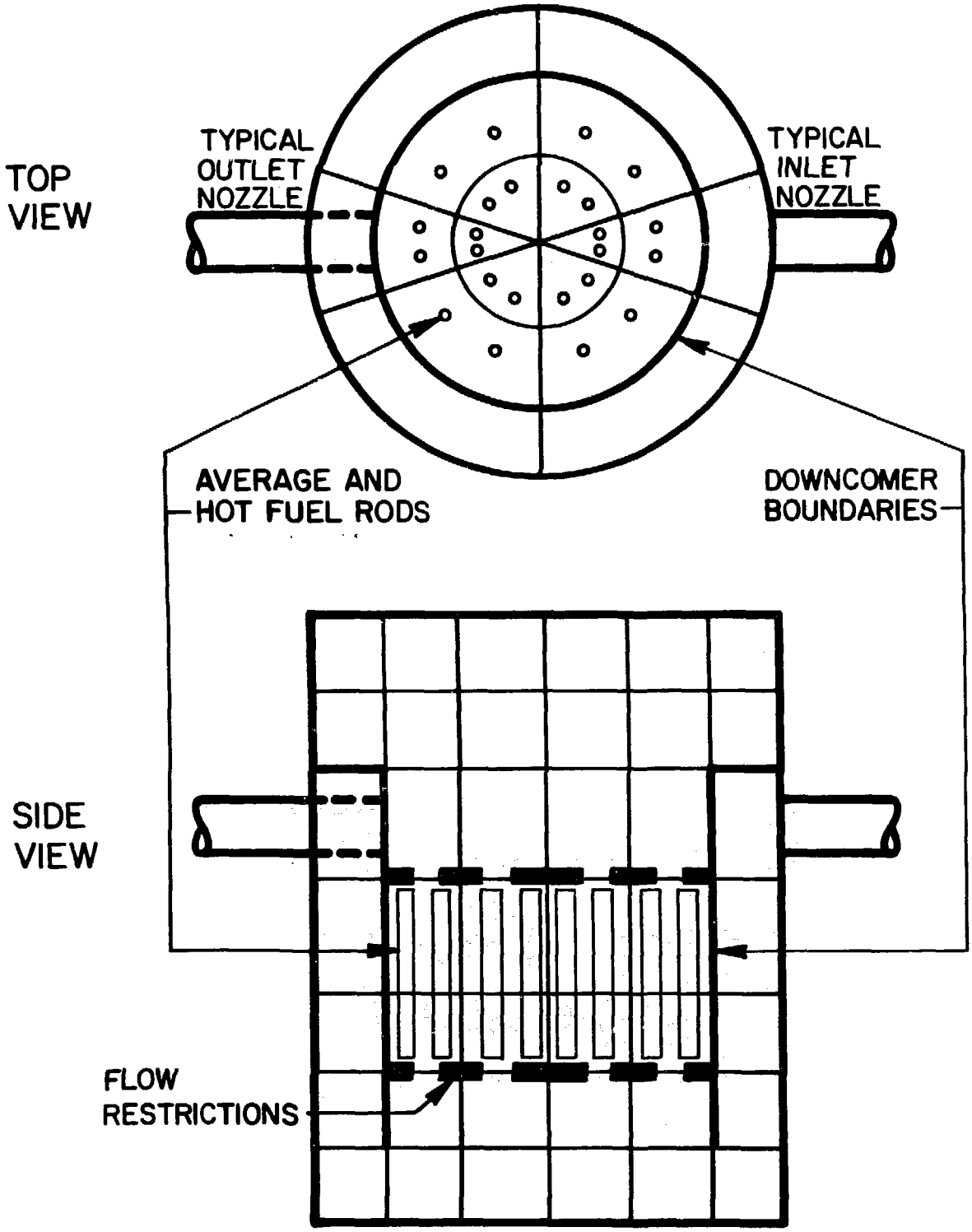

Fig. 25. Illustration of a core region inside the vessel.

V. USER INFORMATION

This chapter describes the details of setting up a problem input data deck, obtaining restart dumps and restarting problems from these dumps, and producing printer and graphics output files.

A. Input Organization and Format

The input deck is divided into five major sections including control, trip, component, PWR initialization, and time step data blocks. These data blocks are contained in a file named TRACIN and are read in the order shown in Fig. 1. The control block contains general control parameters including title cards for problem identification, restart and dump control information, transient and steady-state control information, problem size information, and problem convergence criteria. This data block must always be present in the TRACIN file. Trip control information and detailed specifications for each trip that is included in the problem are provided in the second data block. The trip data block is present only if control parameter NTRX > 0 in the first data block. Trip input data can also be fully or partially provided from a restart dump file.

The main body of the input deck is contained in the component data block. This block contains a detailed description of every component in the problem unless the case is to be reinitiated from a restart dump. For restart problems, only those components that are added to the problem or modified are included in the component block. The rest of the component data is obtained from the restart file. Thus, the component data block is always present in the TRACIN file unless all the component data are obtained from the restart file.

A PWR initialization data block is required only if SIDYST=2 or 3 has been specified in the control data. This block contains several user-specified steady-state operating conditions which the code attempts to match by adjusting certain operating parameters. The time step data block must always be present in the TRACIN file. It is used to specify maximum and minimum time step sizes, edit frequencies, and the end of the problem.

All input data contained on the TRACIN file are read into the code with either a 5E14.6 or 5I14 format statement or by the LOAD subroutine. Standard

FORTRAN statements are used on the formatted reads. The LOAD subroutine provides the user with additional flexibility in specifying data arrays.

The following sections of this chapter cover the trip capability and its input, the dump/restart feature, a detailed description of the input deck, the description of the LOAD subroutine read formats, and a description of the TRAC output files. A sample input deck for a full-scale, four-loop PWR calculation is provided in Appendix C.

B. Trips

Trips provide the means of simulating the actions of a power plant protective system to transient or abnormal conditions. Trips control such actions as reactor scrams, valve openings, and pump startups. In TRAC, the actions are performed by the component modules. The VALVE module, for example, has been coded to open (or close) a valve once an appropriate trip occurs. Other modules have been coded similarly. A trip condition is indicated by a status flag, which is set after a trip has occurred. A problem description can have any number of trips specified with one or more components referencing the same trip.

The criteria for deciding when a trip has occurred are based upon three parameters supplied as input: a signal index (ISID), a signal setpoint (TSP), and a signal delay time (TDT). The signal index defines the type of variable to be observed (i.e., the variable used to activate the trip) and can correspond to a pressure, temperature, water level, or any number of other component parameters. Parameter differentials and multiple parameters may also be chosen. The signal setpoint defines the setting at which the trip will occur. This setting may be an upper limit of the observed variable if ISID > 0, or a lower limit if ISID < 0. The signal delay time serves to simulate the time necessary to process the signal and to initiate the action. A trip status flag is set when the signal delay time has lapsed after the observed variable has reached the signal setpoint.

The component modules determine the status of a trip by the subroutine call statement:

```
CALL TRIP(ITID,ICOND,TLAPS)
```

where ITID is passed and is the trip ID number, ICOND is returned and is equal to zero if a trip has not occurred and is equal to 1 if it has, and TLAPS is returned and is the time since the trip has occurred.

The trips needed in a problem are declared when specifying the component module input. Eight parameters are used to define each trip: ITID, ISID, TSP, TDT, ID1, ID2, ID3, and ID4. ITID is the trip identification number. This number is arbitrarily chosen to distinguish one trip from another. ISID, TSP, and TDT are defined above. Table I provides the correspondence between the signal index and the variable types. The parameters ID1-ID4 are qualifiers that specify the location of the observed variable(s) in the component data base. ID1 identifies the component by the component ID number. ID2 is a second component qualifier and is zero unless the component is a steam generator or vessel. For a steam generator, a value of 1 means that the variable is on the primary side; 2 means that the variable is on the secondary side. If the component is a vessel, then the value of ID2 corresponds to the vessel axial level. Parameters ID3 and ID4 specify the element(s) if the variable is an array. The possible choices of ID3 and ID4 and their meanings are given in Fig. 2.

For illustrative purposes, consider the example:

ITID = 16	ID1 = 6
ISID = 1	ID2 = 0
TSP = 1.7×10^7	ID3 = 3
TDT = 0.1	ID4 = 0

The trip ID number 16 is arbitrary; however, it is this number that must be used in the component input to identify this trip. The positive signal index of 1 means that an upper pressure limit is defined. TSP defines the pressure limit to be 170 bars. TDT defines the trip delay time of 0.1 s after the pressure limit is reached. ID1 = 6 means that the pressure is to be found in the data base for component 6. ID2 = 0 means that this component is something other than a steam generator or vessel. ID3 = 3 and ID4 = 0 means that the third pressure in the array of pressures (pressure of the third cell) is the tested variable.

C. Dump/Restart Feature

TRAC automatically generates a dump/restart data file named TRCDMP, which contains snapshots of the state of the system at various times during problem execution. Any one of these snapshots, called dumps, may be used to initialize all or part of the system for subsequent calculations. The times at which dumps are generated are determined by several criteria. The user may specify, on the time step cards, a dump interval. A dump will be created whenever this interval of time has elapsed since the last dump. These dumps are added sequentially to the end of the TRCDMP file. A dump may also be initiated by the user with one or more of the TRIPS. When the conditions of this TRIP occur, a dump is added to the end of the TRCDMP file. This permits the restart of a problem from the occurrence of particular events of interest.

In addition to these user-specified dumps, TRAC will automatically generate dumps at various times. A dump is generated at the end of the initialization stage. Another dump is generated at the end of the steady-state or transient calculation, and at intermediate points in the calculation based upon CPU time utilized and remaining for the job.

To use a dump file in initializing a subsequent calculation, the name of the file must be changed from TRCDMP to TRCRST. The time step number of the particular dump desired must be specified on Main Control Card 1. (A message containing this dump time step number is sent to the print file TRCOUT whenever a dump is written.) If the time step number specified is negative, TRAC will use the dump with the largest time step number and overwrite the initial time (specified on Main Control Card 1) with the time taken from that dump.

Data retrieved from the selected dump depends on what has already been found in the TRACIN file. Any component not processed by RDCOMP (as determined from the component numbers listed in the IORDER array), is initialized from the dump. Also, any trip found in the dump which has not been initialized by RDTRIP will be initialized in the state found on the dump.

D. TRAC Input Specifications

The TRAC input data may be classified into five general types of data:

1. Main Control,
2. Trip,
3. Component,
4. PWR Initialization, and

5. Time Step.

These classes of data are entered in the above order. All quantities should be entered in standard SI units. Quantities entered in I or E formats should be right justified in their fields and Hollerith information read in A format should be left justified except where noted.

1. Main Control Data

The main control parameters are listed below in the order in which they are entered. This data block must always be supplied in the input.

Card No. 1. (Format I14) NUMTCR

Columns	Variable	Description
1-14	NUMTCR	Number of title cards to be read in. Note: At least one title card must be supplied.

Title Card(s). (Format 20A4) NUMTCR Cards

1-80		Problem title information.

Main Control Card 1. (Format I14,E14.6) DSTEP, TIMET

1-14	DSTEP	Time step number of dump to be used for restart. If DSTEP is less than zero the last dump found will be used for restart.
15-28	TIMET	Problem start time. If DSTEP is less than zero this will be overridden by the time specified for the retrieved dump.

Main Control Card 2. (FORMAT 5I14) STDYST, TRANSI, NCOMP, NJUN, IPAK

1-14	STDYST	Steady-state calculation indicator: =0, no steady-state calculation, =1, generalized steady-state calculation, =2, PWR initialization calculation, and =3, PWR initialization calculation with initial evaluation of operating parameters.
15-28	TRANSI	Transient calculation indicator (0 = no transient calculation, 1 = transient to be calculated).
29-42	NCOMP	Number of components.
43-56	NJUN	Number of junctions.

57-70	IPAK	Water packing option (0=Off, 1=On).

Main Control Card 3. (Format 5E14.6) EPSO, EPSI, EPSS

1-14	EPSO	Convergence criterion for outer iteration (suggested value = 1.0 E-03).
15-28	EPSI	Convergence criterion for inner iteration (suggested value = 1.0 E-03).
29-42	EPSS	Convergence criterion for steady-state calculation (suggested value = 1.0 E-02).
43-56	EPSP	PWR initialization convergence criterion (suggested value = 1.0 E-01).

Main Control Card 4. (Format 5I14) IITMAX, OITMAX, SITMAX, NTRX, NDMPTR

1-14	IITMAX	Maximum number of inner iterations (suggested value = 1).
15-28	OITMAX	Maximum number of outer iterations (suggested value = 20)21
29-42	SITMAX	Maximum number of outer iterations for steady-state calculation (suggested value = 20).
43-56	NTRX	Number of trips specified.
57-70	NDMPTR	Number of trips on which a dump is to be taken.

Iteration Order Card(s). (Format (5(3x,I11)) IORDER(i), i=1, NCOMP

4-14	IORDER(1)	Component number which is first in the iteration sequence.
18-28	IORDER(2)	Component number which is second in the iteration sequence.
29-42	IORDER(3)	etc.

Trip Dump Card(s). (Format 5I14) IDMPTR(i), i=1, NDMPTR

1-14	IDMPTR(1)	First trip ID number which causes dump.
15-28	IDMPTR(2)	Second trip ID number which causes dump.
29-42	IDMPTR(3)	etc.

2. Trip Data

NTRX or fewer sets of trip cards are input. The sets may be input in any order. If less than NTRX sets are input, the end of the trip data is signified by specifying the trip ID to be a negative number. In this case, the second trip card is omitted and the remaining trips are initialized from the TRCRST file. (It should be noted that the state as well as the definition of the trip is obtained from the restart file.) Trips with IDs equal to or greater than 1000 will cause the time step size to be reduced to the minimum allowable size (i.e., DTMIN). See Sec. B above for detailed description of TRIP variables.

TRIP Card 1. (Format 2I14,2E14.6) ITID, ISID, TSP, TDT

Columns	Variable	Description
1-14	ITID	Trip ID number.
15-28	ISID	Trip signal index.
29-42	TSP	Trip setpoint.
43-56	TDT	Trip delay time.

TRIP Card 2. (Format 5I14) ID1, ID2, ID3, ID4

1-14	ID1	First trip qualifier.
15-28	ID2	Second trip qualifier.
29-42	ID3	Third trip qualifier.
43-56	ID4	Fourth trip qualifier.

3. Component Data

NCOMP or fewer sets of component cards are input. The sets may be input in any order. If less than NCOMP sets are input, the end of component data is demarked by a single card containing the characters END in columns 1-3. In this case the remaining components are initialized from the TRCRST file. The format of each set is dependent upon the component type. The input format for the components as presently implemented is as follows. Most of the subscripted component data variables are processed by the LOAD subroutine described in Sec. E below. Additional information on preparing component input

data can be found in Chapter IV where component models are described. All tables which are entered pairs of numbers (x,y) should be supplied in ascending order of the independent variable x.

Each component requires the user to supply a junction number JUN for each of its connecting points. A pipe will require two junction numbers, one for each end. A junction is the point at which two components are connected. A unique junction number must be assigned to each connecting point and referenced by both of the components that are to be connected. For example, if two pipes are to be joined, then the junction numbers of the connecting end of each pipe need to be the same. No component may connect to itself and no function may have only one component connected to it. Any of several single-ended components (BREAK, FILL, etc.) may be used to complete a junction.

a. Accumulator Component (ACCUM)

Card 1. (Format A6,8X,2I14) TYPE, NUM, ID

Columns	Variable	Description
1-6	TYPE	Type of component (ACCUM left justified).
15-28	NUM	Component ID number (must be unique for each component).
29-42	ID	User ID number (arbitrary).

Card 2. (Format 5I14) NCELLS, JUN2

1-14	NCELLS	Number of fluid cells.
15-28	JUN2	Junction number for junction adjacent to cell NCELLS. This must be the accumulator discharge.

Accum Array Cards. 12 sets of cards. One set for each of the following variables. Use LOAD format.

Variable	Dimension	Description
DX	NCELLS	Cell lengths.
VOL	NCELLS	Cell volumes.
FA	NCELLS+1	Cell edge flow areas.
FRIC	NCELLS+1	Additive loss coefficients.
GRAV	NCELLS+1	Cosine of the angle between a vertical vector pointing up and a vector from cell N to cell N+1.
HD	NCELLS+1	Hydraulic diameters.
NFF	NCELLS+1	Friction factor correlation options. 0 = Constant Friction Factor, User Input, 1 = Homogeneous Flow Friction Factor, 2 = Armand Friction Factor, 3 = CISE Friction Factor, 4 = Annular Flow Friction Factor, and 5 = Chisholm Friction Factor. Use negative values for automatic form loss computation (see Sec. III.A.1.d).
ALP	NCELLS	Initial void fractions.

VM	NCELLS+1	Initial mixture velocities.
TL	NCELLS	Initial liquid temperatures.
TV	NCELLS	Initial vapor temperatures.
P	NCELLS	Initial pressures.

b. Break Component (BREAK)

Card 1. (Format A6,8X,2I14) TYPE, NUM, ID

Columns	Variable	Description
1-6	TYPE	Type of component (BREAK left justified).
15-28	NUM	Component ID number (must be unique for each component).
29-42	ID	User ID number (arbitrary).

Card 2. (Format 5I14) JUN1

1-14	JUN1	Junction number at which break is located.

Card 3. (Format 5E14.6) DXIN, VOLIN, ALPIN, TIN, PIN

1-14	DXIN	Length of break cell. (Generally taken to be the same as its neighboring cell in the adjacent pipe.)
15-28	VOLIN	Volume of break cell. (Generally taken to be the same as its neighboring cell in the adjacent pipe.)
29-42	ALPIN	Void fraction of mixture at break. (Usually 1.0.)
43-56	TIN	Temperature of mixture at break. (Usually taken to be the saturation temperature corresponding to the break pressure.)
57-70	PIN	Pressure at break.

c. Fill Component (FILL)

Card 1. (Format A6,8X,2I14) TYPE, NUM, ID

Columns	Variable	Description
1-6	TYPE	Type of component (FILL left justified).
15-28	NUM	Component ID number (must be unique for each component).
29-42	ID	User ID number (arbitrary).

Card 2. (Format 5I14) JUN1, IFTY, IFTR, NFTX

1-14	JUN1	Junction number at which fill is located.
15-28	IFTY	FILL type option 1 - constant velocity 2 - velocity vs time 3 - velocity vs pressure 4 - constant velocity until trip then velocity vs time 5 - constant velocity until trip then velocity vs pressure
29-42	IFTR	Trip ID number
43-56	NFTX	Number of FILL table pairs

Card 3. (Format 5E14.6) DXIN, VOLIN, ALPIN, VIN, TIN

1-14	DXIN	Length of cell. (Generally taken to be the same as its neighboring cell in the adjacent component.)
15-28	VOLIN	Volume of cell. (Generally taken to be the same as that of its neighboring cell in the adjacent component.)
29-42	ALPIN	Void fraction for entrant material.
43-56	VIN	Entrant mixture velocity.
57-70	TIN	Entrant mixture temperature.

Card 4. (Format 5E14.6) PIN

1-14	PIN	Fill pressure.

FILL Table Cards. LOAD format (omit if NFTX = 0).

Variable	Dimension	Description
FTAB	NFTX*2	FILL table (time or pressure, velocity)$_i$ i = 1, NFTX.

d. Pipe Component (PIPE)

Card 1. (Format A6,8X,2I14) TYPE, NUM, ID

1-6	TYPE	Type of component (PIPE left justified).
15-28	NUM	Component ID number (must be unique for each component).
39-42	ID	User ID number (arbitrary).

Card 2. (Format 5I14) NCELLS, NODES, JUN1, JUN2, MAT

1-14	NCELLS	Number of fluid cells in this pipe.
15-28	NODES	Number of radial heat transfer nodes in pipe wall. (0 implies no wall heat transfer.)
29-42	JUN1	Junction number for junction adjacent to cell 1.
43-56	JUN2	Junction number for junction adjacent to cell NCELLS.
57-70	MAT	Material ID of pipe wall. 6 = SS 304, 7 = SS 316, 8 = SS 347, 9 = Carbon Steel A508, and 10= Inconel 718.

Card 3. (Format 2I14) ICHF, IHYDRO

1-14	ICHF	CHF calculation flag. 0 = no CHF calculation, 1 = Zuber/Biasi for rod CHF, 2 = Biasi CHF correlation only, and 3 = Bowring CHF correlation only.
15-28	IHYDRO	1-D hydrodynamics option (0 = partially implicit; 1 = fully implicit).

Card 4. (Format 5E14.6) RADIN, TH, HOUTL, HOUTV, TOUTL

1-14	RADIN	Inner radius of pipe wall.
15-28	TH	Pipe wall thickness.
29-42	HOUTL	Heat transfer coefficient between outer boundary of pipe wall and liquid.

43-56	HOUTV	Heat transfer coefficient between outer boundary of pipe wall and vapor.
57-70	TOUTL	Liquid temperature outside pipe.

Card 5. (Format 5E14.6) TOUTV

1-14	TOUTV	Vapor temperature outside pipe.

Note: The four parameters HOUTL, HOUTV, TOUTL, and TOUTV are provided to allow flexibility in calculating possible heat losses from the outside of pipes. Typically, such heat losses are not important, and HOUTL and HOUTV are set equal to zero. Further, when heat losses are significant, they can often be described by a single heat transfer coefficient (e.g., characteristic of air) and a single external temperature.

Pipe Array Cards. 13 sets of cards. One set for each of the following variables. LOAD format.

Variable	Dimension	Description
DX	NCELLS	Cell lengths.
VOL	NCELLS	Cell volumes.
FA	NCELLS+1	Cell edge flow areas.
FRIC	NCELLS+1	Additive loss coefficients.
GRAV	NCELLS+1	Cosine of the angle between a vertical vector pointing up and a vector from cell N to cell N+1.
HD	NCELLS+1	Hydraulic diameters.
NFF	NCELLS+1	Friction factor correlation options. (See ACCUM input description.)
QPPP	NCELLS	Volumetric heat sources in pipe wall.
ALP	NCELLS	Initial void fractions.
VM	NCELLS+1	Initial mixture velocities.
TL	NCELLS	Initial liquid temperatures.
P	NCELLS	Initial pressures.
TW	NCELLS*NODES	Initial wall temperatures. (Eliminate this card set if NODES=0.)

e. Pressurizer Component (PRIZER)

Card 1. (Format A6,8X,2I14) TYPE, NUM, ID

Columns	Variable	Description
1-6	TYPE	Type of component (PRIZER left justified).
15-28	NUM	Component ID number (must be unique for each component).
29-42	ID	User ID number (arbitrary).

Card 2. (Format 5I14) NCELLS, JUN2

1-14	NCELLS	Number of fluid cells.
15-28	JUN2	Junction number for junction adjacent to cell NCELL. This must be the pressurizer discharge.

Card 3. (Format 5E14.6) QHEAT, PSET, DPMAX, ZHTR

1-14	QHEAT	Total heater power (Watts).
15-28	PSET	Pressure set point for heater/sprayer controller.
29-42	DPMAX	Pressure differential at which heater/sprayer has maximum power.
43-56	ZHTR	Water level for heater cutoff.

PRIZER Array Cards. 12 sets of cards. One set for each of the following variables. LOAD format.

Variable	Dimension	Description
DX	NCELLS	Cell lengths.
VOL	NCELLS	Cell volumes.
FA	NCELLS+1	Cell edge flow areas.
FRIC	NCELLS+1	Additive loss coefficients.
GRAV	NCELLS+1	Cosine of the angle between a vertical vector pointing up and a vector from cell N to cell N+1.
HD	NCELLS+1	Hydraulic diameters.

NFF	NCELLS+1	Friction factor correlation options (see ACCUM input description, NFF=1 is suggested for this component).
ALP	NCELLS	Initial void fractions.
VM	NCELLS+1	Initial mixture velocities.
TL	NCELLS	Initial liquid temperatures.
TV	NCELLS	Initial vapor temperatures.
P	NCELLS	Initial pressures.

f. Pump Component (PUMP)

Card 1. (Format A6,8X,2I14) TYPE, NUM, ID

Columns	Variable	Description
1-6	TYPE	Type of component (PUMP left justified).
15-28	NUM	Component ID number (must be unique for each component).
29-42	ID	User ID number (arbitrary).

Card 2. (Format 5I14) NCELLS, NODES, JUN1, JUN2, MAT

1-14	NCELLS	Number of fluid cells in pump (must be at least two).
15-28	NODES	Number of radial heat transfer nodes in wall. (0 implies no wall heat transfer.)
29-42	JUN1	Junction number for junction adjacent to cell 1.
43-56	JUN2	Junction number for junction adjacent to cell NCELLS.
57-70	MAT	Material ID of wall (see PIPE input description).

Card 3. (Format 5I14) ICHF, IHYDRO, IPMPTY, IRP, IPM

1-14	ICHF	CHF calculation flag. 0 = no calculation 1 = Zuber/Biasi for rod CHF 2 = Biasi CHF correlation only 3 = Bowring CHF correlation only
15-28	IHYDRO	1-D hydrodynamics option (0 = partially implicit; 1 = fully implicit).
29-42	IPMPTY	Pump type (1 or 2). (See PUMP component description).
43-56	IRP	Reverse speed option (0 = reverse rotation not allowed; 1 = allowed).
57-70	IPM	Two-phase option (0 = use single-phase curves; 1 = use two-phase curves).

Card 4. (Format 5I14) IPMPTR, NPMPTX

1-14	IPMPTR	Pump speed table trip I.D.
14-28	NPMPTX	Number of pairs of points in the pump speed table.

Card 5. (Format 5E14.6) RADIN, TH, HOUTL, HOUTV, TOUTL

1-14	RADIN	Inner radius of pump wall.
15-28	TH	Pump wall thickness.
29-42	HOUTL	Heat transfer coefficient between outer boundary of pump wall and liquid.
43-56	HOUTV	Heat transfer coefficient between outer boundary of pump wall and vapor.
57-70	TOUTL	Liquid temperature outside pump wall.

Card 6. (Format 5E14.6) TOUTV

1-14	TOUTV	Vapor temperature outside pump wall.

(See PIPE module description for further comments on these heat transfer parameters.)

Card 7. (Format 5E14.6) RHEAD, RTORK, RFLOW, RRHO, ROMEGA

1-14	RHEAD	Rated head.
15-28	RTORK	Rated torque.
29-42	RFLOW	Rated flow.
43-56	RRHO	Rated density.
57-70	ROMEGA	Rated pump speed.

Card 8. (Format 5E14.6) EFFMI, TFR1, TFR2, OMEGA

1-14	EFFMI	Effective moment of inertia.
15-28	TFR1	Constant torque due to friction.
29-42	TFR2	Bearing and windage torque constant.
43-56	OMEGA	Initial pump speed.

Card 9. (Format 5I14) OPTION PUMP SPEED TABLE CARDS

1-14	OPTION	Pump curve option number. 0 = User specified pump, input following. 1 = Use built in PUMP 1 (Pump 1 = Semi-scale pump).

Card set 10 and pump curve cards are needed only if OPTION = 0. If OPTION = 1 skip to pump array cards. The user is referred to the pump model description in Chapter IV for a definition of the terminology used below.

Card Set 10. (Format 5I14)(NDATA(I),I=1, 16) NHDM, NTDM

First Card.

1-14	NDATA(1)	Number of pairs of points on the HSP1 curve.
15-28	NDATA(2)	Number of pairs of points on the HSP2 curve.
29-42	NDATA(3)	Number of pairs of points on the HSP3 curve.
43-56	NDATA(4)	Number of pairs of points on the HSP4 curve.
57-70	NDATA(5)	Number of pairs of points on the HTP1 curve.

Second Card.

1-14	NDATA(6)	Number of pairs of points on the HTP2 curve.
15-28	NDATA(7)	Number of pairs of points on the HTP3 curve.
29-42	NDATA(8)	Number of pairs of points on the HTP4 curve.
43-56	NDATA(9)	Number of pairs of points on the TSP1 curve.
57-70	NDATA(10)	Number of pairs of points on the TSP2 curve.

Third Card.

1-14	NDATA(11)	Number of pairs of points on the TSP3 curve.

15-28	NDATA(12)	Number of pairs of points on the TSP4 curve.
29-42	NDATA(13)	Number of pairs of points on the TTP1 curve.
43-56	NDATA(14)	Number of pairs of points on the TTP2 curve.
57-70	NDATA(15)	Number of pairs of points on the TTP3 curve.

Fourth Card.

1-14	NDATA(16)	Number of pairs of points on the TTP4 curve.
15-28	NHDM	Number of pairs of points on the HDM curve.
29-42	NTDM	Number of pairs of points on the TDM curve.

Pump Curve Cards. Up to 18 sets of cards. One set for each curve listed in card set 9 which has nonzero data points. LOAD format. Data is entered in pairs $(x,y)_i$, $i = 1,NDATA$ where x is the independent variable and y is the dependent variable.

Variable	Dimension	Description	
HSP1	2*NDATA(1)	HSP1 curve.	single-phase head curves
HSP2	2*NDATA(2)	HSP2 curve.	
HSP3	2*NDATA(3)	HSP3 curve.	
HSP4	2*NDATA(4)	HSP4 curve.	
HTP1	2*NDATA(5)	HTP1 curve.	fully degraded head curves
HTP2	2*NDATA(6)	HTP2 curve.	
HTP3	2*NDATA(7)	HTP3 curve.	
HTP4	2*NDATA(8)	HTP4 curve.	
TSP1	2*NDATA(9)	TSP1 curve.	single-phase torque curves
TSP2	2*NDATA(10)	TSP2 curve.	
TSP3	2*NDATA(10)	TSP3 curve.	

TSP4	2*NDATA(12)	TSP4 curve.	
TTP1	2*NDATA(13)	TTP1 curve.	fully degraded torque curves
TTP2	2*NDATA(14)	TTP2 curve.	
TTP3	2*NDATA(15)	TTP3 curve.	
TTP4	2*NDATA(16)	TTP4 curve.	
HDM	2*NHDM	HDM curve (head degradation multiplier).	
TDM	2*NTDM	TDM curve (torque degradation multiplier).	

Pump Array Cards. 13 sets of cards. One set for each of the following variables. LOAD format.

Variable	Dimension	Description
SPTBL	2*NPMPTX	Time since trip vs pump speed table.
DX	NCELLS	Cell lengths.
VOL	NCELLS	Cell volumes.
FA	NCELLS+1	Cell edge flow areas.
FRIC	NCELLS+1	Additive loss coefficients.
GRAV	NCELLS+1	Cosine of the angle between a vertical vector pointing up and a vector from cell N to cell N+1.
HD	NCELLS+1	Hydraulic diameters.
NFF	NCELLS+1	Friction factor correlation options. (see ACCUM input description)
QPPP	NCELLS	Volumetric heat sources in pipe wall.
ALP	NCELLS	Initial void fractions.
VM	NCELLS+1	Initial mixture velocities.
TL	NCELLS	Initial liquid temperatures.
P	NCELLS	Initial pressures. this card set if NODES = 0.)
TW	NCELLS*NODES	Initial wall temperatures (eliminate this card set if NODES=0).

g. Steam Generator Component (STGEN)

Card 1. (Format A6,8X,2I14) TYPE, NUM, ID

Columns	Variable	Description
1-6	TYPE	Type of component (STGEN left justified).
15-28	NUM	Component ID number (must be unique for each component).
29-42	ID	User ID number (arbitrary).

Card 2. (Format 5I14) NCELL1, NODES, JUN11, JUN12, MAT

1-14	NCELL1	Number of fluid cells on primary side.
15-28	NODES	Number of radial heat transfer nodes in wall. (MUST be greater than or equal to 1.)
29-42	JUN11	Junction number for junction adjacent to cell 1 on primary side.
43-56	JUN12	Junction number adjacent to cell NCELL1 on primary side.
57-70	MAT	Material ID of tube (see PIPE input description).

Card 3. (Format 5I14) KIND, IHYDRO

1-14	KIND	Kind of steam generator (1 = U-tube; 2 = Once-through).
15-28	IHYDRO	Type of hydrodynamics on primary side (0 = partially implicit; 1 = fully implicit).
29-42	ICHF1	Indicator for CHF calculation on primary side (0 = no calculation, 1 = CHF calculation).
43-56	ICHF2	Indicator for CHF calculation on secondary side (0 = no calculation, 1 = CHF calculation).

Card 4. (Format 5E14.6) RADIN, TH

1-14	RADIN	Inner radius of a tube wall.
15-28	TH	Tube wall thickness.

Card 5. (Format 5E14) NCELL2, JUN21, JUN22

1-14	NCELL2	Number of fluid cells on secondary side.
15-28	JUN21	Junction number for junction adjacent to cell 1 on secondary side.
29-42	JUN22	Junction number for junction adjacent to cell NCELL2 on secondary side.

STGEN Array Cards. 27 sets of cards. One set for each of the following variables. LOAD format.

Variable	Dimension	Description
DX1	NCELL1	Cell lengths on primary side.
VOL1	NCELL1	Cell volumes on primary side for all tubes.
FA1	NCELL1+1	Cell edge flow areas on primary side for all tubes.
FRIC1	NCELL1+1	Additive loss coefficients on primary side.
GRAV1	NCELL1+1	Cosine of the angle between a vertical vector pointing up and a vector from cell N to cell N+1.
HD1	NCELL1+1	Hydraulic diameters for primary side for a single tube.
NFF1	NCELL1+1	Friction factor correlation options for primary side (see ACCUM input description).
WA1	NCELL1	Wall areas for primary side for all tubes.
ALP1	NCELL1	Initial void fractions for primary side.
VM1	NCELL1+1	Initial mixture velocities for primary side.
TL1	NCELL1	Initial liquid temperatures for primary side.
TV2	NCELL1	Initial vapor temperatures for primary side.
P1	NCELL1	Initial pressures for primary side.
DX2	NCELL2	Cell lengths on secondary side.

VOL2	NCELL2	Cell volumes on secondary side.
FA2	NCELL2+1	Cell edge flow areas on secondary side.
FRIC2	NCELL2+1	Additive loss coefficients on secondary side.
GRAV2	NCELL2+1	Cosine of the angle between a vertical vector pointing up and a vector from cell N to cell N+1 on the secondary side.
HD2	NCELL2+1	Hydraulic diameters on secondary side.
NFF2	NCELL2+1	Friction factor correlation option for secondary side (see ACCUM input description).
WA2	NCELL2	Wall areas for secondary side for all tubes.
ALP2	NCELL2	Initial void fractions for secondary side.
VM2	NCELL2+1	Initial mixture velocities for secondary side.
TL2	NCELL2	Initial liquid temperatures for secondary side.
TV2	NCELL2	Initial vapor temperatures for secondary side.
P2	NCELL2	Initial pressures for secondary side.
TW	NCELL1*NODES	Initial tube wall temperatures.

h. Tee Component (TEE)

Card 1. (Format A6,8X,2I14) TYPE, NUM, ID

1-6	TYPE	Type of component (TEE left justified).
15-28	NUM	Component ID number (must be unique for each component).
29-42	ID	User ID number (arbitrary).

Card 2. (Format 3I14, E14.6, I14) JCELL, NODES, MATID, COST, ICHF

1-14	JCELL	Junction cell number.
15-28	NODES	Number of radial heat-transfer nodes in the tee wall. (0 implies no wall heat transfer.)
29-42	MATID	Material ID of tee wall (see PIPE input description).
43-56	COST	Cosine of the angle from the low-numbered side of the primary tube to the secondary tube.
57-70	ICHF	CHF calculation flag. 0 = no calculation, 1 = Zuber/Biasi for rod CHF, 2 = Biasi CHF correlation only, 3 = Bowring CHF correlation only.

Card 3. (Format 2I14) IHYDRO, NCELL1, JUN1, JUN2

1-14	IHYDRO	1-D hydrodynamics option (must be set = 0).
15-28	NCELL1	Number of fluid cells in the primary tee tube.
29-42	JUN1	Junction number for the junction adjacent to cell 1.
43-56	JUN2	Junction number for the junction adjacent to cell NCELL1.

Card 4. (Format 5E14.6) RADIN1, TH1, HOUTL1, HOUTV1, TOUTL1

1-14	RADIN1	Inner radius of the primary tube wall.
15-28	TH1	Wall thickness of the primary tube.

29-42	HOUTL1	Heat transfer coefficient to liquid at the outer boundary of the primary tube wall.
43-56	HOUTV1	Heat transfer coefficient to vapor at the outer boundary of the primary tube wall.
57-70	TOUTL1	Temperature of liquid outside primary tube wall.

Card 5. (Format E14.6) TOUTV1

1-14	TOUTV1	Temperature of vapor outside primary tube wall.

(See PIPE module description for further comments on these heat transfer parameters.)

Card 6. (Format 5I14) NCELL2, JUN3

1-14	NCELL2	Number of fluid cells in the secondary tee tube.
15-28	JUN3	Junction number of the free end of the secondary tube (cell NCELL2).

Card 7. (Format 5E14.6) RADIN2, TH2, HOUTL2, HOUTV2, TOUTL2

1-14	RADIN2	Inner radius of the secondary tube wall.
15-28	TH2	Wall thickness of the secondary tube.
29-42	HOUTL2	Heat transfer coefficient to liquid at the outer boundary of the secondary tube wall.
43-56	HOUTV2	Heat transfer coefficient to vapor at the outer boundary of the secondary tube wall.
57-70	TOUTL2	Temperature of liquid outside secondary tube wall.

Card 8. (Format 5E14.6) TOUTV2

1-14	TOUTV2	Temperature of vapor outside secondary tube wall.

(See comment on Card 5.)

Tee Array Cards. 24 sets of cards - Two sets (one for the primary tube and one for the secondary tube) for each of the following variables. LOAD format.

Variable	Dimension	Description
DX	NCELL1	Cell lengths (primary).
DX	NCELL2	Cell lengths (secondary).
VOL	NCELL1	Cell volumes (primary).
VOL	NCELL2	Cell volumes (secondary).
FA	NCELL1+1	Cell edge flow areas (primary).
FA	NCELL2+1	Cell edge flow areas (secondary).
FRIC	NCELL1+1	Additive loss coefficients (primary).
FRIC	NCELL2+1	Additive loss coefficients (secondary).
GRAV	NCELL1+1	Cosine of the angle between a vertical vector pointing up and a vector from cell N to cell N+1 (primary).
GRAV	NCELL2+1	Cosine of the angle between a vertical vector pointing up and the vector from cell N to cell N+1 (secondary).
HD	NCELL1+1	Hydraulic diameters (primary).
HD	NCELL2+1	Hydraulic diameters (secondary).
NFF	NCELL1+1	Friction factor correlation options for primary tube (see ACCUM input description).
NFF	NCELL2+1	Friction factor correlation options for secondary tube (see ACCUM input description).
QPPP	NCELL1	Volumetric heat sources in pipe wall (primary).
QPPP	NCELL2	Volumetric heat sources in pipe wall (secondary).
ALP	NCELL1	Initial void fractions (primary).
ALP	NCELL2	Initial void fractions (secondary).
VM	NCELL1+1	Initial mixture velocities (primary).

VM	NCELL2+1	Initial mixture velocities (secondary).
TL	NCELL1	Initial liquid temperatures (primary).
TL	NCELL2	Initial liquid temperatures (secondary).
P	NCELL1	Initial pressures (primary).
P	NCELL2	Initial pressures (secondary).
TW	NCELL1*NODES	Initial wall temperatures for primary tube. (Eliminate this card set if NODES = 0.)
TW	NCELL2*NODES	Initial wall temperatures for secondary tube. (Eliminate this card set if NODES = 0.)

i. Valve Component (VALVE)

Card 1. (Format A6,8X,2I14) TYPE, NUM, ID

Columns	Variable	Description
1-6	TYPE	Type of component (VALVE left justified).
15-28	NUM	Component ID number (must be unique for each component).
29-42	ID	User ID number (arbitrary).

Card 2. (Format 5I14) NCELLS, NODES, JUN1, JUN2, MAT

1-14	NCELLS	Number of fluid cells (restricted to two).
15-28	NODES	Number of radial heat transfer nodes in valve wall. (0 implies no wall heat transfer.)
29-42	JUN1	Junction number for junction adjacent to cell 1.
43-56	JUN2	Junction number for junction adjacent to cell NCELLS.
57-70	MAT	Material ID of wall (see PIPE input description).

Card 3. (Format 5I14) ICHF, IHYDRO

1-14	ICHF	CHF calculation flag. 0 = no calculation, 1 = Zuber/Biasi for rod CHF, 2 = Biasi CHF correlation only, and 3 = Bowring CHF correlation only.
15-28	IHYDRO	1-D hydrodynamics option (0 = partially implicit; 1 = fully implicit).

Card 4. (Format 5E14.6) RADIN, TH, HOUTL, HOUTV, TOUTL

1-14	RADIN	Inner radius of valve wall.
15-28	TH	Valve wall thickness.
29-42	HOUTL	Heat transfer coefficient between outer boundary of valve wall and liquid.

43-56	HOUTV	Heat transfer coefficient between outer boundary of valve wall and vapor.
57-70	TOUTL	Liquid temperature outside valve.

Card 5. (Format 5E14.6) TOUTV

1-14	TOUTV	Vapor temperature outside pipe.

(See PIPE module description for further comments on these heat transfer parameters.)

Card 6. (Format 5I14) IVTY, IVTR, NVTX, IVPG

1-14	IVTY	Valve type option. IVTY — OPTION 1 — Valve normally open - trip closes it instantaneously. 2 — Valve normally closed - trip opens it instantaneously. 3 — Valve normally open - trip initiated closing specified by time-dependent table. 4 — Valve normally closed- trip initiated opening specified by time-dependent table. 5 — Check valve controlled by static pressure gradient. IVPG = 1, DP = P(1)-P(2) = 2, DP = P(2)-P(1) DP + PVC $\geq$ 0, valve open DP + PVC $<$ 0, valve closed (Note: PVC is defined on Card 7).
15-28	IVTR	Valve trip ID.
29-42	NVTX	Number of valve table entries.
43-56	IVPG	Valve pressure gradient option (used only if IVTY = 5).

Card 7. (Format 3E14.6) AVLVE, HVLVE, PVC

1-14	AVLVE	Valve open area.

15-28	HVLVE	Valve open hydraulic diameter.
29-42	PVC	Check valve set point (use only if IVTY=5).

Valve Array Cards. 14 sets of cards. One set for each of the following variables. LOAD format.

Variable	Dimension	Description
DX	NCELLS	Cell lengths.
VOL	NCELLS	Cell volumes.
FA	NCELLS+1	Cell edge flow areas.
FRIC	NCELLS+1	Additive loss coefficients.
GRAV	NCELLS+1	Cosine of the angle between a vertical vector pointing up and a vector from cell N to cell N+1.
HD	NCELLS+1	Hydraulic diameters.
NFF	NCELLS+1	Friction factor correlation options (see ACCUM input description).
QPPP	NCELLS	Volumetric heat sources in pipe wall.
VLTB	NVTX*2	Valve table data pairs: (Time, Fraction Open)$_i$ i=1,NVTX.
ALP	NCELLS	Initial void fractions.
VM	NCELLS+1	Initial mixture velocities.
TL	NCELLS	Initial liquid temperatures.
P	NCELLS	Initial pressures.
TW	NCELLS*NODES	Initial wall temperatures. (Eliminate this card set if NODES = 0.)

j. Vessel Component (VESSEL)

Card 1. (Format A6,8X2I14) TYPE, NUM, ID

1-6	TYPE	Type of component (VESSEL).
15-28	NUM	Component ID number.
29-42	ID	User ID number.

Card 2. (Format 5I14) NASX, NRSX, NTSX, NCSR

1-14	NASX	Number of axial (z) segments (levels).
15-28	NRSX	Number of radial (r) segments (rings).
29-42	NTSX	Number of azimuthal (θ) segments (sectors).
43-56	NCSR	Number of cell sources (connections to pipes).

Card 3. (Format 5I14) IDCU, IDCL, IDCR, ICRU, ICRL

1-14	IDCU	Downcomer upper boundary axial segment number, Z(IDCU).
15-28	IDCL	Downcomer lower boundary axial segment number, Z(IDCL).
29-42	IDCR	Downcomer inner radial boundary segment number, RAD(IDCR).
43-56	ICRU	Core upper boundary axial segment number, Z(ICRU).
57-70	ICRL	Core lower boundary axial segment number, Z(ICRL).

Card 4. (Format 5I14) ICRR

1-14	ICRR	Core outer radial boundary segment number, RAD(ICRR).

Card 5. (Format 5I14) NFFA, NFFR, NFFT

(Presently all of these must be set to 0).

1-14	NFFA	Axial friction factor correlation option.
15-28	NFFR	Radial friction factor correlation option.

29-42	NFFT	Azimuthal friction factor correlation option.

Card 6. (Format 5E14.6) ROHS, CPHS, CHS, EMHS, HGAP

1-14	ROHS	Density of heat slab material.
15-28	CPHS	Specific heat of heat slab material.
29-42	CHS	Conductivity of heat slab material.
43-56	EMHS	Emissivity of heat slab wall.
57-70	HGAP	Fuel rod gap conductance coefficient. (Constant for NFCI=0, initial value otherwise). NCFI is input on Card 9.

Card 7. (Format 5E14.6) PDRAT

1-14	PDRAT	Fuel rod pitch to diameter ratio.

Card 8. (Format 5I14) NODES, NPWX, IRPOP, IRPTR

1-14	NODES	Number of rod radial heat transfer nodes (must be greater than or equal to four if a core region is specified).
15-28	NPWX	Number of (time,power) pairs in absolute power table.
29-42	IRPOP	Reactor kinetics option (input parameters required for each option are shown in parentheses).

IRPOP	OPTION
1	Constant power (RPOWRI),
2	Reactor kinetics with constant reactivity (RPOWRI, REACT),
3	Reactor kinetics with table lookup of reactivity (RPOWRI, NPWX, PWTB),
4	Reactor kinetics with trip initiated constant reactivity insertion (RPOWRI, IRPTR, REACT),
5	Reactor kinetics with trip-initiated table lookup of reactivity (RPOWRI, IRPTR, NPWX, PWTB),
6	Table lookup of power (NPWX, PWTB), and

	7	Constant initial power with trip-initiated table lookup of power (RPOWRI, NPWX, PWTB, IRPTR).
43-56	IRPTR	Reactor kinetics trip ID.

Card 9. (Format 5I14) NRFDT, NMWRX, NFCI, NFCIL, NCRAZ

1-14	NRFDT	Rod fine mesh trip ID (if zero, no fine mesh calculation is performed).
15-28	NMWRX	Metal-water reaction option (0 = Off, 1 = On).
29-42	NFCI	Fuel-clad interaction (FCI) option (0 = Off, 1 = On).
43-56	NFCIL	Limit on FCI calculations per time step.
57-70	NCRAZ	Total number of axial fine mesh nodes per rod (if NRFDT = 0, set NCRAZ = 0).

Card 10. (Format 5E14.6) RPOWRI, REACT, PLDR

1-14	RPOWRI	Initial reactor power.
15-28	REACT	Total reactivity. (Options 2 and 4 only.)
29-42	PLDR	Pellet dish radius (if zero, no calculation of pellet dishing).

VESSEL Geometry Cards. 3 sets of cards. One set for each of the following variables. LOAD format.

Variable	Dimension	Description
Z	NASX	Upper elevations of axial segments. (Referenced to zero elevation at bottom of vessel.)
RAD	NRSX	Outer radii of radial segments.
TH	NTSX	Theta angles at azimuthal segment ends (radians).

VESSEL Source Cards. One card per pipe connection source. (Format 5I14) LISRL, LISRC, LISRF, LJUNS

Columns	Variable	Description
1-14	LISRL	Axial level number associated with source.

15-28	LISRC	Relative cell number associated with source. (See Sec. I in Chap. IV.)
29-42	LISRF	Face number associated with source. (1 = azimuthal direction, 2 = axial direction, and 3 = radial direction.)
43-56	LJUNS	Junction number associated with source.

VESSEL Core Cards. 15 sets of cards. One set for each of the following variables. Omit these cards if there is no core. LOAD format.

Note: See Chap. IV, Sec. I for a precise definition of the following parameters and the ordering conventions used for reading in the data. A large number of parameters are read in with dimension (ICRR*NTSX). These parameters are supplied for each (r,θ) mesh zone in the core region. Each such zone constitutes one of the axial channels in the core formed by a stack of mesh cells with the same (r,θ) mesh boundaries. Thus, each (r,θ) mesh zone encloses a number of fuel rods and their associated coolant channels.

Variable	Dimension	Description
RDPWR	NODES-1	Relative radial power density within the rods.
CPOWR	ICRR*NTSX	Relative power density per rod.
RPKF	ICRR*NTSX	Hot rod power peaking factors.
ZPOWR	ICRU-ICRL	Relative axial power densities at the center of each axial mesh interval.
NRDX	ICRR*NTSX	Number of rods in each (r,θ) mesh zone.
RADRD	NODES	Rod node radii (cold).
MATRD	NODES-1	Rod material ID numbers (rod must include a gap).

ID	MATERIAL TYPE
1	Mixed oxide fuel
2	Zircaloy
3	Fuel-clad gap
4	Boron nitride insulation
5	Constantan/nichrome heater chrome
6	Stainless steel type 304
7	Stainless steel type 316
8	Stainless steel type 347

		9 Medium carbon steel A508 10 Inconel 718.
PWTB	NPWX*2	Power or reactivity table. Data pairs (time, power or reactivity)$_i$ i=1,NPWX.
NFAX	ICRU-ICRL	Number of fine-mesh intervals per coarse-mesh interval (not used if NRFDT = 0, total per rod must equal NCRAZ).
FPUO2	ICRR*NTSX	Fraction of PUO_2 in mixed oxide fuel.
FTD	ICRR*NTSX	Fuel density (fraction of theoretical).
GMIX	ICRR*NTSX*7	Mole fraction of gap gas constituents. Array not used if NFCI=0. Enter data for each gas in the order indicated.

Index	Gas Type
1	Helium
2	Argon
3	Xenon
4	Krypton
5	Hydrogen
6	Air/nitrogen
7	Water vapor.

GMLES	ICRR*NTSX	Moles of gap gas per rod (not used if NFCI=0).
PGAPT	ICRR*NTSX	Average gap gas pressure (not used if NFCI=0).
PLVOL	ICRR*NTSX	Plenum volume in each fuel rod above pellet stack (not used if NFCI=0).
PSLEN	ICRR*NTSX	Pellet stack length (not used if NFCI=0).
CLENN	ICRR*NTSX	Total cladding length (not used if NFCI=0).

VESSEL Level Cards. 26 Sets of cards. One set for each of the following variables for each level. LOAD format.

Note: The following parameters (dimensioned NRSX*NTSX) are read in for each (r,θ) mesh position at each axial level. In this case they extend over the entire vessel cross section. Since a separate data set is read for each level, these parameters are supplied for every mesh cell in the vessel.

Variable	Dimension	Description
HSA	NRSX*NTSX	Heat slab area.
HSM	NRSX*NTSX	Mass of heat slab.
CFZL-T	NRSX*NTSX	Liquid additive friction loss coefficients (Theta direction).
CFZL-Z	NRSX*NTSX	Liquid additive friction loss coefficients (Z-direction).
CFZL-R	NRSX*NTSX	Liquid additive friction loss coefficients (R-direction).
CFZV-T	NRSX*NTSX	Vapor additive friction loss coefficients (Theta direction).
CFZV-Z	NRSX*NTSX	Vapor additive friction loss coefficients (Z-direction).
CFZV-R	NRSX*NTSX	Vapor additive friction loss coefficients (R-direction).
LVOL	NRSX*NTSX	Cell fluid volume fractions.
FA-T	NRSX*NTSX	Cell fluid edge average area fractions in theta direction.
FA-Z	NRSX*NTSX	Cell fluid edge average area fractions in z-direction.
FA-R	NRSX*NTSX	Cell fluid edge average area fractions in r-direction.
HD-T	NRSX*NTSX	Hydraulic diameters in theta direction.
HD-Z	NRSX*NTSX	Hydraulic diameters in z-direction.
HD-R	NRSX*NTSX	Hydraulic diameters in r-direction.
HSTN	NRSX*NTSX	Heat slab temperatures.
ALPN	NRSX*NTSX	Vapor fraction.
VVN-T	NRSX*NTSX	Vapor velocity in theta direction.
VVN-Z	NRSX*NTSX	Vapor velocity in z-direction.
VVN-R	NRSX*NTSX	Vapor velocity in r-direction.
VLN-T	NRSX*NTSX	Liquid velocity in theta direction.

VLN-Z	NRSX*NTSX	Liquid velocity in z-direction.
VLN-R	NRSX*NTSX	Liquid velocity in r-direction.
TVN	NRSX*NTSX	Vapor temperature.
TLN	NRSX*NTSX	Liquid temperature.
PN	NRSX*NTSX	Pressure.

VESSEL ROD Cards. 2 sets of cards One set for each of the following variables. Omit these cards if there is no core. Use LOAD format.

Variable	Dimension	Description
BURN	(ICRU-ICRL)	Fuel burnup, MWD/MTU.
RDTN	NODES* (ICRU-ICRL)	Rod temperatures.

4. PWR Initialization Data

The following cards are required only if a PWR initialization calculation is to be performed. (This is indicated by setting STDYST=2 or =3 on Main Control Card 1.)

Card 1. (Format I14) NLOOP

Columns	Variable	Description
1-14	NLOOP	Number of primary coolant loops.

Cards 2 through 4 are repeated for each primary coolant loop.

Card 2. (Format I14, E14.6) NLPMP, TILPC1

1-14	NLPMP	Number of pumps in this loop (must be 1 or 2).
15-28	TILPC1	Desired coolant temperature at the vessel junction leading to the outlet side of the first primary loop coolant pump.

Card 3. (Format I14, E14.6) JNLPC1, WLPC1

1-14	JNLPC1	Identification number of the vessel junction which leads to the outlet side of the first primary loop coolant pump.
15-28	WLPC1	Desired mass flow rate through the first primary loop coolant pump.

Card 4. (Format I14, E14.6) JNLPC2, WLPC2

(Omit this card if NLPMP = 1)

1-14	JNLPC2	Identification number of the vessel junction which leads to the outlet side of the second primary loop coolant pump.
15-28	WLPC2	Desired mass flow rate through the second primary loop coolant pump.

5. Time Step Data

The last set of input information is the time step cards for controlling the calculation. The time domain is separated into intervals. Each interval (specified by two cards) may have different minimum and maximum time step

sizes and edit intervals. Any number of time step intervals may be input. The end of the calculation is signified by specifying the minimum time step size to be a negative number. The format of each set of two time step cards is as follows.

Card 1. Format (5E14.6) DTMIN, DTMAX, TEND

Columns	Variable	Description
1-14	DTMIN	Minimum allowable time step size for this time interval.
15-28	DTMAX	Maximum allowable time step size for this time interval.
29-42	TEND	End of this time interval.

Card 2. Format (5E14.6) EDINT, GFINT, DMPINT, RTWFP

1-14	EDINT	Print edit interval for this time interval.
15-28	GFINT	Graphics edit interval for this time interval.
29-42	DMPINT	Restart dump interval for this time interval.
43-56	RTWFP	Ratio between heat transfer and fluid dynamics time step sizes. (Used only for steady-state calculations, suggested value = 1.0.)

E. Load Subroutine

TRAC uses the LOAD subroutine to read most subscripted variables. The arrays may be read in floating point or integer format. If an array is dimensioned zero, then that card should be omitted. The input card images for subscripted variables consist of 5 fields for integer or real format. Each field consists of an operation (A1), a repeat count (I2), and a data constant (E11.2 or I11).

Seven operations are defined. These operations and an explanation of each are listed below.

Operation	Description
E	End of data array.
S	Skip to next card.
BLANK	No action.

R	Repeat data constant I2 times.
M	Multiple repeat. Repeat data constant 10*I2 times.
F	Fill array starting at current data index with data constant.
I	Interpolate between data constant and succeeding data constant with I2 points.

Some restrictions in the use of the LOAD format are:

1. End of data for an array must be signaled by E,
2. Overstore or partial fill of an array are not allowed, and
3. Integer interpolation is not allowed.

Following are examples of the use of the options listed above to fill an array of dimension 11 with data.

EXAMPLE ONE. Fill an integer array with a value of 61.

```
F          61E
```

EXAMPLE TWO. Use of the repeat option to fill an array with a value of 1.2.

```
R11     1.2   E
```

EXAMPLE THREE. Use of the skip option.

```
R 2          15              16S
R 5          17              18              19              20E
```

EXAMPLE FOUR. Use of the multiple repeat option.

```
M 1        1.56E-2          .0156E
```

EXAMPLE FIVE. Use of the interpolation option to get points 1.0, 2.0, 3.0, ... , 11.0.

```
I 9           1.              11.E
```

F. Output Files

Figure 3 shows the files read and written by TRAC during the course of a problem. The two input files, TRACIN and TRCRST, and the dump output file, TRCDMP, have already been discussed. We will now discuss the remaining two output files, TRCOUT and TRCGRF.

The file TRCOUT contains printer output. This file was produced with

standard FORTRAN write statements contained in the various component module output subroutines. Included in this file is a complete description of the problem input file which was read by the code, and time edits which are produced with a frequency specified on the time step cards. Each time edit includes a printout of results from each component in a problem. The component output includes pressures, temperatures, and other important results. TRAC error messages, if any, are also written on the TRCOUT file. These messages are described in Appendix D. A more complete description of individual component output is given in Chap. IV.

The TRCGRF file contains graphics output and is a structured binary file produced with unformatted write statements. The structure of this file is discussed in Chap. VI. A Livermore Time Sharing System (LTSS) library computer code, called GRIT, is used to generate plots of the problem calculation from the TRCGRF file.

TABLE I

TRIP SIGNAL INDEX VALUES AND VARIABLE TYPES

Trip Signal Index (ISID)	Common Usage (all components)	Exceptions
0	Reactor time (values of ID1-ID4 are ignored)	
1	Pressure	
2	Liquid temperature	
3	Vapor temperature	
4	Vapor fraction	
5	Wall temperature	Vessel:slab temperatures
6	(not used in 1-D components)	Vessel:fuel rod surface temperature to liquid
7	(not used in 1-D components)	Vessel:fuel rod surface temperature to vapor Accumulator:water level[a] Pressurizer:water level[a]
8	Mixture velocity	
9	Relative velocity	
10	(not used in 1-D components)	Vessel:reactor power[a]

[a]Note: This is not an array, set ID3 = 1 and ID4 = 0

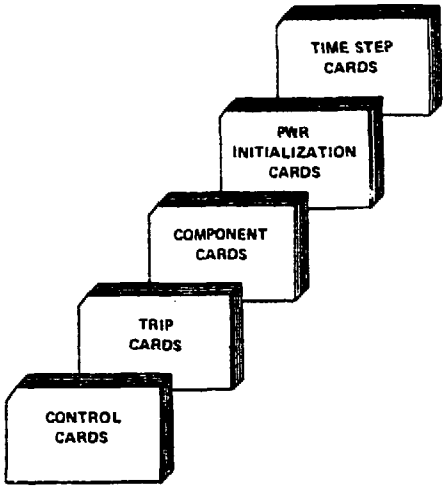

Fig. 1.
TRAC input deck organization.

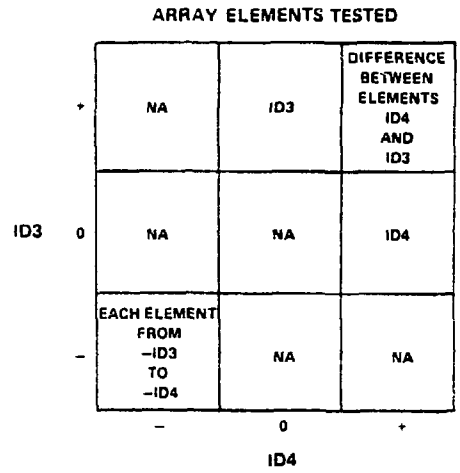

Fig. 2.
Trip array element selection logic (NA means not available).

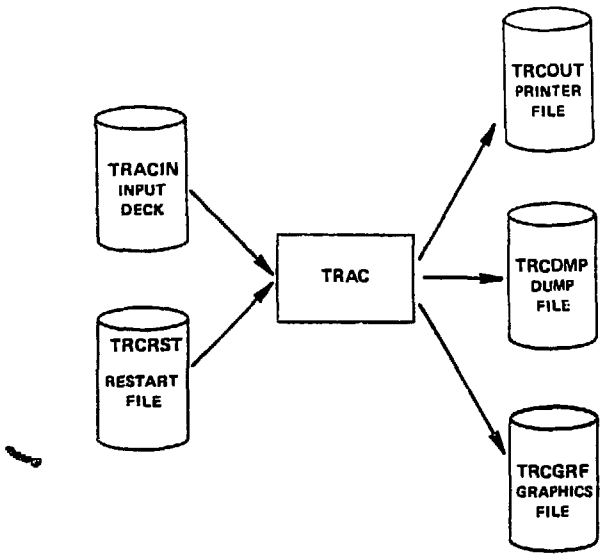

Fig. 3.
TRAC input and output files.

VI. PROGRAMMING DETAILS

A. Overall Code Organization

During the development of TRAC, considerable attention was paid to programming techniques. At the outset, the decision was made to strive for a code structure which minimizes the problems of maintaining and extending the code. In addition, we have attempted to program in a manner which can be understood by others who are knowledgeable in the LWR safety field, and in a fashion which reduces the difficulties of implementing TRAC at other sites and/or computers. At the same time, we recognize the need to take advantage of the efficiency characteristics of the LASL computing environment. In this case, the environment consists of a CDC 7600 computer running the Livermore Time Sharing System (LTSS). In situations of conflict, we have ranked the importance of these goals in the order in which they have been presented. Whenever possible, we have segregated specialized coding to subprograms which perform specific, low-level service functions.

The philosophy which has evolved in response to these goals has been one of modularity. TRAC is modular in two important senses. Because it is designed to analyze reactor systems which consist of specific types of components, the program contains subroutines that treat each component type. The components included in TRAC are described in Chap. IV. This form of modularity simplifies both the programming of subroutines and the data associated with particular components. For example, since fuel rods are only associated with the component type VESSEL, no data concerning fuel rods are referenced nor are any calculations about fuel rods performed by the subroutines which treat any other component type.

The second sense in which TRAC is modular is functionality. Each subprogram in TRAC performs a specific function. If the manner in which a function is to be performed requires modification, only those routines which perform that function need to be altered. For example, if the dump/restart capability is to be modified, only those routines which perform the dump and restart for the affected components will require changes. A number of low-level subprograms are used by all component types, thereby strenghtening this form of modularity. The most important of these routines are listed in Table I with a brief description of their function. A complete listing of all the subroutines in TRAC is given in Appendix E.

Functional modularity within TRAC is taken a step further by its division into overlays. Although the use of an overlay structure was originally mandated by computer size limitations (the small core memory of a 7600, where all executable instructions must reside, is limited to 65 536 60-bit words), this division has been made in a manner which isolates functional subunits within TRAC. Figure 1 displays a calling tree of the overlays in TRAC. Table II describes briefly the function of each overlay.

As mentioned above, the component modularity of TRAC manifests itself in the data structure as well as in the program structure. We have used the modularity of the data in a manner which utilizes the architecture of the CDC 7600 computer in an efficient way. The relevant architectural aspect is the division of the 7600 central memory into two segments: small core memory (SCM) and large core memory(LCM). The Central Processor Unit (CPU) must retrieve the instruction stream from SCM (which is limited in size) but may retrieve data from either segment. Single-word accesses to SCM require 275 nanoseconds to complete. Single-word accesses to the 512 000-word LCM require 1 760 nanoseconds to complete. For transfers of large data blocks between SCM and LCM, the transfer time per word is as low as 27.5 nanoseconds.

To take advantage of this architecture, TRAC divides the data for each component into four blocks. These are: the fixed length table, the variable length table, the pointer table, and the array data. The first three of these blocks are stored in SCM in the COMMON blocks FLTAB, VLTAB, and PTAB, respectively. The structure of the FLTAB COMMON area is the same for all types of components. The identification of words in the VLTAB and PTAB COMMON areas with variable names differs from one component type to another. Descriptions of the fixed length, variable length, and pointer tables for each component are given in Appendix G.

The array data are stored in SCM within the dynamic storage arrays. The location of individual arrays is determined by the value of variables in the pointer table. Dynamic storage of data arrays permits effective use of space for many different types of problems. The array data for one-dimensional components are contained in the SCM blank COMMON dynamic area. The SCM data for the three-dimensional vessel component are contained in both the blank COMMON and SCM3D COMMON dynamic areas, as will be described below.

Data for a particular component are only stored in the dynamic SCM areas while that component is being processed by TRAC. At other times the data are retained in LCM. Two service subroutines, RDLCM and WRLCM, use the efficient block transfer capability described above to transfer data to and from SCM as required. Processing of a component by TRAC begins with the transfer of its component data from LCM to SCM, and the computation of the pointer variables based on the available space in the dynamic storage array. The processing of that component ends with the reverse transfer from SCM to LCM. Figure 2 depicts the relationship between storage areas in SCM and LCM.

In addition to the data which refer to a particular component, TRAC uses many variables to describe the overall state of the calculation. These variables are grouped according to their use into several other COMMON areas. The structure of these COMMON areas, which are identical throughout TRAC, are described in Appendix F.

The overall sequence of calculations is directed by the main program. Overlay INPUT is always invoked at the start of each TRAC execution to read component and control input. The component data is initialized by overlay INIT. The reactor power level is set to zero at this point. The steady-state calculation (if requested) is performed by subroutine STEADY, which performs output operations using the EDIT, GRAF, and DUMP overlays as required. During the steady-state calculation, the reactor power is turned on once the fluid flow rates have been established. This is to prevent high rod temperatures early in the steady-state calculation when the flow rates are small. If no steady-state calculation is performed, the reactor power is turned on by subroutine STEADY in preparation for the transient calculation. This calculation is performed (if requested) by subroutine TRANS. Overlays EDIT, GRAF, and DUMP are invoked by TRANS to generate output as required.

B. Input Processing

The processing of all TRAC input information is performed by the INPUT overlay. This information is of two types: input data cards retrieved from the input file, TRACIN, and restart information from the problem restart file, TRCRST. In addition to obtaining the input data from the appropriate location, overlay INPUT also organizes the component data in LCM, assigns the array pointer variables for every component, allocates the fixed segment of the

blank COMMON area, and analyzes the reactor loop structure for problems which include a PWR initialization calculation.

Subroutine INPUT is the entry point for this overlay and controls the input process. The Main Control parameters (see Chap. V) are read from the TRACIN file by subroutine INPUT. Using this information, INPUT allocates the fixed segment of the SCM blank COMMON areas, as described in Table III. The trip and component data from the TRACIN file are read and processed by subroutines RDTRIP and RDCOMP, respectively. RDTRIP creates the TRIP array described in Table VI. RDCOMP also assigns pointer values and stores the component data in LCM. Component and trip data are retrieved from the restart file TRCRST by subroutine RDREST. This subroutine is analogous to RDCOMP as will be described below. Finally, INPUT utilizes the subroutines ASIGN and RDLOOP to fill the component LCM pointer array and process the PWR initialization input, respectively.

Subroutine RDCOMP invokes a component input routine (a list of these routines is given in Table VII) to process each component. RDCOMP determines the type of each component by reading the first input card. When a component type "END" is encountered, RDCOMP knows that all component input has been read. The component input routines perform the following functions: read input cards for a component, store data in the component data tables and write them to LCM, assign relative pointers for the component array data, and fill in the JUN array.

If it is determined that not all components have been read from the TRACIN file, subroutine RDREST will read the remaining components from the restart file, TRCRST. This file is opened and the dump corresponding to the requested time step number (input on Main Control Card 1) is located. (If the requested time step is negative, RDREST utilizes the last dump.) This dump is then used to initialize the components and trips which were not found in the TRACIN file, using the component restart subroutines listed in Table VII. The detailed structure of the restart file is described in Sec. F below in conjunction with the dump capability.

The PWR initialization input data are read and the loop structure analyzed by subroutine RDLOOP, if a PWR initialization calculation was requested on Main Control Card 2. The analysis of the reactor loop geometry results in the creation of a PWR Initialization Data area, which also resides in the fixed

segment of the blank COMMON area. This data area is described in Fig. 3. The overall prologue, loop prologues, and VESSEL junction data area are created by subroutine RDLOOP. The data structure for each loop is generated by subroutine FNDLP.

The data area depicted in Fig. 3 describes the geometry of PWR systems from a specific point of view. Of principle interest in the PWR initialization calculations are the components through which the primary coolant flows during steady-state conditions. To isolate these components, the components in each primary coolant flow loop are grouped into subloops of three kinds indicated by the associated value of ISLTP. The components through which the primary coolant normally flows are identified by ISLTP=1 and constitute one or two principle subloops (depending on the number of pumps). Subloops with ISLTP=0 are called passive; they are connected to the principle flow loop by a TEE, and have a zero flow at steady-state conditions (e.g., a pressurizer). Components in secondary loops (identified by $|ISLTP| = 2$) are connected to the secondary side of the steam generator. For the system to be processed by the PWR initialization calculation, the secondary loops must be quite simple. One side of the steam generator must be connected by a series of pipes to a FILL component, and the other side to a BREAK. (The first of these is identified by ISLTP=2 and the second by ISLTP=-2.)

C. Component Initialization

The transient or steady-state calculation cannot be initiated directly from the input data. Many arrays and variables for each component are required which are not read by overlay INPUT. Overlay INIT initializes these data based on the values of the input information. It also creates a table that supplies information to the graphics routines. The entry point subroutine, INIT, controls the initialization process by calling ICOMP and IGRAF. Subroutine ICOMP completes the component data tables and IGRAF initializes the graphics capability.

Subroutine ICOMP checks the junction input data (stored in the junction-component pair array, JUN) to ensure that the system is properly configured. then fills in the JSEQ and VSI arrays in the fixed segment of the blank COMMON area (Table III). ICOMP then initializes the data for each component by invoking the appropriate component initialization subroutines, listed in Table VIII. For most types of components there are two levels of initialization

subroutines. The routines of the first level, whose names begin with the letter "C," transfer the component's data from LCM to SCM, adjust the array pointers to reflect the origin of the array data, call the lower level subroutine, and return the initialized data to LCM. These routines exist chiefly to pass the array data through to the lower level subroutines as arguments. This permits referring to elements of these arrays by variable names with mnemonic value in the lower level routine. For example, the volume of mesh cell J in the component is referred to as VOL(J) rather than A(LVOL+J-1), which both shortens and clarifies the programming at this level.

The lower-level component initialization routines initialize geometric and heat transfer arrays, initialize fluid properties by calling subroutines THERMO and FPROP, and initialize the junction data array by using subroutine JlD. Other individual and array variables are initialized for specific component types.

The graphics initialization subroutine, IGRAF, creates the TRCGRF file, writes the header and catalog onto the file, and places the catalog in a LCM storage area. The catalog contains information about the data to be written on the TRCGRF file during the course of a problem and is constructed by the graphics initialization routines associated with the components. The data to be edited for each component are specified in these routines. Each type of data adds one entry to the catalog. This entry describes the location of the data and identifies it with a two-word Hollerith field. The catalog stored in LCM is later interrogated by subroutine GRAF to create each graphics edit.

D. Transient Calculation

1. General

The transient calculation is directed by overlay TRANS. Iteration routines in overlays OUTlD and OUT3D are used by TRANS to advance the calculation through time. Output overlays EDIT, DUMP and GRAF, which are described in Sec. F below, are invoked by TRANS to perform their functions as required.

Subroutine TRANS, which is the entry point for overlay TRANS, is structured as shown in Fig. 4. Each time step in the transient calculation consists of several sweeps through all of the components in the system. These sweeps are called outer iterations. Within each outer iteration, each component solves the thermal-hydraulic equations (see Chap. III) for the cells within its boundaries using a sequence of inner iterations. The purpose of outer iterations is to converge the boundary data passed between components.

Before entering the time step loop, TRANS calls subroutine EDIT to print the state of the system at the beginning of the transient. The major control variables within the time step loop are: NSTEP (the current time step number), TIMET (the time since the transient began), DELT (the size of the current time step), and OITNO (the current outer iteration number). The time step loop begins with the selection of the time step size, DELT, by subroutine TIMSTP. A prepass is performed for each component by overlay OUTER. A summary of the calculations performed during the prepass is given in Table IX. TRANS then enters an outer iteration loop. Each outer iteration is performed by overlay OUTER. The outer iteration loop normally completes when all components require only one inner iteration during the last outer iteration, and the outer iteration criterion (EPSO on Main Control Card 3) is met. This criterion is applied to the maximum fractional change in the pressures throughout the system during the last iteration.

The outer iteration loop may alternatively terminate when the number of outer iterations reaches a user-specified limit (OITMAX on Main Control Card 4). In this case, TRAC restores the state of all components to that at the beginning of the time step, reduces the time step size by an order of magnitude (with the constraint that DELT be greater than or equal to DTMIN), and continues the calculation with the new time step size.

When the outer iteration converges, a postpass is performed by OUTER. A summary of the calculations performed during the postpass is given in Table X. The time step number is then incremented and TIMET is increased by DELT. A calculation is completed when TIMET reaches the last time specified on the time step input cards.

2. Time Step Selection and Output Control

The transient calculation interval is described as a sequence of time domains by the user using the time step input cards. During each of these domains the minimum and maximum time step sizes and the edit, dump, and graphics intervals are fixed. When overlays EDIT, DUMP, and GRAF are invoked, they calculate the time at which the next output of the associated type is to occur. When TRANS finds that TIMET has reached or exceeded the indicated time, the corresponding output overlay is invoked again. Whenever a new time domain is reached, the output indicators are set to the current time plus the new value of the appropriate interval.

Subroutine TIMSTP reads the time step control cards and evaluates the next time step size. At the beginning of the transient, DELT is set to the minimum size specified for the first time domain. At other times TIMSTP applies two algorithms, implemented in subroutine NEWDLT, to evaluate the next time step size. TIMSTP then limits this value of DELT to values between the minimum and maximum for this time domain.

NEWDLT determines the largest total number of inner iterations taken for any component. If this maximum is less than four the time step size is increased by 2%. The time step size is left unchanged if this maximum is between 4 and 10, and reduced if it exceeds 10. The second algorithm in NEWDLT places an upper bound on the time step size. This bound is four-tenths of the Courant stability limit for the differencing scheme used in the TRAC hydrodynamics routines.

3. Component Calculations

Overlay OUTER performs sweeps through all the components of the system. The components are processed in the order specified in the iteration order input cards. The function performed for all components during the outer iteration is signaled by the value of OITNO (set in the calling overlay) as shown in Table XI. Subroutine OUTER is the entry point routine of this overlay. The fixed length table for each component is brought into SCM by OUTER, then either overlay OUT1D or OUT3D is invoked as appropriate. Figure 5 displays the logic for a complete outer iteration.

Overlay OUT1D performs the required calculations for one-dimensional components. The entry point subroutine of this overlay, also called OUT1D, simply calls the subroutine which processes the current component type. These iteration subroutines are listed in Table XII. As with the component initialization routines, the iteration subroutines are divided into two levels. The first-level routines prepare the SCM data areas before calling the lower-level routines, and return data to LCM when the calculation is complete. The aspects of the calculation which are peculiar to each component type are performed by the lower level iteration subroutines. The generic subroutines SLIP, FWALL, MPROP, HTPIPE, TRPSET, DF1D, THERMO, CYLHT, and J1D are used by all of the component iteration subroutines to perform the associated calculations.

The lower-level iteration subroutines solve the hydrodynamics equations for a component. The boundary conditions for the component are transmitted from the adjacent components through the boundary data arrays. The boundary conditions do not change during the inner iterations performed to solve the fluid flow equations. These iterations are performed for one-dimensional components by subroutine DF1DI or DF1DS. The inner iterations for a single component cease when the inner iteration limit (IITMAX from Main Control Card 4) is reached or when the inner convergence criterion (EPSI from Main Control Card 3) is met. This convergence criterion is applied to the fractional change in the fluid pressures throughout the component during the last inner iteration. Upon completion of the inner iterations for a component, the boundary data arrays are updated to reflect the current state of the component.

The three-dimensional VESSEL component is processed by overlay OUT3D. In this overlay the prepass, postpass, and inner iterations are performed by three separate subroutines; VSSL1, VSSL3, and VSSL2, respectively. (Restoration of VESSEL data to the beginning of the time step is also performed by VSSL3.) One of these routines is called by the first-level iteration subroutine CVSSL, as determined from the value of OITNO. The calculational sequence parallels that of the one-dimensional components but the inner iterations are performed by the three-dimensional hydrodynamics routines TF3D, ITR1, and FF3D.

4. Vessel Data Structure

The array data for one-dimensional components are all loaded into core whenever a particular component is processed. Because the amount of array data is much larger for the three-dimensional VESSEL component, this was not possible for components of this type. Therefore, the array data for the VESSEL component is subdivided. There are three categories of VESSEL array data: component data, level data, and rod data. The component data arrays describe the overall state of the VESSEL. These arrays are loaded into the blank COMMON area in SCM before processing of the VESSEL begins and remain there during the VESSEL calculation. The level data arrays contain fluid dynamics and wall temperature data organized by axial level within the VESSEL. A data management subroutine, MANAGE, is used by all VESSEL subroutines to load single levels into SCM and replace them in LCM. There are never more than three levels of data in SCM at one time. The level data reside in the SCM3D

COMMON area when they are in SCM. These arrays are rotated through the SCM area during the fluid dynamics calculation by the VESSEL iteration subroutines.

The rod data arrays contain detailed information about the heat transfer calculation in the fuel rods. These data are organized by fuel rod so that only those data pertaining to the rod under study are in SCM at once. These data arrays are loaded into (and unloaded from) the SCM3D COMMON area by calls to the MANAGE subroutine. Subroutine CORE coordinates the rod heat-transfer calculations including the management of rod data.

In addition to solving the data space problem, the organization of the VESSEL array data improves the efficiency of the calculation by grouping data by their use. However, it introduces a communication problem between the fluid dynamics and heat-transfer calculations since some data need to be in both the rod and level arrays. This problem is resolved by a transfer of data between the rod and level data arrays. This transfer is performed by direct LCM to LCM copies using subroutine LCMOVE during the prepass calculation.

E. Steady-State Calculations

Steady-state calculations are directed by subroutine STEADY. The calculational sequence of this subroutine is similar to that of the transient driver subroutine TRANS. The same sequence of outer and inner iterations used for transient calculations is also used to advance the steady-state calculation. The main difference is the addition of steady-state convergence tests and PWR initialization calculations to STEADY. STEADY also invokes the EDIT, DUMP, and GRAF overlays to provide output as requested by the user. These overlays are described in Sec. F. Overlays TWOTIM and PWRSS, which are described in this section, are called by STEADY to evaluate normalized rates of change and new PWR operating parameters, respectively. STEADY is called by the main program whether or not a steady-state calculation has been requested. If no calculation is required, STEADY simply initializes the VESSEL power and returns control to the main program.

The type of steady-state calculation to be performed is determined by the value of the input variable STDYST on Main Control Card 1 as described in the input specifications in Chap. V. Steady-state calculations begin with the code setting the steady-state indication flag, ISTDY, to one and the transient calculation time, TIMET, to minus 1. (In the steady-state calculation the time variable is STIME instead of TIMET.) These values of ISTDY and TIMET have the effects indicated in Table XIII.

The control of time steps by STEADY is identical to that implemented in TRANS. This includes the selection of the time step size, output timing, and the restarting of time steps if the outer iteration limit is exceeded. (In STEADY the input variable SITMAX, from Main Control Card 4, is used as a delimiter in place of OITMAX.) Within the time step loop, STEADY also calculates normalized rates of change and tests for steady-state convergence. This evaluation is performed every 50 time steps and prior to every edit. The maximum normalized rates of change and their location are included in the printed output, as shown in Table XIV. The maximum normalized rate of change of the fluid velocities is used to determine when the reactor power should be turned on. Once this value falls below one, the reactor power is set to the input value, RPOWRI (specified on card 10 of the VESSEL input data). The generalized steady state completes when all normalized rates of change are below the user-specified convergence criterion, EPSS (from Main Control Card 3), or when STIME reaches the end of the last time domain specified in the time step input cards for the steady state.

Both steady-state and transient calculations may be performed in one computer run. The end of the generalized steady-state time step cards is signified by a single card containing a - 1.0 in columns 12 through 14. The transient time step input cards should immediately follow. If the generalized steady state converges before reaching the end of the last time domain, the remaining steady-state time step input cards are read so the transient calculation will proceed correctly.

Control of the PWR initialization calculation is necessarily more complex. The time domains are divided into groups delimited by negative values of DTMIN. The completion of each group of time step cards or convergence to a steady-state causes a re-evaluation of the loop parameters. The last group of time domains is marked by a card containing negative values of both DTMIN and DTMAX. As with the generalized calculation, a transient calculation may follow the PWR initialization. The time step cards for the transient calculation simply follow those for the PWR initialization.

The PWR initialization calculation completes when the relative errors in the flow rates and inlet temperatures fall below a user-specified criterion (EPSP or Main Control Card 3) for all loops. Figure 6 is a flow diagram for the PWR initialization calculation.

The normalized rates of change for all components are evaluated in overlay TWOTIM. These rates and their locations in the system are transmitted through the variables FMX and LOK in COMMON block SSCON. Overlay TWOTIM is divided into three levels of subroutines. The top level contains only the driver subroutine TWOTIM. TWOTIM calls subroutines in the second level to evaluate the maximum normalized rates of change for each component. These convergence evaluation subroutines are listed in Table XV.

The subroutines in the third level of overlay TWOTIM are called by the convergence evaluation subroutines to analyze specific variables. The subroutines in this level are: FDMXFP, FDMX3D, FDMXTR, FDMXTS, and FDMXTW. The first two of these evaluate in one and three dimensions, respectively, the maximum normalized rates of change for the fluid velocities, masses, and energies . FDMXTR and FDMXTS process the VESSEL rod and SLAB temperatures, while FDMXTW analyzes the temperatures in one-dimensional component walls.

Overlay PWRSS uses the system state, as represented in the LCM component data tables, to evaluate new pump speeds and steam generator fouling factors. The reactor loop data area, depicted in Fig. 3, is used by this overlay for data storage and calculation control.

Subroutine LPSET is the entry point and controlling subroutine for the PWRSS overlay. It calls subroutine VSCON to evaluate the VESSEL pressures and mass and energy flow rates at all VESSEL junctions. These data are retrieved from the boundary data arrays. Each primary coolant loop is then considered in turn by LPSET. The loop flow resistances, specific enthalpy differentials, and the steam generator overall heat transfer coefficient are evaluated by subroutine LPCON. Subroutines PMPP, TEEP, and STGNP provide LPCON with data derived from the PUMP, TEE, and STGEN component data tables, respectively. The equations presented in Sec. III.D.2 are solved for the pump heads and steam generator area by subroutine SLVLP. Finally, LPSET calls subroutine LPRPL to convert these parameters to pump speeds and fouling factors, and store these into the appropriate component data tables.

F. Output Processing

TRAC produces three output files: TRCOUT, TRCGRF, and TRCDMP. The first of these files is in printer format and contains a user-oriented analysis of the course of the calculation. During the input process, a description of the input data is placed into this file. At selected times during the calcula-

tion, overlay EDIT is invoked to add to this file a description of the current state of the system. The TRCGRF and TRCDMP files are binary files designed for analysis by graphics postprocessing programs and restart of problems by TRAC, respectively. The TRCGRF file is created and its header and catalog written during the initialization phase. TRCDMP is created immediately thereafter by overlay DUMP.

Subroutine WCOMP, which is called by the entry point routine EDIT, directs the addition of a time step edit to the TRCOUT file. WCOMP writes certain overall data directly, then uses the component edit subroutines to describe the state of each component in turn. The component edit subroutines, which are listed in Table XVI, are divided into two levels in a manner analogous to the initialization and iteration subroutines. The first level edit subroutines merely load the component data tables into SCM and call the lower level subroutines. These latter routines then add the data which are important for that component type to the TRCOUT file in an appropriate format.

After initialization by IGRAF, the time edit data are added to the TRCGRF file by overlay GRAF. This overlay contains the single subroutine, GRAF, which uses the LCM graph data area which is described in Sec. C. The TRCGRF file is a structured binary file written with unformatted write statements and containing information for graphics processing.

Data contained on the TRCGRF file may be divided into three sections:

1. general information,
2. catalog information, and
3. time edit data.

These data appear on the file in the above order, as illustrated in Fig. 7. The structure of the general information section of the file is given in Fig. 8. This section contains title cards for problem identification and size information needed to describe the problem and the remainder of the file. The catalog section (Fig. 9) contains information which is used to describe the data stored in the time edit section. The time edit section is made up of blocks of data as shown in Fig. 10. Individual arrays within each block are packed to save space. A block is written at each edit taken during the course of a problem. The number of blocks written on the file is determined by the graphics edit frequency specified on the time step cards. The last block is followed by a word "EOF" to signify the "end of file."

The structure and lengths of the blocks are identical to one another to minimize the required catalog information. The catalog is made up of NCTX data entries corresponding to the number of items in each block. This relationship is displayed in Fig. 11. Each data entry contains six words of information which provides a data description and a pointer to the data in the blocks. A data entry may describe a single variable or an array of data. The word count is also included in the catalog. The types of data stored are pressures, temperatures, void fractions, and other important system parameters. The choice of data in the file is made dynamically in the TRAC graphics routines at initialization.

The TRCDMP file is a structured binary file written with unformatted write statements. It contains sufficient data to restart the calculation from the current state as described in Sec. B above. This file is created by a sequence of calls to overlay DUMP. The entry point subroutine, DMPIT, locates the next dump in TRCDMP, writes the dump header data and calls the component dump subroutines which are listed in Table XVII.

The resulting file is structured as shown in Figs. 12 and 13. This structure is designed to permit easy location of particular dumps and particular components within each dump. This reduces the effort required in restarting the problem.

G. Storage Requirements

Although maximum use is made of dynamic storage allocation within TRAC, there are limitations on the complexity of problems that may be simulated. These limitations arise from the finite extent of the component data storage areas, as listed in Table XVIII. These limitations are imposed on the complexity of single components as well as on the system as a whole.

Figure 14 displays the organization of the blank COMMON dynamic storage area in SCM. The fixed segment, which is described in detail in Table III, contains information which is used by all system component subroutines and therefore must remain in SCM throughout the calculation. The PWR initialization data area, shown in detail in Fig. 3, is only required during PWR initialization calculations. Thus, this area does not affect storage requirements when no PWR initialization is performed.

The area which remains, marked as component data area in Fig. 14, is available to each component when its data is in SCM. Each component type

requires varying amounts of array space. For the types of components which are modeled with one-dimensional fluid dynamics, the required space is linear in the number of fluid cells, the number of heat transfer nodes, and the product of these numbers. Table XIX lists the coefficients of these three quantities for each component type (BREAKS require no array space) along with the constant requirement.

The finite size of the component data area also limits certain aspects of the VESSEL description. The arrays stored in this area for VESSEL components require

```
3*NASX+2*NRSX+2*NTSX+34*NCSR+3*NODES+26*ICRR*NTSX+2*(ICRU-ICRL)+2*NPWR+66
```

words of space. The definitions of the individual variables used in this expression are given in the VESSEL input data description in Chap. V.

The complexity of VESSEL components is also limited by the finite extent of the SCM3D COMMON area. This area is used for the storage of level or rod data at different points in the calculation. The hydrodynamic variables for each axial level in the VESSEL are transferred between SCM and LCM as a unit. At certain points in the calculation, three distinct levels of data must be in SCM simultaneously. Therefore, the maximum size of the data associated with a single level is one-third the length of the SCM3D area. Each level of data requires

```
120*NRSX*NTSX+NCSR+7*(ICRU-ICRL)
```

words of space.

In a similar manner, the heat transfer data for each fuel rod are transferred between SCM and LCM as a unit. Because the data for only one rod need be in SCM at any point in the calculation, the rod data may extend over the entire length of the SCM3D COMMON area. Each rod requires

```
(40+15*NODES)*(ICRU-ICRL)+(13+4*NODES)*NCRAZ
```

words of space.

The finite extent of the LCM component storage area (COMMON block LCMSP) limits the total amount of component data which can be handled in a calculation. This amount is found by summing the SCM array requirements as described above, including all VESSEL levels and rods, and adding the space required for the fixed length, variable length, and pointer tables for each component, as listed in Table XX. The graphics catalog, discussed in Sec. F above, is also stored in this LCM block. This area requires one word for each component plus six words for every catalog entry. Figure 15 shows the organization of LCMSP.

TABLE I

IMPORTANT LOW-LEVEL SUBPROGRAMS

Subprogram	Description
CHEN	Uses Chen correlation to evaluate the forced convection nucleate boiling heat transfer coefficient.
CHF	Evaluates the critical heat flux based on a local conditions formulation.
CLEAR	Sets an array to a constant value.
CYLHT	Calculates temperature fields in the radial direction.
DF1D	Controls solution of finite difference equations for the 1-D drift-flux model.
ERROR	Processes different kinds of error conditions.
FF3D	Makes final pass update for all variables in 3-D vessel.
FPROP	Calculates values for fluid enthalpy, transport properties, and surface tension.
FWALL	Computes a two-phase friction factor.
HTCOR	Computes heat transfer coefficients.
HTPIPE	Averages velocities and generates heat transfer coefficients.
HTVSSL	Averages velocities and generates heat transfer coefficients for the vessel.
J1D	Fills boundary array at component junctions.
MFROD	Orders fuel rod property selection and evaluates an average temperature for property evaluation.
MPROP	Orders structure property selection and evaluates an average temperature for property evaluation.
RDLCM	Transfers data from LCM into SCM.
RKIN	Integrates the neutron point kinetics equations.
RODHT	Calculates the fuel rod temperature field.

TABLE I (Cont.)

SLABHT	Calculates the slab temperatures.
SLIP	Calculates drift velocities between phases.
TF3D	Sets up the linearized 3-D finite difference equations.
THERMO	Calculates thermodynamic properties of water.
TRIP	Returns status of a TRIP.
TRPSET	Sets up trip status flags.
WARRAY	Writes a real array to the printer.
WIARR	Writes an integer array to the printer.
WRLCM	Transfers a given number of words from SCM to LCM.

TABLE II

TRAC OVERLAYS

Overlay	Description
MAIN	Controls overall flow of calculation. (The MAIN overlay also contains many service routines used throughout the code.)
INPUT	Reads input and restart files, assigns LCM storage space and saves input data there, and analyzes PWR loops for PWR initialization calculations.
INIT	Initializes component data and graphics tables.
OUTER	Performs one complete outer iteration.
OUT1D	Performs all the inner iterations for a single one-dimensional component during one outer iteration.
OUT3D	Performs all the inner iterations for a VESSEL during one outer iteration.
TWOTIM	Evaluates maximum normalized rates of change throughout the system.
PWRSS	Evaluates new parameter values for the PWR initialization option.
DUMP	Adds a dump at the current time to the TRCDMP file.
EDIT	Adds an edit at the current time to the TRCOUT file.
GRAF	Adds a graphics edit at the current time to the TRCGRF file.

TABLE III

FIXED SEGMENT ALLOCATIONS FOR THE BLANK COMMON AREA

Pointer	Dimension	Array Description
LTITLE	20*NUMTCR	Problem title (stored using only the first four bytes of each word).
LORDER	NCOMP	Component numbers stored in the order used for iteration.
LILCMP	NCOMP	Component LCM pointers stored in the order in which components were read.
LNBR	NCOMP	Component numbers stored in the order in which components were read.
LCOMPT	NCOMP	Component LCM pointers stored in the order used for iteration.
LIITNO	NCOMP	Number of inner iterations during the last outer iteration for each component (in the order used for iteration).
LIITOT	NCOMP	Number of inner iterations during this time step for each component (in the order used for iteration).
LJUN	8*NJUM	Junction-component pair array, described in Table IV.
LJSEQ	NJUN	Junction numbers in the order in which junctions occur in the junction-component array.
LVSI	NJUN	Junction flow reversal indicators in the order in which junctions occur in the junction-component array.
LBD	35*NJUN	Boundary data array, described in Table V.
LTRIP	12*NTRX	Trip data array, described in Table VI.
LDMPTR	NDMPTR	Trip ID numbers of those trips which cause a dump when they are activated.

TABLE IV

JUNCTION-COMPONENT PAIR ARRAY

The JUN array is double subscripted, JUN(4,2*NJUN). The second index indicates the order in which the junction-component pair was encountered during input. The four values of the first index correspond to:

Index	Description
1	Junction number.
2	Component number.
3	Component type.
4	Junction direction flag.
	=0 if positive flow in this component is into the component at this junction, or
	=1 if positive flow in this component is out of the component at this junction.

TABLE V

BOUNDARY ARRAY DATA

The boundary array data are stored in a doubly dimensioned array, BD(35,NJUN), whose second index indicates the order in which the junctions occur in the input data. The data in this array indicate the current condition of the component connected to each junction which was last processed. The fluid properties are evaluated at one of three space points:

1. at the edge of the mesh cell closest to the junction,
2. at the mid-point of that mesh cell, or
3. at the other edge of that mesh cell.

The specific elements of the array are:

Index	Description
1	Width of the adjacent mesh cell.
2	Volume of the adjacent mesh cell.
3	Old mixture density at 2.
4	Product of old vapor density and void fraction at 2.
5	Old energy density at 2.
6	Old mixture mass flow rate at 1.
7	Old void fraction at 2.
8	Old vapor density at 2.
9	Old liquid density at 2.
10	Old mixture velocity at 3.
11	Old relative velocity at 3.
12	Old specific vapor energy at 2.

TABLE V (cont)

Index	Description
13	Old specific liquid energy at 2.
14	Old pressure at 2.
15	New void fraction at 2.
16	New vapor density at 2.
17	New liquid density at 2.
18	New mixture velocity at 3.
19	Flow area at 3.
20	New vapor energy density at 2.
21	New liquid energy density at 2.
22	New pressure at 2.
23	New mixture velocity at 1.
24	New relative velocity at 1.
25	Surface tension at 2.
26	New vapor velocity at 1.
27	New liquid velocity at 1.
28	New vapor velocity at 2.
29	New liquid velocity at 2.
30	Vapor viscosity at 2.
31	Liquid viscosity at 2.
32	Flow area at 1.
33	Hydraulic diameter at 1.
34	Friction factor at 2.
35	Old mixture velocity at 1.

TABLE VI

TRIP DATA ARRAY

Trip data are stored in a doubly dimensioned array, TRIP(12,MTRX), where the second subscript is the trip index. The elements corresponding to the first subscript are:

I	Element	Description
1	TTID	TRIP ID number.
2	TSID	TRIP signal number.
3	ID1	First TRIP qualifier.
4	ID2	Second TRIP qualifier.
5	ID3	Third TRIP qualifier.
6	ID4	Fourth TRIP qualifier.
7	ICOMD	TRIP status flag. 0 = Off 1 = On
8	TSP	TRIP setpoint.
9	TTP	TRIP delay time.
10	TIMTR	Time TRIP turned on.
11	ITSP	Setpoint reached flag. 0 = No 1 = Yes
12	TIMSP	Time setpoint was reached.

TABLE VII

COMPONENT INPUT SUBROUTINES

Component	Card Input	Restart Input
ACCUM	RACCUM	REACCUM
BREAK	RBREAK	REBRK
FILL	RFILL	REFILL
PIPE	RPIPE	REPIPE
PRIZER	RPRIZER	REPRZR
PUMP	RPUMP	REPUMP
REGEN	RREGEN	REREGN
TEE	RTEE	RETEE
VALVE	RVLVE	REVLVE
VESSEL	RVSEL	REVSEL

TABLE VIII

COMPONENT INITIALIZATION SUBROUTINES

Component Type	First Level Initialization Routine	Lower Level Initialization Routine	Graphics Initialization Routine
ACCUM	CIACCUM	IACCUM	IGACCUM
BREAK	none	IBRK	IGBREAK
FILL	none	IFILL	IGFILL
PIPE	CIPIPE	IPIPE	IGPIPE
PRIZER	CIPRIZR	IPRIZR	IGPRIZR
PUMP	CIPUMP	IPUMP	IGPUMP
REGEN	CIREGEN	IREGEN	IGREGEN
TEE	CITEE	ITEE	IGTEE
VALVE	CIVLVE	IVLVE	IGVLVE
VESSEL	CIVSEL	IVSEL	IGVSEL

TABLE IX

SUMMARY OF PREPASS CALCULATIONS

During the prepass, each component performs the following calculations:

1. Copy the values of time-varying quantities calculated during the last time step into the locations for old quantities.

2. Calculate the relative velocity between the liquid and vapor fields using subroutine SLIP.

3. Evaluate the liquid and vapor velocities.

4. Calculate the two-phase wall friction factors using subroutine FWALL.

5. Calculate heat transfer properties using subroutine MPROP.

6. Calculate convective heat transfer coefficients using subroutine HTCOR.

7. Evaluate the current status of TRIP.

TABLE X

SUMMARY OF POSTPASS CALCULATIONS

During the postpass each component performs the following calculations:

1. Calculate new wall, rod, and slab temperature distributions using subroutines CYLHT, RODHT, and SLABHT.

2. Calculate new fluid properties using subroutine FPROP.

3. Update boundary data arrays.

TABLE XI

CALCULATION TYPES IN OVERLAY OUTER

OPTNO	CALCULATION TYPE
0	Prepass (see Table IX).
-1	Postpass (see Table X).
0	Inner Iterations.
-100	Restore variables to start of time step.

TABLE XII

ITERATION SUBROUTINES

Component TYPE	First level Iteration Subroutine	Lower level Iteration Subroutine
ACCUM	CACCUM	ACCUM
BREAK	CBREAK	none
FILL	CFILL	none
PIPE	CPIPE	PIPE
PRIZER	CPRIZR	PRIZER
PUMP	CPUMP	PUMP
PWSEN	CPWSEN	PWSEN
TEE	CTEE	TEE
VALVE	CVALVE	VLVE
VESSEL	CVES	VESL1, VESL2, VESL3

TABLE XIII

STEADY-STATE CALCULATION EFFECTS

Subroutine	Effects
CYLHT	Causes implicit treatment of the convective boundary conditions.
HTCOR	Eliminates CHF calculation.
RODHT	Causes implicit treatment of the convective boundary conditions.
PRIZER	Bypasses calculation of fluid and thermal conditions. Causes cataloging of mass flow through the system junctions.
TRPSET	Trips are not activated.

TABLE XIV

EXAMPLE OF A STEADY-STATE CONVERGENCE EDIT

STEADY-STATE TIME STEP # 8326 CONVERGED IN 3 ITERATIONS.

TIME = 8.001E+01 DELT = 1.023E-02

VARIABLE	MAXIMUM CHANGE RATIO	COMPONENT	CELL
VELOCITY	1.17924E+00	12	1
MIXTURE MASS	9.11400E-03	42	112
VAPOR MASS	0.	0	0
MIXTURE ENERGY	6.42201E-03	42	71
VAPOR ENERGY	4.55970E-01	32	3
TEMPERATURES	6.14202E-04	42	110

TABLE XV

CONVERGENCE EVALUATION SUBROUTINES

Component Type	Subroutine
ACCUM	SACCUM
BREAK	none
FILL	none
PIPE	SPIPE
PRIZER	SPRIZR
PUMP	SPUMP
STGEN	SSTGEN
TEE	STEE
VALVE	SVALVE
VESSEL	SVSSL

TABLE XVI

COMPONENT EDIT SUBROUTINES

Component Type	First-Level Subroutine	Lower-Level Subroutine
ACCUM	CWACCUM	WACCUM
BREAK	none	WBREAK
FILL	none	WFILL
PIPE	CWPIPE	WPIPE
PRIZER	CWPRIZR	WPRIZR
PUMP	CWPUMP	WPUMP
STGEN	CWSTGEN	WSTGEN
TEE	CWTEE	WTEE
VALVE	CWVLVE	WVLVE
VESSEL	CWFSSL	WVSSL

TABLE XVII

COMPONENT DUMP SUBROUTINES

Component Type	Subroutine Name
ACCUM	DACCUM
BREAK	DBRK
FILL	DFILL
PIPE	DPIPE
PRIZER	DPRIZR
PUMP	DPUMP
STGEN	DSTGEN
TEE	DTEE
VALVE	DVLVE
VESSEL	DVSSL

TABLE XVIII

TRAC STORAGE ALLOCATIONS

Storage Area	Size (words)
COMMON/LCMSP/	130 000
COMMON/SCM3D/	15 000
BLANK COMMON	7 000

TABLE XIX

ONE-DIMENSIONAL COMPONENT ARRAY STORAGE REQUIREMENTS

Component Type	Coefficients for Total Array Requirements			
	Fixed	NCELLS	NODES	NCELLS*NODES
ACCUM	52	61	0	0
PIPE	24	70	4	5
PRIZER	62	61	0	0
PUMP[a]	24	70	4	5
STGEN[b]	51	73 69	4	5 4
TEE[c]	58	70	8	5
VALVE[d]	24	70	4	5
FILL[e]				

[a]Each PUMP also requires room in blank COMMON for the pump curves. The standard TRAC pump curves require 215 words. Pumps controlled by time or pressure tables require an additional 2*NPMPTX words.

[b]STGENs have two sets of cells, primary and secondary. The numbers of cells are denoted by NCELL1 and NCELL2.

[c]TEEs have two sets of cells plus one phantom cell. Thus, NCELLS=NCELL1+NCELL2+1.

[d]VALVEs also require 2*NVTX words for the valve table.

[e]FILL requires 2*NFTX words of array space.

TABLE XX

COMPONENT TABLE LENGTHS

Component Type	Fixed Length Table	Variable Length Table	Pointer Table
ACCUM	20	20	100
BREAK	20	50	0
FILL	20	50	0
PIPE	20	100	100
PRIZER	20	20	100
PUMP	20	50	120
STGEN	20	50	175
TEE	20	50	100
VLAVE	20	100	100
VESSEL	20	100	228

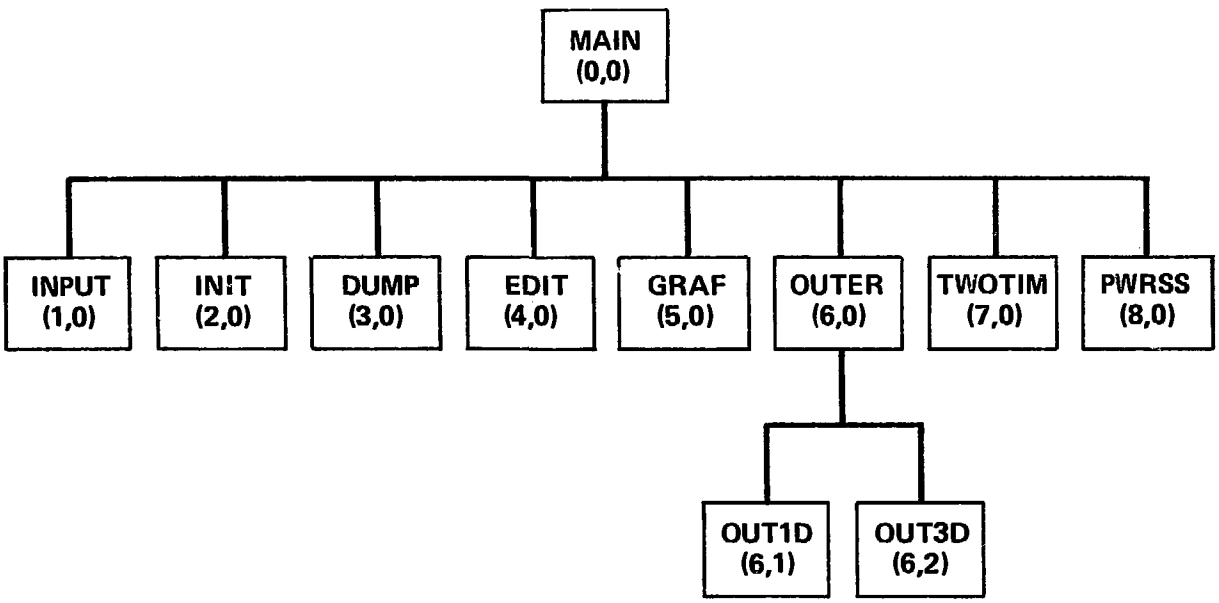

Fig. 1.
TRAC overlay structure.

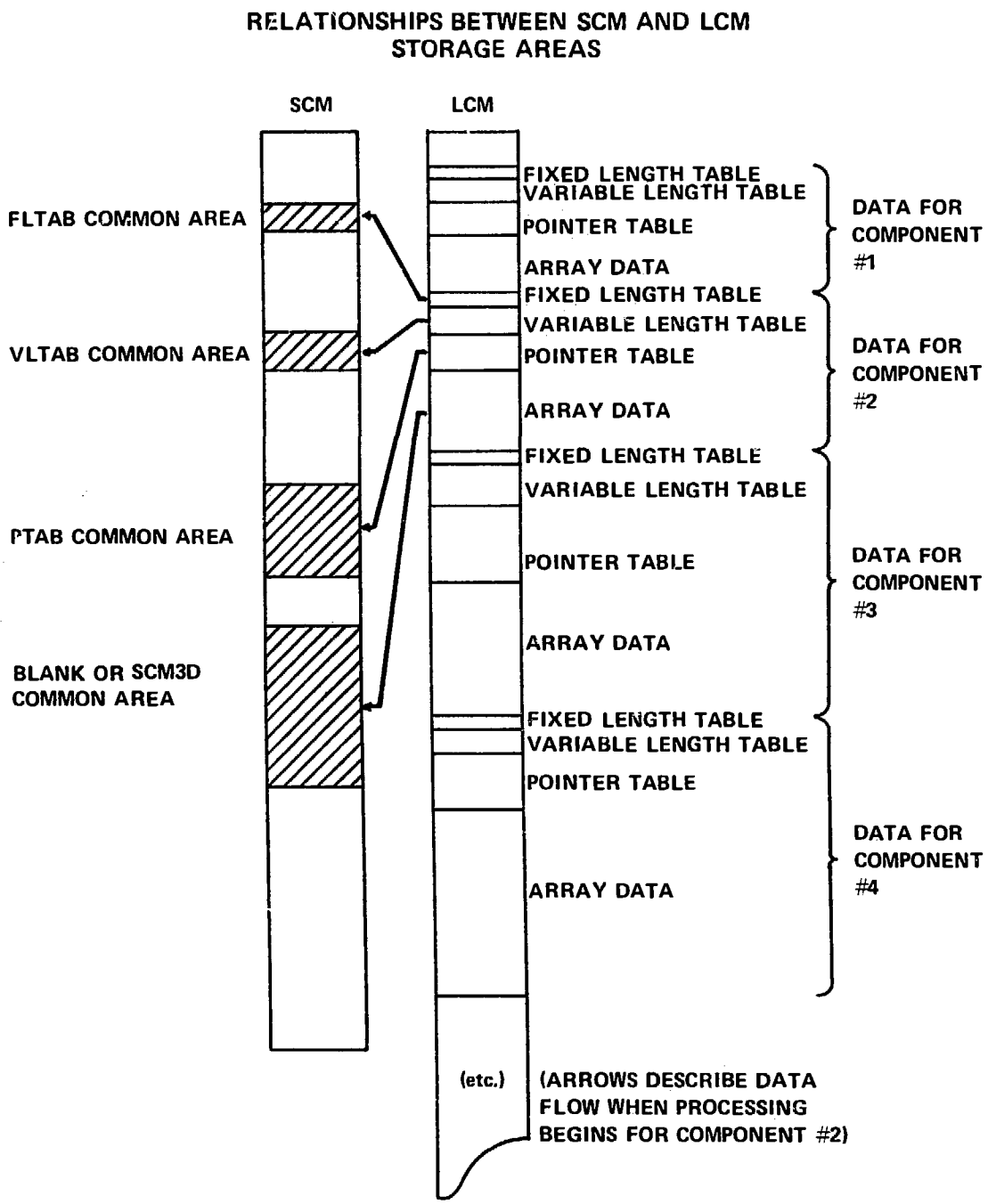

Fig. 2.
Storage areas in LCM and SCM.

Overall Structure

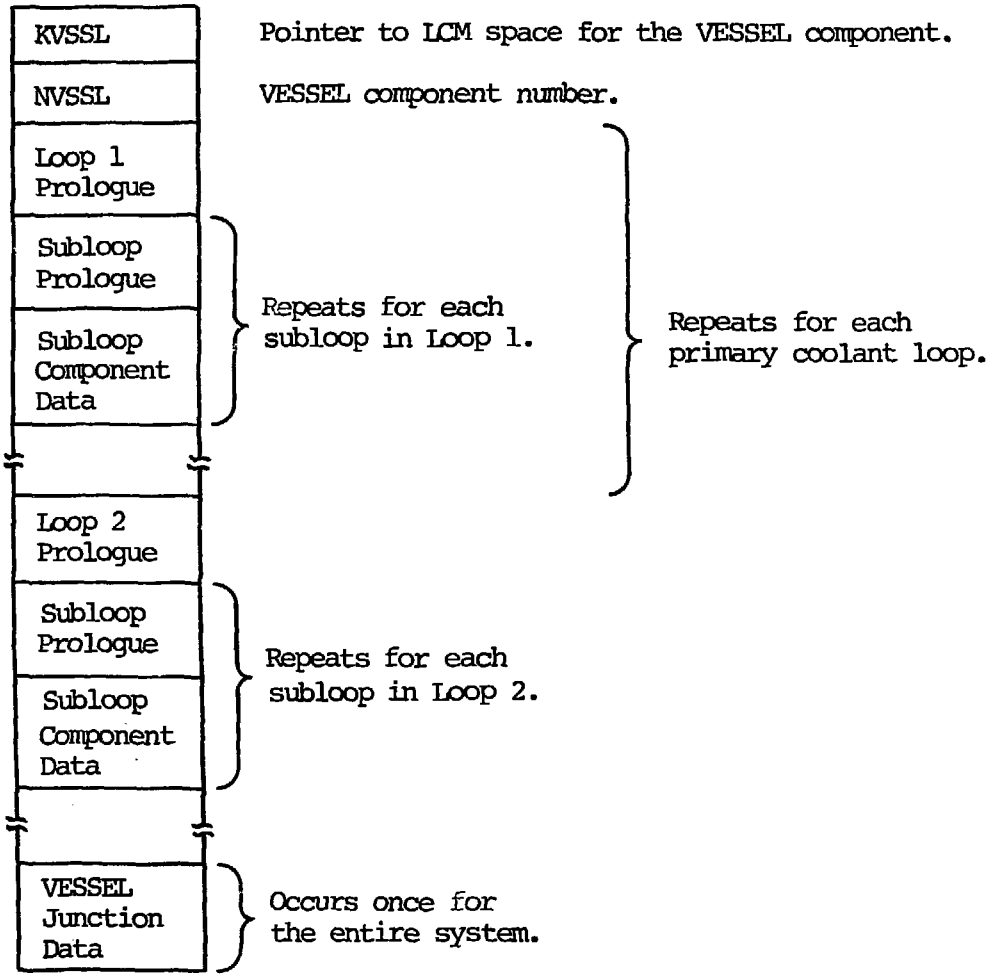

Fig. 3.
PWR initialization data structure.

Loop Prologue Structure

ILOOP	Loop index.
KNLOOP	Pointer to next loop.
JNLPC1	First vessel cold-leg junction.
JNLPC2	Second vessel cold-leg junction.
JNLPCH	Vessel hot-leg junction.
TILPC1	Desired temperature at JNLPC1.
WLPC1	Desired mass flow rate through JNLPC1.
WLPC2	Desired mass flow rate through JNLPC2.
NSLP	Number of subloops in this loop.
KTEE	Pointer to tee which joins loop pumps.

Sub-Loop Prologue Structure

ISL	Subloop index.
KNSL	Pointer to next subloop.
ISLTP	Subloop type index.
NSLCMP	Number of subloop components.
KSLP	Pointer to subloop pump.
KSLS	Pointer to subloop steam generator.
SGAREA	Steam generator area.
PMSPD	Pump speed.

Sub-Loop Component Data Structure (Repeats for each component in the sub-loop.)

KCOMP	Pointer to LCM data.
NUM	Component number.
TYPE	Component type.

VESSEL Junction Data Structure

	NCSR	Number of vessel junctions.
Repeats for each vessel junction.	JN	Junction number.
	P	Pressure inside vessel.
	H	Enthalpy flow rate at junction.
	W	Mass flow rate at junction.

Fig. 3.
(Cont.)

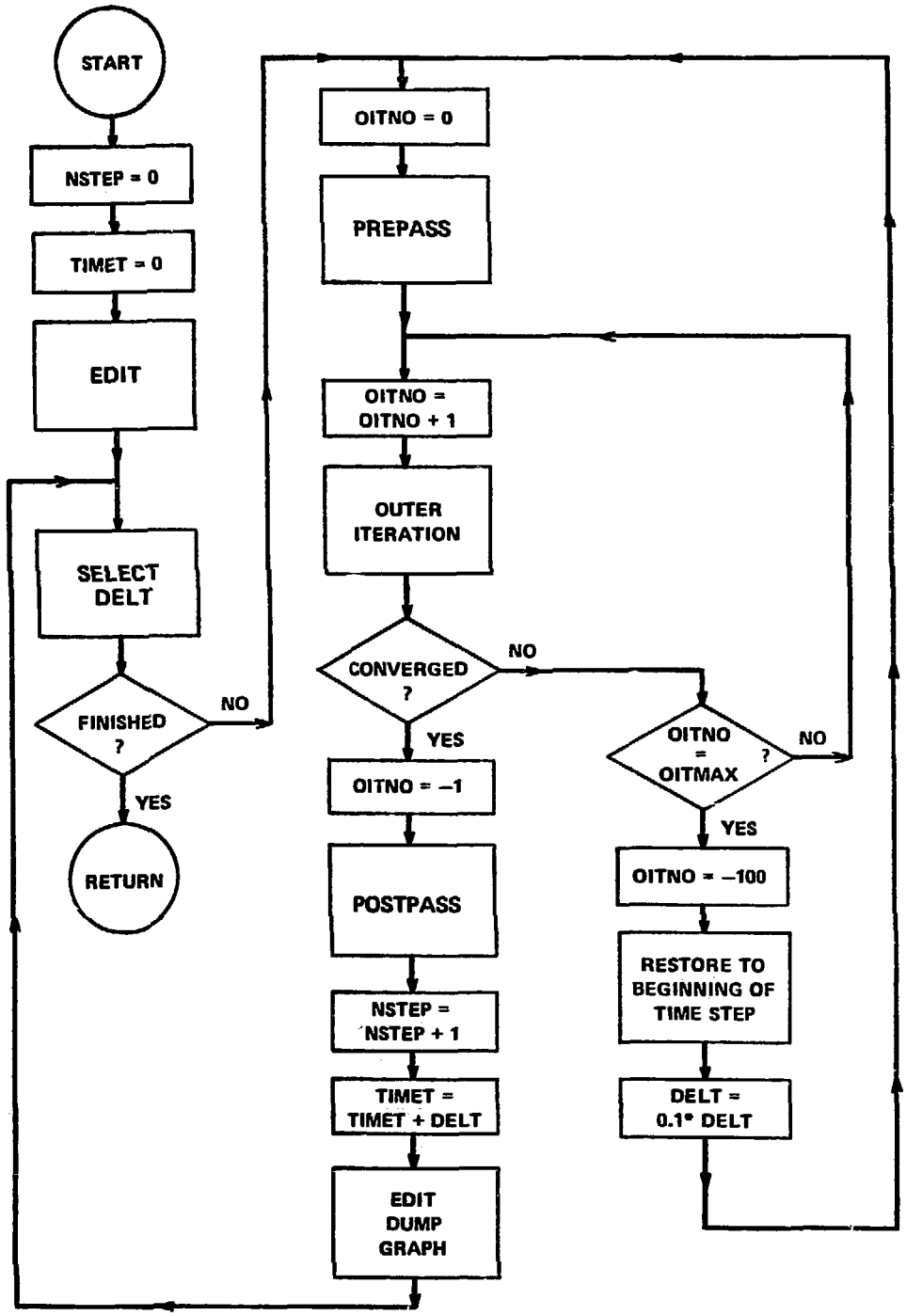

Fig. 4.
Flow diagram for transient calculations.

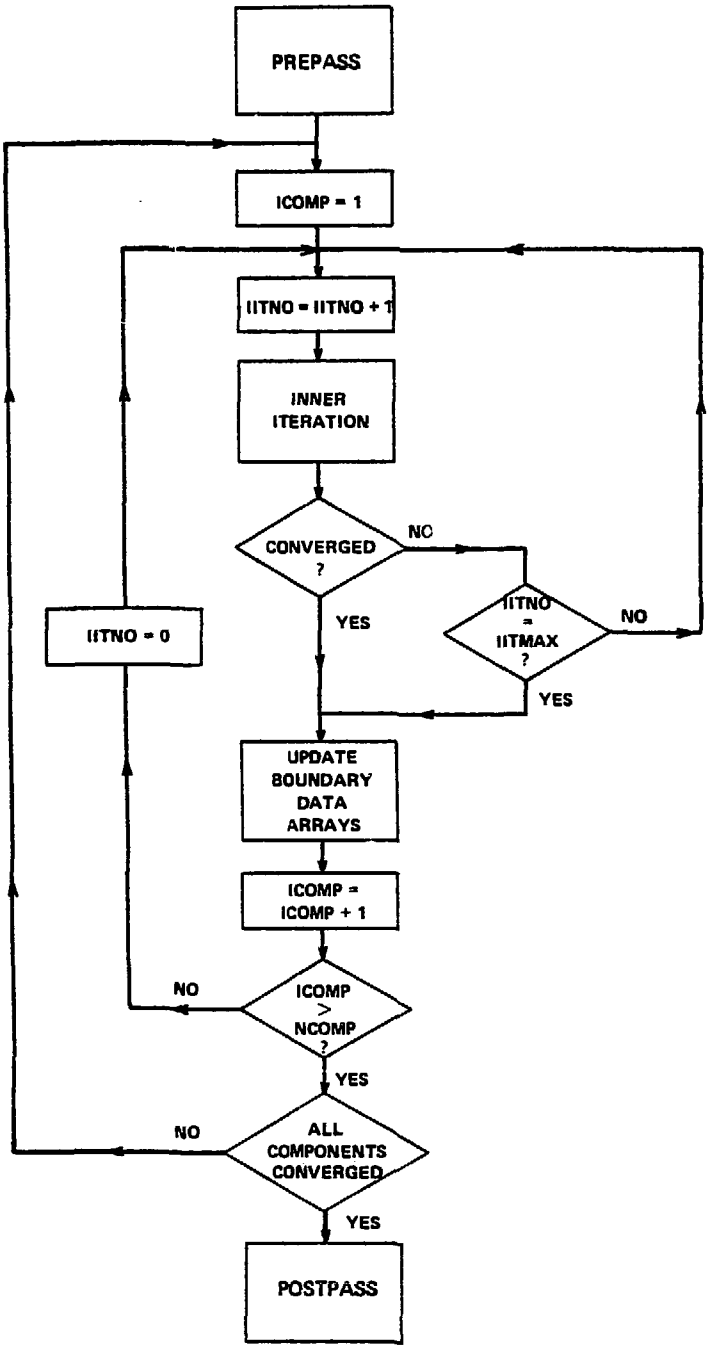

Fig. 5.
Outer iteration flow diagram.

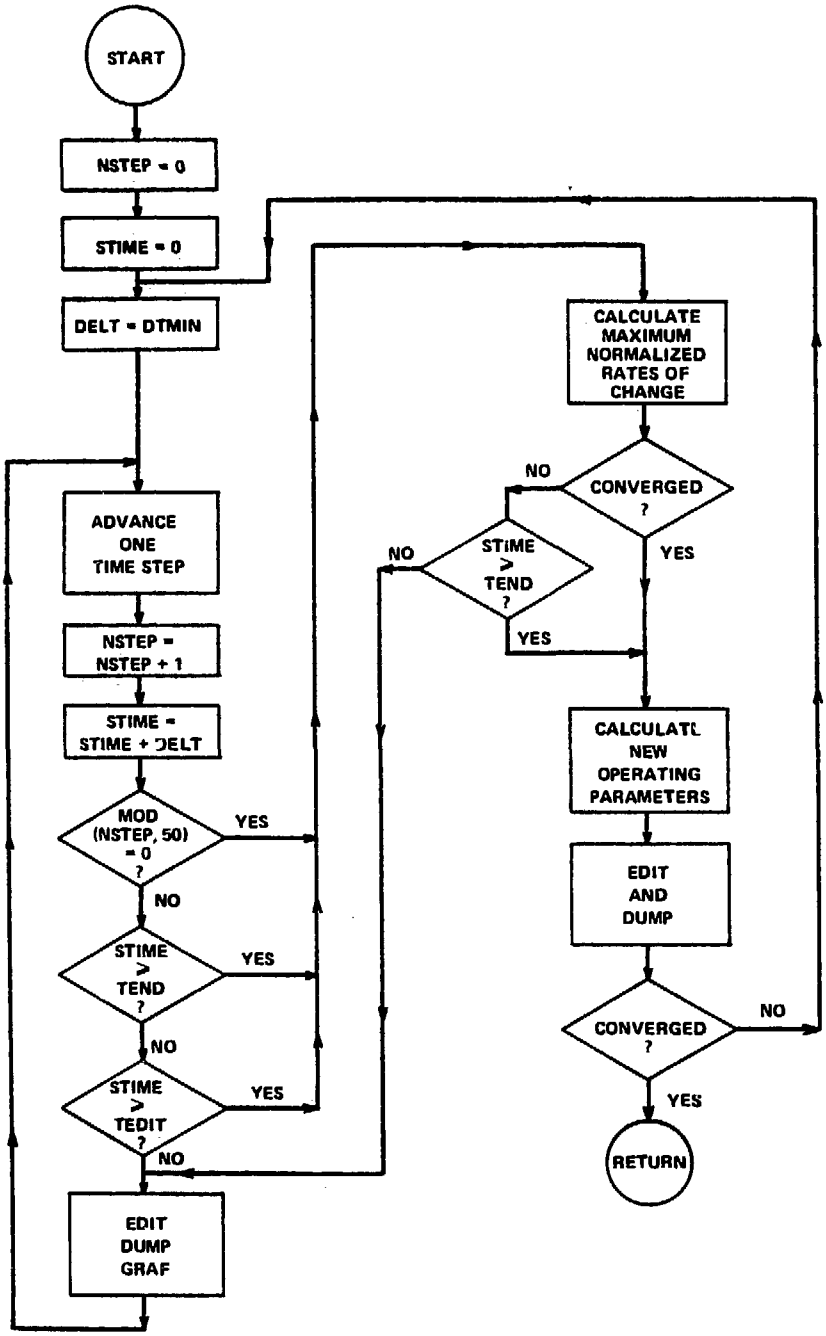

Fig. 6.
PWR initialization flow chart.

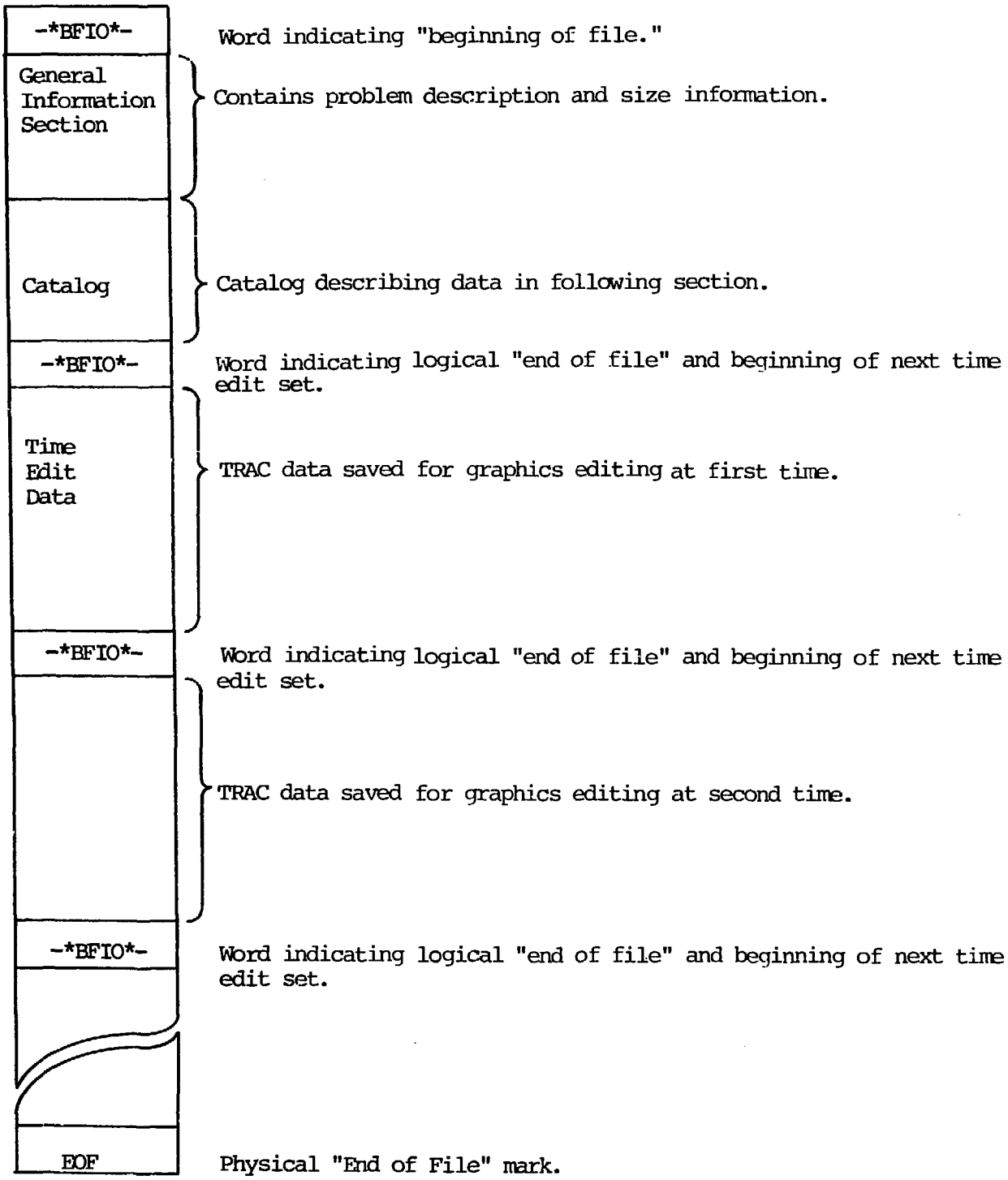

Fig. 7.
Overall graphics file structure.

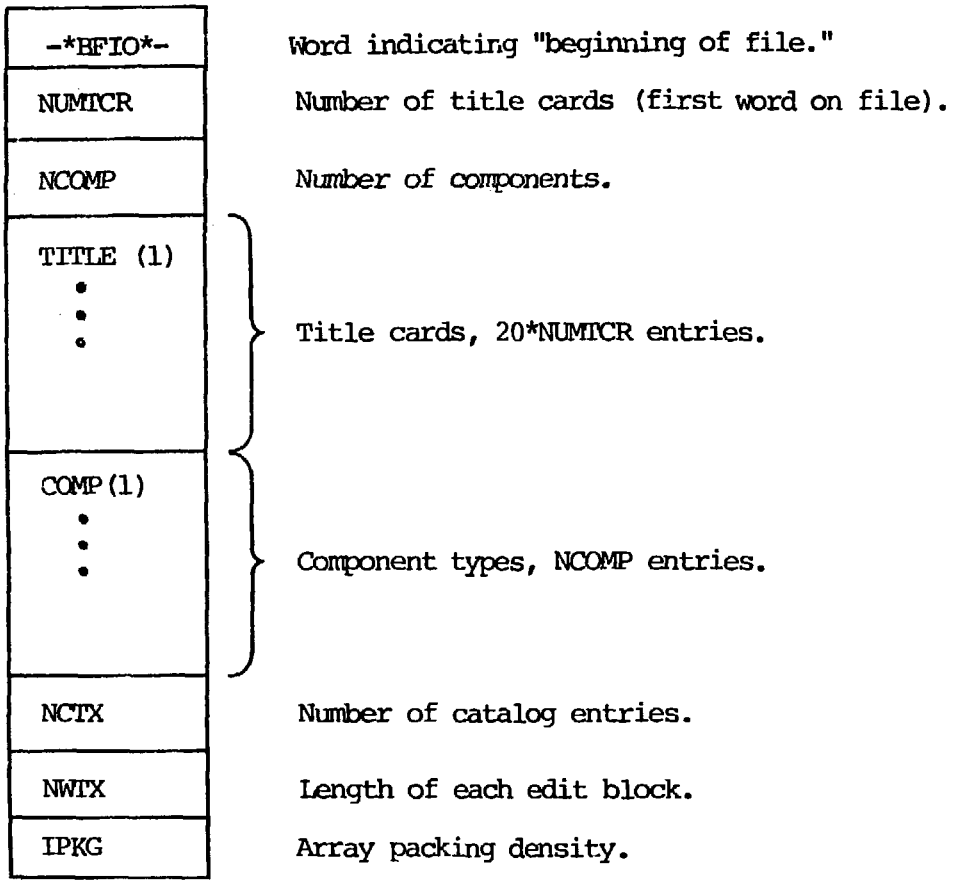

Fig. 8.
Structure of graphics file general information section.

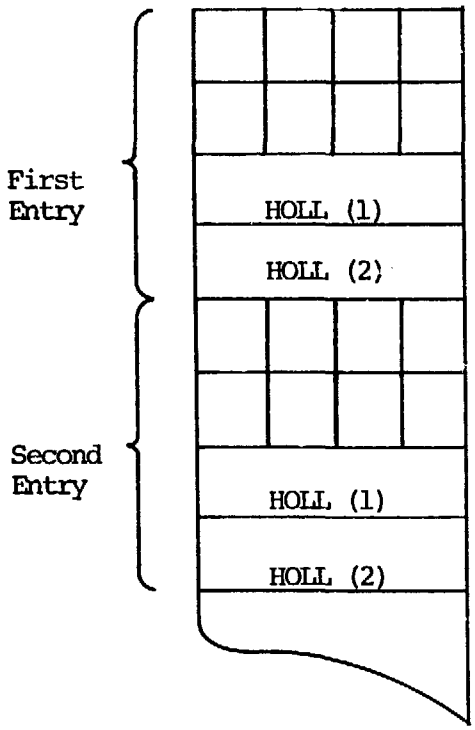

First packed word of description.

Second packed word of description.

First word of Hollerith description.

Second word of Hollerith description.

FIRST PACKED WORD OF DESCRIPTION

ICOMP	NUM	ITYPE	ILRN

SECOND PACKED WORD OF DESCRIPTION

0	NWRD	IPOS	KPT

ICOMP - Component index
NUM - Component number
ITYPE - Data Type
ILRN - Level/rod index
NWRD - Number of data words
IPOS - Location of data in memory
KPT - Location of data on disk

Fig. 9.
Structure of graphics file catalog.

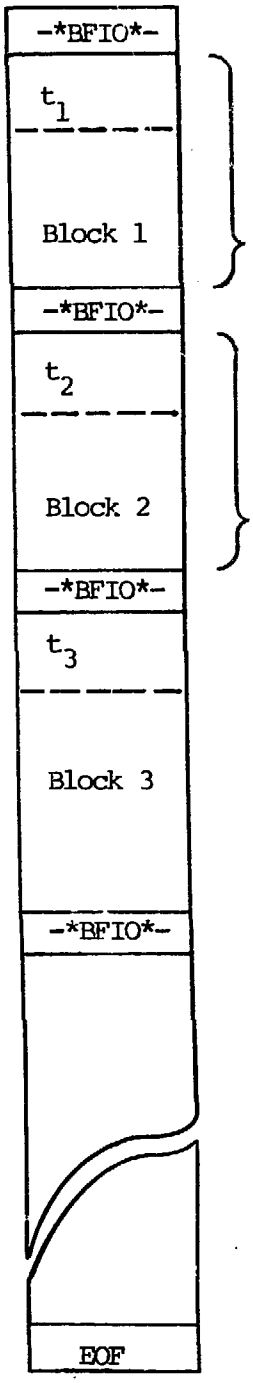

Word indicating "beginning of file."

NWTX words containing first edit block, written at time t_1.

Word indicating logical "end of file" and beginning of next time edit set.

NWTX words containing second edit block, written at time t_2.

Word indicating logical "end of file" and beginning of next time edit step.

etc.

Physical "End of File" mark.

Fig. 10.
Structure of graphics file time-edit data section.

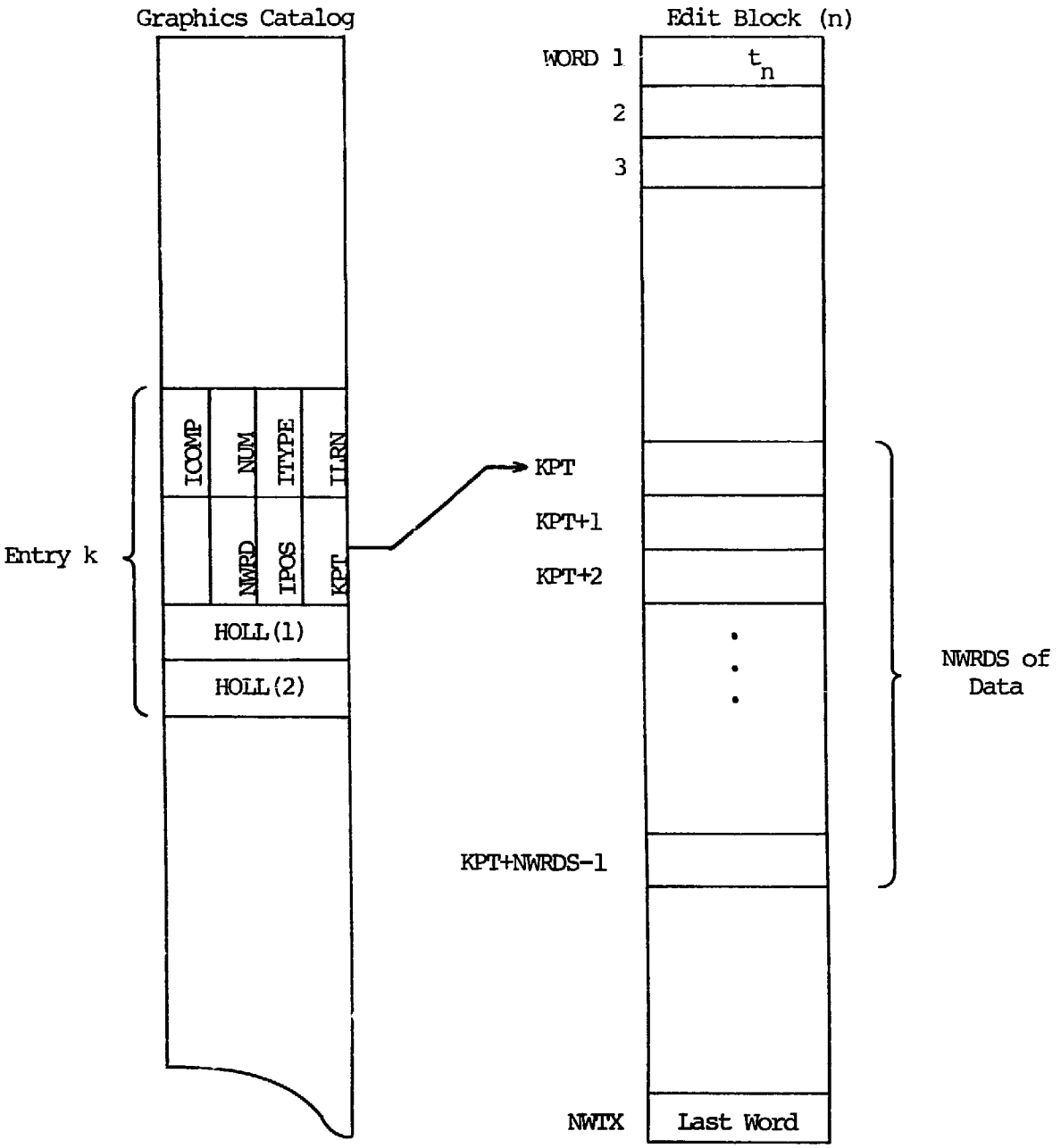

Fig. 11.
Graphics file catalog and time-edit data correspondence.

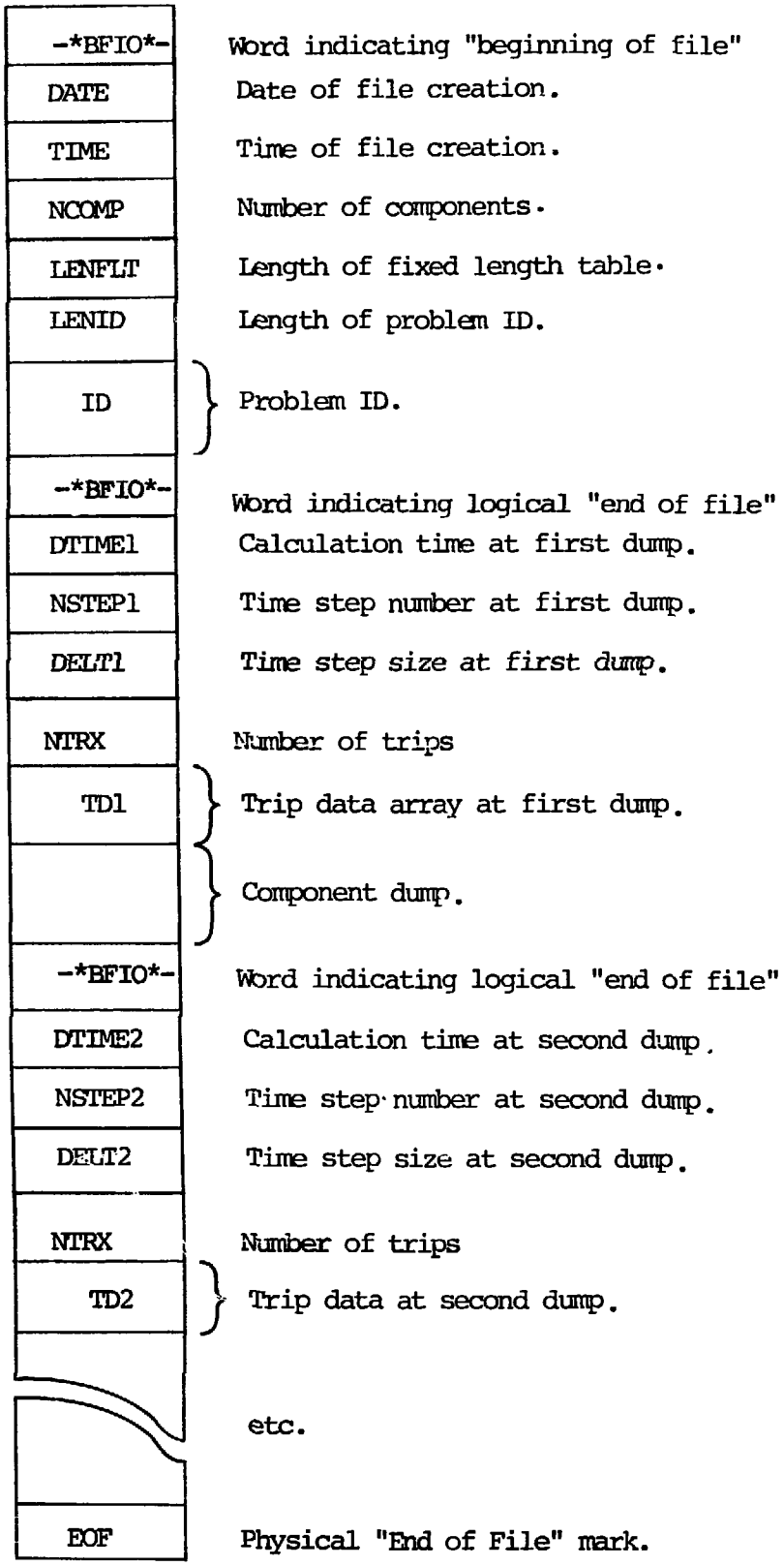

Fig. 12.
Dump file overall structure.

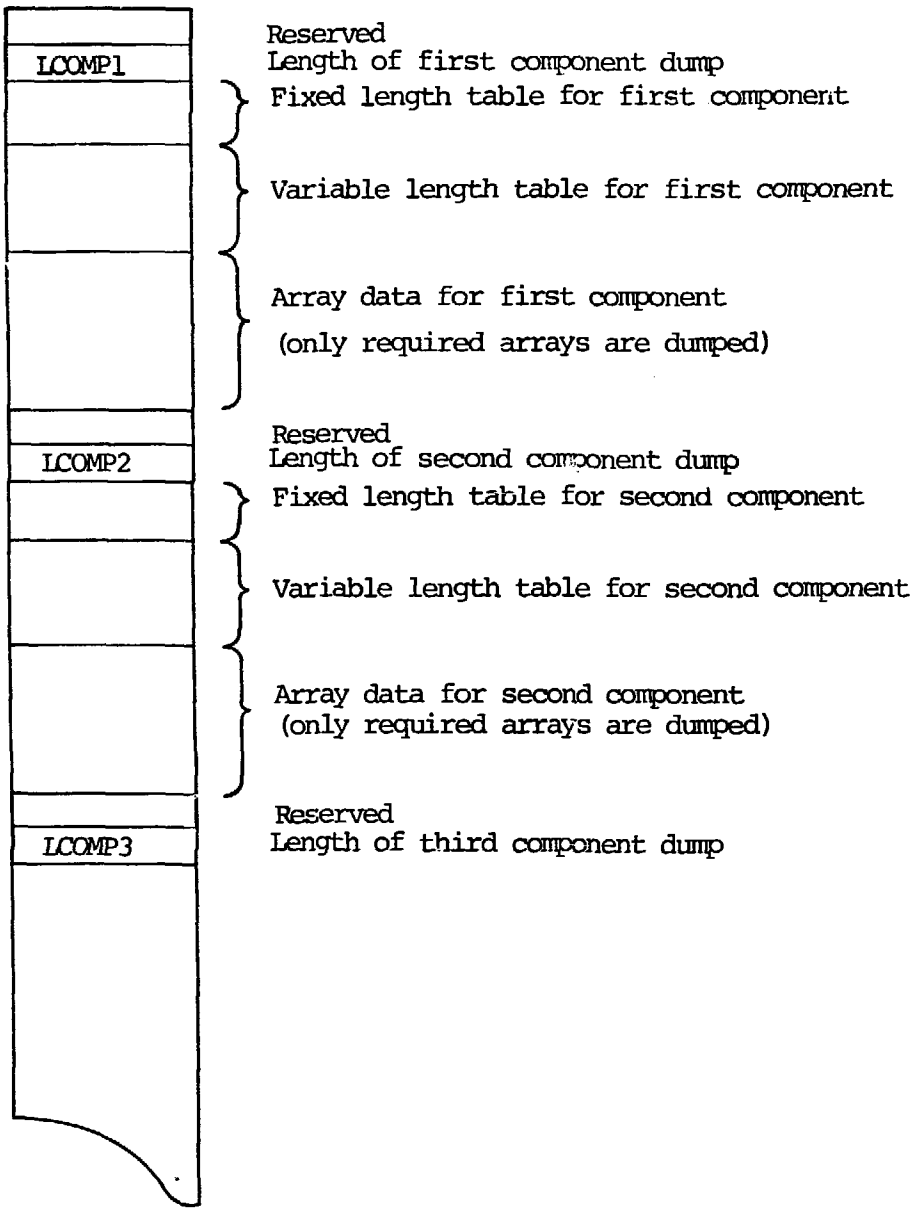

Fig. 13.
Component dump structure.

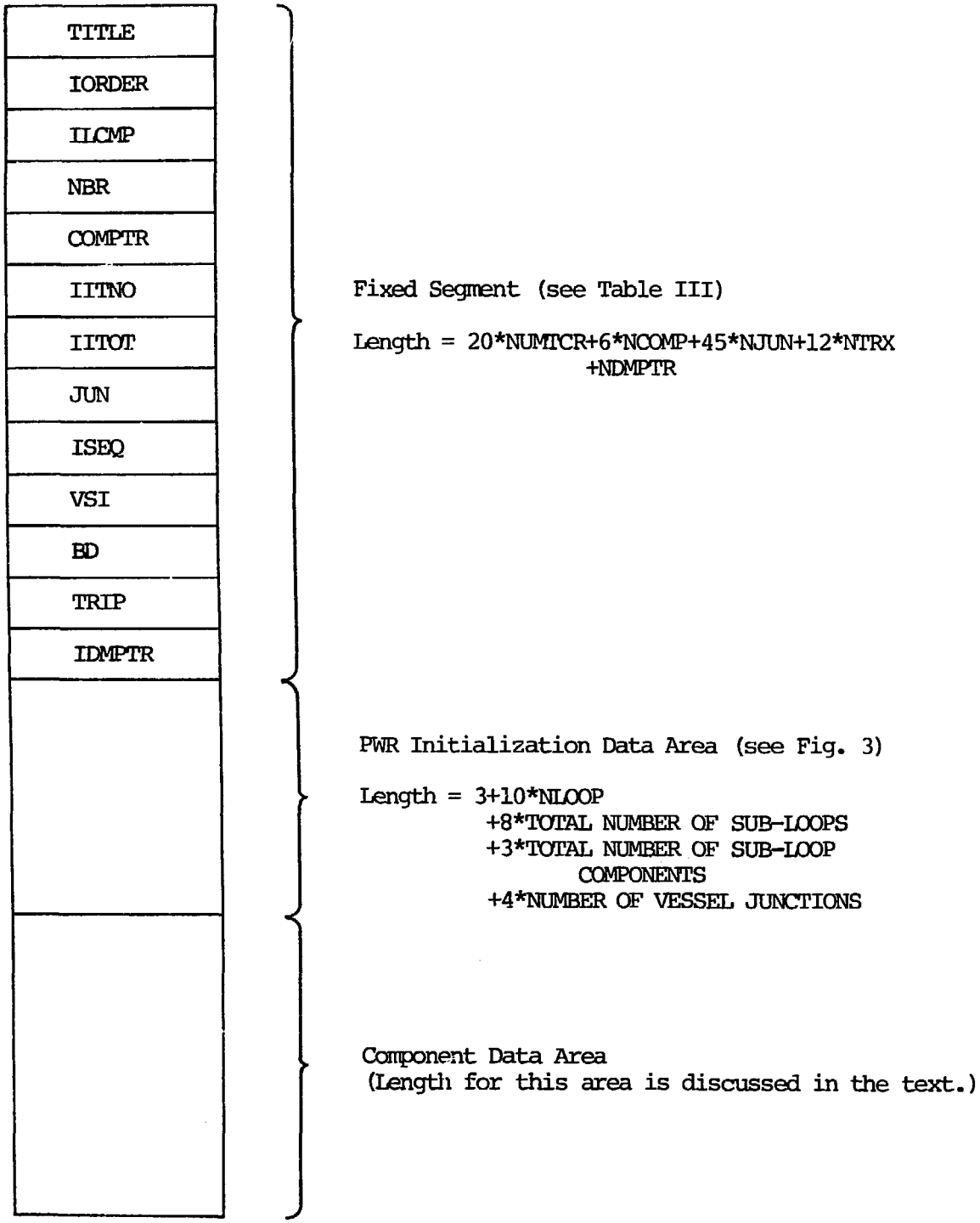

Fig. 14.
Blank common dynamic storage area organization.

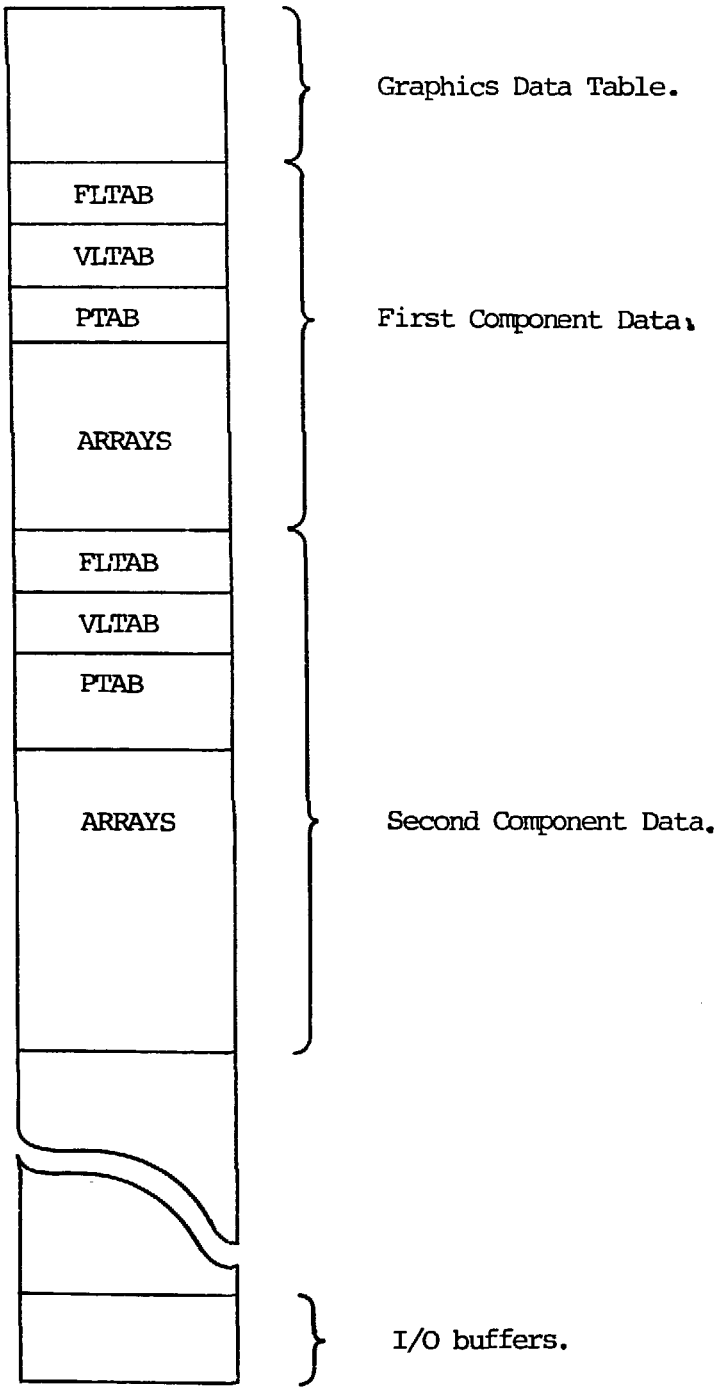

Fig. 15.
LCM data organization.

APPENDIX A
THERMODYNAMIC AND TRANSPORT FLUID PROPERTIES

The thermodynamic and transport properties subroutines used in TRAC are based on polynomial fits to steam table data. Transport property fits were obtained from Ref. 1 and the thermodynamic property fits were obtained from Ref. 2. Both the thermodynamic and transport property routines are used by all of the component modules in TRAC.

I. THERMODYNAMIC PROPERTIES

Figure A-1 shows a generalized flow chart for the THERMO subroutine which supplies thermodynamic water properties for TRAC. The input variables are the pressure and the liquid and vapor temperatures. The output variables include the saturation temperature; derivatives of T_s, T_ℓ, and T_g with respect to pressure; internal energy; density; enthalpy of each phase; the derivatives of internal energy, density, and enthalpy with respect to pressure for each phase; and finally the derivatives of internal energy and density with respect to temperature for each phase. THERMO also includes an ideal gas option for calculating the density and internal energy and their associated derivatives with respect to pressure and temperature.

The range of validity for the thermodynamic properties supplied by THERMO is currently as follows:

$T_\ell > 273.0$ K,

$T_g > 273.0$ K, and

$p < 190.0 \times 10^5$ Pa.

Polynomial equations for the various properties used in THERMO are given below. Values of the polynomial constants are given in Table A-I.

A. Saturation Properties

1. Temperature

$$T_s = c_1 (a_{14}\, p)^{c_2} + c_3 \qquad \text{for } T_s \le 647.3 \text{ K}$$

and

$$\frac{\partial T_s}{\partial p} = a_1 (a_{14}\, p)^{a_2} \qquad \text{for } T_s \leq 647.3\ \text{K} .$$

2. Internal Energy

$$e_s = c_6 + c_7 \left[\frac{1.0}{c_8 + p}\right] \qquad \text{for } p < 2.0 \times 10^6 \text{ Pa},$$

$$e_s = c_{12} + (c_{14}\, p + c_{13})p \qquad \text{for } p > 2.0 \times 10^6 \text{ Pa},$$

$$\frac{\partial e_s}{\partial p} = - c_7 \left[\frac{1.0}{c_8 + p}\right]^2 \qquad \text{for } p < 2.0 \times 10^6 \text{ Pa},$$

and

$$\frac{\partial e_s}{\partial p} = c_{13} + 2\, c_{14}\, p \qquad \text{for } p > 2.0 \times 10^6 \text{ Pa}.$$

3. Heat Capacity

$$c_{ps} = c_4 \left[1.0 - a_{15}\, T_s\right]^{c_5}$$

and

$$\frac{\partial c_{ps}}{\partial p} = a_3 \left[1.0 - a_{15}\, t_s\right]^{a_4} \frac{\partial T_s}{\partial p} .$$

4. Enthalpy

$$h_{gs} = e_s\, g_s$$

and

$$\frac{\partial h_{gs}}{\partial p} = \frac{\partial e_s}{\partial p}\, g_s ,$$

where

$$g_s = c_9 + (c_{11}\, p + c_{10})p \qquad \text{for } p < 2 \times 10^6 \text{ Pa}$$

and

$$g_s = c_{15} + (c_{17}\, p + c_{16})p \qquad \text{for } p > 2 \times 10^6 \text{ Pa} .$$

B. Liquid Properties

1. Internal Energy

$$e_\ell = s_{\ell 0} + s_{\ell 1}\, T_\ell + s_{\ell 2}\, T_\ell^2 + s_{\ell 3}\, T_\ell^3 \qquad \text{for } T_\ell < 573.15\ \text{K} ,$$

$$e_\ell = s_{h0} + s_{h1} T_\ell + s_{h2} T_\ell^2 + s_{h3} T_\ell^3 \qquad \text{for } T_\ell > 573.15 \text{ K},$$

$$\frac{\partial e_\ell}{\partial T_\ell} = s_{\ell 1} + 2 s_{\ell 2} T_\ell + 3 s_{\ell 3} T_\ell^2 \qquad \text{for } T_\ell < 573.15 \text{ K},$$

$$\frac{\partial e_\ell}{\partial T_\ell} = s_{h1} + 2 s_{h2} T_\ell + 3 s_{h3} T_\ell^2 \qquad \text{for } T_\ell > 573.15 \text{ K},$$

and

$$\frac{\partial e_\ell}{\partial p} = 0.0 \quad (e_\ell \text{ is not a function of pressure}).$$

2. Density

$$\rho_\ell = c_{47} + (c_{45} e_\ell) [c_{48} (c_{45} e_\ell) + c_{49}] + c_{51} p,$$

$$\frac{\partial \rho_\ell}{\partial p} = c_{51},$$

and

$$\frac{\partial \rho_\ell}{\partial T_\ell} = [a_5 + (c_{45} e_\ell) a_6] \frac{\partial e_\ell}{\partial T_\ell}.$$

3. Enthalpy

$$h_\ell = e_\ell + \frac{p}{\rho_\ell}$$

and

$$\frac{\partial h_{s\ell}}{\partial p} = \left[\frac{\partial e_{s\ell}}{\partial T_s} \frac{\partial T_s}{\partial p}\right] + \frac{1}{\rho_{s\ell}} - \frac{p}{(\rho_{s\ell})^2} \left[\frac{\partial \rho_{s\ell}}{\partial T_s} \frac{\partial T_s}{\partial p} + \frac{\partial \rho_{s\ell}}{\partial p}\right].$$

Note that at saturation T_ℓ is replaced by T_s in the above equations ($\frac{\partial h_{s\ell}}{\partial p}$ is an example).

C. Vapor Properties

1. Superheated Vapor: $(T_g - T_s) > 0$

a. Internal Energy

$$e_g = e_s + a_{12} \left[(T_g - T_s) + (T_g^2 - \beta)^{\frac{1}{2}} - \frac{T_s}{(a_{11} c_{ps} - 1.0)}\right],$$

where

$$\beta = T_s^2 \left[1.0 - \frac{1.0}{(a_{11} \; c_{ps} - 1.0)^2}\right] ,$$

$$\frac{\partial e_g}{\partial T_g} = \left[\frac{a_1}{2}\left(1.0 - \frac{\beta}{k^2}\right)\right]^{-1.0} ,$$

where

$$k = a_{13} \; (e_g - e_s) + T_s \left[1.0 + \frac{1.0}{(a_{11} \; c_{ps} - 1.0)}\right] ,$$

$$\frac{\partial e_g}{\partial p} = -\frac{1}{2}\left(\frac{\partial e_g}{\partial T_g}\right)\left[\left(1.0 - \frac{\beta}{k^2}\right)\frac{\partial k}{\partial p} + \frac{1}{k}\frac{\partial \beta}{\partial p}\right] ,$$

where

$$\frac{\partial k}{\partial p} = -a_{13}\frac{\partial e_s}{\partial p} + \left[1.0 + \frac{1.0}{(a_{11} \; c_{ps} - 1.0)}\right]\frac{\partial T_s}{\partial p}$$

$$- T_s \, a_{11}\left[\frac{1.0}{(a_{11} \; c_{ps} - 1.0)^2}\right]\frac{\partial c_{ps}}{\partial p} ,$$

and

$$\frac{\partial \beta}{\partial p} = \frac{2.0}{T_s}\left[\beta\left(\frac{\partial T_s}{\partial p}\right) + \frac{T_s^3 \, a_{11}}{(a_{11} \; c_{ps} - 1.0)^3}\left(\frac{\partial c_{ps}}{\partial p}\right)\right] .$$

b. Density

$$\rho_g = \frac{p}{[(g_s - 1.0) \; e_s + c_{26} \; (e_g - e_s)]} ,$$

$$\frac{\partial \rho_g}{\partial T_g} = -\left(\frac{\partial e_g}{\partial T_g}\right)\left[\frac{c_{26} \; \rho_g}{(g_s - 1.0) \; e_s + c_{26} \; (e_g - e_s)}\right] ,$$

and

$$\frac{\partial \rho_g}{\partial p} = \rho_g \left\{ \frac{1.0}{p} - \left[e_s \left(\frac{\partial g_s}{\partial p} \right) + (g_s - 1.0 - c_{26}) \frac{\partial e_s}{\partial p} \right] \cdot \left[\frac{1.0}{(g_s - 1.0)\, e_s + c_{26}\, (e_g - e_s)} \right] \right\} + \left(\frac{\partial \rho_g}{\partial e_g} \right) \left(\frac{\partial e_g}{\partial p} \right) ,$$

where

$$\frac{\partial g_s}{\partial p} = c_{10} + a_{16}\ p \qquad \text{for } p < 2.0 \times 10^6 \text{ Pa} ,$$

$$\frac{\partial g_s}{\partial p} = c_{16} + a_{18}\ p \qquad \text{for } p > 2.0 \times 10^6 \text{ Pa} ,$$

and

$$\frac{\partial \rho_g}{\partial e_g} = \frac{- c_{26}\, \rho_g}{[(g_s - 1.0)\, e_s + c_{26}\, (e_g - e_s)]} .$$

c. Enthalpy

$$h_g = e_g + \frac{p}{\rho_g}$$

and

$$\frac{\partial h_g}{\partial p} = \frac{\partial e_g}{\partial p} + \frac{1}{\rho_g} - p \frac{\partial \rho_g}{\partial p} .$$

2. Subcooled Vapor $(T_g - T_s) \leq 0$

a. Internal Energy

$$e_g = e_s + (T_g - T_s) \frac{c_{ps}}{c_{24}} ,$$

$$\frac{\partial e_g}{\partial T_g} = \frac{c_{ps}}{c_{24}} ,$$

and

$$\frac{\partial e_g}{\partial p} = - \left(\frac{\partial e_g}{\partial T_g} \right) \left\{ \frac{\partial T_s}{\partial p} - \left(\frac{c_{24}}{c_{ps}} \right) \left[\frac{\partial e_s}{\partial p} + \frac{(e_g - e_s)}{c_{ps}} \left(\frac{\partial c_{ps}}{\partial p} \right) \right] \right\} .$$

b. Density

$$\rho_g = \frac{p}{[(g_s - 1.0)\ e_g]} \quad ,$$

$$\frac{\partial \rho_g}{\partial T_g} = - \frac{\rho_g}{e_g} \left(\frac{\partial e_g}{\partial T_g} \right) \quad ,$$

and

$$\frac{\partial \rho_g}{\partial p} = \rho_g \left[\frac{1.0}{p} - \frac{1.0}{(g_s - 1.0)} \left(\frac{\partial g_s}{\partial p} \right) \right] - \left(\frac{\rho_g}{e_g} \right) \left(\frac{\partial e_g}{\partial p} \right) \quad .$$

3. Ideal Gas (Air)

These properties are presently used only for the vapor phase in an accumulator component.

a. Internal Energy

$$e_g = c_{vg}\ T_g \quad ,$$

$$\frac{\partial e_g}{\partial T_g} = c_{vg} \quad ,$$

and

$$\frac{\partial e_g}{\partial p} = 0.0 \quad .$$

b. Density

$$\rho_g = \frac{p}{R\ T_g} \quad ,$$

$$\frac{\partial \rho_g}{\partial p} = \frac{1.0}{R\ T_g} \quad ,$$

and

$$\frac{\partial \rho_g}{\partial T_g} = - R\ \rho_g \left(\frac{\partial \rho_g}{\partial p} \right) \quad ,$$

where R is the universal gas constant divided by the molecular weight for air.

This completes the equation set description for the thermodynamics properties. Next, we proceed to a description of the transport properties.

II. TRANSPORT PROPERTIES

Figure A-2 shows a generalized flow chart for the FPROP subroutine which is used to obtain transport water properties for TRAC. The input variables for this routine are the saturation temperature, pressure, enthalpies of each phase, vapor density, and the vapor temperature. The output transport variables include the latent heat of vaporization, surface tension, constant pressure specific heat, viscosity, and thermal conductivity of each phase. The transport property calls are function calls within the FPROP subroutine. The polynomial equation fits for the transport properties used in FPROP are now described.

A. Latent Heat of Vaporization

$$h_{\ell g} = h_{sg} - h_{s\ell},$$

where

$$h_{sg} = h_{g0} + h_{g1}\ p + h_{g2}\ p^2 + h_{g3}\ p^3 + h_{g4}\ p^4\ ,$$

$$h_{s\ell} = h_{\ell 0} + h_{\ell 1}\ p + h_{\ell 2}\ p^2 + h_{\ell 3}\ p^3 + h_{\ell 4}\ p^4 + h_{\ell 5}\ p^5\ ,$$

and

$$h_{g0} = 2.739623397 \times 10^{6} \qquad h_{\ell 0} = 5.747471844 \times 10^{5}$$

$$h_{g1} = 3.758844554 \times 10^{-2} \qquad h_{\ell 1} = 2.092062386 \times 10^{-1}$$

$$h_{g2} = -7.163990945 \times 10^{-9} \qquad h_{\ell 2} = -2.805106994 \times 10^{-8}$$

$$h_{g3} = 4.200231947 \times 10^{-16} \qquad h_{\ell 3} = 2.380982843 \times 10^{-15}$$

$$h_{g4} = -9.850752122 \times 10^{-24} \qquad h_{\ell 4} = -1.004266028 \times 10^{-22}$$

$$h_{\ell 5} = 1.658695956 \times 10^{-30}\ .$$

B. Constant Pressure Specific Heats

$$c_{p\ell} = \left\{ h_\ell \left[h_\ell \ (d_{0\ell} + d_{1\ell} \ p) + (c_{0\ell} + c_{1\ell} \ p) \right] + b_{0\ell} + b_{1\ell} \ p \right\}^{-1.0}$$

and

$$c_{pg} = \frac{1.0}{(z_1 + z_2 \ h_g)} ,$$

where

$$z_1 = p \ (b_{2g} \ p + b_{1g}) + b_{0g} ,$$

$$z_2 = p \ (c_{2g} \ p + c_{1g}) + c_{0g} ,$$

and

$b_{0\ell} = 2.394907 \times 10^{-4}$ $\qquad$ $b_{1\ell} = -5.196250 \times 10^{-13}$

$c_{0\ell} = 1.193203 \times 10^{-11}$ $\qquad$ $c_{1\ell} = 2.412704 \times 10^{-18}$

$d_{0\ell} = -3.944067 \times 10^{-17}$ $\qquad$ $d_{1\ell} = -1.680771 \times 10^{-24}$

$b_{0g} = -5.2568962 \times 10^{-4}$ $\qquad$ $c_{0g} = 3.2441688 \times 10^{-10}$

$b_{1g} = -3.4405779 \times 10^{-11}$ $\qquad$ $c_{1g} = 3.7348130 \times 10^{-18}$

$b_{2g} = 7.0081327 \times 10^{-19}$ $\qquad$ $c_{2g} = -2.9133521 \times 10^{-26}$

C. Fluid Viscosities

1. Liquid

Polynomial coefficients for the data in this section are given in Table A-II. The polynomial data for liquid viscosity is divided into three different enthalpy ranges. For $h_\ell < 2.76 \times 10^5$ J/kg,

$$\mu_\ell = \left[a_{0\ell} + a_{1\ell} \ x_i + a_{2\ell} \ x_i^2 + a_{3\ell} \ x_i^3 + a_{4\ell} \ x_i^4 \right]$$

$$- \left[b_{0\ell} + b_{1\ell} \ \eta + b_{2\ell} \ \eta^2 + b_{3\ell} \ \eta^3 + b_{4\ell} \ \eta^4 \right] (p - p_i) ,$$

where

$$x_i = (h_\ell - 42658.84) \ h_C$$

and

$$\eta = (h_\ell - 55358.8) \ e_{h0} .$$

In the range $2.76 \times 10^5 < h < 3.94 \times 10^5$ J/kg,

$$\mu_\ell = \left[e_{0\ell} + e_{1\ell} h_\ell + e_{2\ell} h_\ell^2 + e_{3\ell} h_\ell^3 \right] + \left[f_{0\ell} + f_{1\ell} h_\ell + f_{2\ell} h_\ell^2 + f_{3\ell} h_\ell^3 \right] (p - p_i) .$$

For $h_\ell > 3.94 \times 10^5$ J/kg,

$$\mu_\ell = \left[d_{0\ell} + d_{1\ell} z_i + d_{2\ell} z_i^2 + d_{3\ell} z_i^3 + d_{4\ell} z_i^4 \right] ,$$

where

$$z_i = (h_\ell - 401467.6) h_{00} .$$

2. Vapor

Polynomial coefficients for the vapor viscosity data are given in Table A-III. The data are divided into three vapor temperature ranges. For $T_g \leq 300^\circ$C,

$$\mu_g = (b_{1g} T_g + c_{1g}) - \rho_g (d_{1g} - e_{1g} T_g) ,$$

where T_g is in $^\circ$C. For $300 < T_g < 375^\circ$C,

$$\mu_g = (b_{1g} T_g + c_{1g}) + \rho_g \left[f_{0g} + f_{1g} T_g + f_{2g} T_g^2 + f_{3g} T_g^3 \right] + \rho_g \left[g_{og} + g_{1g} T_g + g_{2g} T_g^2 + g_{3g} T_g^3 \right] \left[a_{0g} + a_{1g} \rho_g + a_{2g} \rho_g^2 \right] .$$

For the range $T_g \geq 375^\circ$C,

$$\mu_g = (b_{1g} T_g + c_{1g}) + \rho_g \left[a_{og} + a_{1g} \rho_g + a_{2g} \rho_g^2 \right] .$$

D. Fluid Thermal Conduc ivities

The liquid thermal conductivity is given by

$$k_\ell = a_{k0} + a_{k1} x_k + a_{k2} x_k^2 + a_{k3} x_k^3 ,$$

where

$$x_k = h_\ell / 5.815 \times 10^5$$

and

$$a_{k0} = 0.573738622$$

$$a_{k1} = 0.2536103551$$

$$a_{k2} = -0.145468269$$

$$a_{k3} = -0.01387472485 \ .$$

For the vapor, the thermal conductivity is given by

$$k_g = x_1 + \rho_g \left[x_2 + \frac{\rho_g \ 2.1482 \times 10^5}{T_g^{4.2}} \right] ,$$

where T_g is in ^{o}C,

$$x_1 = k_{g0} + k_{g1} T_g + k_{g2} T_g^2 + k_{g3} T_g^3 \ ,$$

$$x_2 = b_{k0} + b_{k1} T_g + b_{k2} T_g^2 \ ,$$

and

$$k_{g0} = 1.76 \times 10^{-2} \qquad b_{k0} = 1.0351 \times 10^{-4}$$

$$k_{g1} = 5.87 \times 10^{-5} \qquad b_{k1} = 0.4198 \times 10^{-6}$$

$$k_{g2} = 1.04 \times 10^{-7} \qquad b_{k2} = -2.771 \times 10^{-11}$$

$$k_{g3} = -4.51 \times 10^{-11} \ .$$

E. Surface Tension

$$\sigma = 0.0755 \left[1.0 - \frac{T_s}{374.15} \right]^{1.2} \quad \text{for } T_s \leq 374.15 \ ^{o}C \quad \text{and}$$

$$\sigma = 0 \qquad \text{for } T_s > 374.15 \ ^{o}C \ .$$

This completes the description of the functional fits to the water transport properties.

III. VERIFICATION

The thermodynamic and transport property fits used in TRAC have been compared (see Ref. 2) with steam table data over a wide range of parameters.

The agreement is satisfactory in the saturation region and in the superheated steam region for 1.0×10^5 Pa $< p < 100 \times 10^5$ Pa and 423.0 K $< T_g <$ 823.0 K. The agreement is also good in the subcooled water region for 373.0 K $< T_\ell <$ 523.0 K and 0.4178×10^6 J/kg $< e_\ell < 1.0808 \times 10^6$ J/kg.

Further verification was performed by comparing the TRAC polynomial fits with the WATER package (Ref. 1) over a wider range of nonequilibrium (99 K of both superheat and subcooling) for a pressure variation of 1.0×10^5 Pa to 2.0×10^7 Pa. The comparisons showed good agreement for both the thermodynamic and transport properties throughout the saturation and nonequilibrium regions except for very extreme cases. For instance, the vapor specific heat equation fit used in TRAC diverges to infinity at saturation conditions above 1.8×10^7 Pa pressure. Also, at high degrees of subcooling or superheat, some inconsistencies are noticed. However, it should be pointed out that since there are no data to compare with in these extreme cases, it is impossible to make an adequate comparison between TRAC and the WATER package.

In conclusion, for most of the applications that TRAC will be used for, the thermodynamic and transport property routines provide realistic values over a wide range of interest. Also, the simplified polynomial fits provide an efficient and low-cost method compared to other approaches such as steam table interpolation.

REFERENCES

1. W. A. Coffman and L. L. Lynn, "WATER: A Large Range Thermodynamic and Transport Water Property FORTRAN-IV Computer Program," Bettis Atomic Power Laboratory report WAPD-TM-568 (December 1966).

2. W. C. Rivard and M. D. Torrey, "Numerical Calculation of Flashing from Long Pipes Using a Two-Field Model," Appendix A, Los Alamos Scientific Laboratory report LA-6104-MS (November 1975).

TABLE A-I

POLYNOMIAL CONSTANTS FOR THERMO

$c_1 = 117.8$

$c_2 = 0.223$

$c_3 = 255.2$

$c_4 = 958.75$

$c_5 = -0.8566$

$c_6 = 2619410.618$

$c_7 = -4.995 \times 10^{10}$

$c_8 = 3.403 \times 10^{5}$

$c_9 = 1.0665545$

$c_{10} = 1.02 \times 10^{-8}$

$c_{11} = -2.548 \times 10^{-15}$

$c_{12} = 2589600.0$

$c_{13} = 6.350 \times 10^{-3}$

$c_{14} = -1.0582 \times 10^{-9}$

$c_{15} = 1.0764$

$c_{16} = 3.625 \times 10^{-10}$

$c_{17} = -9.063 \times 10^{-17}$

$c_{20} = 461.7$

$c_{21} = 2.0 \times 10^{6}$

$c_{23} = 647.3$

$c_{24} = 1.3$

$c_{26} = 0.3$

$c_{28} = 1.0 \times 10^{5}$

$c_{40} = 273.0$

$c_{41} = 239.36$

$c_{42} = 2.7867$

$c_{43} = -5.77626$

$c_{44} = 3.938$

$c_{45} = 1.0 \times 10^{-6}$

$c_{47} = 1000.0$

$c_{48} = -0.15 \times 10^{3}$

$c_{49} = -20.0$

$c_{51} = 0.657 \times 10^{-6}$

$a_1 = C_1 \cdot C_2 / C_{28}$

$a_2 = C_2 - 1.0$

$a_3 = -C_4 \cdot C_5 / C_{23}$

$a_4 = C_5 - 1.0$

$a_5 = C_{45} \cdot C_{49}$

$a_6 = 2 \cdot C_{45} \cdot C_{48}$

$a_7 = 4 \cdot C_{44} \cdot C_{45}$

$a_8 = 3 \cdot C_{43} \cdot C_{45}$

$a_9 = 2 \cdot C_{42} \cdot C_{45}$

$a_{10} = C_{41} \cdot C_{45}$

$a_{11} = 2 \cdot C_{26} / (C_{24} + C_{20})$

$a_{13} = A_{11} \cdot (1.0 + C_{26})$

$a_{12} = 1.0 / A_{13}$

$a_{14} = 1.0 / C_{28}$

$a_{15} = 1.0 / C_{23}$

$a_{16} = 2 \cdot C_{11}$

$a_{17} = 2 \cdot C_{14}$

$a_{18} = 2 \cdot C_{17}$

$s_{\ell 0} = -1.4655677 \times 10^{6}$

$s_{\ell 1} = 6.926955 \times 10^{3}$

$s_{\ell 2} = -7.7423067$

$s_{\ell 3} = 7.2803006 \times 10^{-3}$

$s_{h0} = -8.9$

$s_{h1} = 2.3639439 \times 10^{4}$

$s_{h2} = -77.434017$

$s_{h3} = 7.0215574 \times 10^{-2}$

TABLE A-II

LIQUID VISCOSITY POLYNOMIAL COEFFICIENTS

$a_{0\ell} = 1.299470229 \times 10^{-3}$

$a_{1\ell} = -9.264032108 \times 10^{-4}$

$a_{2\ell} = 3.81047061 \times 10^{-4}$

$a_{3\ell} = -8.219444458 \times 10^{-5}$

$a_{4\ell} = 7.022437984 \times 10^{-6}$

$b_{0\ell} = -6.5959 \times 10^{-12}$

$b_{1\ell} = 6.763 \times 10^{-12}$

$b_{2\ell} = -2.88825 \times 10^{-12}$

$b_{3\ell} = 4.4525 \times 10^{-13}$

$d_{0\ell} = 3.026032306 \times 10^{-4}$

$d_{1\ell} = -1.836606896 \times 10^{-4}$

$d_{2\ell} = 7.567075775 \times 10^{-5}$

$d_{3\ell} = -1.647878879 \times 10^{-5}$

$d_{4\ell} = 1.416457633 \times 10^{-6}$

$e_{0\ell} = 1.4526052612 \times 10^{-3}$

$e_{1\ell} = -6.9880084985 \times 10^{-9}$

$e_{2\ell} = 1.5210230334 \times 10^{-14}$

$e_{3\ell} = -1.2303194946 \times 10^{-20}$

$f_{0\ell} = -3.8063507533 \times 10^{-11}$

$f_{1\ell} = 3.9285207677 \times 10^{-16}$

$f_{2\ell} = -1.2585799292 \times 10^{-21}$

$f_{3\ell} = 1.2860180788 \times 10^{-27}$

$h_0 = 8.581289699 \times 10^{-6}$

$c_{0n} = 4.265884 \times 10^{4}$

$p_i = 6.894575293 \times 10^{5}$

$h_{00} = 3.892077365 \times 10^{-6}$

$e_{c0n} = 5.53588 \times 10^{4}$

$e_{h0} = 6.484503981 \times 10^{-6}$

$c_n = 4.014676 \times 10^{5}$

TABLE A-III

VAPOR VISCOSITY POLYNOMIAL COEFFICIENTS

$a_{0g} = 3.53 \times 10^{-8}$

$a_{1g} = 6.765 \times 10^{-11}$

$a_{2g} = 1.021 \times 10^{-14}$

$b_{1g} = 0.407 \times 10^{-7}$

$c_{1g} = 8.04 \times 10^{-6}$

$d_{1g} = 1.858 \times 10^{-7}$

$e_{1g} = 5.9 \times 10^{-10}$

$f_{0g} = -0.2885 \times 10^{-5}$

$f_{1g} = 0.2427 \times 10^{-7}$

$f_{2g} = -0.678933 \times 10^{-10}$

$f_{3g} = 0.6317037 \times 10^{-13}$

$g_{0g} = 176.0$

$g_{1g} = -1.6$

$g_{2g} = 0.0048$

$g_{3g} = -0.474074074 \times 10^{-5}$

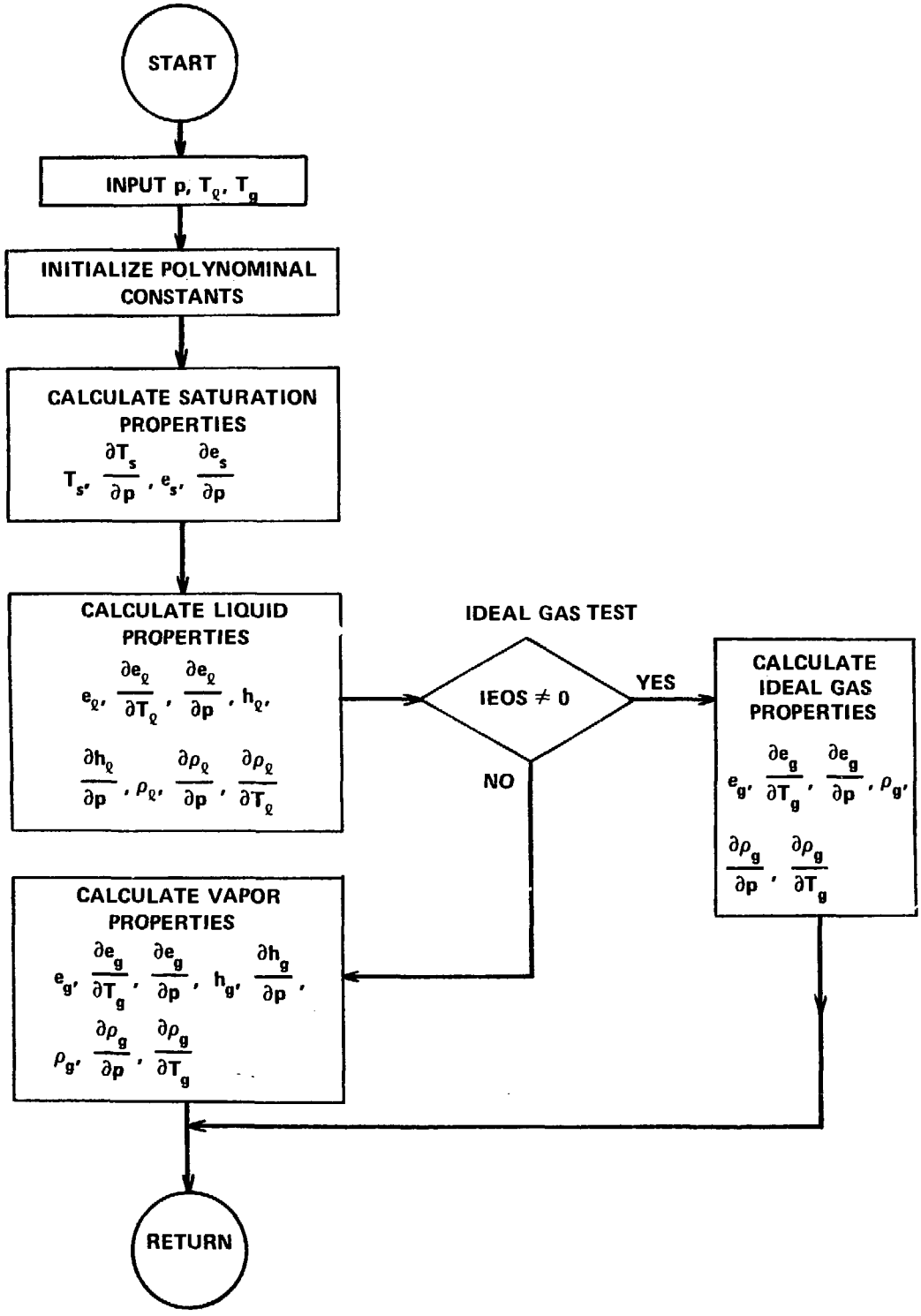

Fig. A-1.
Flow chart for thermodynamic water properties routine THERMO.

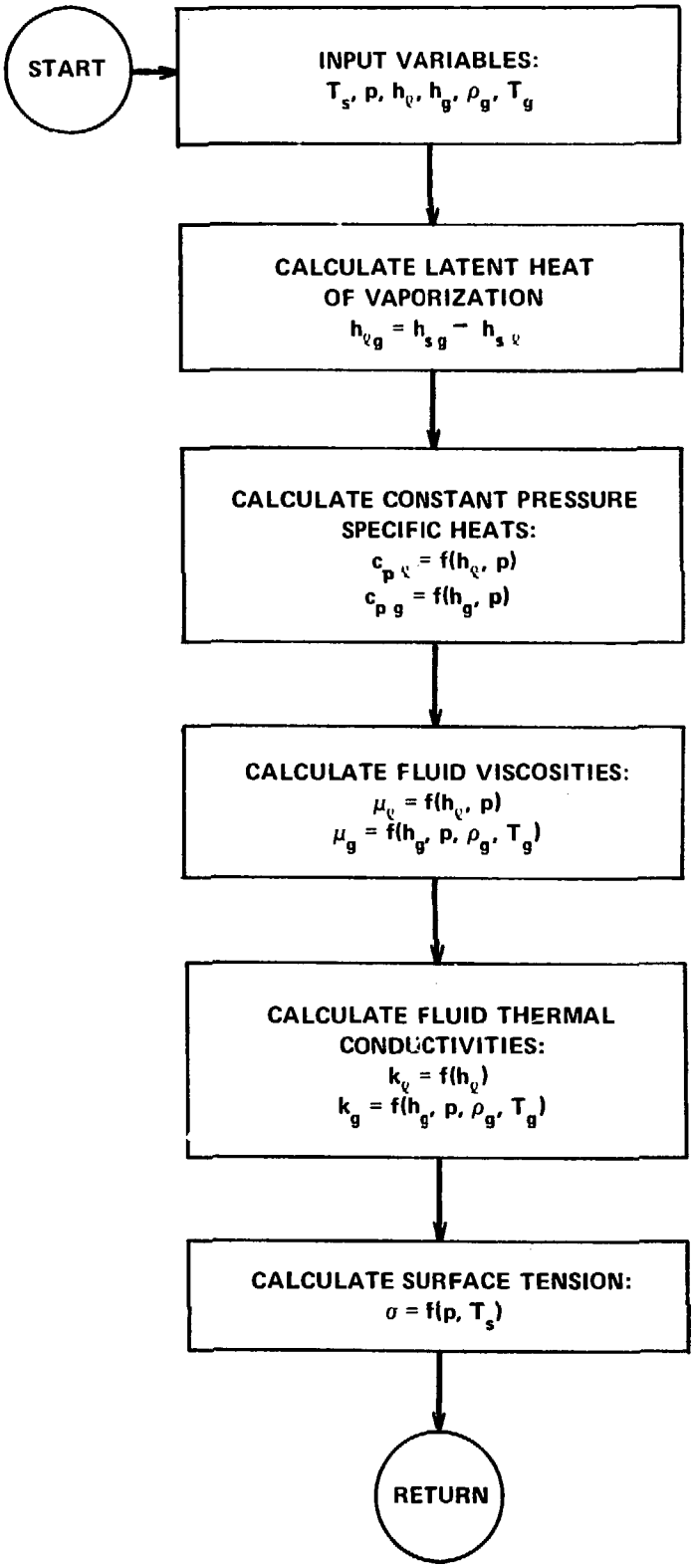

Fig. A-2.
Flow chart for transport water properties routine FPROP.

APPENDIX B
MATERIAL PROPERTIES

I. INTRODUCTION

An extensive library of temperature-dependent material properties is incorporated in the TRAC code. The entire library is accessible by the vessel component, while ex-vessel components have access to structural materials property sets only. There are 10 sets of materials properties which comprise the library, each set supplying values for thermal conductivity, specific heat, density, and spectral emissivity for use in heat transfer calculations. The first five sets contain properties for nuclear heated or electrically heated fuel rod simulation. Included are: nuclear fuels Zircaloy cladding, fuel-cladding gap gases, electrical heater rod filaments, and electrical heater rod insulating material. The last five sets are for structural materials including stainless steels, carbon steel, and Inconel.

Figure B-1 illustrates the calling tree for obtaining the property values. The subroutines MFROD and MPROP are simple processors for calculating the average temperature and calling the appropriate subroutine based on the user-supplied material index. Subroutine FROD controls the fuel-clad gap conductance and fuel rod thermal conduction calculations. The material indexes used in the library are:

1 - mixed oxide fuel
2 - Zircaloy
3 - gap gases
4 - boron nitride insulation
5 - Constantan/Nichrome heater
6 - stainless steel type 304
7 - stainless steel type 316
8 - stainless steel type 347
9 - carbon steel type A508
10 - Inconel type 718.

Gap gas properties are calculated only when the dynamic fuel-clad gap heat transfer coefficient option is used.

II. NUCLEAR FUEL (UO_2-PuO_2) PROPERTIES

Subroutine MFUEL calculates the properties for mixed oxide nuclear fuels. Values obtained are influenced by three user-supplied input variables: fraction of theoretical density, fraction of plutonium oxide in the fuel, and fuel burnup. Property changes upon melting are not included in this code version.

A. Density

The mixed oxide fuel density is calculated with a correction factor to account for thermal expansion, which is assumed to be axisymmetric:

$$\rho = d/(1 + 3\,\Delta L/L),$$

where

ρ = density (kg/m^3),

$d = f_{TD}\,[(1 - f_{PuO_2})\rho_{UO_2} + f_{PuO_2}\,\rho_{PuO_2}]$,

f_{TD} = fraction of theoretical fuel density,

f_{PuO_2} = weight fraction of PuO_2 in fuel,

$\rho_{UO_2} = 1.097 \times 10^4$,

$\rho_{PuO_2} = 1.146 \times 10^4$, and

$\Delta L/L$ = linear thermal expansion.

The value calculated for the linear thermal expansion is based on the MATPRO formulation:[1]

$$\Delta L/L = a_o + a_1 T_c + a_2 T_c^2 + a_3 T_c^3 ,$$

where

T_c = fuel temperature (^oC)

and

	UO_2	$UO_2 - PuO_2$
a_o	-4.972×10^{-4}	-3.935×10^{-4}
a_1	7.107×10^{-6}	$8.495\ 5 \times 10^{-6}$
a_2	2.581×10^{-9}	$2.151\ 3 \times 10^{-9}$
a_3	1.140×10^{-13}	$3.714\ 3 \times 10^{-16}$.

B. Specific Heat

The mixed oxide fuel specific heat correlations are taken from the MATPRO report:[1]

$$c_p = 15.496 \left[\frac{b_1 b_4^2 \exp(b_4/T)}{T^2 (\exp(b_4/T) - 1)^2} + 2b_2 T + \frac{b_3 b_5}{b_6 T^2} \exp(-b_5/b_6 T) \right] ,$$

where

c = specific heat capacity (J/kg K),

T = fuel temperature (K),

and

	UO_2	$UO_2 - PuO_2$
b_1	19.145	19.53
b_2	$7.847\ 3 \times 10^{-4}$	9.25×10^{-4}
b_3	$5.643\ 7 \times 10^{6}$	6.02×10^{6}
b_4	535.285	539.0
b_5	37 694.6	40 100.0
b_6	1.987	1.987 .

C. Thermal Conductivity

The mixed oxide fuel thermal conductivity correlations are taken from the MATPRO report[1] and include porosity and density correction factors.

For $T_c \leq T_1$,

$$k = c \left[\frac{c_1}{c_2 + T_c} + c_3 \exp (c_4 T_c) \right] ,$$

and for $T_c > T_1$,

$$k = c \left[c_5 + c_3 \exp (c_4 T_c) \right] ,$$

where

T_c = temperature (^{o}C),

$$c = 100.0 \left[\frac{1 - \beta (1 - f_{TD})}{1 - 0.05 \beta} \right] ,$$

$$\beta = c_6 + c_7 T_c ,$$

f_{TD} = fraction of theoretical density,

and

	UO_2	$UO_2 - PuO_2$
c_1	40.4	33.0
c_2	464.0	375.0
c_3	1.216×10^{-4}	1.54×10^{-4}
c_4	1.867×10^{-3}	1.71×10^{-3}
c_5	0.019 1	0.017 1
c_6	2.58	1.43
c_7	-5.8×10^{-4}	0.0
T_1	1 650.0	1 550.0 .

D. Spectral Emissivity

The mixed oxide spectral emissivity is calculated as a function of temperature based on the MATPRO correlations. The values for UO_2 fuel and UO_2-PuO_2 fuel are assumed to be equivalent:

$$\varepsilon = 0.870\ 7 \qquad \text{for } T \leq 1\ 000\ ^\circ C$$

$$\varepsilon = 1.311 - 4.404 \times 10^{-4}\ T \qquad \text{for } 1\ 000 < T \leq 2\ 050\ ^\circ C,$$

and

$$\varepsilon = 0.408\ 3 \qquad \text{for } T > 2\ 050\ ^\circ C.$$

III. ZIRCALOY CLADDING PROPERTIES

Subroutine MZIRC calculates the properties for Zircaloy and oxidized zircaloy cladding. The values obtained are for Zircaloy-4. Zircaloy-2 properties are assumed to be identical. The equations used are based on the correlations in the MATPRO report.[1]

A. Density

Zircaloy cladding exhibits an asymmetric thermal expansion behavior. Thermal expansion is calculated in the radial and axial directions and these effects are included in the density calculation:

$$\rho = \frac{6\ 551.4}{1 + 1.5\ [(\Delta L/L)_r + (\Delta L/L)_z]}\ ,$$

where

$$(\Delta L/L)_r = - 2.373 \times 10^{-4} + 6.721 \times 10^{-6}\ T_c$$

$$(\Delta L/L)_z = - 2.506 \times 10^{-4} + 4.441 \times 10^{-6}\ T_c$$

for $T \leq 1073.15$,

$$(\Delta L/L)_r = 5.1395 \times 10^{-3} - 1.12 \times 10^{-5}\ (T_c - 1073.15)$$

$$(\Delta L/L)_z = 3.5277 \times 10^{-3} - 1.06385 \times 10^{-5}\ (T_c - 1073.15)$$

for $1073.15 < T \leq 1273.15$,

$$(\Delta L/L)_r = - 6.8 \times 10^{-3} + 9.7 \times 10^{-6}\ T_c$$

$$(\Delta L/L)_z = - 8.3 \times 10^{-3} + 9.7 \times 10^{-6}\ T_c$$

for t_c 1273.15 and

T_c = temperature (^{o}C).

B. Specific Heat

Since zircaloy undergoes a phase change (alpha to beta) from 1 090 to 1 248 K, with a resultant sharp spike in the specific heat value during the transition, the specific heat is calculated by linear interpolation. The following table of specific heat vs temperature is used for $T \leq 1\ 248$ K:

T (K)	c_p (J/kg K)
300	281
400	302
640	381
1 090	375
1 093	502
1 113	590
1 133	615
1 153	719
1 173	816
1 193	770
1 213	619
1 233	469
1 248	356

and for $T > 1\ 248$ K,

$c_p = 356$ J/kg K.

C. Thermal Conductivity

Four-term polynomials are used to calculate the Zircaloy and oxidized Zircaloy thermal conductivities. Temperature in kelvins is the independent variable and the polynomial constants are given below:

	Zr	ZrO_2
a_o	7.51	1.96
a_1	2.09×10^{-2}	-2.41×10^{-4}
a_2	-1.45×10^{-5}	6.43×10^{-7}
a_3	7.67×10^{-9}	1.95×10^{-10}

The form of the polynomial used in this section and the subsequent materials properties sections is:

$$y = a_o + a_1 x + a_2 x^2 + \ldots + a_m x^m \quad .$$

D. Spectral Emissivity

The emissivity of Zircaloy is temperature dependent and the emissivity of Zircaloy oxide is temperature and time dependent. For simplicity, a constant value of $\varepsilon = 0.75$ is currently used.

IV. FUEL-CLADDING GAP GAS PROPERTIES

Subroutine MGAP calculates values for the gap gas mixture thermal conductivity which are used in predicting gap heat transfer coefficients. The method is taken from the MATPRO report[1] and is based on calculating mixture values for a possible seven constituent gases:

$$k_{gap} = \sum_{i=1}^{n} \left(\frac{k_i x_i}{x_i + \sum_{\substack{j=1 \\ j \neq 1}}^{n} \psi_{ij} x_j} \right) ,$$

where

k_{gap} = gap mixture thermal conductivity (W/m K),

$$\psi_{ij} = \phi_{ij} \left[1 + 2.41 \frac{(M_i - M_j)(M_i - 0.142 M_j)}{(M_i + M_j)^2} \right] ,$$

$$\phi_{ij} = \frac{\left[1 + \left(\frac{k_i}{k_j} \right)^{1/2} \left(\frac{M_i}{M_j} \right)^{1/4} \right]^2}{2^{3/2} \left(1 + \frac{M_i}{M_j} \right)^{1/2}} ,$$

k_i = constituent gas thermal conductivity (W/m K),

M_i = constituent gas molecular weight, and

x_i = constituent gas mole fraction.

The seven constituent gases considered are helium, argon, xenon, krypton, hydrogen, air/nitrogen, and water vapor. Except for water vapor, their thermal conductivities are defined as follows:

$$k = aT^b,$$

where

T = temperature (K),

and

	a	b
helium	3.36×10^{-3}	0.668
argon	3.421×10^{-4}	0.701
xenon	$4.028\ 8 \times 10^{-5}$	0.872
krypton	4.726×10^{-5}	0.923
hydrogen	$1.635\ 5 \times 10^{-4}$	0.821 3
air/nitrogen	2.091×10^{-3}	0.846 .

For water vapor the following correlation is used:

$$k = (2.2428 \times 10^{-7} + 5.0534 \times 10^{-10}\ T - 1.853 \times 10^{-14}\ T^2)\ \frac{p_g}{T}$$

$$+ \frac{1.0086\ p_g^2}{T^2\ (T-273)^{4.2}} + 1.76 \times 10^{-4} + 3.261 \times 10^{-5}\ T$$

$$+ 3.209 \times 10^{-8}\ T^2 - 7.733 \times 10^{-12}\ T^3,$$

where

p = gap gas pressure (N/m^2).

When the gap dimension shrinks to the order of the gas mean free path, a correction factor is applied to the light gas thermal conductivities to account for the change in energy exchange between gas and surface. Once again utilizing the MATPRO recommendations,[1] the correction factor for hydrogen and helium is:

$$k = \frac{k_i}{1 + f\ k_i},$$

where

$$f = \frac{0.2103\ \sqrt{T_g}}{p_g\ \lambda}\ ,$$

T_g = average gap gas temperature (K), and
λ = characteristic fuel RMS roughness = 4.389×10^{-6} m.

V. ELECTRICAL FUEL ROD INSULATOR (BN) PROPERTIES

Subroutine MBN calculates values for boron nitride insulators which are used in electrically heated nuclear fuel rod simulators. Magnesium oxide insulators are assumed to have roughly equivalent values.

A. Density

A constant value of 2002 kg/m^3 from Ref. 2 is used.

B. Specific Heat

A four-term polynomial is used to calculate the specific heat. The independent variable is temperature in degrees Fahrenheit and the constants are modifications of those reported in an EPRI report:[3]

a_0	a_1	a_2	a_3
760.59	1.7955	8.6704×10^{-4}	1.5896×10^{-7}

C. Thermal Conductivity

The boron nitride thermal conductivity is calculated based on a conversion to SI units of a curve fit reported in Ref. 4:

$$k = 25.27 - 1.365 \times 10^{-3}\ T_f\ ,$$

where

k = thermal conductivity (W/m K), and
T_f = temperature (^{o}F).

D. Spectral Emissivity

A constant value of unity is used for the boron nitride spectral emissivity.

VI. ELECTRICAL FUEL ROD HEATER COIL (CONSTANTAN) PROPERTIES

Subroutine MHTR calculates property values for Constantan heater coils as used in electrically heated nuclear fuel rod simulators. Nichrome coils, used in some installations in place of Constantan, are assumed to have similar properties. The correlations used are from Ref. 4.

A. Density

A constant value of 8393.4 kg/m^3 is used.

B. Specific Heat

$$c_p = 110\ T^{0.2075},$$

where

c_p = specific heat (J/kg K) and
T_f = temperature (^oF).

C. Thermal Conductivity

$$k = 29.18 + 2.683 \times 10^{-3}\ (T_f - 100),$$

where

k = thermal conductivity (W/m K) and
T_f = temperature (^oF).

D. Spectral Emissivity

A constant value of unity is used.

VII. STRUCTURAL MATERIAL PROPERTIES

Subroutine MSTRCT supplies property values for five types of structural materials normally used in light water power reactor plants: stainless steel type 304, stainless steel type 316, stainless steel type 347, carbon steel type A508, and Inconel type 718. A tabulation of the correlations used and a list of associated references are given in Table B-I.

REFERENCES

1. "MATPRO-Version 09: A Handbook of Materials Properties for Use In The Analysis Of Light Water Reactor Fuel Rod Behavior," Idaho National Engineering Laboratory report TREE-NUREG-1005 (December 1976).

2. Y. S. Touloukian, ed., Thermophysical Properties of High Temperature Solid Materials (MacMillan Co., New York, 1967).

3. "A Prediction of the SEMISCALE Blowdown Heat Transfer Test S-02-8 (NRC Standard Problem Five)," Electric Power Research Institute report EPRI NP-212 (October 1976).

4. W. L. Kirchner, "Reflood Heat Transfer In A Light Water Reactor," U.S. Nuclear Regulatory Commission report NUREG-0106, Vols. I & II (August 1976).

5. "Properties for LMFBR Safety Analysis," Argonne National Laboratory report ANL-CEN-RSD-76-1 (1976).

6. J. C. Spanner, ed., "Nuclear Systems Materials Handbook - Vol. 1 Design Data," Hanford Engineering Development Laboratory report TID-26666 (1976).

TABLE B-I. STRUCTURAL MATERIALS PROPERTIES

Material	Property	Indep. Variable	Polynomial Constants a_0	a_1	a_2	a_3	a_4	a_5	a_6	a_7	Ref.
SS 304	ρ	T	7984.0	-2.651×10^{-1}	-1.158×10^{-4}						5
	c_p	T_f	426.17	0.43816	-6.3759×10^{-4}	4.4803×10^{-7}	-1.0729×10^{-10}				
	k	T	8.116	1.618×10^{-2}							
	ϵ	-	0.84								
SS 316	ρ	T	8084.0	-4.209×10^{-1}	-3.894×10^{-5}						5
	c_p	T_f	426.17	0.43816	-6.3759×10^{-4}	4.4803×10^{-7}	-1.0729×10^{-10}				
	k	T	9.248	1.571×10^{-2}							
	ϵ	-	0.84								
SS 347	ρ	-	7913.0								4
	c_p	(T_f-240)	502.416	0.0984							
	k	T_f	14.1926	7.269×10^{-3}							
	ϵ	-	0.84								
A 508	ρ	T_f	7859.82	-2.6428×10^{-2}	-4.5471×10^{-4}	3.311×10^{-7}					6
	c_p	T_f	400.48	0.4582	6.5532×10^{-4}	5.3607×10^{-7}					
	k	T_f	66.1558	-1.4386×10^{-2}	-2.6987×10^{-4}	1.8306×10^{-6}	-6.0673×10^{-9}	1.0524×10^{-11}	-9.1603×10^{-15}	3.1597×10^{-18}	
	ϵ	-	0.84								
In-718	ρ	T_f	8233.4	-1.8351×10^{-1}	-9.8415×10^{-6}	-6.5343×10^{-9}					6
	c_p	T_f	418.18	0.1204							
	k	T_f	10.8046	8.829×10^{-3}							
	ϵ	-	0.84								

ρ = density (kg/m^3)
c_p = specific heat (J/kg K)
k = thermal conductivitiy (W/m K)
ϵ = spectral emissivity

T = temperature (K)
T_f = temperature (°F)
$y = a_o + a_1x + a_2x^2 + \ldots a_mx^m$

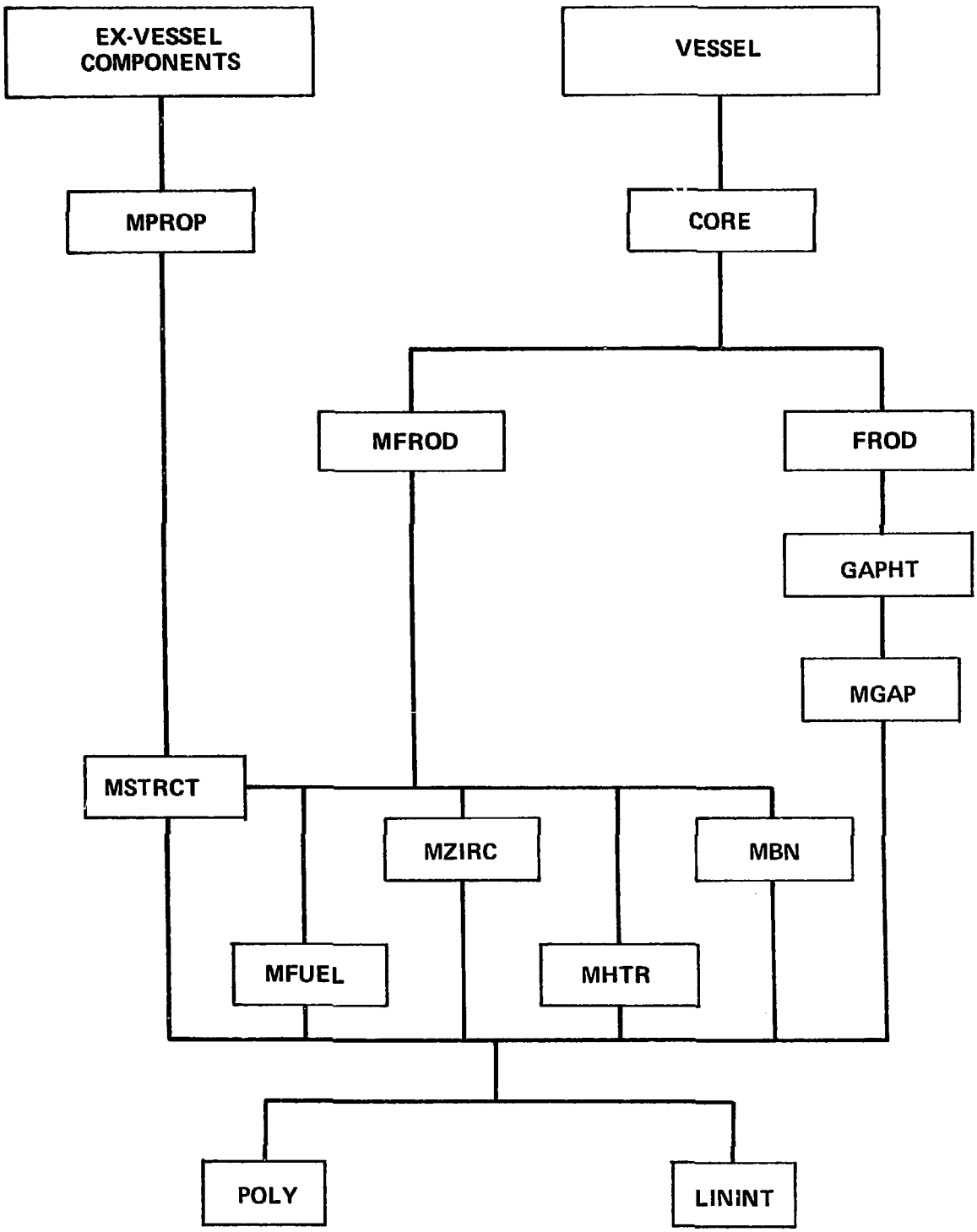

Fig. B-1.
Material properties code organization.

APPENDIX C
PWR SAMPLE PROBLEM

The purpose of the PWR sample problem presented in this appendix is to give the user an idea of how a large, complicated TRAC problem is set up. A typical U.S. four-loop PWR design, which combines features of a variety of different Westinghouse PWR designs,[1-4] has been chosen for the sample problem. The first part of this appendix discusses, in some detail, the TRAC geometry and noding for the four loops, the vessel, and the emergency core cooling (ECC) systems. The second part discusses the results of a steady-state calculation performed for this PWR. Also included in this appendix is a listing of the steady-state input deck and a listing of a restart input deck used to begin the transient calculation (a double-ended guillotine cold-leg break).

I. GEOMETRY AND NODING

Figure C-1 shows a schematic of the loop and vessel arrangement used to model the PWR. Shown in this figure is the loop which contains the pressurizer, another loop which represents two of the other typical PWR loops (these two loops are modeled separately in the actual TRAC calculation), and a third loop which represents the broken loop. Also shown in the figure are junction numbers (circled numbers) and component numbers (numbers in squares). These junction and component numbers can be used as a guide when referring to the input listing shown at the end of this appendix. There are a total of 42 components and 45 junctions. As can be seen from Figure C-1, each of the three intact cold legs includes a TEE connected to a FILL, which models both the high- (HPIS) and low-pressure (LPIS) injection systems, and also a TEE connected to a VALVE and an ACCUM component. There are no ECC systems included in the broken cold leg because it was assumed this system was not operational and would not significantly affect the transient. It should be mentioned that this PWR setup includes at least one of every type of TRAC component module.

Almost all of the dimensions for the pipes and tees in each of the loops were obtained from the RELAP input[5] for the BE/EM study.[3] Figure C-2

shows the noding for the three unbroken cold legs from the vessel to the steam generators including the ECC systems. Most of the cells in the pipes and tees are on the order of 1 - 2 m long, except where geometry considerations forced the use of smaller cells. As a rule of thumb, 1 - 2 m cells are optimal for most one-dimensional components. The HPIS and LPIS are combined into one injection tee connected to a FILL module on each of the three unbroken cold legs. The actual HPIS and LPIS flow rates, which also were obtained from the BE/EM study, are combined through this tee when these two systems are actuated by trips during the transient. The accumulator size and initial conditions (shown on the input listing) were obtained from the BE/EM study. As can be seen from Figure C-2, the accumulators are connected to a valve which is tripped open when the valve pressure on the loop side decreases below 4.08×10^6 Pa. The pump characteristics such as speed, head, torque, and dimensions, were also obtained from Ref. 3. These details for the pump components can be found in the input listing.

Figure C-3 shows the dimensions and noding for the hot leg which contains the pressurizer. A tee connects the vessel to the steam generator and the secondary side of the tee is used to model the long surge line connecting the pressurizer to the hot leg. Data for the tee dimensions and the pressurizer conditions were again obtained from Ref. 3. Geometrical data for the steam generators were obtained from a steam generator sample problem.[6] The only difference between the hot leg containing the pressurizer, shown in the figure, and the other three hot legs is that the tee is replaced with a pipe connecting the vessel to the steam generators. The mesh cell sizes in the pressurizer are quite large away from the water exit (2.0 m) and are 1 m long near the exit.

Figure C-4 shows the noding for the broken cold-leg pipe and gives the noding used for the pipe during steady state and the noding chosen for the break. During the steady-state calculation all the pipes are calculated using the semi-implicit option in TRAC. At the beginning of the transient (as shown in the transient restart listing), the pipe is divided into two fully implicit pipes connected to two breaks (at atmospheric pressure) to model a double-ended pipe break.

The three-dimensional vessel is the most complicated and time-consuming TRAC module to set up because the user must accurately calculate the three-dimensional flow areas, volumes, and other parameters to ensure a proper

geometrical representation of the vessel. Figure C-5 shows the noding scheme used for the PWR pressure vessel and its associated internals. As can be seen, there are 8 angular, 5 radial, and 10 axial nodes totaling 400 TRAC cells. This noding distribution was chosen to define the following regions in the vessel: core, upper and lower plenums, upper head, barrel-baffle section, and the downcomer. The positions of the axial nodes correspond to major flow restriction locations such as the flow distributor plate, lower core support plate, and upper core support plate. The location of the azimuthal nodes accounts for the eight vessel penetrations (four hot legs and four cold legs), while the radial noding accounts for the three major radial power regions (orifice zones). The radial noding also defines the barrel-baffle region and the downcomer.

The lower plenum consists of two axial levels, one of which extends from the vessel bottom to the flow distributor (mixer) plate. The other level extends from the flow distributor plate to the lower core support plate. There is a large amount of structure in the first level such as instrumentation tubes and guides, the core support dome, outer support ring, and the flow distributor plate. The instrumentation assemblies are nonuniformly distributed throughout the first, second, and third radial zones, and they extend from the bottom of the vessel to the core. The flow distributor plate is located at the top of the first axial level above the core support dome. It has various penetrations in it to allow for core orificing and instrumentation tubes. All of these structures and penetrations are accounted for in the TRAC input by calculating the appropriate flow areas in the r,θ,z directions, the liquid volume fractions, and the heat slab areas and masses.

The second axial level in the lower plenum consists of the flow distributor plate, core barrel, lower part of the thermal shield in the fifth radial region, lower core support plate, and the upper portion of the instrumentation assemblies and supports. The lower core support plate, as well as the flow distributor plate, extend radially into the fourth region where the core barrel is located. The thermal shield extends about half the axial distance into the second level and is located in the fifth radial region between the core barrel and the vessel wall.

The core region consists of five axial levels. The axial boundaries of the core are located at the upper and lower core support plates while the radial core boundary is located at the core shroud. Five axial levels in the core were used to give a good representation of the axial power distribution. The flow areas in all directions in the core are symmetrical because the control assembly arrangement is symmetrical. A small amount of flow is allowed to pass radially through the core shroud into the barrel-baffle region to allow for cooling and depressurization in this area.

The upper plenum extends from the upper core support plate to the upper support assembly structure and consists of two axial levels. The top of the first level is just below the hot-leg outlet nozzle. The flow and heat slab areas calculated for the upper plenum account for the asymmetric distribution of the upper plenum internals.

The downcomer extends from the ninth axial level to the first level. The upper boundary for the downcomer is the lower part of the upper support assembly. The only major structure in the downcomer region is the thermal shield which surrounds the core region in axial levels two through eight.

The upper head is modeled by the tenth axial level. The upper head volume is essentially void with the exception of the control rod shroud tubes, thermocouple sleeves, and the upper parts of the control rod guide tube.

II. STEADY-STATE CALCULATION

Based on the geometry and noding described in the previous section, a steady-state calculation was performed using the generalized steady-state option. The calculation was run to 140 s of reactor steady-state time in 3 h on the CDC 7600. The average time step size during the calculation was approximately 0.01 s. As can be seen from the input in the next section, all the initial velocities were zero. Until the pumps reach full speed, the reactor power is also internally zeroed to prevent boiling in the core. At approximately 17 s, the velocities in the system have almost reached a zero power steady state and the power is turned on. It thus takes approximately another 120 s before all the temperatures, velocities, and pressures converge to a steady state.

Figures C-6 to C-11 show some representative steady-state results for velocities, pressures, and temperatures. Figures C-6 and C-7 show the mixture velocity time histories for the four cold legs at the cell connecting to the vessel. Figure C-7 shows the velocities for the four hot legs at the vessel connection and the pressurizer which is connected to hot leg #4 (HL #4). It should be pointed out that the pressurizer is treated simply as a constant pressure break during the steady-state calculation to prevent it from emptying.

As can be seen from these figures, the cold-leg velocities essentially converge within 60 s. It takes longer for HL #4 since the pressurizer is connected to it. Since the initial condition guesses for the system (shown in the input listing) were only rough estimates, it takes the pressurizer about 100 s to converge to a zero discharge velocity. Steady-state pressure time histories for the hot- and cold-leg cells at the vessel junctions, and for two axial locations in the vessel (at the same r and θ locations), are shown in Figures C-8 and C-9, respectively. As with the velocities, these pressures take 60-80 s to converge. The parameters which limited convergence are the temperatures since the reactor power is not turned on until 17 s into the calculation. Figures C-10 and C-11 show average hot- and cold-leg temperatures at the vessel junctions and two vessel locations, respectively. Initially, these temperatures decrease but after the power is turned on they increase and eventually converge to the expected ΔT of about 33 K. Finally, Table C-I summarizes the steady-state initial conditions that are used for the transient calculation.

III. INPUT LISTINGS

This section contains two separate input listings. The first is the complete system input listing used for the steady-state calculation. The next listing is a sample input which would be used to begin the transient by replacing pipe component #1 with two implicit pipes and two breaks as shown in Figure C-4. This second listing is a restart input deck which requires the last steady-state dump file (PWRD3SS) to begin the transient.

A. Steady-State Input Deck

```
          2
PRESSURIZED WATER REACTOR (PWR) SAMPLE PROBLEM.
TYPICAL U.S. PWR WITH FOUR LOOPS---STEADY STATE CALCULATION.
      USPWR              0              0.                                  RESTART
          1              0              42             45                   CLC TYPE
    0.00100         0.0010          0.010                                  CONV
          1             20              20              7              3    ITER
          1              2               3              4              5    IORDER
          6              7               8              9             10
         11             12              13             14             15
         16             17              18             19             20
         21             22              23             24             25
         26             27              28             29             30
         31             32              33             34             35
         36             37              38             39             40
         41             42
          6              7               8                                  DMP TRPS
          2             -1       4.080E06              0.                  TRIPS
         24              0               2              0
          3             -1       4.080E06              0.
         25              0               2              0
          4             -1       4.080E06              0.
         26              0               2              0
          6             -1        1.02E07              0.
          2              0               7              0
          7             -1        1.02E07              0.
          3              0               7              0
          8             -1        1.02E07              0.
          4              0               7              0
         13             -1        1.00E06              0.
         42              3               1              0
PIPE                     1               1                                  CL-1
          7              1               5              1              6
          0              0
  0.34925000       0.058400         0.00
        325.
     0.7542          1.2200          0.6100         1.7710         1.7710
     1.7710         0.9320E
     0.2930          0.4670          0.2338         0.6786         0.6786
     0.6786         0.5000E
R 7  0.38300        0.5520E
F       0.0E
F       0.0E
R 7  0.69850        0.8382E
F         1E
F       0.0E
F       0.0E
F       0.0E
F     550.00E
F   1.55E 07E
F     550.00E
TEE                      2               2                                  CL-2
          1              1               6           0.00               0
          0              5               6              2
  0.3492500       0.058400
```

```
           325.
              1          35
       0.02540         0.01
           325.
         0.6100R 3     1.7710       0.93200E
F           1.0E
         0.2338R 3     0.6786        0.5000E
F        0.0020E
R 5      0.3830        0.5520E
F        0.0020E
F           0.0E
F           0.0E
F           0.0E
F          -1.0E
R 5      0.6985        0.8382E
F        0.0508E
F             1E
F             1E
F           0.0E
F           0.0E
F           0.0E
F           0.0E
F           0.0E
F           0.0E
F         550.0E
F         550.0E
F      1.55E 07E
F      1.55E 07E
F         550.0E
F         550.0E
TEE                         3          3                              CL-3
              1             1          6          0.00          0
              0             5          7             3
     0.3492500      0.058400
           325.
              1          36
       0.02540         0.01
           325.
         0.6100R 3     1.7710       0.93200E
F           1.0E
         0.2338R 3     0.6786        0.5000E
F        0.0020E
R 5      0.3830        0.5520E
F        0.0020E
F           0.0E
F           0.0E
F           0.0E
F          -1.0E
R 5      0.6985        0.8382E
F        0.0508E
F             1E
F             1E
F           0.0E
F           0.0E
F           0.0E
```

```
F       0.3830E
F       0.0507E
F          0.0E
F          0.0E
F          0.0E
R 9       -1.0          0.0E
F       0.6985E
F       0.2540E
F            1E
F            1E
F          0.0E
F          0.0E
F          0.0E
F          0.0E
F         0.00E
F          0.0E
F        550.0E
F        550.0E
F     1.550E07E
F     1.550E07E
F        550.0E
F        550.0E
TEE                        6          6                              CL-3
              2            1          6         0.00
              0            2         15            7
     0.3492500       0.05840
          325.0
              9           44
         0.1270         0.02
          325.0
         0.7642       1.220E
          1.0R 8        2.0E
         0.2930      0.4670E
      0.05070R 8    0.10140E
F       0.3830E
F       0.0507E
F          0.0E
F          0.0E
F          0.0E
R 9       -1.0          0.0E
F       0.6985E
F       0.2540E
F            1E
F            1E
F          0.0E
F          0.0E
F          0.0E
F          0.0E
F         0.00E
F          0.0E
F        550.0E
F        550.0E
F     1.550E07E
F     1.550E07E
F        550.0E
```

```
F          0.0E
F          0.0E
F          0.0E
F        550.0E
F        550.0E
F     1.55E 07E
F     1.55E 07E
F        550.0E
F        550.0E
TEE                         4              4                          CL-4
             1              1              6         0.00         0
             0              5              8            4
     0.3492500      0.058400
          325.
             1             37
       0.02540           0.01
          325.
        0.6100R 3      1.7710      0.93200E
F          1.0E
        0.2338R 3      0.6786       0.5000E
F       0.0020E
R 5     0.3830         0.5520E
F       0.0020E
F          0.0E
F          0.0E
F          0.0E
F         -1.0E
R 5     0.6985         0.8382E
F       0.0508E
F            1E
F            1E
F          0.0E
F          0.0E
F          0.0E
F          0.0E
F          0.0E
F          0.0E
F        550.0E
F        550.0E
F     1.55E 07E
F     1.55E 07E
F        550.0E
F        550.0E
TEE                         5              5                          CL-2
             2              1              6         0.00
             0              2             14            6
     0.3492500        0.05840
         325.0
             9             43
        0.1270           0.02
         325.0
        0.7642         1.220E
         1.0R 8          2.0E
        0.2930        0.4670E
      0.05070R 8     0.10140E
```

```
F        550.0E
TEE                        7           7                        CL-4
           2               1           6          0.00
           0               2          16             8
    0.3492500        0.05840
        325.0
            9             45
       0.1270           0.02
        325.0
       0.7642         1.220E
         1.0R 8         2.0E
       0.2930        0.4670E
     0.05070R 8      0.10140E
F      0.3830E
F      0.0507E
F         0.0E
F         0.0E
F         0.0E
R 9      -1.0           0.0E
F      0.6985E
F      0.2540E
F           1E
F           1E
F         0.0E
F         0.0E
F         0.0E
F         0.0E
F        0.00E
F         0.0E
F       550.0E
F       550.0E
F    1.550E07E
F    1.550E07E
F       550.0E
F       550.0E
PIPE                       8           8                        CL-1
           3               1          21            17        6
           0
    0.3937000       0.065300
        325.0
         1.5R 2         2.0E
      0.7300R 2      0.9740E
F      0.4870E
F         0.0E
        -1.0R 3         0.0E
F      0.7874E
F           1E
F         0.0E
F         0.0E
F        0.00E
F       550.0E
F     1.5E 07E
F       550.0E
PIPE                       9           9                        CL-2
           3               1          22            18        6
```

```
             0
     0.3937000        0.065300
         325.0
            1.5R 2        2.0E
        0.7300R 2      0.9740E
F       0.4870E
F          0.0E
          -1.0R 3         0.0E
F       0.7874E
F            1E
F          0.0E
F          0.0E
F         0.00E
F        550.0E
F      1.5E 07E
F        550.0E
PIPE                      10            10                                CL-3
             3             1            23            19            6
             0
     0.3937000        0.065300
         325.0
            1.5R 2        2.0E
        0.7300R 2      0.9740E
F       0.4870E
F          0.0E
          -1.0R 3         0.0E
F       0.7874E
F            1E
F          0.0E
F          0.0E
F         0.00E
F        550.0E
F      1.5E 07E
F        550.0E
PIPE                      11            11                                CL-4
             3             1            24            20            6
             0
     0.3937000        0.065300
         325.0
            1.5R 2        2.0E
        0.7300R 2      0.9740E
F       0.4870E
F          0.0E
          -1.0R 3         0.0E
F       0.7874E
F            1E
F          0.0E
F          0.0E
F         0.00E
F        550.0E
F      1.5E 07E
F        550.0E
PIPE                      12            12                                HL-1
             6             1            29            25            6
             0
```

```
        0.36830           0.062
          325.0
             1.5R 4       1.810          0.457E
        0.63900R 4        0.771          0.250F
R 6       0.4260          0.603E
F            0.0E
           -1.0R 6         0.0E
R 6       0.7366         0.8763E
F              1E
F            0.0E
F            0.0E
F            0.0E
F       583.000E
F       1.53E07E
F       583.000E
PIPE                        13             13                                HL-2
               6             1             30            26            6
               0
        0.36830           0.062
          325.0
             1.5R 4       1.810          0.457F
        0.63900R 4        0.771          0.250E
R 6       0.4260          0.603E
F            0.0E
           -1.0R 6         0.0E
R 6       0.7366         0.8763E
F              1E
F            0.0E
F            0.0E
F            0.0E
F       583.000E
F       1.53E07E
F       583.000E
PIPE                        14             14                                HL-3
               6             1             31            27            6
               0
        0.36830           0.062
          325.0
             1.5R 4       1.810          0.457E
        0.63900R 4        0.771          0.250E
R 6       0.4260          0.603E
F            0.0E
           -1.0R 6         0.0E
R 6       0.7366         0.8763E
F              1E
F            0.0E
F            0.0E
F            0.0E
F       583.000E
F       1.53E07E
F       583.000E
TEE                         15             15                                HL-4
               5             1              6           0.0            0
               0             8             32            28
        0.36830          0.0620
```

```
         325.0
            12            33
       0.17760          0.03
         325.0
          1.5R 3       1.312        0.8060          1.0          1.5
         0.457E
         0.750R10      2.010        0.7500E
         0.639R 3      0.559        0.3430        0.426        0.639
         0.195E
        0.0743R10      0.199        0.0743E
R 8      0.426         0.603E
F       0.0991E
F          0.0E
F          0.0E
         -1.0R 8          0.E
          1.0R10          0.R 2        1.00E
R 8     0.7366        0.8763E
F      0.3556E
F           1E
F           1E
F          0.0E
F          0.0E
F          0.0E
F          0.0E
F          0.0E
F          0.0E
F      583.00E
F      583.00E
F     1.53E07E
F     1.53E07E
F      583.00E
F      583.00E
PRIZER                   16           16                                HL-4
             5           33
      1.70E 06     1.53E 07     2.00E 05          3.0
R 3      4.30R 2        1.0E
R 3      14.7R 2     3.4140E
R 5     3.4140     0.099100E
F        0.00E
F       -1.00E
R 5     2.0840       0.3556E
F           1E
         1.000         0.4R 3        0.00E
F         0.0E
         616.4        616.4        605.0        594.0        583.0E
         616.4        616.4        605.0        594.0        583.0E
F     1.52E07E
PUMP                     17           17                                CL-1
             3            1           17            5            6
             0            0            1            0            1
        0.2540        0.100
        325.00
         828.0       4.285E4        5.58       1000.0     124.4000
      3.46E 03         0.00         0.00        123.7
             1
```

```
F         1.120E
F         0.227E
          0.487R 2        0.203          0.3830E
F           0.0E
F           0.0E
         0.78740R 2       0.508          0.6985E
F             1E
F           0.0E
F           0.0E
F           0.0E
F         550.00E
F        1.53E07E
F         550.00E
PUMP                        18             18                                  CL-2
               3             1             18             14             6
               0             0              1              0             1
          0.2540         0.100
          325.00
           828.0       4.285E4           5.58         1000.0        124.4000
        3.46E 03          0.00           0.00          123.7
               1
F         1.120E
F         0.227E
          0.487R 2        0.203          0.3830E
F           0.0E
F           0.0E
         0.78740R 2       0.508          0.6985E
F             1E
F           0.0E
F           0.0E
F           0.0E
F         550.00E
F        1.53E07E
F         550.00E
PUMP                        19             19                                  CL-3
               3             1             19             15             6
               0             0              1              0             1
          0.2540         0.100
          325.00
           828.0       4.285E4           5.58         1000.0        124.4000
        3.46E 03          0.00           0.00          123.7
               1
F         1.120E
F         0.227E
          0.487R 2        0.203          0.3830E
F           0.0E
F           0.0E
         0.78740R 2       0.508          0.6985E
F             1E
F           0.0E
F           0.0E
F           0.0E
F         550.00E
F        1.53E07E
F         550.00E
```

```
P MP                          20             20                           CL-4
             3                 1             20            16         6
             0                 0              1             0         1
        0.2540             0.100
        325.00
         828.0          4.285E4            5.58        1000.0   124.4000
      3.46E 03              0.00           0.00         123.7
             1
F       1.120E
F       0.227E
        0.487R 2          0.203         0.3830E
F         0.0E
F         0.0E
      0.78740R 2          0.508         0.6985E
F           1E
F         0.0E
F         0.0E
F         0.0E
F      550.00E
F     1.53E07E
F      550.00E
FILL                          21             21                           HPIS-2
            35
           1.0             0.002            0.0          0.00      325.0
    1.020E 07
FILL                          22             22                           HPIS-3
            36
           1.0             0.002            0.0          0.00      325.0
    1.020E 07
FILL                          23             23                           HPIS-4
            37
           1.0             0.002            0.0          0.00      325.0
    1.020E 07
VALVE                         24             24                           CL-2
             2                 1             47            43         6
             0
         0.127              0.02            0.0
         325.0
             2                 2              0             0
      0.050700            0.2540           0.00
F         2.0E
F     0.10140E
F     0.05070E
F         0.0E
R 2       -1.0              0.0E
F      0.2540E
F           1E
F         0.0E
F         0.0E
F         0.0E
        325.00           550.00E
      4.08E 06         1.55E 07E
        325.00           550.00E
VALVE                         25             25                           CL-3
             2                 1             48            44         6
```

```
                0
            0.127          0.02          0.0
            325.0
                2             3             0             0
        0.050700        0.2540          0.00
F            2.0E
F        0.10140E
F        0.05070E
F            0.0E
R 2         -1.0           0.0E
F         0.2540E
F              1E
F            0.0E
F            0.0E
F            0.0E
          325.00        550.00E
        4.08E 06      1.55E 07E
          325.00        550.00E
VALVE                     26            26                                 CL-4
                2             1            49            45           6
                0
            0.127          0.02           0.0
            325.0
                2             4             0             0
        0.050700        0.2540          0.00
F            2.0E
F        0.10140E
F        0.05070E
F            0.0E
R 2         -1.0           0.0E
F         0.2540E
F              1E
F            0.0E
F            0.0E
F            0.0E
          325.00        550.00E
        4.08E 06      1.55E 07E
          325.00        550.00E
ACCUM                     27            27                                 CL-2
                3         47
F       1.48600E
F         13.20E
R 3        6.890      0.05070E
F            0.0E
F         -1.00E
R 3       3.3650        0.2540E
F              1E
             1.0          0.07           0.E
F            0.0E
F        325.00E
F        325.00E
F      4.08E 06E
ACCUM                     28            28                                 CL-3
                3         48
F       1.48600E
```

```
F          13.20E
R 3         8.890          0.05070E
F             0.0E
F            -1.00E
R 3         3.3650           0.2540E
F               1E
              1.0              0.07              0.E
F             0.0E
F           325.00E
F           325.00E
F        4.08E 06E
ACCUM                          29                29                                  CL-4
                3              49
F         1.48600E
F          13.20E
R 3         8.890          0.05070E
F             0.0E
F            -1.00E
R 3         3.3650           0.2540E
F               1E
              1.0              0.07              0.E
F             0.0E
F           325.00E
F           325.00E
F        4.08E 06E
STGEN                          30                30                                  LEG-2
               12               3                29              21                6
                1               0
          0.00991        0.001220
                5              50                54
            1.0R10           1.740             1.0E
           5.59R10           1.887           5.980E
          0.4260R11          1.005          0.4870E
F             0.0E
R 6           1.0R 1           0.0R 6         -1.00E
          0.7366R11          0.0198          0.7874E
F               1E
            0.00R10          367.6             0.0E
F             0.00E
F              0.0E
           583.00           580.0             577.0           573.00           570.00
           567.00           563.0             560.0           557.00           553.00
           550.00           550.0E
           583.00           580.0             577.0           573.00           570.00
           567.00           563.0             560.0           557.00           553.00
           550.00           550.0E
R 6       1.53E7R 6      1.50E07E
F          1.740E
F          9.920E
F          5.700E
F            0.0E
F            1.0E
F         0.03417E
F               1E
F          412.80E
```

```
F          0.0E
F          0.1E
F        497.00E
F        497.00E
F       5.80E06E
F        550.00E
STGEN                        31               31                                    LEG-2
              12              3               30             22            6
               1              0
        0.00991         0.001220
               5             51               55
           1.0R10         1.740              1.0E
          5.59R10         1.887            5.980E
        0.4260R11         1.005           0.4870E
F          0.0E
R 6        1.0R 1          0.0R 6          -1.00E
        0.7366R11        0.0198           0.7874E
F           1E
          0.00R10         367.6              0.0E
F         0.00E
F          0.0E
        583.00          580.0           577.0          573.00          570.00
        567.00          563.0           560.0          557.00          553.00
        550.00          550.0E
        583.00          580.0           577.0          573.00          570.00
        567.00          563.0           560.0          557.00          553.00
        550.00          550.0E
R 6     1.53E7R 6     1.50E07E
F       1.740E
F       9.920E
F       5.700E
F          0.0E
F          1.0E
F      0.03417E
F           1E
F      412.80E
F          0.0E
F          0.1E
F      497.00E
F      497.00E
F     5.80E06E
F      550.00E
STGEN                        32               32                                    LEG-3
              12              3               31             23            6
               1              0
        0.00991         0.001220
               5             52               56
           1.0R10         1.740              1.0E
          5.59R10         1.887            5.980E
        0.4260R11         1.005           0.4870E
F          0.0E
R 6        1.0R 1          0.0R 6          -1.00E
        0.7366R11        0.0198           0.7874E
F           1E
          0.00R10         367.6              0.0E
```

```
F          0.00E
F           0.0E
         583.00           580.0         577.0        573.00       570.00
         567.00           563.0         560.0        557.00       553.00
         550.00           550.0E
         583.00           580.0         577.0        573.00       570.00
         567.00           563.0         560.0        557.00       553.00
         550.00           550.0E
R 6      1.53E7R 6      1.50E07E
F         1.740E
F         9.920E
F         5.700E
F           0.0E
F           1.0E
F       0.03417E
F            1E
F        412.80E
F           0.0E
F           0.1E
F        497.00E
F        497.00E
F       5.80E06E
F        550.00E
STGEN                        33            33                                    LEG-4
             12               3            32            24             6
              1               0
        0.00991        0.001220
              5              53            57
         1.0R10           1.740          1.0E
        5.59R10           1.887        5.980E
      0.4260R11           1.005       0.4870E
F           0.0E
R 6      1.0R 1          0.0R 6        -1.00E
      0.7366R11          0.0198       0.7874E
F            1E
        0.00R10           367.6          0.0E
F         0.00E
F          0.0E
         583.00           580.0         577.0        573.00       570.00
         567.00           563.0         560.0        557.00       553.00
         550.00           550.0E
         583.00           580.0         577.0        573.00       570.00
         567.00           563.0         560.0        557.00       553.00
         550.00           550.0E
R 6      1.53E7R 6      1.50E07E
F         1.740E
F         9.920E
F         5.700E
F           0.0E
F           1.0E
F       0.03417E
F            1E
F        412.80E
F           0.0E
F           0.1E
```

```
F        497.00E
F        497.00E
F      5.80E06E
F        550.00E
FILL                        34           34                                    SGFN-1
              50
            1.00          1.00           0.          0.50          497.0
     5.800E 06
FILL                        35           35                                    SGEN-2
              51
            1.00          1.00           0.          0.50          497.0
     5.800E 06
FILL                        36           36                                    SGEN-3
              52
            1.00          1.00           0.          0.50          497.0
     5.800E 06
FILL                        37           37                                    SGEN-4
              53
            1.00          1.00           0.          0.50          497.0
     5.800E 06
BREAK                       38           38                                    SGEN-1
              54
            1.00          1.00          0.0        547.00        5.80E06
BREAK                       39           39                                    SGEN-2
              55
            1.00          1.00          0.0        547.00        5.80E06
BREAK                       40           40                                    SGEN-3
              56
            1.00          1.00          0.0        547.00        5.80E06
BREAK                       41           41                                    SGEN-4
              57
            1.00          1.00          0.0        547.00        5.80E06
VESSEL                      42           42                                    VESSEL
              10             5            8             8
               9             1            4             7              2
               3
               0
          8026.0        502.00        17.30          0.60         6000.0
          1.3340
               8            14            6             0
              13             1            1             1             15
       3.238E09            0.0          0.0
          2.4960         2.975       3.9750         4.775         5.2520 GEOM
          6.0520         7.052       7.5810        10.820     12.5090E
          0.7500         1.350       1.6134        1.9411        2.1971E
          0.7854        1.5708       2.3562        3.1416         3.9270
          4.7124        5.4978      6.2832E
               9            25            3            25                  SOURCES
               9            34            3             1
               9            35            3             2
               9            28            3            26
               9            29            3            27
               9            38            3             3
               9            39            3             4
               9            32            3            28
```

```
R 4       1.00R 3         0.E                                                  CORE CDS
          0.83            0.84          0.83          0.84          0.84
          0.80            0.82          0.84S
          0.97            1.00          0.97          0.96          0.94
          0.93            0.92          0.97S
          0.76            0.75          0.74          0.77          0.74
          0.70            0.68          0.77E
F          1.0E
          0.75           1.125         1.185         1.100         0.64E
           943             944           943           944           943
           944             943           944R 8       2295R 8       1683E
           0.0           0.002         0.003         0.004      0.004647
    0.00475500      0.00500000    0.005359400E
R 4          1              3R 2            2E
           0.0         3.238E9          0.10       2.27E8S
           1.0         1.950E8          2.00       1.88E8S
           5.0         1.750E8          10.0       1.62E8S
          15.0         1.520E8          20.0       1.46E8S
          50.0         1.230E8          75.0       1.13E8S
         100.0         1.070E8         125.0       1.04E8S
         150.0         1.000E8         200.0       0.94E8E
F           3E
F         0.0E
F      0.9450E
          1.0R 6            0.S
          1.0R 6           0.0S
          1.0R 6           0.0S
          1.0R 6            0.S
          1.0R 6           0.0S
          1.0R 6           0.0S
          1.0R 6           0.0S
          1.0R 6           0.0S
          1.0R 6           0.0S
          1.0R 6            0.S
          1.0R 6           0.0S
          1.0R 6           0.0S
          1.0R 6            0.S
          1.0R 6           0.0S
          1.0R 6           0.0S
          1.0R 6            0.S
          1.0R 6           0.0S
          1.0R 6           0.0S
          1.0R 6           0.0S
          1.0R 6           0.0S
          1.0R 6           0.0S
          1.0R 6            0.S
          1.0R 6           0.0S
          1.0R 6           0.0E
F         0.0E
F    10.00E06E
F         0.0E
F         0.0E
F         0.0E
R 8    2.5883R 8     5.1604R 8     2.9336R 8     3.1458R 8     3.2213E LEVEL 1
R 8    539.81R 8    2319.02R 8    1798.92R 8    1739.61R 8    3988.71E
```

```
F          0.0E
F          0.0E
F          0.0E
F          0.0E
F          0.0E
F          0.0E
R 8     0.9138R 8      0.8433R 8      0.8135R 8      0.9145R 8      0.9612E
        0.6661         0.9279         0.5352         0.6662         0.8283
        0.9279         0.8283         0.7970S
        0.5798         0.7294         0.5798         0.7294         0.2810
        0.7294         0.2810         0.5800S
        0.2301         0.5294         0.2301         0.8283         0.9836
        0.8283         0.9836         0.8283S
R 8     0.9142R 8      0.8485E
R 2     0.3323         0.4500R 2      0.4676         0.3504         0.5174
        0.4002S
        0.4790         0.3822         0.4006         0.5502         0.4612
        0.5963         0.5519         0.4265S
R 2     0.5279         0.4460         0.5767         0.4433         0.5051
R 2     0.5767S
        0.4620         0.4707         0.4840         0.3918         0.4840
        0.4379         0.4620         0.4928R 8         1.0E
        0.9388         0.5882R 6      0.9388S
R 3     0.7848         0.8578         0.7848         0.8578         0.9371
        0.8578S
        0.7204         0.8275         0.7204R 3      0.7777         0.7204
        0.8275R 8      0.7159R 8         0.0E
F          1.0E
F          1.0E
F          1.0E
R 8     511.00R 8      506.00R 8      502.00R16      439.00E
F          0.0E
F          0.0E
F          0.0E
F          0.0E
F          0.0E
F          0.0E
F          0.0E
F        550.00E
F        550.00E
F      1.550E07E
R 8     0.3657R 8      0.7033R 8      0.3728R 8      1.3796R 8      2.5728E LEVEL 2
R 8     60.410R 8      114.55R 8      58.660R 8      331.39R 8      2043.11E
F          0.0E
F          0.0E
F          0.0E
F          0.0E
F          0.0E
F          0.0E
R 8     0.9108R 8      0.9247R 8      0.9421R 8      0.6421R 8      0.7977E
        0.6674         0.9081         0.5329          .6393         0.8263
        0.9081         0.8263         0.7737S
        0.5668         0.7175         0.5668         0.7175         0.2307
        0.7175         0.2307         0.5494S
        0.1300         0.5127         0.1300         0.8952         0.9651
```

```
        0.8952          0.9651          0.8952S
R 8      .6300R 8       0.8057E
R 8     0.6578R 8       0.7143R 8       0.8454R 8       0.0066R 8       0.6925E
        0.9001          0.5442R 6       0.9001S
R 3     0.9493          0.9646          0.9493          0.9646          0.9822
        0.9646S
R24        0.0E
F          1.0E
F          1.0E
F          1.0E
R32     550.00R 8       466.00E
F          0.0E
F          0.0E
F          0.0E
F          0.0E
F          0.0E
F          0.0E
F          0.0E
F         550.00E
F         550.00E
F        1.55E07E
R 8     0.0756R 8       0.1414R 8       1.3146R 8       3.1690R 8       6.4745E LEVEL 3
R 8     15.290R 8       28.600R 8       156.31R 8       577.25R 8       4513.32E
F          0.0E
F          0.0E
F          0.0E
F          0.0E
F          0.0E
F          0.0E
R 8     0.5607R 8       0.5229R 8       0.4353R 8       0.7296R 8       0.6925E
        0.2191          0.4422          0.2191          0.4422          0.2191
        0.4422          0.2191          0.4422S
        0.1633          0.4422          0.1633          0.4422          0.1633
        0.4422          0.1633          0.4422S
R 8     0.3647R 8       0.7357R 8       0.6900E
R 8     0.5607R 8       0.5229R 8       0.4353R 8       0.7296R 8       0.6925E
R 8     0.4723R 8       0.4945R 8       0.0080R16          0.0E
F          1.0E
F          1.0E
F          1.0E
R24     555.00R16       467.00E
F          0.0E
F          0.0E
F          0.0E
F          0.0E
F          0.0E
F          0.0E
F          0.0E
F         555.00E
F         555.00E
F        1.55E07E
R16        0.0R 8       1.0137R 8       2.2149R 8       5.1796E                 LEVEL 4
R16        0.0R 8       117.38R 8       397.01R 8       3610.66E
F          0.0E
F          0.0E
```

```
F          0.0E
F          0.0E
F          0.0E
F          0.0E
R 8     0.5607R 8      0.5229R 8      0.4353R 8      0.7296R 8      0.6925E
        0.2191         0.4422         0.2191         0.4422         0.2191
        0.4422         0.2191         0.4422S
        0.1633         0.4422         0.1633         0.4422         0.1633
        0.4422         0.1633         0.4422S
R 8     0.3647R 8      0.7357R 8      0.6900E
R 8     0.5607R 8      0.5229R 8      0.4353R 8      0.7296R 8      0.6925E
R 8     0.4723R 8      0.4945R 8      0.0040R16        0.0E
F          1.0E
F          1.0E
F          1.0E
R24     562.00R16      465.00E
F          0.0E
F          0.0E
F          0.0E
F          0.0E
F          0.0E
F          0.0E
F          0.0E
F        562.00E
F        562.00E
F       1.55E07E
R16        0.0R 8      0.6044R 8      1.3206R 8      3.0883E                  LEVEL 5
R16        0.0R 8       69.99R 8      419.53R 8     2152.86E
F          0.0E
F          0.0E
F          0.0E
F          0.0E
F          0.0E
F          0.0E
R 8     0.5607R 8      0.5229R 8      0.4353R 8      0.7296R 8      0.6925E
        0.2191         0.4422         0.2191         0.4422         0.2191
        0.4422         0.2191         0.4422S
        0.1633         0.4422         0.1633         0.4422         0.1633
        0.4422         0.1633         0.4422S
R 8     0.3647R 8      0.7357R 8      0.6900E
R 8     0.5607R 8      0.5229R 8      0.4353R 8      0.7296R 8      0.6925E
R 8     0.4723R 8      0.4945R 8      0.0040R16        0.0E
F          1.0E
F          1.0E
F          1.0E
R24     569.00R16      465.00E
F          0.0E
F          0.0E
F          0.0E
F          0.0E
F          0.0E
F          0.0E
F          0.0E
F        569.00E
F        569.00E
```

```
F       1.55E07E
R16        0.0R 8      1.0137R 8      2.2149R 8       5.1796E                  LEVEL 6
R16        0.0R 8      117.38R 8      397.01R 8     3610.66E
F          0.0E
F          0.0E
F          0.0E
F          0.0E
F          0.0E
F          0.0E
R 8     0.5607R 8      0.5229R 8      0.4353R 8     0.7296R 8     0.6925E
        0.2191         0.4422         0.2191        0.4422        0.2191
        0.4422         0.2191         0.4422S
        0.1633         0.4422         0.1633        0.4422        0.1633
        0.4422         0.1633         0.4422S
R 8     0.3647R 8      0.7357R 8      0.6900E
R 8     0.5607R 8      0.5229R 8      0.4353R 8     0.7296R 8     0.6925E
R 8     0.4723R 8      0.4945R 8      0.0080R16        0.0E
F          1.0E
F          1.0E
F          1.0E
R24     576.00R16      465.00E
F          0.0E
F          0.0E
F          0.0E
F          0.0E
F          0.0E
F          0.0E
F          0.0E
F       576.00E
F       576.00E
F       1.54E07E
R 8     0.0756R 8      0.1414R 8      1.3146R 8     3.1502R 8     6.4745E LEVEL 7
R 8     15.410R 8      28.830R 8      156.39R 8     574.06R 8     4513.32E
F          0.0E
F          0.0E
F          0.0E
F          0.0E
F          0.0E
F          0.0E
R 8     0.5607R 8      0.5229R 8      0.4353R 8     0.7296R 8     0.6925E
        0.2191         0.4422         0.2191        0.4422        0.2191
        0.4422         0.2191         0.4422S
        0.1633         0.4422         0.1633        0.4422        0.1633
        0.4422         0.1633         0.4422S
R 8     0.3647R 8      0.7357R 8      0.6900E
R 8     0.2185R 8      0.2372R 8      0.2807R 8        0.0R 8     0.6925E
R 8     0.4723R 8      0.4945R 8      0.0040R16        0.0F
F          1.0E
F          1.0E
F          1.0E
R24     580.00R16      467.00E
F          0.0E
F          0.0E
F          0.0E
F          0.0E
```

```
F          0.0E
F          0.0E
F          0.0E
F        580.00E
F        580.00E
F       1.54E07E
         1.3529          0.9756          1.2363          0.8590          1.2363  LEVEL 8
         0.8590          1.4694          1.0921S
         3.1902          2.9571          3.4233          2.9571          3.7729
         3.3067          3.1902          2.9571S
         1.4415          1.9354          1.4415          2.0519          1.4415
         2.0519          1.4415          1.9354R 8       1.5413R 8       2.9854E
         234.61          62.780          227.78          56.020          227.78
         56.020          241.29          69.530S
         259.18          245.67          272.69          245.67          292.94
         265.93          259.18          245.67S
         84.080          262.59          84.080          269.34          84.080
         269.34          84.080          262.59R 8       434.15R 8       2206.51E
F          0.0E
F          0.0E
F          0.0E
F          0.0E
F          0.0E
F          0.0E
         0.7499          0.9331          0.7571          0.9403          0.7571
         0.9403          0.7427          0.9259S
         0.8766          0.8831          0.8702          0.8831          0.8606
         0.8734          0.8766          0.8831S
         0.9354          0.7982          0.9354          0.7930          0.9354
         0.7930          0.9354          0.7982R 8       0.7765R 8       0.6903E
         0.2001          0.5485          0.2001          0.3615          0.2001
         0.5485          0.2001          0.3615S
         0.0672          0.2765          0.0672           .2765          0.0672
         0.2765          0.0672          0.2765S
R 8      0.4444R 8       0.7417R 8       0.7932E
         0.5600          0.7433          0.5704          0.7536           .5704
         0.7536          0.5497          0.7329S
         0.4949          0.5042          0.4857          0.5042          0.4718
         0.4903          0.4949          0.5042S
         0.7409          0.6014          0.7409          0.5939          0.7409
         0.5939          0.7409          0.6014R 8       0.7210R 8          1.0E
         0.1700          0.2878          0.1700          0.4933          0.1700
         0.4933          0.1700          0.2878S
R 2      0.4714          0.3481          0.4714          0.3481R 3        .4714
         0.5595          0.4417R 2       0.5068          0.5595R 2       0.5068
         0.4417R16          0.0E
F          1.0E
F          1.0E
F          1.0E
R24      583.00R16       468.00E
F          0.0E
F          0.0E
F          0.0E
F          0.0E
F          0.0E
```

```
F          0.E
F          0.0E
F        583.00E
F        583.00E
F       1.54E07E
          7.7503          5.4404          7.1993          4.8894          7.1993  LEVEL 9
          4.8894          8.3012          5.9913S
         18.5263         17.4244         19.6283         17.4244         21.2812
         19.0773         18.5263         17.4244S
          8.9254         11.7862          8.9254         12.3372          8.9254
         12.3372          8.9254         11.7862S
          7.7221R 2       8.2513R 2       7.7221R 2       8.2513          7.7221
         12.8561R 2      12.7630R 2      12.8561R 2      12.7630         12.8561E
       1409.70          357.610         1377.780         325.690         1377.780
        325.69         1441.64          389.550S
       1545.89         1482.00         1609.74          1482.00         1705.53
       1577.75         1545.89         1482.000S
        670.57         1754.60          670.570          1786.5          670.57
       1786.52          670.57         1754.60S
       2231.51R 2      2394.84R 2      2231.51R 2      2394.84         2231.51
      10070.22R 2     10203.05R 2     10070.22R 2     10203.05        10070.22E
F          0.00E
F          0.0E
F          0.0E
F          0.0E
F          0.0E
F          0.0E
          0.7545          0.9377          0.7601          0.9433          0.7601
          0.9433          0.7489          0.9322S
          0.8798          0.8848          0.8749          0.8848          0.8674
          0.8773          0.8798          0.8848S
          0.9158          0.7798          0.9158          0.7758          0.9158
          0.7758          0.9158          0.7798S
          0.8124R 2       0.7986R 2       0.8124R 2       0.7986          0.8124
          0.9104R 2       0.8953R 2       0.9104R 2       0.8953          0.9104E
          0.2235          0.5182          0.2235          0.3738          0.2235
          0.5182          0.2235          0.3738S
          0.0314          0.2128          0.0314          0.2128          0.0314
          0.2128          0.0314          0.2128S
R 8       0.5593R 8       0.8026R 8       0.8505E
R 2       0.7296R 4       0.7434R 2        .7159S
          0.5237          0.5359          0.5114          0.5359          0.4929
          0.5175          0.5237          0.5359S
          0.7237          0.7138          0.7237          0.7038          0.7237
          0.7038          0.7237          0.7138R 8       0.8096R 8          0.0E
          0.2541          0.4154          0.2541          0.5992          0.2541
          0.5992          0.2541          0.4154S
R 2       0.5075          0.4054          0.5075          0.4054R 3       0.5075
          0.6368          0.5114R 2       0.5855          0.6368R 2       0.5855
          0.5114R16          0.0E
F          1.0E
F          1.0E
F          1.0E
R24      583.00R16       466.00E
F          0.0E
```

```
F          0.0E
F          0.0E
F          0.0E
F          0.0E
F          0.0E
F          0.0E
R33      583.00R 2      550.00R 2      583.00R 2      550.00         583.00E
R33      583.00R 2      550.00R 2      583.00R 2      550.00         583.00E
R33    1.530E07R 2    1.55E07R 2     1.53E07R 2     1.55E07       1.530E07E
R 2      2.6885R 4      2.4550R 2      2.9220S                                  LEVEL 10
         7.2051         6.7589         7.6513         6.7589         8.3206
         7.4282         7.2051         6.7589S
         4.1796         4.3574         4.1796         4.5352         4.1796
         4.5352         4.1796         4.3574R 8      1.9187R 8      0.6982E
R 2       601.15R 4       559.9R 2      642.40S
        2068.14        1988.68        2146.63        1988.68        2264.86
        2107.23        2068.14        1988.68S
        1595.71        1627.17        1595.71        1658.47        1595.71
        1658.47        1595.71        1627.17R 8     2023.35R 8     1916.35E
F          0.0E
F          0.0E
F          0.0E
F          0.0E
F          0.0E
F          0.0E
R 2      0.7992R 4      0.8130R 2      0.7856S
         0.6917         0.7035         0.6800         0.7035         0.6623
         0.6858         0.6917         0.7035S
         0.6160         0.6084         0.6160         0.6009         0.6160
         0.6009         0.6160         0.6084R 8      0.9660R 8        1.0E
         0.4508         0.6968         0.4508         0.5795         0.4508
         0.6968         0.4508         0.5795S
         0.3940         0.7419         0.3940         0.7419         0.3940
         0.7419         0.3940         0.7419S
R 8       .7938R 8       0.9610R 8        1.0E
F          0.0E
         0.6561         0.5366         0.6561         0.6859         0.6561
         0.6859         0.6561         0.5366S
R 2      0.6375         0.5546         0.6375         0.5546R 3       .6375
R 2      0.8050R 2      0.7864         0.8050R 2      0.7864         0.8050
R 8      0.9444R 8         0.0E
F          1.0E
F          1.0E
F          1.0E
R 8      511.00R 8      489.00R 8      482.00R16      436.00E
F          0.0E
F          0.0E
F          0.0E
F          0.0E
F          0.0E
F          0.0E
F          0.0E
F        569.00E
F        569.00E
F       1.53E07E
```

```
         12158.0        18237.0        19210.0        17832.0        10375.0E ROD CRDS
R 8        560.0R 8       567.0R 8       574.0R 8       581.0R 8       585.00E
         12158.0        18237.0        19210.0        17832.0        10375.0E
R 8        560.0R 8       567.0R 8       574.0R 8       581.0R 8       585.00E
         12158.0        18237.0        19210.0        17832.0        10375.0E
R 8        560.0R 8       567.0R 8       574.0R 8       581.0R 8       585.00E
         12158.0        18237.0        19210.0        17832.0        10375.0E
R 8        560.0R 8       567.0R 8       574.0R 8       581.0R 8       585.00E
         12158.0        18237.0        19210.0        17832.0        10375.0E
R 8        560.0R 8       567.0R 8       574.0R 8       581.0R 8       585.00E
         12158.0        18237.0        19210.0        17832.0        10375.0E
R 8        560.0R 8       567.0R 8       574.0R 8       581.0R 8       585.00E
         12158.0        18237.0        19210.0        17832.0        10375.0E
R 8        560.0R 8       567.0R 8       574.0R 8       581.0R 8       585.00E
         12158.0        18237.0        19210.0        17832.0        10375.0E
R 8        560.0R 8       567.0R 8       574.0R 8       581.0R 8       585.00E
         14000.0        21000.0        22120.0        20534.0        11947.0E
R 8        560.0R 8       567.0R 8       574.0R 8       581.0R 8       585.00E
         14000.0        21000.0        22120.0        20534.0        11947.0E
R 8        560.0R 8       567.0R 8       574.0R 8       581.0R 8       585.00E
         14000.0        21000.0        22120.0        20534.0        11947.0E
R 8        560.0R 8     . 567.0R 8       574.0R 8       581.0R 8       585.00E
         14000.0        21000.0        22120.0        20534.0        11947.0E
R 8        560.0R 8       567.0R 8       574.0R 8       581.0R 8       585.00E
         14000.0        21000.0        22120.0        20534.0        11947.0E
R 8        560.0R 8       567.0R 8       574.0R 8       581.0R 8       585.00E
         14000.0        21000.0        22120.0        20534.0        11947.0E
R 8        560.0R 8       567.0R 8       574.0R 8       581.0R 8       585.00E
         14000.0        21000.0        22120.0        20534.0        11947.0E
R 8        560.0R 8       567.0R 8       574.0R 8       581.0R 8       585.00E
         14000.0        21000.0        22120.0        20534.0        11947.0E
R 8        560.0R 8       567.0R 8       574.0R 8       581.0R 8       585.00E
         10788.0        16182.0        17045.0        15822.0        9206.0E
R 8        560.0R 8       567.0R 8       574.0R 8       581.0R 8       585.00E
         10788.0        16182.0        17045.0        15822.0        9206.0E
R 8        560.0R 8       567.0R 8       574.0R 8       581.0R 8       585.00E
         10788.0        16182.0        17045.0        15822.0        9206.0E
R 8        560.0R 8       567.0R 8       574.0R 8       581.0R 8       585.00E
         10788.0        16182.0        17045.0        15822.0        9206.0E
R 8        560.0R 8       567.0R 8       574.0R 8       581.0R 8       585.00E
         10788.0        16182.0        17045.0        15822.0        9206.0E
R 8        560.0R 8       567.0R 8       574.0R 8       581.0R 8       585.00E
         10788.0        16182.0        17045.0        15822.0        9206.0E
R 8        560.0R 8       567.0R 8       574.0R 8       581.0R 8       585.00E
         10788.0        16182.0        17045.0        15822.0        9206.0E
R 8        560.0R 8       567.0R 8       574.0R 8       581.0R 8       585.00E
         10788.0        16182.0        17045.0        15822.0        9206.0E
R 8        560.0R 8       567.0R 8       574.0R 8       581.0R 8       585.00E
         1.000E-5       0.100          200.0                                       TIME STP
         10.0000        0.100          10.            1.00
-1.                                                                                END DATA
```

B. Restart Input Deck for Transient Calculation

```
             3
   PRESSURIZED WATER REACTOR (PWR) SAMPLE PROBLEM.
   TYPICAL U.S. PWR WITH FOUR LOOPS---BEGINNING OF TRANSIENT CALCULATION--
   READ RESTART FILE PWRD3SS STARTING AT STEP 6904 WITH NEW TIME=0.0.
       PWRD3SS          6904              0.                              RESTART
             0             1              45              47              CLC TYPE
       0.00100        0.0010          0.010                              CONV
             1            20              20               7           3  ITER
             1            43              44              45           2  NIORDER
             3             4               5               6           7
             8             9              10              11          12
            13            14              15              16          17
            18            19              20              21          22
            23            24              25              26          27
            28            29              30              31          32
            33            34              35              36          37
            38            39              40              41          42
             6             7               8                              DMP TRPS
             2            -1        4.080E06              0.              TRIPS
            24             0               2               0
             3            -1        4.080E06              0.
            25             0               2               0
             4            -1        4.080E06              0.
            26             0               2               0
             6            -1         1.02E07              0.
             2             0               7               0
             7            -1         1.02E07              0.
             3             0               7               0
             8            -1         1.02E07              0.
             4             0               7               0
            13            -1         1.00E06              0.
            42             3               1               0
   PIPE                    1               1                              BKN-PIP
            13             1             100               1           6
             0             1
       0.3492500      0.058400
            325.
   R 2       0.1R 2        0.2R 2        0.3R 2        0.5R 2        0.75
             0.8          0.813         0.932E
   R 2    0.0383R 2     0.0766R 2     0.11490R 2     0.1915S
   R 2  0.287250        0.3064       0.3113800       0.5000E
   R13     0.3830       0.5520E
   F         0.0E
   F         0.0E
   R13     0.6985       0.8382E
   F           4E
   F          0.E
   F         0.0E
   R13      16.89       11.720E
   F      559.600E
   F    1.567E 07E
   F      559.550E
   PIPE                   45              45                              BKN-PIP
             8             1               5             101           6
             0             1
```

```
      0.349250        0.058400
         325.0
       0.76420          0.6300R 2       0.30R 2       0.20R 2       0.10E
       0.29270          0.2413R 2     0.11490R 2    0.07660R 2    0.03830E
F      0.38300E
F         0.0E
F         0.0E
F      0.6985E
F           4E
F        0.00E
F         0.0E
F      16.890E
F      559.60E
F    1.567E07E
F      559.55E
BREAK                       43            43                                  CONT-BK
           100
           0.1    0.038300            1.         373.0       1.0E 05
BREAK                       44            44                                  CONT-BK
           101
           0.1    0.038300            1.         373.0       1.0E 05
END                                                                           END CDAT
     1.000e-5        0.100         0.100                                      time stp
      0.10000        0.100           0.1          0.10
-1.                                                                           end
```

REFERENCES

1. L. Shotkin, Nuclear Regulatory Commission, personal communication (1977).

2. Commonwealth Edison Company, "Zion Nuclear Power Station, Unit 1, Startup Test Report," Docket No. 50-295, License No. DPR-39 (November 1974).

3. G. W. Johnson, F. W. Childs, and J. M. Broughton, "A Comparison of 'Best-Estimate' and 'Evaluation Model,' LOCA Calculations: The BE/EM Study," Idaho National Engineering Laboratory report PG-R-76-009 (December 1976).

4. Westinghouse Nuclear Energy Systems, "Reference Safety Analysis Report," RESAR 41 (December 1975).

5. "RELAP4/MOD5 User's Manual-Volume II," Idaho National Engineering Laboratory report ANCR-NUREG-1335 (September 1976).

6. K. A. Williams, Los Alamos Scientific Laboratory, personal communication (1977).

TABLE C-I

INITIAL STEADY-STATE CONDITIONS

Parameter	Value
Core Power[a]	3.238×10^9 W
Fuel[a]	Equilibrium cycle
Core-Average Burnup[a] at mid-plane	16 386 MWD/MTU
Relative Axial Power Shape (5 axial levels - bottom to top)[a]	0.75, 1.125, 1.185, 1.10, 0.64
Relative Radial Power Shape (Average for each of three radial regions - center-to-core shroud)[a]	0.99, 1.14, 0.88
Cold-leg Vessel Entrance Temperature	559.6 K
Lower Plenum Average Temperature	559.5 K
Hot-leg Vessel Outlet Temperature	593.0 K
Cold-leg Vessel Entrance Pressure	1.567×10^7 Pa
Hot-leg Vessel Outlet Pressure	1.535×10^7 Pa
Pump Suction Side Pressure	1.50×10^7 Pa
Pump Discharge Pressure	1.55×10^7 Pa
HPIS Setpoint[a]	1.02×10^7 Pa
LPIS Setpoint[a]	1.27×10^6 Pa
Accumulator Valve Setpoint[a]	4.08×10^6 Pa

[a]Values not calculated during steady state.

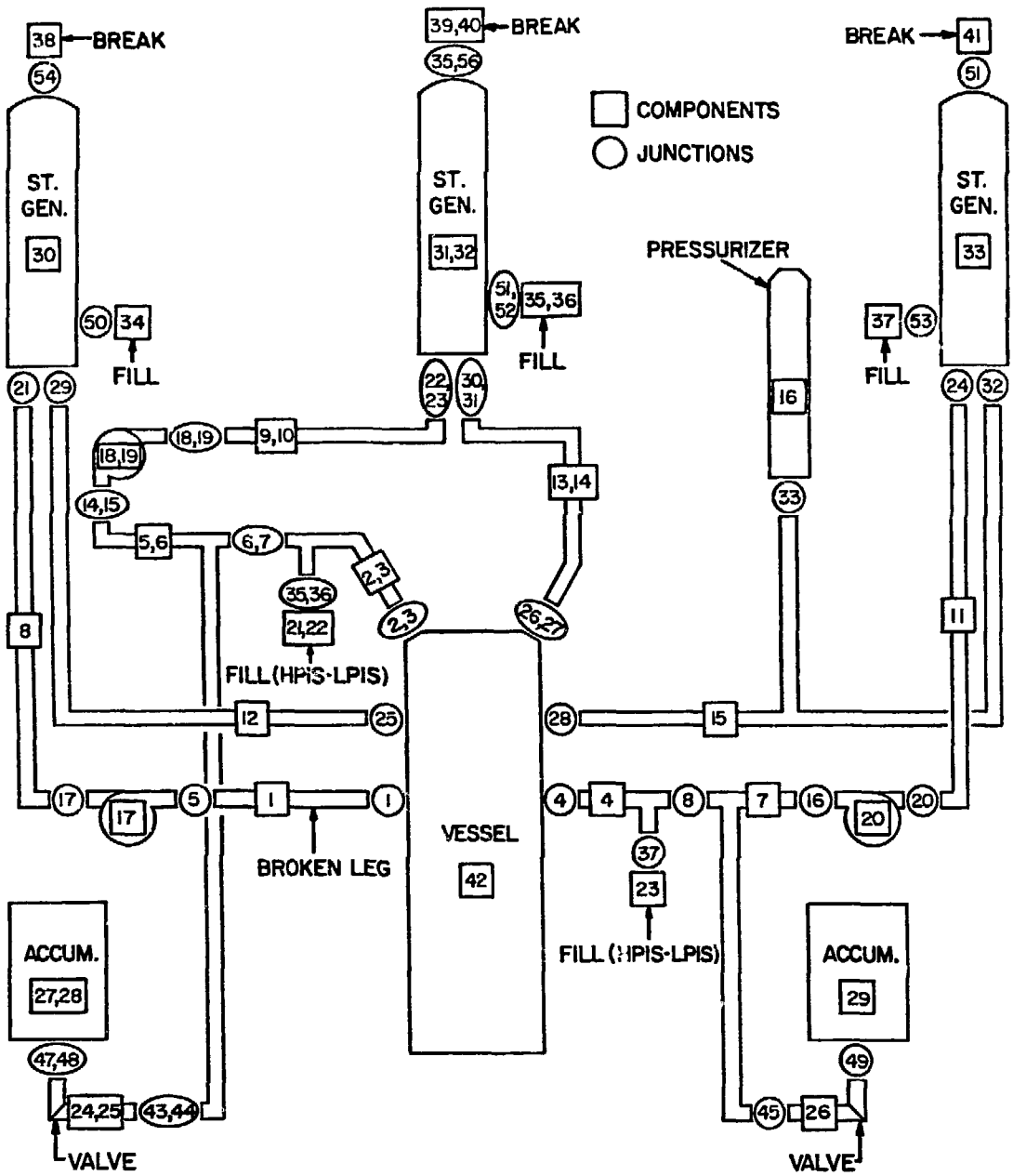

Fig. C-1.
PWR sample problem TRAC schematic.

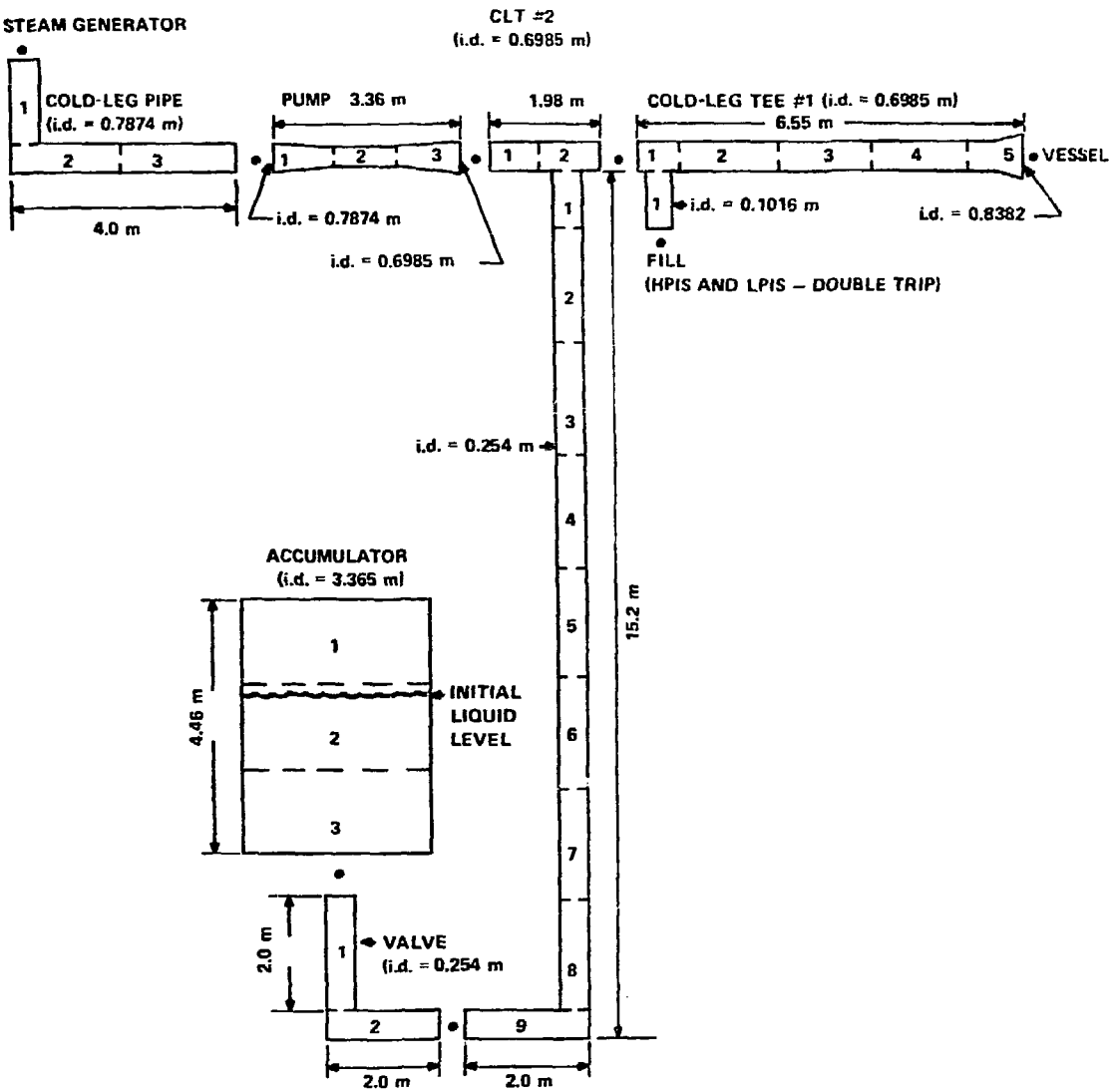

Fig. C-2.
TRAC noding for unbroken cold legs.

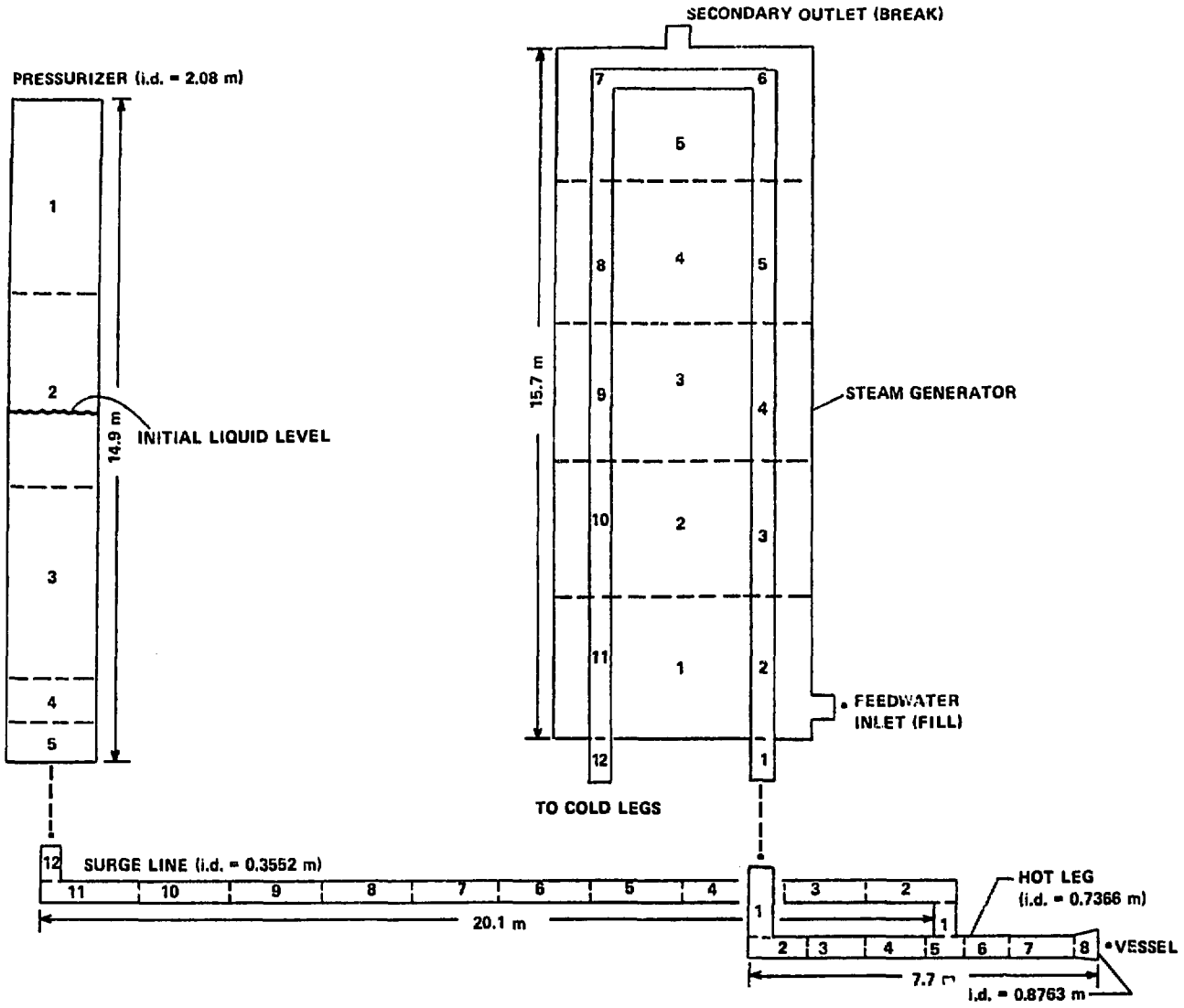

Fig. C-3.
TRAC noding for pressurizer hot leg.

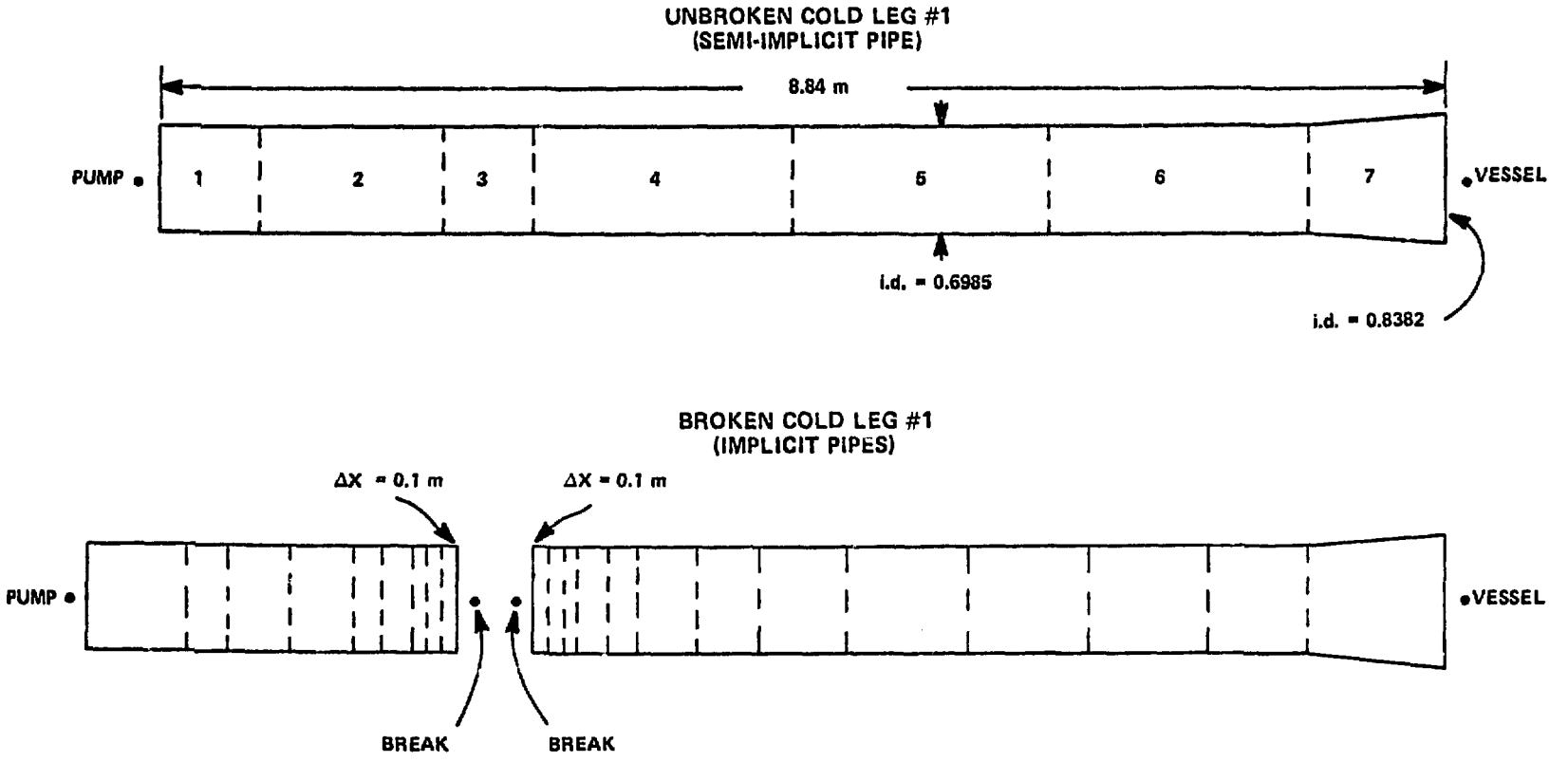

Fig. C-4.
TRAC noding for broken cold leg.

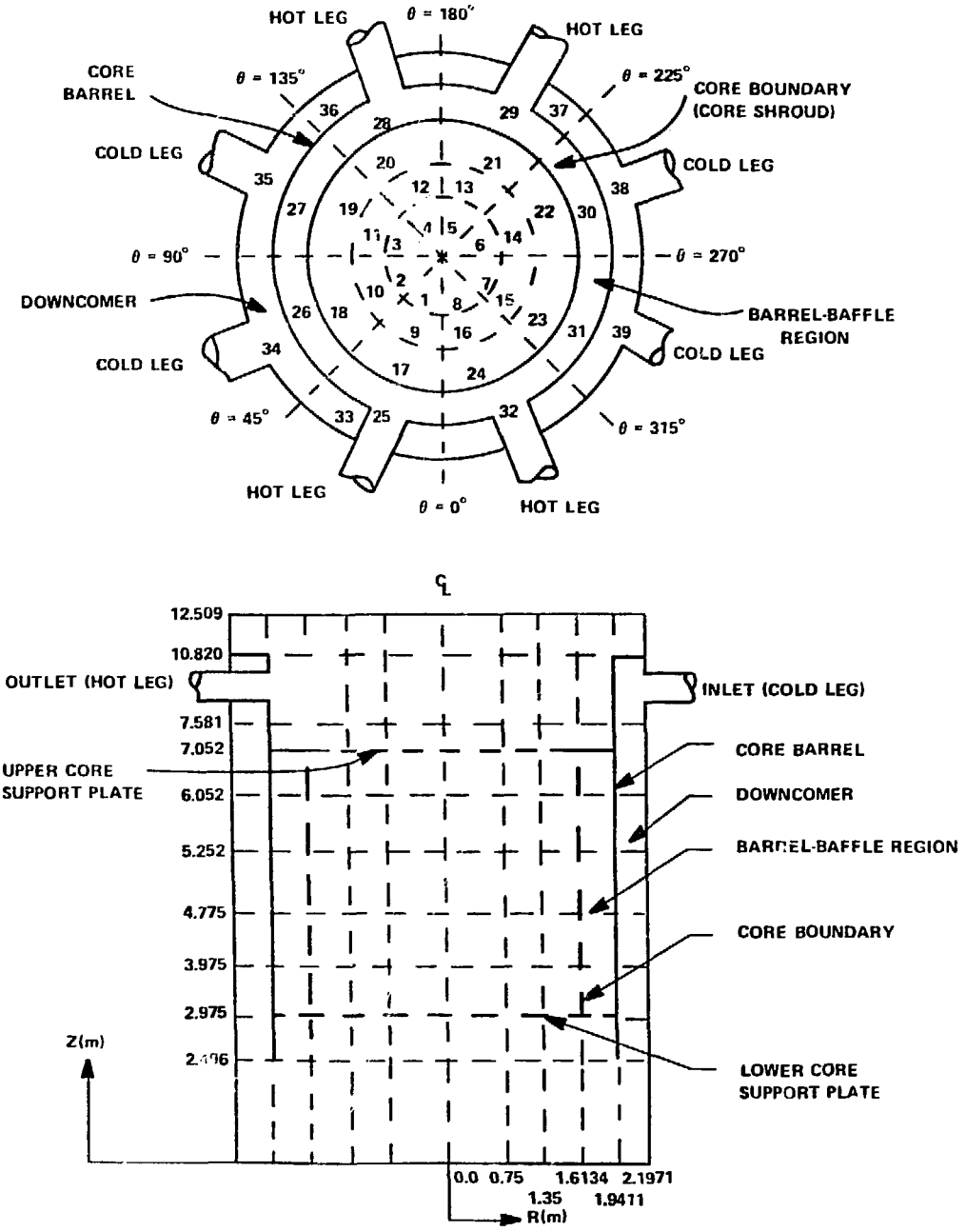

Fig. C-5.
TRAC noding for pressure vessel.

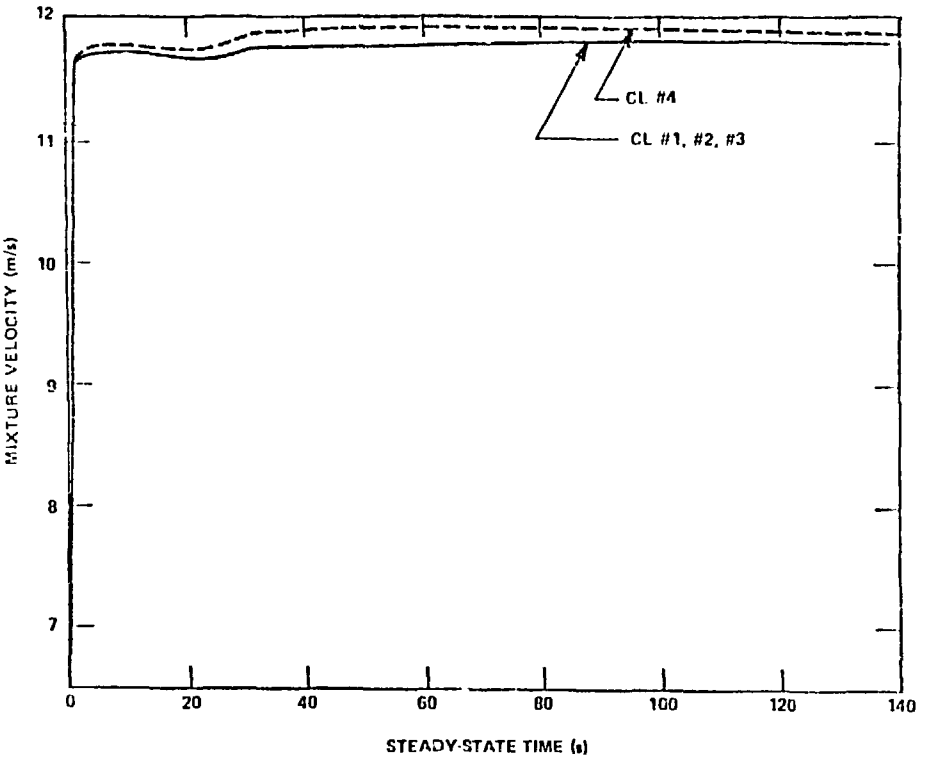

Fig. C-6.
Cold-leg mixture velocities at vessel entrance.

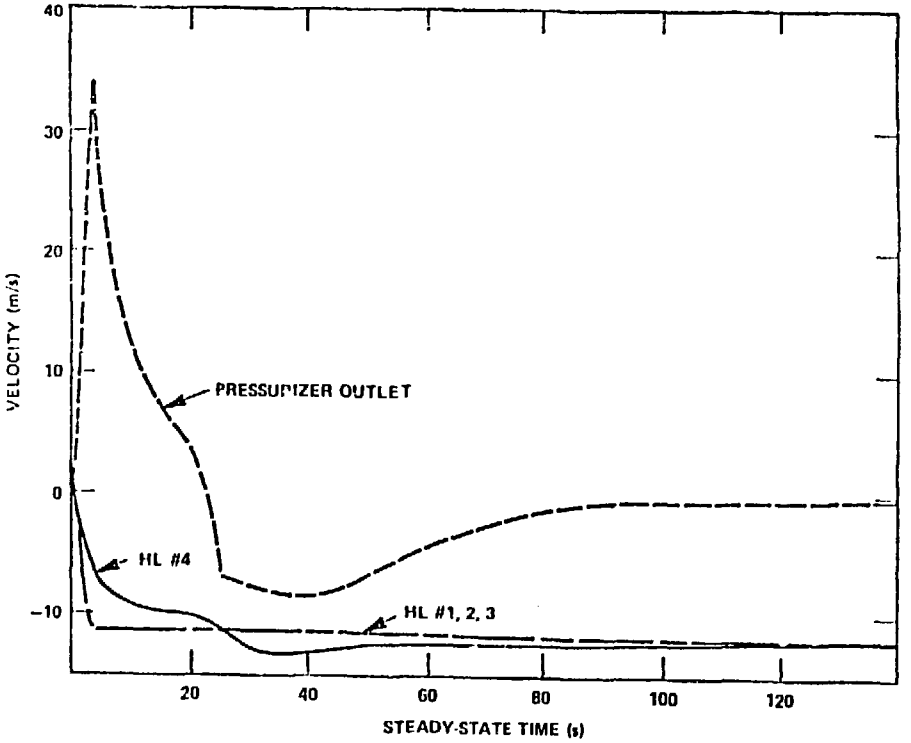

Fig. C-7.
Hot-leg and pressurizer velocities.

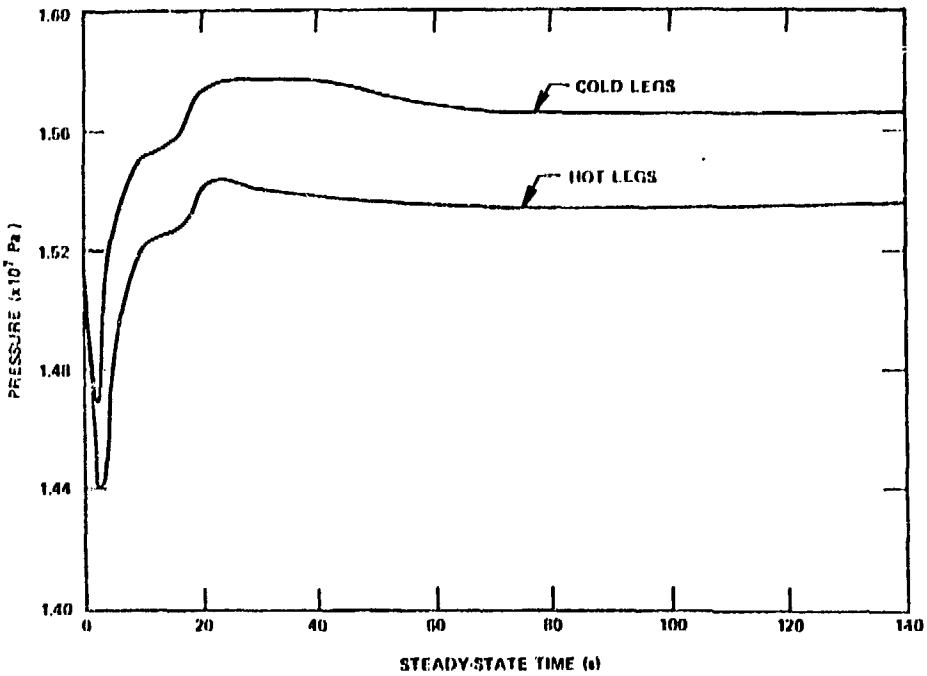

Fig. C-8.
Cold- and hot-leg pressures at vessel.

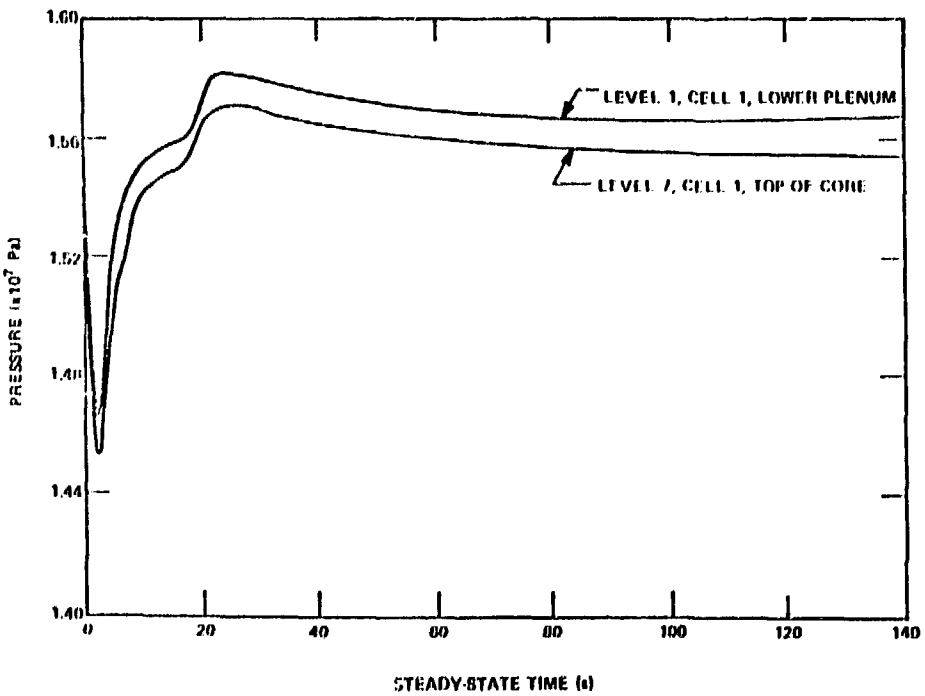

Fig. C-9.
Pressure in vessel.

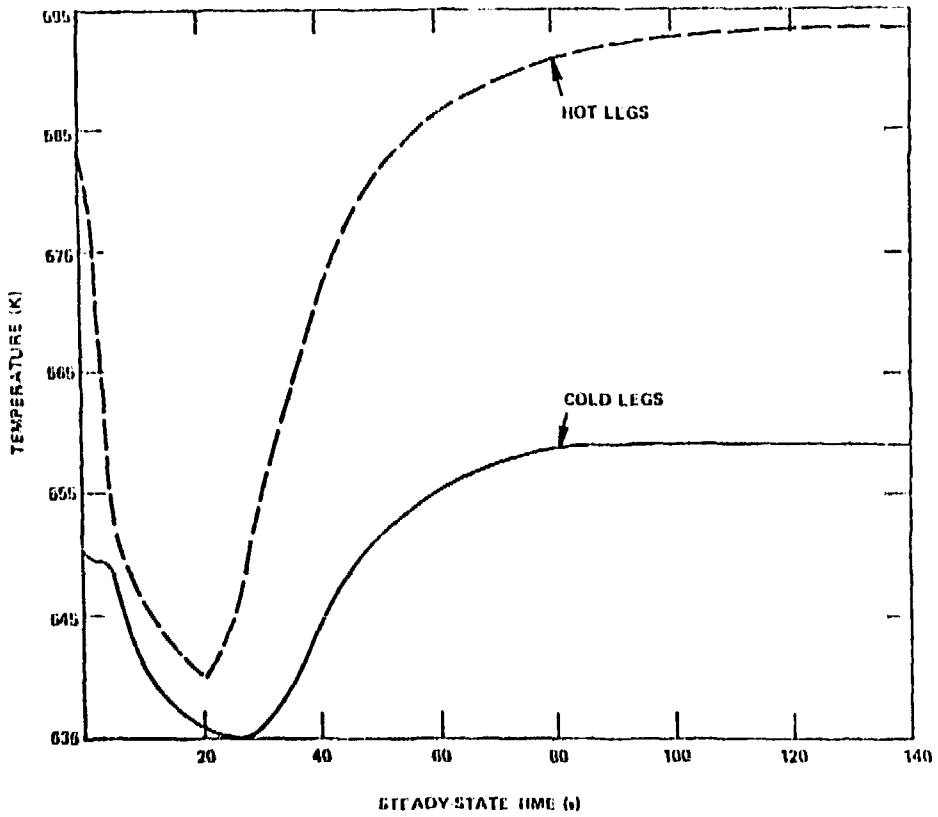

Fig. C-10.
Steady-state cold- and hot-leg temperatures.

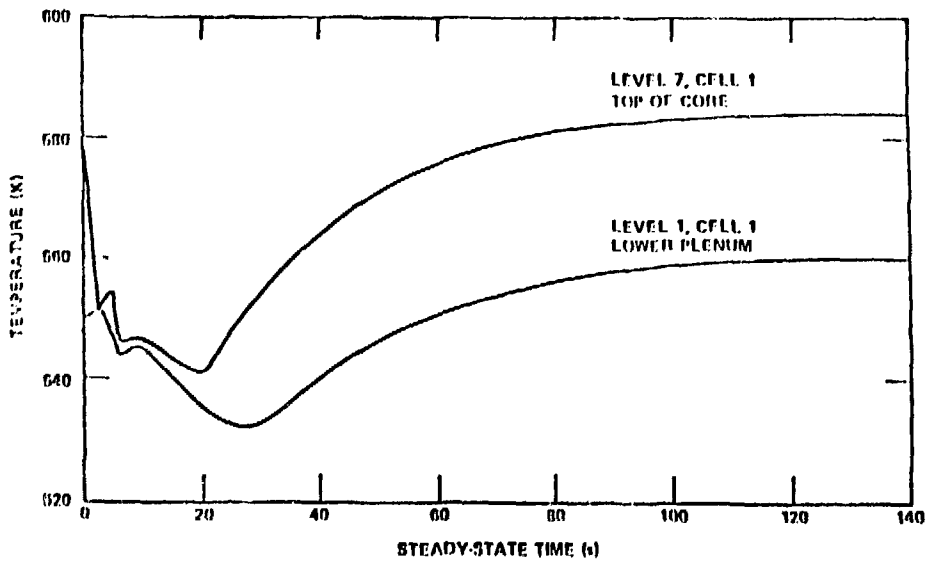

Fig. C-11.
Liquid temperature in vessel.

APPENDIX D

TRAC ERROR MESSAGES

Errors diagnosed by TRAC are handled by subroutine ERROR. This subroutine writes error messages to both the teletype and the TRCOUT file. The level number associated with each error below is used by ERROR to determine its course of action:

Level	Actions
1,3	Fatal error, stop problem.
2	Nonfatal error, continue problem.
4	Fatal error, add dump to the TRCDMP file, then stop problem.

OVERLAY MAIN

Subroutine	Level	Message*	Explanation
BFIN	3	READ ERROR	Error reading data in binary format.
BFOUT	3	WRITE ERROR	Error writing data in binary format.
CHBD	2	BOUNDARY ERROR DETECTED	Mismatched geometry for adjacent components.
ENDDMP	2	DUMP FILE NOT CLOSED	I/O error while attempting to close file TRCDMP.
ENDGRF	2	GRAPHICS FILE NOT CLOSED	I/O error while attempting to close file TRCGRF.

*Each message also identifies the subroutine detecting the error.

Subroutine	Level	Message	Explanation
MANAGE	1	LEVEL PROBLEM	The core level or rod number requested does not exist.
PUMPD	1	CANNOT LOCATE HEAD CURVE	Pump regime outside of data base.
PUMPD	1	CANNOT LOCATE TORQUE CURVE	Pump regime outside of data base.
STEADY	1	INVALID TIME STEP RATIO	Ratio between heat transfer and fluid flow time steps is ≤ 0.
STEADY	1	EXCESSIVE OUTER ITERATION FAILURES	More than three outer iteration failures encountered.
STEADY	1	STEADY-STATE NOT REACHED	Steady-state conditions not reached during specified time interval.
STEADY	1	OUT OF TIME FOR STEADY-STATE	Allocated CPU time exhuasted before steady-state was reached.
THERMO	2	PRESSURE LIMIT EXCEEDED	Pressure in some cell has fallen below 1.0E+03 or risen above 1.9E+07.
THERMO	2	VAPOR TEMPERATURE LIMIT EXCEEDED	Vapor temperature in some cell has fallen below 280 K.
THERMO	2	LIQUID TEMPERATURE LIMIT EXCEEDED	Liquid temperature in some cell has fallen below 280 K or risen above 647 K.
TIMSTP	1	CANNOT REDUCE TIME STEP FURTHER	Time step has been reduced to the minimum allowable and the outer iteration failed to converge.
TRANS	1	OUTER ITERATION DID NOT CONVERGE	The outer iteration procedure failed three consecutive times.
TRIP	1	TRIP NUMBER NOT DEFINED	A request was made for the status of a trip that was never defined.

Subroutine	Level	Message	Explanation
TRPSET	1	TRIP DATA ERROR	Illegal values for trip qualifiers ID3 and ID4.
OVERLAY INPUT			
INPUT	1	FATAL INPUT ERROR	A fatal input error occurred while reading an input and/or restart file.
FNDLP	1	INVALID VESSEL JUNCTION	PWR Initialization input error. A junction was specified which is not connected to the vessel.
FNDLP	1	TEE MISSING FROM JUN ARRAY	PWR Initialization input error. A loop tee was not found in the JUN array.
FNDLP	1	STGEN MISSING FROM JUN ARRAY	PWR Initialization input error. A loop steam generator was not found in the JUN array.
FNDLP	1	COMPLEX SECONDARY LOOP	PWR Initialization input error. The secondary side of the steam generator must be connected to only pipe, fill, and break.
FNDLP	1	LAST COMMON COMPONENT NOT FOUND	PWR Initialization input error. In a two-pump loop, the connecting tee was not located.
FNDLP	1	LAST COMMON COMPONENT NOT A TEE	PWR Initialization input error. In a two-pump loop, the connecting component is not a tee.
PATH	1	ADJACENT COMPONENT MISSING	PWR Initialization input error. A junction was encountered which is connected to only one component.

Subroutine	Level	Message	Explanation
PATH	1	COMPONENT NOT FOUND IN IORDER ARRAY	PWR Initialization input error. A component was encountered which is not listed in the IORDER array.
PATH	1	PIPE JUNCTION NOT ADJACENT	PWR Initialization input error. The two entries in JUN for a pipe are not consecutive.
RACCUM	2	LCM OVERFLOW	LCM area overflowed during input of data for an accumulator.
RACCUM	2	SCM OVERFLOW	SCM area overflowed during input of data from an accumulator.
RBREAK	2	LCM OVERFLOW	LCM area overflowed during input of data for a break.
RDCOMP	1	COMPONENT TYPE NOT RECOGNIZED	An invalid component type was encountered.
RDCOMP	1	DUPLICATE COMPONENT NUMBERS	At least 2 components were assigned the same NUM during input.
RDLOOP	1	VESSEL NOT FOUND IN JUN ARRAY	PWR Initialization input error. The vessel is not listed in the JUN array.
RDLOOP	1	VESSEL NOT FOUND IN IORDER ARRAY	PWR Initialization input error. The vessel is not listed in the IORDER array.
RDLOOP	1	INSUFFICIENT SCM ARRAY SPACE	PWR Initialization input error. The PWR Initialization Data Area is larger than the available space.
RDREST	1	BUFFERS EXCEED LCM SPACE	Insufficient LCM space remains for allocation of restart file buffers.

Subroutine	Level	Message	Explanation
RDREST	1	RESTART FILE OPEN ERROR	I/O error while attempting to open the restart file.
RDREST	1	RESTART FILE INCOMPATIBLE WITH THIS PROBLEM	The restart file cannot be used with this version of TRAC.
RDREST	1	DUMP TIME NOT FOUND ON RESTART FILE	Restart dump at time indicated on input file is not on the restart file.
RDREST	1	RESTART FILE NOT CLOSED PROPERLY	The file TRCRST was not closed properly when created.
RDREST	1	COMPONENT DATA NOT FOUND	Data for a particular component was not found in either input or restart file.
RDREST	1	TYPE NOT RECOGNIZED IN RESTART	An invalid component type was encountered.
RDREST	1	ERROR RETRIEVING DUMP DATA	I/O error occurred while attempting to read restart file.
REACCM	2	SCM OVERFLOW	SCM area overflowed while reading accumulator data from restart file.
REACCM	2	LCM OVERFLOW	LCM area overflowed while reading accumulator data from restart file.
REBRK	2	LCM OVERFLOW	LCM area overflowed while reading break data from restart file.
REFILL	2	LCM OVERFLOW	LCM area overflowed while reading fill data from restart file.

Subroutine	Level	Message	Explanation
REPIPE	2	SCM OVERFLOW	SCM area overflowed while reading pipe data from a restart file.
REPIPE	2	LCM OVERFLOW	LCM area overflowed while reading pipe data from a restart file.
REPRZR	2	SCM OVERFLOW	SCM area overflowed while reading pressurizer data from restart file.
REPRZR	2	LCM OVERFLOW	LCM area overflowed while reading pressurizer data from restart file.
REPUMP	2	SCM OVERFLOW	SCM area overflowed while reading pump data from restart file.
REPUMP	2	LCM OVERFLOW	LCM area overflowed while reading pump data from restart file.
RESTGN	2	SCM OVERFLOW	SCM area overflowed while reading steam generator data from restart file.
RESTGN	2	LCM OVERFLOW	LCM overflowed while reading steam generator data from restart file.
RETEE	2	SCM OVERFLOW	SCM area overflowed while reading tee data from restart file.
RETEE	2	LCM OVERFLOW	LCM area overflowed while reading tee data from restart file.
RETRIP	1	TRIP BLOCK TOO SMALL	Too many trips found in the restart file.

Subroutine	Level	Message	Explanation
REVLVE	2	SCM OVERFLOW	SCM area overflowed while reading valve data from restart file.
REVLVE	2	LCM OVERFLOW	LCM area overflowed while reading valve data from restart file.
REVSSL	2	SCM3D OVERFLOW	SCM3D area overflowed while reading rod and level data from restart file.
REVSSL	2	LCM OVERFLOW	LCM area overflowed while reading vessel data from restart file.
REVSSL	2	SCM OVERFLOW	SCM area overflowed while reading vessel data from restart file.
RFILL	2	LCM OVERFLOW	LCM area overflowed while reading fill data from input file.
RFILL	1	FILL INPUT ERROR	An error in fill input parameters has been made.
RPIPE	2	LCM OVERFLOW	LCM area overflowed while reading pipe data from input file.
RPIPE	2	SCM OVERFLOW	SCM area overflowed while reading pipe data from input file.
RPRIZR	2	LCM OVERFLOW	LCM area overflowed while reading pressurizer data from input file.
RPRIZR	2	SCM OVERFLOW	SCM area overflowed while reading pressurizer data from input file.
RPUMP	2	WARNING-IPMPTY SET EQUAL TO 1 ******	IMPPTY is only allowed to be 1 or 2. Anything other than 2 will default to 1.

Subroutine	Level	Message	Explanation
RPUMP	2	WARNING PUMP TYPE 1 BUT NO POINTS IN THE SPEED TABLE	Pump trip was specified but no speed table provided.
RPUMP	2	LCM OVERFLOW	LCM area overflowed while reading pump data from input file.
RPUMP	2	SCM OVERFLOW	SCM area overflowed while reading pump data from input file.
RVLVE	2	SCM OVERFLOW	SCM area overflowed while reading valve data from an input file.
RSTGEN	2	LCM OVERFLOW	LCM area overflowed while reading steam generator data from input file.
RSTGEN	2	SCM OVERFLOW	SCM area overflowed while reading steam generator data from input file.
RTEE	2	WRONG HYDRO OPTION	AN IMPLICIT TEE CANNOT BE SPECIFIED IN THIS VERSION OF THE CODE.
RTEE	2	LCM OVERFLOW	LCM area overflowed while reading tee data from input file.
RTEE	2	SCM OVERFLOW	SCM area overflowed while reading tee data from input file.
RVLVE	1	NUMBER OF CELLS MUST BE TWO	The number of fluid cells for a valve must be input as 2.
RVLVE	1	NO VALVE TABLE SPECIFIED	Input indicated that opening or closing of a valve would be specified in a valve table, but length of table was input as zero.
RVLVE	1	PRESSURE GRADIENT OPTION	Input indicated a value to be controlled by static pressure gradient,

Subroutine	Level	Message	Explanation
			but a nonexistent pressure gradient option was input.
RVLVE	1	NO TRIP NUMBER SPECIFIED FOR VLVE	Input specified a value to be controlled by a trip, but no ID number was assigned to it.
RVLVE	2	SCM OVERFLOW	SCM area overflowed while reading valve data from an input file.
RVLVE	2	LCM OVERFLOW	LCM area overflowed while reading valve data from an input file.
RVSSL	1	INCONSISTENT CORE INPUT	Error in specifying the core positional parameters ICRV, ICRL, ICRR, or the number of heat transfer nodes.
RVSSL	1	INCONSISTENT DOWNCOMER INPUT	Error in specifying the downcomer positional parameters IDCU, IDCL, and IDCR.
RVSSL	2	SCM3D OVERFLOW	SCM3D area overflowed while reading rod and level data from an input file.
RVSSL	2	LCM OVERFLOW	LCM area overflowed while reading vessel data from an input file.
RVSSL	2	SCM OVERFLOW	SCM area overflowed while reading vessel data from an input file.
TRCE	1	TOO MANY NESTED TEES	PWR Initialization input error. More than 5 tees are connected together.
TRCE	1	COMPONENT TYPE NOT LOCATED	PWR Initialization input error. A steam generator, pump, or

Subroutine	Level	Message	Explanation
			vessel hot leg not connected to the vessel cold leg.
TRCE	1	TEE JUNCTIONS NOT ADJACENT	PWR Initialization input error. The entries in the JUN array for a tee are not consecutive.
TRCE	1	COMPONENT JUNCTIONS NOT ADJACENT	PWR Initialization input error. The entries in the JUN array for a component are not adjacent.
OVERLAY INIT			
CIVSSL	1	JUNCTION PROBLEM	Cannot find component adjacent to the vessel.
CIVSSL	1	IORDER PROBLEM	The calculational sequence must be such that the vessel is calculated after the component it is connected to.
CIVSSL	1	CONNECTIONS COMPUTED AFTER VESSEL	The component calculational sequence must be such that the connections are computed before the vessel.
CIVSSL	1	VESSEL CONNECTED TO BREAK	A vessel cannot be connected to a break.
ICOMP	1	JUNCTION COUNT ERROR	The number of junctions specified is inconsistent with the number found.
ICOMP	1	INCONSISTENT JUNCTION NUMBERS	Inconsistent specification of junction numbers.
ICOMP	1	JUNCTION NUMBERS WRONG	The junctions are assigned incorrectly.

Subroutine	Level	Message	Explanation
IGRAF	1	GRAPHICS FILE ALLOCATION FAILURE	I/O error occurred while attempting to allocate space for graphics file.
IGRAF	1	BUFFERS EXCEED LCM SPACE	Insufficient LCM space remains for allocation of graphics file buffers.
IGRAF	1	ERROR WRITING GRAPHICS FILE HEADER	I/O error while writing the header of the TRCGRF file.
IVSSL	1	KINETICS CONSTANTS PROBLEM	Number of delayed neutron groups does not agree with built-in data.
IVSSL	1	ROD POWER PROBLEM	Reactor power option specified is not within allowable limits.
IVSSL	1	ROD HAS NO GAP	Fuel rod must contain a gap.
IVSSL	1	GAP POSITION ERROR	Gap must lie between the fuel and clad.
JFIND	1	JUNCTION PROBLEM	A junction number could not be located in junction sequence array.
OVERLAY DUMP			
DMPIT	1	INSUFFICIENT SPACE LEFT FOR DUMP	File TRCDMP has insufficient space for the next dump.
DMPIT	3	TYPE NOT RECOGNIZED IN DUMP	An invalid component type has been encountered.
DMPIT	1	ERROR EMPTYING DUMP BUFFERS FILE	I/O error at completion of a dump.
DMPIT	3	ERROR INITIALIZING DUMP FILE	Could not create file TRCDMP.
OVERLAY TWOTIM			
TWOTIM	1	COMPONENT TYPE NOT LOCATED	An invalid component type was encountered

Subroutine	Level	Message	Explanation
OVERLAY PWRSS			
LDSET	1	ZERO FLOW OR POWER FOUND AT PWR INITIALIZATION	The PWR Initialization calculation began with a zero value of reactor power or flow rate.
LPCON	1	NO PUMP IN PRINCIPAL LOOP	No pump was found in the loop description.
LPCON	1	NO STGEN IN PRINCIPAL LOOP	No steam generator was found in the loop description.
LPCON	1	MISSING VESSEL JUNCTION	An invalid vessel junction number was found in the vessel junction data area.
ORIENT	1	NO JUNCTION MATCH	Unable to locate a junction connected to a tee or steam generator in the JUN array.
RPPH	1	CONVERGENCE FAILURE EVALUATING PUMP SPEED	Unable to calculate the pump speed to achieve the needed head.
TEMPL	1	TOO MANY ITERATIONS	Unable to evaluate the temperature from values of enthalpy and pressure.
OVERLAY OUTlD			
OUTlD	1	COMPONENT TYPE NOT RECOGNIZED	Invalid component type encountered.
CFILL	1	ERROR IN TABLE LOOKUP	Fill table was specified incorrectly.
PUMP	4	ERROR IN PUMP SPEED TABLE LOOKUP	Pump speed table was specified incorrectly.
PUMP	1	TERMINATING DUE TO ERROR IN PUMPX	An error has been encountered while evaluating a pump head or torque.

Subroutine	Level	Message	Explanation
VLVE	1	ERROR IN TABLE LOOKUP	Error retrieving data from a valve table.
OVERLAY OUT3D			
OUT3D	1	COMPONENT TYPE NOT RECOGNIZED	An invalid component type was encountered.
RKIN	1	TABLE LOOKUP PROBLEM	Error retrieving data from a reactivity or power table.

APPENDIX E

LIST OF TRAC SUBPROGRAMS

Name	Code Block	Function
ACCUM	OUT1D	Models accumulators and calculates discharge when check valves open.
ASIGN	INPUT	Assigns the component LCM pointers according to the iteration number.
BFALOC	MAIN	Allocates files and buffers for buffered I/O.
BFBUSY	MAIN	Wait if buffered I/O is busy and return completion status.
BFCLOS	MAIN	Empties buffers and closes files.
BFIN	MAIN	Buffered input without error status.
BFLAST	MAIN	Skip to last logical restart dump file.
BFLUSH	MAIN	Flush output buffers.
BFREW	MAIN	Rewind I/O file.
BFRIN	MAIN	Buffered input with error status.
BFROUT	MAIN	Buffered output with error status.
BFSKIP	MAIN	Skip to beginning of next logical input file.
BFOUT	MAIN	Buffered output without error status.
BLOCK-DATA	MAIN	Set compile time data via data statements.
BLSHT	MAIN	Force loads certain subprograms into MAIN codeblock.
C3CELL	OUT1D	Sets up flux terms and derivatives for fully implicit hydrodynamics.
CACCUM	OUT1D	Transfers accumulator data to be used in a calculation from LCM to SCM.
CBREAK	OUT1D	Transfers break data from LCM to SCM.
CFILL	OUT1D	Transfers fill data from LCM to SCM.

Name	Code Block	Function
CHAIN	MAIN	Codeblock overlay controller.
CHBD	MAIN	Checks boundary data.
CHEN	OUTER	Uses Chen correlation to evaluate the forced convection nucleate boiling heat transfer coefficient.
CHF	OUTER	Evaluates the critical heat flux based on a local conditions formulation.
CHF1	OUTER	Biasi CHF correlation.
CHF2	OUTER	Bowring CHF correlation.
CIACUM	INIT	Transfers accumulator data from LCM to SCM so that remaining data can be initialized.
CIPIPE	INIT	Transfers pipe data from LCM to SCM so that remaining data can be initialized.
CIPRZR	INIT	Transfers pressurizer data from LCM to SCM so that remaining data can be initialized.
CIPUMP	INIT	Transfers pump data from LCM to SCM so that remaining data can be initialized.
CISTGN	INIT	Transfers steam generator data from LCM to SCM so that remaining data can be initialized.
CITEE	INIT	Transfers tee data from LCM to SCM so that remaining data can be initialized.
CIVLVE	INIT	Tranfers valve data from LCM to SCM so that remaining data can be initialized.
CIVSSL	INIT	Transfers vessel data from LCM to SCM so that remaining data can be initialized.
CLEAR	MAIN	Sets an array to a constant value.
CORE	OUT3D	Controls fuel rod thermal analysis calculations and generates heat transfer coefficients.
CPIPE	OUT1D	Transfers pipe data to be used in a calculation from LCM to SCM.
CPLL	MAIN	Calculates specific heat of liquid water as a function of enthalpy and pressure.
CPRIZR	OUT1D	Transfers pressurizer data to be used in a calculation from LCM to SCM.

Name	Code Block	Function
CPUMP	OUT1D	Transfers pump data to be used in a calculation from LCM to SCM.
CPVV	MAIN	Calculates specific heat of water vapor as a function of enthalpy and pressure.
CSTGEN	OUT1D	Transfers steam generator data to be used in a calculation from LCM to SCM.
CTEE	OUT1D	Transfers tee data to be used in a calculation from LCM to SCM.
CVLVE	OUT1D	Transfers valve data to be used in a calculation from LCM to SCM.
CVSSL	OUT3D	Transfers vessel data to be used in a calculation from LCM to SCM.
CWACUM	EDIT	Transfers accumulator data from LCM to SCM so that it can be printed.
CWPIPE	EDIT	Transfers pressurizer data from LCM to SCM so that it can be printed.
CWPRZR	EDIT	Transfers pressurizer data from LCM to SCM so that it can be printed.
CWPUMP	EDIT	Transfers pump data from LCM to SCM so that it can be printed.
CWSTGN	EDIT	Transfers steam generator data from LCM to SCM so that it can be printed.
CWTEE	EDIT	Transfers tee data from LCM to SCM so that it can be printed.
CWVLVE	EDIT	Transfers valve data from LCM to SCM so that it can be printed.
CWVSSL	EDIT	Transfers vessel data from LCM to SCM so that it can be printed.
CYLHT	OUT1D	Calculates temperature fields in a cylinder.
DACCUM	DUMP	Generates accumulator data dump.
DBRK	DUMP	Generates break data dump.

Name	Code Block	Function
DF1D	OUT1D	Controls solution of finite difference equations for the 1-D drift-flux model of a pipe.
DF1DI	OUT1D	Solves the fully implicit finite difference equations for the 1-D drift-flux model of a pipe.
DF1DS	OUT1D	Solves the semi-implicit finite difference equations for the 1-D drift-flux model of a pipe.
DFILL	DUMP	Generates fill data dump.
DMPIT	DUMP	Dump code block entry routine which controls generation of dumps.
DPIPE	DUMP	Generates pipe data dump.
DPRIZR	DUMP	Generates pressurizer data dump.
DPUMP	DUMP	Generates pump data dump.
DSTGEN	DUMP	Generates steam generator data dump.
DTEE	DUMP	Generates tee data dump.
DVLVE	DUMP	Generates valve data dump.
DVSSL	DUMP	Generates vessel data dump.
EDIT	EDIT	Entry routine for code block edit.
EMPBUF	MAIN	Empty output buffer.
ENDDMP	MAIN	Calls routine to empty dump buffers and close dump file.
ENDGRF	MAIN	Calls routine to empty graphics buffers and close graphics file.
ERRGET	MAIN	Trap interrupts for subsequent handling by TRAC.
ERROR	MAIN	Processes different kinds of error conditions.
ERRTRP	MAIN	Handles trapped errors.
FDMX3D	TWOTIM	Calculates normalized rates of change for 3-D component variables.
FDMXFP	TWOTIM	Calculates normalized rates of change for 1-D component variables.

Name	Code Block	Function
FDMXTR	TWOTIM	Calculates normalized rates of change for rod temperatures.
FDMXTS	TWOTIM	Calculates normalized rates of change for vessel heat slabs.
FDMXTW	TWOTIM	Calculates normalized rates of change for wall temperatures.
FF3D	OUT3D	Makes final pass update for all variables in 3-D vessel.
FILM	OUT3D	Calculates quench front propagation and axial conduction for a falling film.
FLOOD	OUT3D	Calculates quench front propagation and axial conduction for bottom flooding.
FNDLP	INPUT	Catalogs one primary loop configuration.
FPROP	MAIN	Calculates values for fluid enthalpy, transport properties, and surface tension.
FROD	OUT3D	Calculates temperature profiles in nuclear or electrically heated fuel rods.
FWALL	OUT1D	Computes a two-phase friction factor.
GAPHT	OUT3D	Calculates fuel-clad gap heat transfer coefficient.
GETCRV	MAIN	Gets appropriate pump curves from data base.
GRAF	GRAF	Edits graphics data during transient.
GRFGET	MAIN	Returns entries in graphics catalog block.
GRFPUT	INIT	Places entries in graphics catalog block.
HLS	MAIN	Calculates enthalpy of saturated water as function of pressure.
HTCOR	OUTER	Computes heat transfer coefficients.
HTPIPE	OUT1D	Averages velocities and generates heat transfer coefficients for pipe.
HTVSSL	OUT3D	Averages velocities and generates heat transfer coefficients for vessel.
HVS	MAIN	Calculates enthalpy of saturated steam as a function of pressure.

Name	Code Block	Function
IACCUM	INIT	Initializes the accumulator data arrays which are not read in from cards.
IBRK	INIT	Initializes the break data arrays which are not read in from cards.
ICOMP	INIT	Controls the routines which initialize component data.
IFILL	INIT	Initializes the fill data arrays which are not read in from cards.
IGACUM	INIT	Supplies accumulator data for graphics.
IGBRAK	INIT	Initializes the data which are not read in from cards.
IGFILL	INIT	Supplies fill data for graphics.
IGPIPE	INIT	Supplies pipe data for graphics.
IGPRZR	INIT	Supplies pressurizer data for graphics.
IGPUMP	INIT	Supplies pump data for graphics.
IGRAF	INIT	Initializes graphics variables and writes header to graphics file.
IGSTGN	INIT	Supplies steam generator data for graphics.
IGTEE	INIT	Supplies tee data for graphics.
IGVLVE	INIT	Supplies valve data for graphics.
IGVSSL	INIT	Supplies vessel data for graphics.
INIT	INIT	Entry routine for code block INIT.
INPUT	INPUT	Entry routine for code block INPUT.
IPIPE	INIT	Initializes the pipe data arrays which are not read in from cards.
IPRIZR	INIT	Initializes the pressurizer data arrays which are not read in from cards.
IPUMP	INIT	Initializes the pump data arrays which are not read in from cards.
ISTGEN	INIT	Initializes the steam generator data arrays which are not read in from cards.

Name	Code Block	Function
ITEE	INIT	Initializes the tee data arrays which are not read in from cards.
ITRl	OUT3D	Gives iterative solution of reduced, linearized 3-D finite difference equations.
IVLVE	INIT	Initializes the valve data arrays which are not read in from cards.
IVSSL	INIT	Initializes the vessel data arrays which are not read in from cards.
JlD	MAIN	Fills boundary array at component junctions.
JFIND	INIT	Locates junctions in junction sequence array.
LCMOVE	MAIN	Copies data from one part of LCM to another.
LENPCK	MAIN	Computes packed data array lengths.
LININT	MAIN	Performs linear interpolation on arrays.
LOAD	INPUT	Reads in specially formatted input data.
LPCON	PWRSS	Evaluates loop properties.
LPRPL	PWRSS	Replaces pump heads and steam generator areas and checks for convergence of steady-state calculation.
LPSET	PWRSS	PWRSS code block entry point; resets PWR loop parameters for steady state.
MANAGE	MAIN	Performs all level data file operations for the vessel.
MBN	OUT3D	Calculates values for electrically heated nuclear fuel rod insulator properties.
MFROD	OUT3D	Orders fuel rod property selection and evaluates an average temperature for property evaluation.
MFUEL	OUT3D	Calculates values for UO_2 and UO_2-PUO_2 properties.
MGAP	OUT3D	Calculates values for the thermal conductivity of the gap gas mixture.
MHTR	OUT3D	Calculates values for electrically heated fuel rod heater coil properties.
MPROP	OUTER	Orders structure property selection and evaluates an average temperature for property evaluation.

Name	Code Block	Function
MSTRCT	OUTER	Calculates properties for certain types of steel.
MWRX	OUT3D	Calculates the zircaloy steam reaction in the cladding at high temperatures.
MZIRC	OUT3D	Calculates properties for zircaloy-4.
NEWDLT	MAIN	Evaluates prospective new time increment.
ORIENT	PWRSS	Determines adjacent junction index given component number.
OUT1D	OUT1D	Controls calculation for 1-D components.
OUT3D	OUT3D	Controls calculation for the vessel.
OUTER	OUTER	Controls calculation for one time step.
PACKIT	MAIN	Packs data from one array into another.
PATH	INPUT	Catalogs a path beginning at a given junction of a given component.
PIPE	OUT1D	Models the fluid and heat flow in a pipe.
PMPP	PWRSS	Calculates pump enthalpy, pressure, and density.
POLY	MAIN	Evaluates a polynomial through successive multiplications.
PRIZER	OUT1D	Models pressurizers.
PUMP	OUT1D	Models pumps.
PUMP1	INPUT	Supplies built-in pump characteristics.
PUMPD	MAIN	Calculates head and torque from pump curves.
PUMPX	OUT1D	Calculates pump head and torque.
RACCUM	INPUT	Reads accumulator data from cards and sets up pointer table for that data.
RBREAK	INPUT	Reads break data from cards and sets up a pointer table for that data.
RDCOMP	INPUT	Controls reading of component data from cards.
RDCRVS	INPUT	Reads pump curves from card data.

Name	Code Block	Function
RDDIM	INPUT	Reads number of points on pump curves from card data.
RDLCM	MAIN	Reads data from LCM into SCM.
RDLOOP	INPUT	Reads loop data and sets up geometry data for steady state.
RDREST	INPUT	Controls reading of component data from a restart dump file.
RDTRIP	INPUT	Reads trip data from cards.
REACCM	INPUT	Reads accumulator data from a restart dump and sets up a pointer table for that data.
REBRK	INPUT	Reads break data from a restart dump and sets up a pointer table for that data.
REFILL	INPUT	Reads fill data from a restart dump and sets up a pointer table for that data.
REPIPE	INPUT	Reads pipe data from a restart dump and sets up a pointer table for that data.
REPRZR	INPUT	Reads pressurizer data from a restart dump and sets up a pointer table for that data.
REPUMP	INPUT	Reads pump data from a restart dump and sets up a pointer table for that data.
RESTGN	INPUT	Reads steam generator data from a restart dump and sets up a pointer table for that data.
RETEE	INPUT	Reads tee data from a restart dump and sets up a pointer table for that data.
RETRIP	INPUT	Reads trip data from a restart dump file.
REVLVE	INPUT	Reads valve data from a restart dump and sets up a pointer table for that data.
REVSSL	INPUT	Reads vessel data from a restart dump and sets up a pointer table for that data.
RFILL	INPUT	Reads fill data from cards and sets up a pointer table for that data.
RKIN	OUT3D	Integrates the neutron point-kinetics equations.
RODHT	OUT3D	Calculates the fuel rod temperature field.

Name	Code Block	Function
RPIPE	INPUT	Reads pipe data from cards and sets up a pointer table for that data.
RPPH	PWRSS	Tests and replaces pump speed.
RPRIZR	INPUT	Reads pressurizer data from cards and sets up a pointer table for that data.
RPSCA	PWRSS	Tests and replaces steam generator heat transfer area.
RPUMP	INPUT	Reads pump data from cards and sets up a pointer table for that data.
RSTGEN	INPUT	Reads steam generator data from cards and sets up pointer tables for that data.
RTEE	INPUT	Reads tee data from cards and sets up a pointer table for that data.
RVLVE	INPUT	Reads valve data from cards and sets up pointer tables for that data.
RVSSL	INPUT	Reads vessel data from cards and sets up pointer tables for that data.
SACCUM	TWOTIM	Compares two time steps for an accumulator.
SCMOVE	MAIN	Copies a given number of words from one SCM array into another.
SECOND	MAIN	Return problem CPU elapsed time.
SETPOW	MAIN	Initialize reactor power.
SETPRP	MAIN	Determines pump speed and steam generator heat transfer area.
SIGMA	MAIN	Returns surface tension of water as a function of pressure.
SLABHT	OUT3D	Calculates the slab temperatures.
SLIP	OUT1D	Calculates drift velocities between phases.
SLVLP	PWRSS	Solves one primary loop in steady state.
SOLVE	OUTER	Solves linear system of the form: A*X =B.
SPIPE	TWOTIM	Compares two time steps for a pipe.
SPLIT	MAIN	Reads appropriate data from pump curves.

Name	Code Block	Function
SPUMP	TWOTIM	Compares two time steps for a pump.
SSTGEN	TWOTIM	Compares two time steps for a steam generator.
STEADY	MAIN	Generates a steady-state solution.
STEE	TWOTIM	Compares two time steps for a tee.
STGEN	OUTlD	Models steam generators.
STGNP	PWRSS	Calculates thermal properties for steam generator for steady state.
SVALVE	TWOTIM	Compares two time steps for a valve.
SVSSL	TWOTIM	Compares two time steps for a vessel.
TEE	OUTlD	Models a tee.
TEEP	PWRSS	Calculates central cell pressure and enthalpy flow rate.
TEMPL	PWRSS	Evaluates temperature based on liquid enthalpy and pressure.
TF3D	OUT3D	Sets up the linearized 3-D finite difference equations.
THCL	MAIN	Returns thermal conductivity of water as function of pressure and enthalpy.
THCV	MAIN	Returns thermal conductivity of steam as function of pressure and enthalpy.
THERMO	MAIN	Calculates thermodynamic properties of water.
TIMCHK	MAIN	Checks elapsed time to see whether certain functions should be performed.
TIMSTP	MAIN	Sets up time step size and edit interval time.
TRAC	MAIN	Main program.
TRANS	MAIN	Controls overall calculation for each time step.
TRCE	INPUT	Traces paths to locate a given component.
TRIP	MAIN	Returns status of a trip.
TRPSET	MAIN	Sets up trip status flags.
TWOTIM	TWOTIM	Controls time step comparison for steady state.

Name	Code Block	Function
VISCL	MAIN	Returns viscosity of water as a function of pressure and enthalpy.
VISCV	MAIN	Returns viscosity of steam as a function of pressure and enthalpy.
VLVE	OUT1D	Models valves.
VSCON	PWRSS	Evaluates vessel constants and junction properties.
VSSL1	OUT3D	Performs prepass calculations for vessel dynamics.
VSSL2	OUT3D	Performs inner iterations for vessel dynamics.
VSSL3	OUT3D	Performs postpass calculations for vessel dynamics.
WACCUM	EDIT	Writes selected accumulator data to the printer.
WARRAY	MAIN	Writes a real array to the printer.
WBREAK	EDIT	Writes selected break data to the printer.
WCOMP	EDIT	Controls the writing of selected component data to the printer.
WFILL	EDIT	Writes selected fill data to the printer.
WIARR	MAIN	Writes an integer array to the printer.
WPIPE	EDIT	Writes selected pipe data to the printer.
WPRIZR	EDIT	Writes selected pressurizer data to the printer.
WPUMP	EDIT	Writes selected pump data to the printer.
WRLCM	MAIN	Writes a given number of words from SCM to LCM.
WRSLP	INPUT	Prints out subloop description.
WSTGEN	EDIT	Writes selected steam generator data to the printer.
WTEE	EDIT	Writes selected tee data to the printer.
WVLVE	EDIT	Writes selected valve data to the printer.
WVSSL	EDIT	Writes selected vessel data to the printer.

APPENDIX F

DESCRIPTION OF COMMON BLOCK VARIABLES

COMMON A(6500)

A(6500)	Dynamic storage area for component data.

COMMON/CONST/PI,GC,AERO,ONE

PI	Constant π .
GC	Gravitational constant.
ZERO	Real constant zero.
ONE	Real constant one.

COMMON/CONTRL/STDYST,TRANSI,DSTEP,ICP,LCMPTR,TIMEL,DELT,TIMET,EPSO,EPSI,EPSS,
OITMAX,IITMAX,SITMAX,IEOS,VMAXT,DAMX,VARER,ICMP,DTMIN,DTMAX,
ISTDY,TEND,IPAK,EPSP

STDYST	Steady-state calculation indicator.
TRANSI	Transient calculation indicator.
DSTEP	Time step number of dump to be used for restart.
ICP	Temporary pointer to next free location in the dynamic storage area for component data.
LCMPTR	Pointer to end of component data for last component read in.
TIMEL	Variable used to increase length of code by one word.
DELT	Current time increment for advancement of finite difference equations.
TIMET	Current calculation time.
EPSO	Convergence criterion for outer iteration.
EPSI	Convergence criterion for inner iteration.
EPSS	Convergence criterion for steady-state calculation.

OITMAX	Maximum number of outer iterations.
IITMAX	Maximum number of inner iterations.
SITMAX	Maximum number of outer iterations for steady-state calculation.
IEOS	Flag to indicate either steam (0) or air (1).
VMAXT	Maximum Courant number.
DAMX	Error due to relative change in void fraction.
VARER	Variable error.
ICMP	Component indicator.
DTMIN	Minimum allowable time step size for time interval.
DTMAX	Maximum allowable time step size for time interval.
ISTDY	Flag to indicate type of calculation (0 = transient; 1 = steady state).
TEND	End of time domain.
IPAK	Flag to indicate water packer option (0 = off, 1 = On).
EPSP	Convergence criteria for PWR initialization calculation.

COMMON/CTRLDP/ICTRLD(13),DMPFLG,TDUMP,DMPINT,LTDUMP,LDMPTR,NDMPTR

ICTRLD(13)	Array which contains buffering information about the dump output file.
DMPFLG	Flag which signals whether the dump output file has been initialized (0 = not, 1 = initialized).
TDUMP	Calculation time at which next dump is to be taken.
DMPINT	Dump interval for time domain.
LTDUMP	CPU time when last dump was taken.
LDMPTR	Pointer to dump trip data.
NDMPTR	Number of trips on which a dump is to be taken.

COMMON/DF1DC/IDF1D,ISRB,ISLB,JSTART,SSMC2,SSMC,SSVE,SSVC,SSMOM,SSE,VJS,DVJP,
SSAC,SRHE,SRHVC,SRHEV,SRHAC,MSC

IDF1D	Hydrodynamics trigger.
ISRB	Right-hand boundary switch.

ISLB	Left-hand boundary switch.
JSTART	Cell number at left end of one-dimensional segment.
SSMC2	Momentum source to right-hand boundary of cell.
SSMC	Mass source.
SSVE	Vapor energy source.
SSVC	Vapor mass source.
SSMOM	Momentum source to left cell boundary.
SSE	Energy source.
VJS	Source velocity.
DVJP	Pressure derivative of source velocity.
SSAC	Air source.
SRHE	Energy source due to drift terms.
SRHVC	Vapor mass due to drift terms.
SRHEV	Vapor energy due to drift terms.
SRHAC	Air mass due to drift terms.
MSC	Cell number for source terms.

COMMON/DIMEN/NUMCTR,NCOMP,NJUN,LENTBL,IFREE,LAST,LFREE,LLAST,LENBD,NTRX,
L3DLT,NTHM

NUMCTR	Number of title cards.
NCOMP	Number of components.
NJUN	Number of junctions.
LENTBL	Length of fixed length table.
IFREE	First free word in the dynamic storage area.
LAST	Last word in the dynamic storage area.
LFREE	First free location in LCM.
LLAST	Last location in LCM.
LENBD	Length of boundary data array for each junction.
NTRX	Number of trips specified.
L3DLT	Last location of dynamic storage area for vessel, rod, and level data (A3D array).
NTHM	Number of elements per cell in the DRIV array.

```
COMMON/GRAPH/IBUFF,LCMGCT,NCTX,NWTX,KLENTH,KP,LCAT,TEDIT,EDINT,TGRAF,GFINT,
            IPKG,ICTRLG(13)
```

IBUFF	Length of graphics buffer.
LCMGCT	Address of graphics catalog in LCM.
NCTX	Number of graphics catalog entries.
NWTX	Number of words written to disk per graphics edit.
KLENTH	Length of the graphics disk file.
KP	Pointer in graphics catalog block.
LCAT	Address of graphics catalog in SCM.
TEDIT	Time of next print edit.
EDINT	Print edit interval for time domain.
TGRAF	Time of next graphics edit.
GFINT	Graphics edit interval for time domain.
IPKG	Graphics file packing density.
ICTRLG(13)	Array which contains buffering information about the graphics output file.

```
COMMON/HOLL/PIPEH,PUMPH,TEEH,VALVEH,BREAKH,FILLH,CTAINH,PRIZRH,STGENH,ACCUMH,
            VSSLH
```

PIPEH	Hollerith representation of word "PIPE."
PUMPH	Hollerith representation of word "PUMP."
TEEH	Hollerith representation of word "TEE."
VALVEH	Hollerith representation of word "VALVE."
BREAKH	Hollerith representation of word "BREAK."
FILLH	Hollerith representation of word "FILL."
CTAINH	Hollerith representation of word "CTAIN."
PRIZRH	Hollerith representation of word "PRIZER."
STGENH	Hollerith representation of word "STGEN."
ACCUMH	Hollerith representation of word "ACCUM."
VSSLH	Hollerith representation of word "VESSEL."

COMMON/ISTAT/NSTEP,OITNO,IITNO,VERR,VARERM,IIBIG,IIFAIL

NSTEP	Number of time steps taken.
OITNO	Outer iteration number.
IITNO	Inner iteration number.
VERR	Velocity error at component junction.
VARERM	Maximum variable error.
IIBIG	Maximum number of inner iterations per outer iteration.
IIFAIL	Flag to indicate failure of hydrodynamics to converge.

COMMON/JUNCT/JPTR

JPTR	Number of junction-component pairs.

COMMON/LCMSP/ALCM(150000)

ALCM(150000)	Dynamic LCM storage area.

COMMON/PTRS/LTITLE,LORDER,LILCMP,LNBR,LCOMPT,LIITNO,LIITOT,LJUN,LJSEQ,LVSI,
LBD,LTRIP

LTITLE	Location of title information in A array.
LORDER	Location of iteration order array in A array.
LILCMP	Location (in A array) of component LCM pointer array according to order components were read in.
LNBR	Location of component number array in A array.
LCOMPT	Location (in A array) of component LCM pointer array according to order of iteration.
LIITNO	Location (in A array) of array containing the inner iteration number by component at a given outer iteration.
LIITOT	Location (in A array) of array containing the total number of inner iterations by component at a given time step.

LJUN	Location in A array of junction array.
LJSEQ	Location in A array of junction sequence array.
LVSI	Location in A array of velocity sign indicators by junction.
LBD	Location in A array of boundary data array.
LTRIP	Location in A array of trip data array.

```
COMMON/PWRS/NLOOP,LENLDP,LENLPP,LENSLP,LLOOP,LVJN,NITPWR,QV,QVS,FLOW,FLOWS,W,
            W1,W2,TVIS,AREA,PH1,PH2,PVO,TVI,MTD,RHOP1,RHOP2,RS,RP1,RP2,RV1,
            RV2,DHS,USG,ISGK,DHP1,DHP2,DHV1,DHV2
```

NLOOP	Number of primary coolant loops.
LENLDP	Length of overall loop data area prologue.
LENLPP	Length of loop prologue.
LENSLP	Length of subloop prologue.
LLOOP	Pointer to beginning of loop data area.
LVJN	Pointer to vessel junction data area within loop data area.
NITPWR	Parameter iteration counter for PWR initialization.
QV	Total energy entering fluid through the vessel.
QVS	Desired total energy entering fluid through the vessel.
FLOW	Total mass flow rate through vessel.
FLOWS	Desired total mass flow rate through vessel.
W	Mass flow rate through loop hot leg.
W1	Mass flow rate through first loop pump.
W2	Mass flow rate through second loop pump.
TVIS	Desired temperature at vessel inlet.
AREA	Steam generator heat transfer area.
PH1	Head for first loop pump.
PH2	Head for second loop pump.
PVO	Pressure at vessel hot-leg junction.
TVI	Current temperature at VESSEL inlet.
MTD	Steam generator mean temperature difference.
RHOP1	Fluid density at first loop pump source cell.
RHOP2	Fluid density at second loop pump source cell.
RS	Flow resistance of steam generator.

RP1	Flow resistance of first loop pump.
RP2	Flow resistance of second loop pump.
RV1	Flow resistance of vessel as seen by first loop pump.
RV2	Flow resistance of vessel as seen by second loop pump.
DHS	Specific enthalpy differential for steam generator.
USG	Overall heat transfer coefficient for steam generator.
ISGK	Steam generator kind flag.
DHP1	Specific enthalpy differential for first loop pump.
DHP2	Specific enthalpy differential for second loop pump.
DHV1	Specific enthalpy differential for vessel as seen by first loop pump.
DHV2	Specific enthalpy differential for vessel as seen by second loop pump.

COMMON/RESTART/ICTRLR(13),DDATE,DDTIME,DNCOMP,DLNFLT,

ICTRLR(13)	Array which contains buffering information about the restart file.
DDATE	Date restart file was created.
DDTIME	Time restart file was created.
DNCOMP	Number of components in the restart file.
DLNFLT	Length of fixed length tables read from restart file.

COMMON/SCM3D/A3D(15000)*

A3D(15000)	Dynamic storage area for vessel, rod, and level data.

*In some overlays this COMMON block has only 10 000 words.

COMMON/SSCON/FMAX(7),LOK(7,2),RTWFP

FMAX(7)	Maximum normalized errors.
LOK(7,2)	Location of maximum normalized errors.
RTWFP	Ratio of heat transfer to fluid dynamics time step sizes.

COMMON/TF3DC/KU,KL,ORG,IZ

KU	Displacement of level IZ+1 from level IZ in A3D array.
KL	Displacement of level IZ-1 from level IZ in A3D array.
ORG	Origin of level IZ data A3D array.
IZ	Vessel level number currently being used.

COMMON/TIMER/CPUO,ADATE,ATIME,CPTIME

CPUO	CPU time used at time zero.
ADATE	Problem start date.
ATIME	Problem start time.
CPTIME	CPU time used by calculation.

COMMON/UNITS/IN,IOUT,ITTY,IGOUT,IDOUT,IRSTRT

IN	I/O unit number for input data file.
IOUT	I/O unit number for output data file.
ITTY	I/O unit number for terminal output.
IGOUT	I/O unit number for graphics output file.
IDOUT	I/O unit number for dump output file.
IRSTRT	I/O unit number for restart input file.

APPENDIX G

COMPONENT DATA TABLES

I. FIXED LENGTH TABLES

The structure of the fixed length data tables is shown below and is identical for all the components in TRAC. Refer to Chap. VI for a detailed discussion of the TRAC data base.

Position	Parameter	Description
1	NUM	Component number.
2	TYPE	Component type.
3	ID	Component ID.
4	NCELLT	Total number of cells.
5	LENVLT	Length of variable length table.
6	LENPTR	Length of pointer table.
7	LENARR	Length of array block.
8	LFV	Relative position of old fundamental variables.
9	LFVN	Relative position of new fundamental variables.
10	LENFV	Length of fundamental variables.
11	LTDVO	Relative position of time-dependent variables in variable length table (old time).
12	LTDVN	Relative position of time-dependent variables in variable length table (new time).
13	LENTDV	Number of time-dependent variables in the variable length table.
14	IREST	Component restart indicator.

II. ACCUMULATOR MODULE

A. ACCUM Variable Length Table

Position	Parameter	Description
1	NCELLS	Number of fluid cells.
2	JUN2	Junction number at accumulator discharge (high-numbered end).
3	QINT	Initial water volume in accumulator.
4	QOUT	Volume of liquid that has discharged from the accumulator.
5	TYPE2	Adjacent component type (PIPE or TEE).
6	ICJ	Adjacent component COMPTR number.
7	IUV1	Indicator for velocity update at Junction 1 (=0).
8	IUV2	Indicator for velocity update at Junction 2.
9	JS2	Junction sequence number at accumulator discharge.
10	Z	Water height above discharge.
11	FLOW	Volume flow rate at discharge.
12	ISTOP	Indicator that accumulator has emptied (=1).

B. ACCUM Pointer Table

Word	Name	Array	Dimension	Description
1	LDX	DX	NCELLS	Delta x.
2	LVOL	VOL	NCELLS	Cell volumes.
3	LFA	FA	NCELLS+1	Cell edge flow areas.
4	LFRIC	FRIC	NCELLS+1	Additive friction factors.
5	LGRAV	GRAV	NCELLS+1	Gravitation terms (cosine theta).
6	LHD	HD	NCELLS+1	Hydraulic diameters.
7	LNFF	NFF	NCELLS+1	Friction correlation options.

Word	Name	Array	Dimension	Description
8	LWA	WA	NCELLS	Wall areas.
9	LBD1	BD1	40	Dummy BD1 array.
10	LRHS	RHS	3*NCELLS	Right-hand side for vapor continuity and energy equations.
11	LVISL	VISL	NCELLS	Viscosity of liquid.
12	LVISV	VISV	NCELLS	Viscosity of vapor.
13	LHIL	HIL	NCELLS	Heat transfer coefficient between inside wall and liquid (not used).
14	LHIV	HIV	NCELLS	Heat transfer coefficient between inside wall and vapor (not used).
15	LHLV	HLV	NCELLS	Interfacial heat transfer coefficient.
16	LALV	ALV	NCELLS	Interfacial surface area.
17	LSIG	SIG	NCELLS	Surface tension.
18	LQPPL	QPPL	NCELLS	Heat flux from wall to liquid (not used).
19	LROM	ROM	NCELLS	Mixture density.
20	LARV	ARV	NCELLS	ALP*ROV.
21	LRMEM	RMEM	NCELLS	Mixture internal energy.
22	LRMVM	RMVM	NCELLS+1	ROM*VM.
23	LCFZ	CFZ	NCELLS+1	Friction coefficients.
24	LDRIV	DRIV	NCELLS*15	Storage array for thermodynamic derivatives and enthalpies.
25	LTSAT	TSAT	NCELLS	Saturation temperatures.
26	LVR	VR	NCELLS+1	Old relative velocities.
27	LVL	VL	NCELLS+1	Old liquid velocities.
28	LVV	VV	NCELLS+1	Old vapor velocities.
29	LALP	ALP	NCELLS	Old vapor fractions.

Word	Name	Array	Dimension	Description
30	LROV	ROV	NCELLS	Old vapor densities.
31	LROL	ROL	NCELLS	Old liquid densities.
32	LVM	VM	NCELLS+1	Old mixture velocities.
33	LEV	EV	NCELLS	Old vapor internal energy.
34	LEL	EL	NCELLS	Old liquid internal energy.
35	LTV	TV	NCELLS	Old vapor temperatures.
36	LTL	TL	NCELLS	Old liquid temperatures.
37	LP	P	NCELLS	Old pressures.
38	LALPN	ALPN	NCELLS	New vapor fractions.
39	LROVN	ROVN	NCELLS	New vapor densities.
40	LROLN	ROLN	NCELLS	New liquid densities.
41	LVMN	VMN	NCELLS+1	New mixture velocities.
42	LEVN	EVN	NCELLS	New vapor internal energies.
43	LELN	ELN	NCELLS	New liquid internal energies.
44	LTVN	TVN	NCELLS	New vapor temperatures.
45	LTLN	TLN	NCELLS	New liquid temperatures.
46	LPN	PN	NCELLS	New pressures.
47	LALPD	ALPD	0	Droplet volume fraction.[a]
48	LROVA	ROVA	0	Old air density.[a]
49	LEVA	EVA	0	Old air internal energy.[a]
50	LVRD	VRD	0	Droplet drift velocity.[a]
51	LALPND	ALPND	0	New droplet volume fraction.[a]
52	LROVAN	ROVAN	0	New air density.[a]

[a]Not presently implemented.

Word	Name	Array	Dimension	Description
53	LEVAN	EVAN		New air internal energy.[a]
54	LTSSN	TSSN		New vapor saturation temperature.[a]
55	LB	B	NCELLS*30	Temporary storage for 1-D implicit block tridiagonal matrix solution.[a]

III. BREAK MODULE VARIABLE LENGTH TABLE

Position	Parameter	Description
1	JUN1	Junction at which break is located.
2	DXIN	Delta x outside break.
3	VOLIN	Volume outside break.
4	ALPIN	Void fraction outside break.
5	TIN	Temperature outside break.
6	PIN	Pressure outside break.
7	DX	Delta x outside break.
8	VOL	Volume outside break.
9	ROM	Mixture density.
10	ARV	ALP*ROV.
11	RMEM	Mixture internal energy.
12	RMVM	ROM*VM.
13	ALP	Void fraction outside break.
14	ROV	Old vapor density.

---

[a]Not presently implemented.

Position	Parameter	Description
15	ROL	Old liquid density.
16	VM2	Old mixture velocity.
17	VR2	Old relative velocity.
18	EV	Old vapor internal energy.
19	EL	Old liquid internal energy.
20	P	Old pressure.
21	ALPN	New vapor fraction.
22	ROVN	New vapor density.
23	ROLN	New liquid density.
24	VMN2	New mixture velocity one cell from boundary.
25	VRN2	New relative velocity one cell from boundary.
26	EVN	New vapor internal energy.
27	ELN	New liquid internal energy.
28	PN	New pressure.
29	VMN1	New mixture velocity at the boundary.
30	VRN1	New relative velocity at the boundary.
31	SIG	Surface tension.
32	VVN1	Vapor velocity at the boundary.
33	VLN1	Liquid velocity at the boundary.
34	VVN2	Vapor velocity one cell from the boundary.
35	VLN2	Liquid velocity one cell from the boundary.
36	VISV	Viscosity of vapor.
37	VISL	Viscosity of liquid.
38	ICJ	Adjacent component COMPTR number.

Position	Parameter	Description
39	TYPE1	Type of component adjacent to break.
40	JS1	Junction sequence number.
41	BXMASS	Current mass flow rate out of break.
42	BSMASS	Time-integrated mass flow rate out of break.

IV. FILL MODULE

A. FILL Variable Length Table

Position	Parameter	Description
1	JUN1	Junction at which fill is located.
2	DXIN	Delta x outside fill.
3	VOLIN	Volume outside fill.
4	ALPIN	Void fraction of entrant material.
5	VIN	Velocity of entrant material.
6	TIN	Temperature outside fill.
7	PIN	Pressure outside fill.
8	DX	Delta x outside fill.
9	VOL	Volume outside fill.
10	ROM	Mixture density.
11	ARV	ALP*ROV.
12	RMEM	Mixture internal energy.
13	RMVM	ROM*VM.
14	ALP	Void fraction outside fill.
15	ROV	Old vapor density.
16	ROL	Old liquid density.

Position	Parameter	Description
17	VM2	Old mixture velocity.
18	VR2	Old relative velocity.
19	EV	Old vapor internal energy.
20	EL	Old liquid internal energy.
21	P	Old pressure.
22	ALPN	New vapor fraction.
23	ROVN	New vapor density.
24	ROLN	New liquid density.
25	VMN2	New mixture velocity one cell from boundary.
26	VRN2	New relative velocity one cell from boundary.
27	EVN	New vapor internal energy.
28	ELN	New liquid internal energy.
29	PN	New pressure.
30	VMN1	New mixture velocity at the boundary.
31	VRN1	New relative velocity at the boundary.
32	SIG	Surface tension.
33	VVN1	Vapor velocity at the boundary.
34	VLN1	Liquid velocity at the boundary.
35	VVN2	Vapor velocity one cell from the boundary.
36	VLN2	Liquid velocity one cell from the boundary.
37	VISV	Viscosity of vapor.
38	VISL	Viscosity of liquid.
39	ICJ	Adjacent component COMPTR number.
40	TYPE1	Type of component adjacent to fill.
41	JS1	Junction sequence number at junction 1.

Position	Parameter	Description
42	FXMASS	Current mass flow rate out of fill.
43	FSMASS	Time-integrated mass flow rate out of fill.
44	IFTY	FILL type.
45	IFTR	FILL trip number.
46	NFTX	Number of FILL table pairs.

B. FILL Pointer Table

Word	Name	Array	Dimension	Description
1	LFTAB	FTAB	NFTX*2	FILL velocity table

V. PIPE MODULE

A. PIPE Variable Length Table

Position	Parameter	Description
1	NCELLS	Number of fluid cells.
2	NODES	Number of heat transfer nodes.
3	JUN1	Junction number of low-numbered pipe end.
4	JUN2	Junction number of high-numbered pipe end.
5	MAT	Material ID.
6	RADIN	Inner radius of pipe wall.
7	TH	Thickness of pipe wall.
8	HOUTL	Heat transfer coefficient between outer boundary of pipe wall and liquid.
9	HOUTV	Heat transfer coefficient between outer boundary of pipe wall and vapor.
10	TOUTL	Liquid temperature outside pipe.
11	TOUTV	Vapor temperature outside pipe.
12	ICJ1	Adjacent component at junction 1.

Position	Parameter	Description
13	ICJ2	Adjacent component at junction 2.
14	TYPE1	Type of adjacent component at junction 1.
15	TYPE2	Type of adjacent component at junction 2.
16	JS1	Junction sequence number at low-numbered pipe end.
17	JS2	Junction sequence number at high-numbered pipe end.
18	ISOLLB	Indication for velocity update at junction 1.
19	ISOLRB	Indication for velocity update at junction 2.
20	ICHF	CHF calculation.
21	IHYDRO	1-D hydrodynamics option.

B. PIPE Pointer Table

Word	Name	Array	Dimension	Description
1	LDX	DX	NCELLS	Delta x.
2	LVOL	VOL	NCELLS	Cell volumes.
3	LFA	FA	NCELLS+1	Cell edge areas.
4	LFRIC	FRIC	NCELLS+1	Additive friction factors.
5	LGRAV	GRAV	NCELLS+1	Gravitation terms (cosine theta).
6	LHD	HD	NCELLS+1	Hydraulic diameters.
7	LNFF	NFF	NCELLS+1	Friction correlation options.
8	LWA	WA	NCELLS	Wall areas.
9	LMATID	MATID	NODES-1	Material IDs.
10	LRHS	RHS	3*(NCELLS)	Right-hand side for vapor continuity and energy equations.
11	LCPL	CPL	NCELLS	C sub P liquid.
12	LCPV	CPV	NCELLS	C sub P vapor.
13	LCL	CL	NCELLS	Conductivity of liquid.

Word	Name	Array	Dimension	Description
14	LCV	CV	NCELLS	Conductivity of vapor.
15	LVISL	VISL	NCELLS	Viscosity of liquid.
16	LVISV	VISV	NCELLS	Viscosity of vapor.
17	LHFG	HFG	NCELLS	Latent heat of vaporization.
18	LEMIS	EMIS	NCELLS	Emissivity of pipe wall.
19	LRN	RN	NODES	Radii at nodes.
20	LRN2	RN2	NODES-1	Radii at cell centers.
21	LDR	DR	NODES-1	Delta r.
22	LIDR	IDR	NCELLS	Heat transfer regime.
23	LHIL	HIL	NCELLS	Heat transfer coefficient between inside wall and liquid.
24	LHIV	HIV	NCELLS	Heat transfer coefficient between inside wall and vapor.
25	LHLV	HLV	NCELLS	Interfacial heat transfer coefficient.
26	LALV	ALV	NCELLS	Interfacial surface area.
27	LHOL	HOL	NCELLS	Heat transfer coefficient between outside wall and liquid.
28	LHOV	HOV	NCELLS	Heat transfer coefficient between outside wall and vapor.
29	LTOL	TOL	NCELLS	Liquid temperature outside pipe.
30	LTOV	TOV	NCELLS	Vapor temperature outside pipe.
31	LSIG	SIG	NCELLS	Surface tension.
32	LROW	ROW	(NODES-1)*NCELLS	Density of wall.
33	LCPW	CPW	(NODES-1)*NCELLS	Specific heat of wall.
34	LCW	CW	(NODES-1)*NCELLS	Conductivity of wall.
35	LQPPC	QPPC	NCELLS	Critical heat flux.
36	LQPPP	QPPP	NCELLS	Wall heat source.

Word	Name	Array	Dimension	Description
37	LROM	ROM	NCELLS	Mixture density.
38	LARV	ARV	NCELLS	ALP*ROV.
39	LRMEM	RMEM	NCELLS	Mixture internal energy.
40	LRMVM	RMVM	NCELLS+1	ROM*VM.
41	LCFZ	CFZ	NCELLS+1	Total friction factor.
42	LDRIV	DRIV	NCELLS*15	Storage array for thermodynamic derivatives and enthalpies.
43	LTSAT	TSAT	NCELLS	Saturation temperatures.
44	LVR	VR	NCELLS+1	Relative velocities.
45	LVL	VL	NCELLS+1	Liquid velocities.
46	LVV	VV	NCELLS+1	Vapor velocities.
47	LTW	TW	NCELLS*NODES	Old wall temperatures.
48	LALP	ALP	NCELLS	Old vapor fractions.
49	LROV	ROV	NCELLS	Old vapor densities.
50	LROL	ROL	NCELLS	Old liquid densities.
51	LVM	VM	NCELLS+1	Old mixture velocities.
52	LEV	EV	NCELLS	Old vapor internal energy.
53	LEL	EL	NCELLS	Old liquid internal energy.
54	LTV	TV	NCELLS	Old vapor temperature.
55	LTL	TL	NCELLS	Old liquid temperature.
56	LP	P	NCELLS	Old pressure.
57	LTWN	TWN	NCELLS*NODES	New wall temperatures.
58	LALPN	ALPN	NCELLS	New vapor fraction.
59	LROVN	ROVN	NCELLS	New vapor density.
60	LROLN	ROLN	NCELLS	New liquid density.

Word	Name	Array	Dimension	Description
61	LVMN	VMN	NCELLS+1	New mixture velocity.
62	LEVN	EVN	NCELLS	New vapor internal energy.
63	LELN	ELN	NCELLS	New liquid internal energy.
64	LTVN	TVN	NCELLS	New vapor temperature.
65	LTLN	TLN	NCELLS	New liquid temperature.
66	LPN	PN	NCELLS	New pressure.
67	LALPD	ALPD	0	Droplet volume fraction.[a]
68	LROVA	ROVA	0	Old air density.[a]
69	LEVA	EVA	0	Old air internal energy.[a]
70	LVRD	VRD	0	Droplet drift velocity.[a]
71	LALPND	ALPND	0	New droplet volume fraction.[a]
72	LROVAN	ROVAN	0	New air density.[a]
73	LEVAN	EVAN	0	New air internal energy.[a]
74	LTSSN	TSSN	0	New vapor saturation temperature.[a]
75	LB	B	NCELLS*30	Temporary storage of 1-D implicit block tridiagonal matrix solution.[a]

VI. PRESSURIZER MODULE

A. PRIZER Variable Length Table

Position	Parameter	Description
1	NCELLS	Number of fluid cells.

---

[a]Not presently implemented.

Position	Parameter	Description
2	JUN2	Junction number at pressurizer discharge (high-numbered end).
3	QHEAT	Total heater power.
4	PSET	Pressurizer pressure set point for heater-spray control.
5	DPMAX	Differential pressure at which heaters have maximum power.
6	QINT	Initial water volume in accumulator.
7	ZHTR	Water height for heater cut off.
8	QOUT	Volume of liquid that has discharged from the pressurizer.
9	TYPE2	Adjacent component type.
10	ICJ	Adjacent component COMPTR number.
11	IUV1	Indicator for velocity update at Junction 1 (=0).
12	IUV2	Indicator for velocity update at Junction 2.
13	JS2	Junction sequence number at pressurizer discharge.
14	Z	Water height above discharge.
15	QIN	Heater power being input to water.
16	FLOW	Volume flow rate at discharge.
17	BXMASS	Current mass flow rate during steady state.
18	BSMASS	Time-integrated mass flow rate out of pressurizer.

B. PRIZER Pointer Table

Word	Name	Array	Dimension	Description
1	LDX	DX	NCELLS	Delta x.

Word	Name	Array	Dimension	Description
2	LVOL	VOL	NCELLS	Cell volumes.
3	LFA	FA	NCELLS+1	Cell edge flow areas.
4	LFRIC	FRIC	NCELLS+1	Additive friction factors.
5	LGRAV	GRAV	NCELLS+1	Gravitation terms (cosine theta).
6	LHD	HD	NCELLS+1	Hydraulic diameters.
7	LNFF	NFF	NCELLS+1	Friction correlation options.
8	LWA	WA	NCELLS	Wall areas.
9	LBD1	BD1	40	Dummy BD1 array.
10	LRHS	RHS	3*NCELLS	Right-hand side for vapor continuity and energy equations.
11	LVISL	VISL	NCELLS	Viscosity of liquid.
12	LVISV	VISV	NCELLS	Viscosity of vapor.
13	LHIL	HIL	NCELLS	Heat transfer coefficient between inside wall and liquid.
14	LHIV	HIV	NCELLS	Heat transfer coefficient between inside wall and vapor.
15	LHLV	HLV	NCELLS	Interfacial heat transfer coefficient.
16	LALV	ALV	NCELLS	Interfacial surface area.
17	LSIG	SIG	NCELLS	Surface tension.
18	LQPPL	QPPL	NCELLS	Heat flux from wall to liquid.
19	LROM	ROM	NCELLS	Mixture density.
20	LARV	ARV	NCELLS	ALP*ROV.
21	LRMEM	RMEM	NCELLS	Mixture internal energy.
22	LRMVM	RMVM	NCELLS+1	ROM*VM.
23	LCFZ	CFZ	NCELLS+1	Total friction factors.
24	LDRIV	DRIV	NCELLS*15	Storage array for thermodynamic derivatives and enthalpies.

Word	Name	Array	Dimension	Description
25	LTSAT	TSAT	NCELLS	Saturation temperatures.
26	LVR	VR	NCELLS+1	Relative velocities.
27	LVL	VL	NCELLS+1	Liquid velocities.
28	LVV	VV	NCELLS+1	Vapor velocities.
29	LALP	ALP	NCELLS	Vapor fractions.
30	LROV	ROV	NCELLS	Old vapor densities.
31	LROL	ROL	NCELLS	Old liquid densities.
32	LVM	VM	NCELLS+1	Old mixture velocities.
33	LEV	EV	NCELLS	Old vapor internal energy.
34	LEL	EL	NCELLS	Old liquid internal energy.
35	LTV	TV	NCELLS	Old vapor temperatures.
36	LTL	TL	NCELLS	Old liquid temperatures.
37	LP	P	NCELLS	Old pressures.
38	LALPN	ALPN	NCELLS	New vapor fractions.
39	LROVN	ROVN	NCELLS	New vapor densities.
40	LROLN	ROLN	NCELLS	New liquid densities.
41	LVMN	VMN	NCELLS+1	New mixture velocities.
42	LEVN	EVN	NCELLS	New vapor internal energies.
43	LELN	ELN	NCELLS	New liquid internal energies.
44	LTVN	TVN	NCELLS	New vapor temperatures.
45	LTLN	TLN	NCELLS	New liquid temperatures.
46	LPN	PN	NCELLS	New pressures.
47	LALPD	ALPD	0	Droplet volume fraction.[a]
48	LROVA	ROVA	0	Old air density.[a]
49	LEVA	EVA	0	Old air internal energy.[a]

Word	Name	Array	Dimension	Description
50	LVRD	VRD	0	Droplet drift velocity.[a]
51	LALPND	ALPND	0	New droplet volume fraction.[a]
52	LROVAN	ROVAN	0	New air density.[a]
53	LEVAN	EVAN	0	New air internal energy.[a]
54	LTSSN	TSSN	0	New vapor saturation temperature.[a]
55	LB	B	NCELLS*30	Temporary storage for 1-D implicit block tridiagonal matrix solution.[a]

VII. PUMP MODULE

A. PUMP Variable Length Table

Position	Parameter	Description
1	NCELLS	Number of fluid cells.
2	JUN1	Junction number of low-numbered end of pump.
3	JUN2	Junction number of high-numbered end of pump.
4	IPMPTY	Pump type (1 or 2).
5	IRP	Reverse speed indicator (1=Reverse allowed; 0=Reverse not allowed).
6	IPM	Two-phase indicator (1=Use two-phase curves; 0=Use single-phase curves).
7	RHEAD	Rated head.
8	RTORK	Rated torque.
9	RFLOW	Rated flow.
10	RRHO	Rated density.
11	EFFMI	Moment of inertia.

---

[a]Not presently implemented.

Position	Parameter	Description
12	TFR1	Frictional torque constant 1.
13	TFR2	Frictional torque constant 2.
14	ROMEGA	Rated angular velocity.
15	INDXHM	Index on head degradation multiplier curve.
16	INDXTM	Index on torque degradation multiplier curve.
17	NHDM	Number of points on the head degradation multiplier curve.
18	NTDM	Number of points on the torque degradation multiplier curve.
19	ICJ1	Adjacent component at junction 1.
20	ICJ2	Adjacent component at junction 2.
21	TYPE1	Type of adjacent component at junction 1.
22	TYPE 2	Type of adjacent component at junction 2.
23	ISOL1	Indication for velocity update at junction 1.
24	ISOL2	Indication for velocity update at junction 2.
25	OMEGA	Angular velocity at old time.
26	OMEGAN	Angular velocity at new time.
27	RHO	Pump mixture density.
28	FLOW	Pump volumetric flow rate.
29	ALPHA	Pump void fraction.
30	HEAD	Pump head.
31	TORQUE	Pump torque.
32	SMOM	Momentum source.
33	DELP	Delta - P across pump.
34	NODES	No. of radial heat transfer nodes.
35	MAT	Material I.D. of wall.

Position	Parameter	Description
36	RADIN	Inner radius of wall.
37	TH	Wall thickness.
38	HOUTL	Heat transfer coefficient between outer boundary of pipe wall and liquid.
39	HOUTV	Heat transfer coefficient between outer boundary of pipe wall and vapor.
40	TOUTL	Liquid temperature outside wall.
41	TOUTV	Vapor temperature outside wall.
42	JS1	Junction sequence number at low-numbered pipe end.
43	JS2	Junction sequence number at high-numbered pipe end.
44	ICHF	CHF calculation indicator.
45	IHYDRO	1-D hydrodynamics option.
46	NDMAX	Size of scratch storage array.
47	MFLOW	Pump mass flow rate.
48	IPMPTR	Pump trip I.D.
49	NPMPTX	Number of pump speed table entries.
50	ISAVE	Index in pump speed table.
51	ICOND	Trip condition.

B. PUMP Pointer Table

Word	Name	Array	Dimension	Description
1	LDX	DX	NCELLS	Delta x.
2	LVOL	VOL	NCELLS	Cell volumes.
3	LFA	FA	NCELLS+1	Cell edge flow areas.
4	LFRIC	FRIC	NCELLS+1	Additive friction factors.
5	LGRAV	GRAV	NCELLS+1	Gravitation terms (cosine theta).

Word	Name	Array	Dimension	Description
6	LHD	HD	NCELLS+1	Hydraulic diameters.
7	LNFF	NFF	NCELLS+1	Friction correlation options.
8	LWA	WA	NCELLS	Wall areas.
9	LMATID	MATID	NODES-1	Material IDs.
10	LRHS	RHS	3(NCELLS)	Right-hand side for vapor continuity and energy equations.
11	LCPL	CPL	NCELLS	C sub P liquid.
12	LCPV	CPV	NCELLS	C sub P vapor.
13	LCL	CL	NCELLS	Conductivity of liquid.
14	LCV	CV	NCELLS	Conductivity of vapor.
15	LVISL	VISL	NCELLS	Viscosity of liquid.
16	LVISV	VISV	NCELLS	Viscosity of vapor.
17	LHFG	HFG	NCELLS	Latent heat of vaporization.
18	LEMIS	EMIS	NCELLS	Emissivity of wall.
19	LRN	RN	NODES	Radii at nodes.
20	LRN2	RN2	NODES-1	Radii at cell centers.
21	LDR	DR	NODES-1	Delta r.
22	LIDR	IDR	NCELLS	Heat transfer regime.
23	LHIL	HIL	NCELLS	Heat transfer coefficient between inside wall and liquid.
24	LHIV	HIV	NCELLS	Heat transfer coefficient between inside wall and vapor.
25	LHLV	HLV	NCELLS	Interfacial heat transfer coefficient.
26	LALV	ALV	NCELLS	Interfacial surface area.
27	LHOL	HOL	NCELLS	Heat transfer coefficient between outside wall and liquid.

Word	Name	Array	Dimension	Description
28	LHOV	HOV	NCELLS	Heat transfer coefficient between outside wall and vapor.
29	LTOL	TOL	NCELLS	Liquid temperature outside pump.
30	LTOV	TOV	NCELLS	Vapor temperature outside pump.
31	LSIG	SIG	NCELLS	Surface tension.
32	LROW	ROW	(NODES-1)*NCELLS	Density of wall.
33	LCPW	CPW	(NODES-1)*NCELLS	Specific heat of wall.
34	LCW	CW	(NODES-1)*NCELLS	Conductivity of wall.
35	LQPPC	QPPC	NCELLS	Critical heat flux.
36	LQPPP	QPPP	NCELLS	Wall heat source.
37	LROM	ROM	NCELLS	Mixture density.
38	LARV	ARV	NCELLS	ALP*ROV.
39	LRMEM	RMEM	NCELLS	Mixture internal energy.
40	LRMVM	RMVM	NCELLS+1	ROM*VM.
41	LCFZ	CFZ	NCELLS+1	Total friction factor.
42	LDRIV	DRIV	NCELLS*15	Storage array for thermodynamic derivatives and enthalpies.
43	LTSAT	TSAT	NCELLS	Saturation temperature.
44	LVR	VR	NCELLS+1	Relative velocity.
45	LVL	VL	NCELLS+1	Liquid velocity.
46	LVV	VV	NCELLS+1	Vapor velocity.
47	LTW	TW	NCELLS*NODES	Old wall temperatures.
48	LALP	ALP	NCELLS	Old vapor fraction.
49	LROV	ROV	NCELLS	Old vapor density.
50	LROL	ROL	NCELLS	Old liquid density.
51	LVM	VM	NCELLS+1	Old mixture velocity.

Word	Name	Array	Dimension	Description
52	LEV	EV	NCELLS	Old vapor internal energy.
53	LEL	EL	NCELLS	Old liquid internal energy.
54	LTV	TV	NCELLS	Old vapor temperature.
55	LTL	TL	NCELLS	Old liquid temperature.
56	LP	P	NCELLS	Old pressure.
57	LTWN	TWN	NCELLS*NODES	New wall temperatures.
58	LALPN	ALPN	NCELLS	New vapor fraction.
59	LROVN	ROVN	NCELLS	New vapor density.
60	LROLN	ROLN	NCELLS	New liquid density.
61	LVMN	VMN	NCELLS+1	New mixture velocity.
62	LEVN	EVN	NCELLS	New vapor internal energy.
63	LELN	ELN	NCELLS	New liquid internal energy.
64	LTVN	TVN	NCELLS	New vapor temperature.
65	LTLN	TLN	NCELLS	New liquid temperature.
66	LPN	PN	NCELLS	New pressure.
67	LALPD	ALPD	0	Droplet volume fraction.[a]
68	LROVA	ROVA	0	Old air density.[a]
69	LEVA	EVA	0	Old air internal energy.[a]
70	LVRD	VRD	0	Droplet drift velocity.[a]
71	LALPND	ALPND	0	New droplet volume fraction.[a]
72	LROVAN	ROVAN	0	New air density.[a]
73	LEVAN	EVAN	0	New air internal energy.[a]
74	LTSSN	TSSN	0	New vapor saturation temperature.[a]

[a]Not presently implemented.

Word	Name	Array	Dimension	Description
75	LB	B	NCELLS*30	Temporary storage for 1-D implicit block tridiagonal matrix solution.
76	LSPTBL	SPTBL	NPMTX*2	Pump speed table.
77	LNDATA	NDATA	16	Number of sets of points head and torque curves.
78	LHSP1	HSP1	2*NDATA(1)	Single-phase head curve 1.
79	LHSP2	HSP2	2*NDATA(2)	Single-phase head curve 2.
80	LHSP3	HSP3	2*NDATA(3)	Single-phase head curve 3.
81	LHSP4	HSP4	2*NDATA(4)	Single-phase head curve 4.
82	LHTP1	HTP1	2*NDATA(5)	Two-phase head curve 1.
83	LHTP2	HTP2	2*NDATA(6)	Two-phase head curve 2.
84	LHTP3	HTP3	2*NDATA(7)	Two-phase head curve 3.
85	LHTP4	HTP4	2*NDATA(8)	Two-phase head curve 4.
86	LTSP1	TSP1	2*NDATA(9)	Single-phase torque curve 1.
87	LTSP2	TSP2	2*NDATA(10)	Single-phase torque curve 2.
88	LTSP3	TSP3	2*NDATA(11)	Single-phase torque curve 3.
89	LTSP4	TSP4	2*NDATA(12)	Single-phase torque curve 4.
90	LTTP1	TTP1	2*NDATA(13)	Two-phase torque curve 1.
91	LTTP2	TTP2	2*NDATA(14)	Two-phase torque curve 2.
92	LTTP3	TTP3	2*NDATA(15)	Two-phase torque curve 3.
93	LTTP4	TTP4	2*NDATA(16)	Two-phase torque curve 4.
94	LHDM	HDM	NHDM	Head degradation multiplier curve.
95	LTDM	TDM	NTDM	Torque degradation multiplier curve.
96	LIDXCS	IDXCS	16	Curve set index array.

VIII. STEAM GENERATOR MODULE

A. STGEN Variable Length Table

Position	Parameter	Description
1	NCELL1	No. of fluid cells on tube side (PS).
2	NCELL2	No. of fluid cells on shell side (SS).
3	NODES	No. of wall temperature nodes.
4	JUN11	Junction no. adjacent to cell 1 on tube side.
5	JUN12	Junction no. adjacent to cell NCELL1 on tube side.
6	JUN21	Junction no. adjacent to cell 1 on shell side.
7	JUN22	Junction no. adjacent to cell NCELL2 on shell side.
8	MAT	Material ID for tubes.
9	RADIN	Inner radius of a tube wall.
10	TH	Tube wall thickness.
11	NFF1	Friction factor correlation option for tube side.
12	NFF2	Friction factor correlation option for shell side.
13	ICJ11	Adjacent component at JUN11.
14	ICJ12	Adjacent component at JUN12.
15	ICJ21	Adjacent component at JUN21.
16	ICJ22	Adjacent component at JUN22.
17	TYPE11	Type of adjacent component at JUN11.
18	TYPE12	Type of adjacent component at JUN12.
19	TYPE21	Type of adjacent component at JUN21.
20	TYPE22	Type of adjacent component at JUN22.
21	ISVLB1	Indicator for velocity update at JUN11.

Position	Parameter	Description
22	ISVRB1	Indicator for velocity update at JUN12.
23	ISVLB2	Indicator for velocity update at JUN21.
24	ISVRB2	Indicator for velocity update at JUN22.
25	KIND	STGEN type: 1=u-tube; 2=once through.
26	IITOT1	Total no. of inner iterations during this time step for tube side.
27	IITOT2	Total no. of inner iterations during this time step for shell side.
28	JS11	Junction sequence number at primary side inlet.
29	JS12	Junction sequence number at primary side discharge.
30	JS21	Junction sequence number at secondary side inlet.
31	JS22	Junction sequence number at secondary side discharge.
32	IHYDRO	Type of hydrodynamics on primary side (0=partition implicit; 1=full implicit).

B. STGEN Pointer Table

Word	Name	Array	Dimension	Description
1	LDX1	DX1	NCELL1	Delta x primary side (PS).
2	LVOL1	VOL1	NCELL1	Cell volumes PS.
3	LFA1	FA1	NCELL1+1	Cell edge areas PS.
4	LFRIC1	FRIC1	NCELL1+1	Additive friction factors PS.
5	LGRAV1	GRAV1	NCELL1+1	Gravitation terms (cosine theta).
6	LHD1	HD1	NCELL1+1	Hydraulic diameters PS.
7	LNFF1	NFF1	NCELL1+1	Friction correlation options PS.
8	LWA1	WA1	NCELL1	Wall areas PS.

Word	Name	Array	Dimension	Description
9	LMATID	MATID	NODES-1	Material IDs.
10	LRHS1	RHS1	3*(NCELL1)	Right-hand side for vapor continuity and energy equations PS.
11	LCPL1	CPL1	NCELL1	C sub P liquid PS.
12	LCPV1	CPV1	NCELL1	C sub P vapor PS
13	LDRIV1	DRIV1	NCELLS*15	Storage array for thermodynamic derivatives and enthalpies.
14	LTSAT1	TSAT1	NCELL1	Saturation temperature PS.
15	LCL1	CL1	NCELL1	Conductivity of liquid PS.
16	LCV1	CV1	NCELL1	Conductivity of vapor PS.
17	LVISL1	VISL1	NCELL1	Viscosity of liquid PS.
18	LVISV1	VISV1	NCELL1	Viscosity of vapor PS.
19	LHFG1	HFG1	NCELL1	Latent heat of vaporization PS.
20	LEMIS	EMIS	NCELL1	Emissivity of wall PS.
21	LRN	RN	NODES	Radii at nodes.
22	LRN2	RN2	NODES-1	Radii at cell centers of tube wall.
23	LDR	DR	NODES-1	Delta r of tube.
24	LIDR1	IDR1	NCELL1	Heat transfer regime.
25	LHIL1	HIL1	NCELL1	Heat transfer coefficient between inside wall and liquid PS.
26	LHIV1	HIV1	NCELL1	Heat transfer coefficient between inside wall and vapor PS.
27	LHLV1	HLV1	NCELL1	Interfacial heat transfer coefficient PS.
28	LALV1	ALV1	NCELL1	Interfacial surface area PS.
29	LQPPC1	QPPC1	NCELL1	Critical heat flux PS.
30	LSIG1	SIG1	NCELL1	Surface tension PS.

Word	Name	Array	Dimension	Description
31	LROW	ROW	(NODES-1)*NCELL1	Density of wall.
32	LCPW	CPW	(NODES-1)*NCELL1	Specific heat of wall.
33	LCW	CW	(NODES-1)*NCELL1	Conductivity of wall.
34	LQPPL1	QPPL1	NCELL1	Wall to liquid heat flux PS.
35	LQPPV1	QPPV1	NCELL1	Wall to vapor heat flux PS.
36	LQPPP1	QPPP1	NCELL1	Wall heat source PS.
37	LROM1	ROM1	NCELL1	Mixture density PS.
38	LARV1	ARV1	NCELL1	ALP*ROV PS.
39	LRMEM1	RMEM1	NCELL1	Mixture internal energy PS.
40	LRMVM1	RMVM1	NCELL1+1	ROM*VM PS.
41	LHLEFF	HLEFF	NCELL2	Effective wall to liquid heat transfer coefficient.
42	LHVEFF	HVEFF	NCELL2	Effective wall to vapor heat transfer coefficient.
43	LTWEFF	TWEFF	NODES*(NCELL2)	Effective wall temperatures.
44	LHLO	HLO	NCELL1	Wall to liquid heat transfer coefficient secondary side (SS).
45	LHVO	HVO	NCELL1	Wall to liquid heat transfer coefficient SS.
46	LTLO	TLO	NCELL1	Liquid temperature SS.
47	LTVO	TVO	NCELL1	Vapor temperature SS.
48	LCFZ1	CFZ1	NCELL1+1	Total friction factor PS.
49	LVR1	VR1	NCELL1+1	Relative velocity PS.
50	LVL1	VL1	NCELL1+1	Liquid vapor velocity PS.
51	LVV1	VV1	NCELL1+1	Vapor velocity PS.
52	LDX2	DX2	NCELL2	Delta x SS.
53	LVOL2	VOL2	NCELL2	Cell volumes SS.

Word	Name	Array	Dimension	Description
54	LFA2	FA2	NCELL2+1	Cell edge areas SS.
55	LFRIC2	FRIC2	NCELL2+1	Additive friction factors SS.
56	LGRAV2	GRAV2	NCELL2+1	Gravitation terms (cosine theta) SS.
57	LHD2	HD2	NCELL2+1	Hydraulic diameters SS.
58	LNFF2	NFF2	NCELL2+1	Friction correlation options SS.
59	LWA2	WA2	NCELL2	Wall areas SS.
60	LRHS2	RHS2	3*(NCELL2)	Right-hand side for vapor continuity and energy equations SS.
61	LCPL2	CPL2	NCELL2	C sub P liquid SS.
62	LCPV2	CPV2	NCELL2	C sub P vapor SS.
63	LDRIV2	DRIV2	NCELL2*15	Storage array for thermodynamic derivatives and enthalpies SS.
64	LTSAT2	TSAT2	NCELL2	Saturation temperature SS.
65	LCL2	CL2	NCELL2	Conductivity of liquid SS.
66	LCV2	CV2	NCELL2	Conductivity of vapor SS.
67	LVISL2	VISL2	NCELL2	Viscosity of liquid SS.
68	LVISV2	VISV2	NCELL2	Viscosity of vapor SS.
69	LHFG2	HFG2	NCELL2	Latent heat of vaporization SS.
70	LIDR2	IDR2	NCELL2	Heat transfer regime.
71	LHIL2	HIL2	NCELL2	Heat transfer coefficient between inside wall and liquid SS.
72	LHIV2	HIV2	NCELL2	Heat transfer coefficient between inside wall and vapor SS.
73	LHLV2	HLV2	NCELL2	Interfacial heat transfer coefficient SS.
74	LALV2	ALV2	NCELL2	Interfacial surface area SS.
75	LQPPC2	QPPC2	NCELL2	Critical heat flux SS.
76	LSIG2	SIG2	NCELL2	Surface tension SS.

Word	Name	Array	Dimension	Description
77	LQPPL2	QPPL2	NCELL2	Wall to liquid heat flux SS.
78	LQPPV2	QPPV2	NCELL2	Wall to vapor heat flux SS.
79	LQPPP2	QPPP2	NCELL2	Wall heat source SS.
80	LROM2	ROM2	NCELL2	Mixture density SS.
81	LARV2	ARV2	NCELL2	ALP*ROV SS.
82	LRMEM2	RMEM2	NCELL2	Mixture internal energy SS.
83	LRMVM2	RMVM2	NCELL2+1	ROM*VM SS.
84	LCFZ2	CFZ2	NCELL2+1	Total friction factor SS.
85	LVR2	VR2	NCELL2+1	Relative velocity SS.
86	LVL2	VL2	NCELL2+1	Liquid vapor velocity SS.
87	LVV2	VV2	NCELL2+1	Vapor velocity SS.
88	LTMASS	TMASS	NCELL1	Tube wall mass (not used).
89	LTW	TW	NCELL1*NODES	Old wall temperatures.
90	LALP1	APL1	NCELL1	Old vapor fraction PS.
91	LROV1	ROV1	NCELL1	Old vapor density PS.
92	LROL1	ROL1	NCELL1	Old liquid density PS.
93	LVM1	VM1	NCELL1+1	Old mixture velocity PS.
94	LEV1	EV1	NCELL1	Old vapor internal energy PS.
95	LEL1	EL1	NCELL1	Old liquid internal energy PS.
960	LTV1	TV1	NCELL1	Old vapor temperature PS.
97	LTL1	TL1	NCELL1	Old liquid temperature PS.
98	LP1	P1	NCELL1	Old pressure PS.
99	LALP2	ALP2	NCELL2	Old vapor fraction SS.
100	LROV2	ROV2	NCELL2	Old vapor density SS.
101	LROL2	ROL2	NCELL2	Old liquid density SS.

Word	Name	Array	Dimension	Description
102	LVM2	VM2	NCELL2+1	Old mixture velocity SS.
103	LEV2	EV2	NCELL2	Old vapor internal energy SS.
104	LEL2	EL2	NCELL2	Old liquid internal energy SS.
105	LTV2	TV2	NCELL2	Old vapor temperature SS.
106	LTL2	TL2	NCELL2	Old liquid temperature SS.
107	LP2	P2	NCELL2	Old pressure SS.
108	LTWN	TWN	NCELL1*NODES	New wall temperatures.
109	LALPN1	ALPN1	NCELL1	New vapor fraction PS.
110	LROVN1	ROVN1	NCELL1	New vapor density PS.
111	LROLN1	ROLN1	NCELL1	New liquid density PS.
112	LVMN1	VMN1	NCELL1+1	New mixture velocity PS.
113	LEVN1	EVN1	NCELL1	New vapor internal energy PS.
114	LELN1	ELN1	NCELL1	New liquid internal energy PS.
115	LTVN1	TVN1	NCELL1	New vapor temperature PS.
116	LTLN1	TLN1	NCELL1	New liquid temperature PS.
117	LPN1	PN1	NCELL1	New pressure PS.
118	LALPN2	ALPN2	NCELL2	New vapor fraction SS.
119	LROVN2	ROVN2	NCELL2	New vapor density SS.
120	LROLN2	ROLN2	NCELL2	New liquid density SS.
121	LVMN2	VMN2	NCELL2+1	New mixture velocity SS.
122	LEVN2	EVN2	NCELL2	New vapor internal energy SS.
123	LELN2	ELN2	NCELL2	New liquid internal energy SS.
124	LTVN2	TVN2	NCELL2	New vapor temperature SS.
125	LTLN2	TLN2	NCELL2	New liquid temperature SS.
126	LPN2	PN2	NCELL2	New pressure SS.

Word	Name	Array	Dimension	Description
127	LALPD1	ALPD1	0	Droplet volume fraction PS.[a]
128	LALPD2	ALPD2	0	Droplet volume fraction SS.[a]
129	LROVA1	ROVA1	0	Old air density PS.[a]
130	LROVA2	ROVA2	0	Old air density SS.[a]
131	LEVA1	EVA1	0	Old air internal energy PS.[a]
132	LEVA2	EVA2	0	Old air internal energy SS.[a]
133	LVRD1	VRD1	0	Droplet drift velocity PS.[a]
134	LVRD2	VRD2	0	Droplet drift velocity PS.[a]
135	LALND1	ALND1	0	New droplet volume fraction PS.[a]
136	LALND2	ALND2	0	New droplet volume fraction SS.[a]
137	LRVAN1	RVAN1	0	New air density PS.[a]
138	LRVAN2	RVAN2	0	New air density SS.[a]
139	LEVAN1	EVAN1	0	New air internal energy PS.[a]
140	LEVAN2	EVAN2	0	New air internal energy PS.[a]
141	LTSSN1	TSSN1	0	New vapor saturation temperature PS.[a]
142	LTSSN2	TSSN2	0	New vapor saturation temperature SS.[a]
143	LB	B	NCELLS*30	Temporary storage for 1-D implicit block tridiagonal matrix solution.

[a]Not presently implemented.

IX. TEE MODULE

A. TEE Variable Length Table

Position	Parameter	Description
1	NCELLS	NCELL1 + NCELL2 + 1.
2	NCELL1	Number of fluid cells in the primary tube of the tee.
3	NCELL2	Number of fluid cells in the side tube of the tee.
4	NODES	Number of heat transfer nodes.
5	JCELL	Index of the junction cell within primary tube.
6	JUN1	Junction number of the low-numbered end of the primary tube.
7	JUN2	Junction number of the high-numbered end of the primary cube.
8	JUN3	Junction number of the high-numbered end of the secondary tube.
9	MATID	Material ID for tee.
10	COST	Cosine of the angle from the low-numbered segment.
11	RADIN1	Inner radius of the primary tube.
12	RADIN2	Inner radius of the secondary tube.
13	TH1	Wall thickness of the primary tube.
14	TH2	Wall thickness of the secondary tube.
15	HOUTL1	Heat transfer coefficient to liquid at the outer boundary of the primary tube wall.
16	HOUTV1	Heat transfer coefficient to vapor at the outer boundary of the primary tube wall.
17	HOUTL2	Heat transfer coefficient to liquid at the outer boundary of the secondary tube wall.
	HOUTV2	Heat transfer coefficient to vapor at the outer boundary of the secondary tube wall.

Position	Parameter	Description
19	TOUTL1	Temperature of liquid outside the primary tube wall.
20	TOUTV1	Temperature of vapor outside the secondary tube wall.
21	TOUTL2	Temperature of liquid outside the secondary tube wall.
22	TOUTV2	Temperature of vapor outside the secondary tube wall.
23	ICJ1	Adjacent component to tee at junction 1.
24	ICJ2	Adjacent component to tee at junction 2.
25	ICJ3	Adjacent component to tee at junction 3.
26	TYPE1	Type of adjacent component at junction 1.
27	TYPE2	Type of adjacent component at junction 2.
28	TYPE3	Type of adjacent component at junction 3.
29	JS1	Junction sequence number at junction 1.
30	JS2	Junction sequence number at junction 2.
31	JS3	Junction sequence number at junction 3.
32	ISOL1	Indication for velocity update at junction 1.
33	ISOL2	Indication for velocity update at junction 2.
34	ISOL3	Indication for velocity update at junction 3.
35	ICHF	CHF calculation (0=no; 1=yes).
36	IHYDRO	Not used.

B. TEE Pointer Table

Word	Name	Array	Dimension	Description
1	LDX	DX	NCELLS	Delta x.
2	LVOL	VOL	NCELLS	Cell volumes.

Word	Name	Array	Dimension	Description
3	LFA	FA	NCELLS+1	Cell edge flow areas.
4	LFRIC	FRIC	NCELLS+1	Additive friction factors.
5	LGRAV	GRAV	NCELLS+1	Gravitation terms (cosine theta).
6	LHD	HD	NCELLS+1	Hydraulic diameters.
7	LNFF	NFF	NCELLS+1	Friction correlation options.
8	LWA	WA	NCELLS	Wall areas.
9	LMATID	MATID	2*NODES	Material IDs.
10	LRHS	RHS	3*NCELLS	Right-hand side for continuity and energy equations.
11	LCPL	CPL	NCELLS	C sub P liquid.
12	LCPV	CPV	NCELLS	C sub P vapor.
13	LCL	CL	NCELLS	Conductivity of liquid.
14	LCV	CV	NCELLS	Conductivity of vapor.
15	LVISL	VISL	NCELLS	Viscosity of liquid.
16	LVISV	VISV	NCELLS	Viscosity of vapor.
17	LHFG	HFG	NCELLS	Latent heat of vaporization.
18	LEMIS	EMIS	NCELLS	Emissivity of wall.
19	LRN	RN	2*(NODES)	Radii at nodes.
20	LRN2	RN2	2*(NODES-1)	Radii at cell centers.
21	LDR	DR	2*(NODES-1)	Delta r.
22	LIDR	IDR	NCELLS	Heat transfer regime.
23	LHIL	HIL	NCELLS	Heat transfer coefficient between inside wall and liquid.
24	LHIV	HIV	NCELLS	Heat transfer coefficient between inside wall and vapor.

*NCELLS=NCELL1+NCELL2+1.

Word	Name	Array	Dimension	Description
25	LHLV	HLV	NCELLS	Interfacial heat transfer coefficient.
26	LALV	ALV	NCELLS	Interfacial surface area.
27	LHOL	HOL	NCELLS	Heat transfer coefficient between outside wall and liquid.
28	LHOV	HOV	NCELLS	Heat transfer coefficient between outside wall and vapor.
29	LTOL	TOL	NCELLS	Liquid temperature outside pump.
30	LTOV	TOV	NCELLS	Vapor temperature outside pump.
31	LSIG	SIG	NCELLS	Surface tension.
32	LROW	ROW	(NODES-1)*NCELLS	Density of wall.
33	LCPW	CPW	(NODES-1)*NCELLS	Specific heat of wall.
34	LCW	CW	(NODES-1)*NCELLS	Conductivity of wall.
35	LQPPC	QPPC	NCELLS	Critical heat flux.
36	LQPPP	QPPP	NCELLS	Wall heat source.
37	LROM	ROM	NCELLS	Mixture density.
38	LARV	ARV	NCELLS	ALP*ROV.
39	LRMEM	RMEM	NCELLS	Mixture internal energy.
40	LRMVM	RMVM	NCELLS+1	ROM*VM.
41	LCFZ	CFZ	NCELLS+1	Total friction factor.
42	LDRIV	DRIV	NCELLS*15	Storage array for thermodynamic derivatives and enthalpies.
43	LTSAT	TSAT	NCELLS	Saturation temperature.
44	LVR	VR	NCELLS+1	Relative velocity.
45	LVL	VL	NCELLS+1	Liquid vapor velocity.
46	LVV	VV	NCELLS+1	Vapor velocity.
47	LBD4	BD4	50	Dummy BD4 array.

Word	Name	Array	Dimension	Description
48	LTW	TW	NCELLS*NODES	Old wall temperatures.
49	LALP	ALP	NCELLS	Old vapor fraction.
50	LROV	ROV	NCELLS	Old vapor density.
51	LROL	ROL	NCELLS	Old liquid density.
52	LVM	VM	NCELLS+1	Old mixture velocity.
53	LEV	EV	NCELLS	Old vapor internal energy.
54	LEL	EL	NCELLS	Old liquid internal energy.
55	LTV	TV	NCELLS	Old vapor temperature.
56	LTL	TL	NCELLS	Old liquid temperature.
57	LP	P	NCELLS	Old pressure.
58	LTWN	TWN	NCELLS*NODES	New wall temperatures.
59	LALPN	ALPN	NCELLS	New vapor fraction.
60	LROVN	ROVN	NCELLS	New vapor density.
61	LROLN	ROLN	NCELLS	New liquid density.
62	LVMN	VMN	NCELLS+1	New mixture velocity.
63	LEVN	EVN	NCELLS	New vapor internal energy.
64	LELN	ELN	NCELLS	New liquid internal energy.
65	LTVN	TVN	NCELLS	New vapor temperature.
66	LTLN	TLN	NCELLS	New liquid temperature.
67	LPN	PN	NCELLS	New pressure.
68	LALPD	ALPD	0	Droplet volume fraction.[a]
69	LROVA	ROVA	0	Old air density.[a]

[a]Not presently implemented.

Word	Name	Array	Dimension	Description
70	LEVA	EVA	0	Old air internal energy.[a]
71	LVRD	VRD	0	Droplet drift velocity.[a]
72	LALPND	ALPND	0	New droplet volume fraction.[a]
73	LROVAN	ROVAN	0	New air density.[a]
74	LEVAN	EVAN	0	New air internal energy.[a]
75	LTSSN	TSSN	0	New vapor saturation temperature.[a]
76	LB	B	NCELLS*30	Temporary storage for 1-D implicit block tridiagonal matrix solution.

X. VALVE MODULE

A. VALVE Variable Length Table

Position	Parameter	Description
1	NCELLS	Number of fluid cells.
2	NODES	Number of heat transfer nodes.
3	JUN1	Junction number of low-numbered valve end.
4	JUN2	Junction number of high-numbered valve end.
5	MAT	Material ID.
6	RADIN	Inner radius of pipe wall.
7	TH	Thickness of pipe wall.
8	HOUTL	Heat transfer coefficient between outer boundary of valve wall and liquid.
9	HOUTV	Heat transfer coefficient between outer boundary of valve wall and vapor.

[a]Not presently implemented.

Position	Parameter	Description
10	TOUTL	Liquid temperature outside valve.
11	TOUTV	Vapor temperature outside valve.
12	ICJ1	Adjacent component at junction 1.
13	ICJ2	Adjacent component at junction 2.
14	TYPE1	Type of adjacent component at junction 1.
15	TYPE2	Type of adjacent component at junction 2.
16	JS1	Junction sequence number at low-numbered valve end.
17	JS2	Junction sequence number at high-numbered valve end.
18	ISOLLB	Indication for velocity update at junction 1.
19	ISOLRB	Indication for velocity update at junction 2.
20	ICHF	CHF calculation.
21	IHYDRO	1-D hydrodynamics option.
22	IVTY	Valve type index.
23	IVTR	Valve trip ID.
24	NVTX	Number of valve table entries.
25	IVPG	Valve pressure gradient option (IVTY=5).
26	PVC	Pressure gradient setpoint.
27	AVLVE	Valve open flow area.
28	HVLVE	Valve open hydraulic diameter.

B. VALVE Pointer Table

Word	Name	Array	Dimension	Description
1	LDX	DX	NCELLS	Delta x.
2	LVOL	VOL	NCELLS	Cell volumes.

Word	Name	Array	Dimension	Description
3	LFA	FA	NCELLS+1	Cell edge areas.
4	LFRIC	FRIC	NCELLS+1	Additive friction factors.
5	LGRAV	GRAV	NCELLS+1	Gravitation terms (cosine theta).
6	LHD	HD	NCELLS+1	Hydraulic diameters.
7	LNFF	NFF	NCELLS+1	Friction correlation options.
8	LWA	WA	NCELLS	Wall areas.
9	LMATID	MATID	NODES-1	Material IDs.
10	LRHS	RHS	3*NCELLS	Right-hand side for vapor continuity and energy equations.
11	LCPL	CPL	NCELLS	C sub P liquid.
12	LCPV	CPV	NCELLS	C sub P vapor.
13	LCL	CL	NCELLS	Conductivity of liquid.
14	LCV	CV	NCELLS	Conductivity of vapor.
15	LVISL	VISL	NCELLS	Viscosity of liquid.
16	LVISV	VISV	NCELLS	Viscosity of vapor.
17	LHFG	HFG	NCELLS	Latent heat of vaporization.
18	LEMIS	EMIS	NCELLS	Emissivity of pipe wall.
19	LRN	RN	NODES	Radii at nodes.
20	LRN2	RN2	NODES-1	Radii at cell centers.
21	LDR	DR	NODES-1	Delta r.
22	LIDR	IDR	NCELLS	Heat transfer regime.
23	LHIL	HIL	NCELLS	Heat transfer coefficient between inside wall and liquid.
24	LHIV	HIV	NCELLS	Heat transfer coefficient between inside wall and vapor.
25	LHLV	HLV	NCELLS	Interfacial heat transfer coefficient.

Word	Name	Array	Dimension	Description
26	LALV	ALV	NCELLS	Interfacial surface area.
27	LHOL	HOL	NCELLS	Heat transfer coeffcient between outside wall and liquid.
28	LHOV	HOV	NCELLS	Heat transfer coefficient between outside wall and vapor.
29	LTOL	TOL	NCELLS	Liquid temperature outside valve.
30	LTOV	TOV	NCELLS	Vapor temperature outside valve.
31	LSIG	SIG	NCELLS	Surface tension.
32	LROW	ROW	(NODES-1)*NCELLS	Density of wall.
33	LCPW	CPW	(NODES-1)*NCELLS	Specific heat of wall.
34	LCW	CW	(NODES-1)*NCELLS	Conductivity of wall.
35	LQPPC	QPPC	NCELLS	Critical heat flux.
36	LQPPP	QPPP	NCELLS	Wall heat source.
37	LROM	ROM	NCELLS	Mixture density.
38	LARV	ARV	NCELLS	ALP*ROV.
39	LRMEM	RMEM	NCELLS	Mixture internal energy.
40	LRMVM	RMVM	NCELLS+1	ROM*VM.
41	LCFZ	CFZ	NCELLS+1	Total friction factor.
42	LDRIV	DRIV	NCELLS*15	Storage array for thermodynamic derivatives and enthalpies.
43	LTSAT	TSAT	NCELLS	Saturation temperature.
44	LVR	VR	NCELLS+1	Relative velocity.
45	LVL	VL	NCELLS+1	Liquid velocity.
46	LVV	VV	NCELLS+1	Vapor velocity.
47	LVLTB	VLTB	NVTX*2	Valve table.
48	LTW	TW	NCELLS*NODES	Old wall temperatures.
49	LALP	ALP	NCELLS	Old vapor fraction.

Word	Name	Array	Dimension	Description
50	LROV	ROV	NCELLS	Old vapor density.
51	LROL	ROL	NCELLS	Old liquid density.
52	LVM	VM	NCELLS+1	Old mixture velocity.
53	LEV	EV	NCELLS	Old vapor internal energy.
54	LEL	EL	NCELLS	Old liquid internal energy.
55	LTV	TV	NCELLS	Old vapor temperature.
56	LTL	TL	NCELLS	Old liquid temperature.
57	LP	P	NCELLS	Old pressure.
58	LTWN	TWN	NCELLS*NODES	New wall temperatures.
59	LALPN	ALPN	NCELLS	New vapor fraction.
60	LROVN	ROVN	NCELLS	New vapor density.
61	LROLN	ROLN	NCELLS	New liquid density.
62	LVMN	VMN	NCELLS+1	New mixture velocity.
63	LEVN	EVN	NCELLS	New vapor internal energy.
64	LELN	ELN	NCELLS	New liquid internal energy.
65	LTVN	TVN	NCELLS	New vapor temperature.
66	LTLN	TLN	NCELLS	New liquid temperature.
67	LPN	PN	NCELLS	New pressure.
68	LALPD	ALPD	0	Droplet volume fraction.[a]
69	LROVA	ROVA	0	Old air density.[a]
70	LEVA	EVA	0	Old air internal energy.[a]
71	LVRD	VRD	0	Droplet drift velocity.[a]

[a]Not presently implemented.

Word	Name	Array	Dimension	Description
72	LALPND	ALPND	0	New droplet volume fraction.[a]
73	LROVAN	ROVAN	0	New air density.[a]
74	LEVAN	EVAN	0	New air internal energy.[a]
75	LTSSN	TSSN	0	New vapor saturation temperature.[a]
76	LB	B	NCELLS*30	Temporary storage for 1-D implicit block tridiagonal matrix solution.

[a]Not presently implemented.

XI. VESSEL MODULE

A. VSSL Variable Length Table

Position	Parameter	Description
1	NCELLS	Total number of fluid cells.
2	NCLX	Number of fluid cells per level.
3	NASX	Number of axial segments (levels).
4	NRSX	Number of radial segments.
5	NTSX	Number of theta segments.
6	IDCU	Downcomer upper boundary segment number, Z(IDCU).
7	IDCL	Downcomer lower boundary segment number, Z(IDCL).
8	IDCR	Downcomer radial boundary segment number, RAD(IDCR).
9	ICRU	Core upper boundary segment number, Z(ICRU).
10	ICRL	Core lower boundary segment number, Z(ICRL).
11	ICRR	Core outer radial boundary segment number, RAD(ICRR).
12	LNPTRL	Number of pointers of level data.
13	LENLD	Length of level data.
14	LFVL	Relative position of old fundamental variables of level data.
15	LFVNL	Relative position of new fundamental variables of level data.
16	LNFVL	Length of fundamental variables of level data.
17	LNPTRR	Number of pointers of rod data.
18	LENRD	Length of rod data.
19	LFVR	Relative position of old fundamental variables of rod data.

Position	Parameter	Description
20	LFVNR	Relative position of new fundamental variables of rod data.
21	LNFVR	Length of fundamental variables of rod length.
22	NCSR	Number of cell sources (connections).
23	ROHS	Density of heat slab material.
24	CPHS	Specific heat of heat slab material.
25	CHS	Conductivity of heat slab material.
26	EMHS	Emissivity of heat slab wall.
27	NCRXX	Total number of core volumes.
28	NCRX	Maximum number of core volumes per level.
29	NCRZ	Number of core levels.
30	NCRAZ	Axial fine-mesh nodes per rod.
31	NODES	Number of rod heat transfer nodes.
32	NDM1	Nodes - 1.
33	HGAPO	Rod fuel gap conductance coefficient (MATRD=3).
34	NFUEL	Number of nodes in fuel pellet.
35	NMWRX	Metal-water reaction flag (0 = no calculation, 1 = yes).
36	NFCI	Fuel-clad interaction flag (0 = no calculation, 1 = calculation).
37	NFCIL	Limit on FCI calculations per time stop.
38	PLDR	Pellet dish radius (=0.0, no calculation of pellet dishing).
39	PDRAT	Rod pitch diameter ratio.
40	NRFDS	Rod fine-mesh status flag (0 = coarse mesh on, 1 = fine mesh on).
41	NRFD	Reflood flag (0 = no action, 1 = turn fine mesh on if off).

Position	Parameter	Description
42	NRFDT	Rod fine-mesh flag trip ID.
43	NFFA	Axial friction factor correlation option.
44	NFFR	Radial friction factor correlation option.
45	NFFT	Theta friction factor correlation option.
46	NDGX	Number of delayed neutron groups.
47	NDHX	Number of decay heat groups.
48	TNEUT	Neutron generation time.
49	BEFF	Total delayed neutron fraction.
50	ENEFF	Total decay heat fraction.
51	REACT	Total reactivity.
52	NPWX	Number of absolute power entries.
53	IRPOP	Reactor kinetics option flag.
54	IRPTR	Reactor kinetics trip ID.
55	RPOWR	Old reactor power.
56	RPOWRN	New reactor power.
57	RPOWRI	Initial reactor power.
58	NRMAX	Rod location for peak clad temperature search.
59	NLMAX	Core level location for peak clad temperature search.
60	TIMAX	Time for peak clad temperature search.
61	TCMAX	Temperature for peak clad temperature search.

B. VSSL Pointer Table

Word	Name	Array	Dimension	Description
1	LZ	Z	NASX	Axial segment upper elevation.

Word	Name	Array	Dimension	Description
2	LDZ	DZ	NASX	Axial segments lengths (delta-Z).
3	LRAD	RAD	NRSX	Radial segments outer radius.
4	LDR	DR	NRSX	Radial segment lengths (delta-R).
5	LTH	TH	NTSX	Theta segment angle.
6	LDTH	DTH	NTSX	Theta segment length (delta-theta).
7	LISRL	ISRL	NCSR	Level number associated with source.
8	LISRC	ISRC	NCSR	Relative cell number associated with source.
9	LISRF	ISRF	NCSR	Face number associated with source.
10	LJUNS	JUNS	NCSR	Junction number associated with source.
11	LJSN	JSN	NCSR	Junction sequence number associated with source.
12	LICJ	ICJ	NCSR	Adjacent component associated with source.
13	LMSC	MSC	NCSR	Absolute cell number of source.
14	LNSRL	NSRL	NASX	Number of sources on level.
15	LISOLB	ISOLB	NCSR	Indicate for velocity update.
16	LSVC	SVC	NCSR*2	Vapor continuity source.
17	LSLC	SLC	NCSR*2	Liquid continuity source.
18	LSVE	SVE	NCSR*2	Vapor energy source.
19	LSLE	SLE	NCSR*2	Liquid energy source.
20	LDVVDP	DVVDP	NCSR	Derivative of vapor source velocity WRT pressure.
21	LDVLDP	DVLDP	NCSR	Derivative of liquid source velocity WRT pressure.
22	LSMOMV	SMOMV	NCSR*6	Vapor momentum source.

Word	Name	Array	Dimension	Description
23	LSMOML	SMOML	NCSR*6	Liquid momentum source.
24	LVELSV	VELSV	NCSR	Vapor source velocity.
25	LVELSL	VELSL	NCSR	Liquid source velocity.
26	LPSOLD	PSOLD	NCSR	Old source pressure.
27	LPSNEW	PSNEW	NCSR	New source pressure.
28	LRDPWR	RDPWR	NODES-1	Relative rod radial power density.
29	LCPOWR	CPOWR	NCRX	Relative power per unit rod.
30	LZPOWR	ZPOWR	NCRZ	Relative axial power density.
31	LNRDX	NRDX	NCRX	Number of rods in volume.
32	LRPKF	RPKF	NCRX	Rod power peaking factor.
33	LRADRD	RADRD	NODES	Rod node radius (cold).
34	LMATRD	MATRD	NODES-1	Rod material ID.
35	LNFAX	NFAX	NCRZ	Rod fine mesh noding factor.
36	LBETA	BETA	NDGX	Delayed neutron fraction of groups.
37	LLAMDA	LAMDA	NDGX	Decay constant on delaved groups.
38	LLAMDH	LAMDH	NDHX	Decay constant of decay heat groups.
39	LEDH	EDH	NDHX	Energy yield fraction of decay heat groups.
40	LPWTB	PWTB	NPWX*2	Power table.
41	LFPUO2	FPUO2	NCRX	Fraction of PUO_2 in UO_2 fuel.
42	LFTD	FTD	NCRX	Fuel fraction of theoretical density.
43	LGMIX	GMIX	NCRX*7	Mole fraction of gap gas constituents.
44	LGMLES	GMLES	NCRX	Moles of gap gas.
45	LPGAPT	PGAPT	NCRX	Total gap gas pressure.

Word	Name	Array	Dimension	Description
46	LPLVOL	PLVOL	NCRX	Rod plenum volume.
47	LPSLEN	PSLEN	NCRX	Pellet stack length.
48	LVBF	VBF	NCRX	Bottom flood velocity.
49	LVBFH	VBFH	NCRX	Bottom flood velocity (HR).
50	LVFF	VFF	NCRX	Falling film velocity.
51	LVFFH	VFFH	NCRX	Falling film velocity (HR).
52	LZBF	ZBF	NCRX	Bottom flood quench position.
53	LZBFH	ZBFH	NCRX	Bottom flood quench position (HR).
54	LZFF	ZFF	NCRX	Falling film quench position.
55	LZFFH	ZFFH	NCRX	Falling film quench position (HR).
56	LCDG	CDG	NDGX	Old concentration of delayed neutron groups.
57	LCDH	CDH	NDHX	Old concentration of decay heat groups.
58	LCLEN	CLEN	NCRX	Old total cladding length.
59	LCDGN	CDGN	NDGX	New concentration of delayed neutron groups.
60	LCDHN	CDHN	NDHX	New concentration of decay heat groups.
61	LCLENN	CLENN	NCRX	New total cladding length.
62	LDRIV	DRIV	NCELLS*22	Storage array for thermodynamic derivatives, enthalpies, and temporary storage for matrix inversions.
		----Items below are repeated for each level----		
63	LISRN	ISRN	NCSR	Source numbers on level.
64	LC4P	C4P	NCLX*7	Solution matrix storage area.
65	LC3P	C3P	NCLX*2	Solution matrix storage area.

Word	Name	Array	Dimension	Description
66	LDROP	DROP	NCLX*4	Droplet field storage area.
67	LGCOND	GCOND	NCLX	Vapor condensation rate.
68	LGEVAP	GEVAP	NCLX	Liquid evaporation rate.
69	LSIG	SIG	NCLX	Surface tension.
70	LICRN	ICRN	NCLX	Core volume number.
71	LTCHF	TCHF	NCRX	Critical temperature-rod.
72	LIDRG	IDRG	NCRX	Flow regime flag.
73	LRDHL	RDHL	NCRX	Average rod heat transfer coefficient (liquid).
74	LRDHV	RDAV	NCRX	Average rod heat transfer coefficient (vapor).
75	LRDA	RDA	NCRX	Total rod area.
76	LIHSN	IHSN	NCLX	Heat slab number.
77	LHSA	HSA	NCLX	Heat slab area.
78	LHSM	HSM	NCLX	Mass of heat slab.
79	LTCHFS	TCHFS	NCLX	Slab critical temperature.
80	LIDRGS	IDRGS	NCLX	Slab heat transfer regime flag.
81	LHSHL	HSHL	NCLX	Slab heat transfer coefficient (liquid).
82	LHSHV	HSHV	NCLX	Slab heat transfer coefficient (vapor).
83	LHLV	HLV	NCLX	Interfacial heat transfer coefficient.
84	LALV	ALV	NCLX	Interfacial area.
85	LARV	ARV	NCLX	ALPHA*ROV.
86	LRMEM	RMEM	NCLX	Mixture internal energy.
87	LROM	ROM	NCLX	Mixture density.
88	LVM	VM	NCLX*3	Mixture velocity.

Word	Name	Array	Dimension	Description
89	LVLC	VLC	NCLX	Liquid cross-flow velocity.
90	LVVC	VVC	NCLX	Vapor cross-flow velocity.
91	LCFZL	CFZL	NCLX*3	Total friction factors (liquid).
92	LCFZV	CFZV	NCLX*3	Total friction factors (vapor).
93	LFRICL	FRICL	NCLX*3	Friction multipliers (liquid).
94	LFRICV	FRICV	NCLX*3	Friction multipliers (vapor).
95	LFRICI	FRICI	NCLX*3	Interfacial friction factors.
96	LDVV	DVV	NCLX*3	Derivative used in momentum update (liquid).
97	LDLL	DLL	NCLX*3	Derivative used in momentum update (vapor).
98	LVOL	VOL	NCLX	Cell fluid volumes.
99	LVOLG	VOLG	NCLX	Cell geometric volumes.
100	LFA	FA	NCLX*3	Cell fluid edge areas.
101	LFAG	FAG	NCLX*3	Cell geometric edge areas.
102	LGRAV	GRAV	NCLX	Gravitation terms.
103	LHD	HD	NCLX*3	Hydraulic diameters.
104	LCPL	CPL	NCLX	C sub P liquid.
105	LCPV	CPV	NCLX	C sub P vapor.
106	LTSAT	TSAT	NCLX	Saturation temperature.
107	LCL	CL	NCLX	Conductivity of liquid.
108	LCV	CV	NCLX	Conductivity of vapor.
109	LVISL	VISL	NCLX	Viscosity of liquid.
110	LVISV	VISV	NCLX	Viscosity of vapor.
111	LHFG	HFG	NCLX	Latent heat of vaporization.
112	LRDTL	RDTL	NCRX	Average rod temperature to liquid.

Word	Name	Array	Dimension	Description
113	LRDTV	RDTV	NCRX	Average rod temperature to vapor.
114	LALD	ALD	NCLX	Old droplet fraction.
115	LHST	HST	NCLX	Old heat slab temperatures.
116	LALP	ALP	NCLX	Old vapor fraction.
117	LROV	ROV	NCLX	Old vapor density.
118	LROL	ROL	NCLX	Old liquid density.
119	LVV	VV	NCLX*3	Old vapor velocity.
120	LVL	VL	NCLX*3	Old liquid velocity.
121	LEV	EV	NCLX	Old vapor internal energy.
122	LEL	EL	NCLX	Old liquid internal energy.
123	LTV	TV	NCLX	Old vapor temperature.
124	LTL	TL	NCLX	Old liquid temperature.
125	LP	P	NCLX	Old pressure.
126	LALDN	ALDN	NCLX	New droplet fraction.
127	LHSTN	HSTN	NCLX	New heat slab temperatures.
128	LALPN	ALPN	NCLX	New vapor fraction.
129	LROVN	ROVN	NCLX	New vapor density.
130	LROLN	ROLN	NCLX	New liquid density.
131	LVVN	VVN	NCLX*3	New vapor velocity.
132	LVLN	VLN	NCLX*3	New liquid velocity.
133	LEVN	EVN	NCLX	New vapor internal energy.
134	LELN	ELN	NCLX	New liquid internal energy.
135	LTVN	TVN	NCLX	New vapor temperature.
136	LTLN	TLN	NCLX	New liquid temperature.
137	LPN	PN	NCLX	New pressure.

Word	Name	Array	Dimension	Description
		----Items Below are Repeated for Each Rod----		
138	LALPR	ALPR	NCRZ	Vapor fraction.
139	LALVR	ALVR	NCRZ	Interfacial area.
140	LBURN	BURN	NCRZ	Fuel burnup.
141	LCLR	CLR	NCRZ	Liquid conductivity.
142	LCND	CND	NDM1*NCRZ	Rod conductivity.
143	LCNDH	CNDH	NDM1*NCRZ	Rod conductivity (HR).
144	LCPLR	CPLR	NCRZ	Liquid specific heat.
145	LCPND	CPND	NDM1*NCRZ	Rod specific heat.
146	LCPNDH	CPNDH	NDM1*NCRZ	Rod specific heat (HR).
147	LCPVR	CPVR	NCRZ	Vapor specific heat.
148	LCVR	CVR	NCRZ	Vapor conductivity.
149	LDZF	DZF	NCRAZ	Axial fine-mesh length.
150	LEMIS	EMIS	NDM1*NCRZ	Rod emissivity.
151	LEMISH	EMISH	NDM1*NCRZ	Rod emissivity (HR).
152	LHDR	HDR	NCRZ	Rod bundle hydraulic diameter.
153	LHFGR	HFGR	NCRZ	Latent heat of vaporization.
154	LHGAP	HGAP	NCRZ	Gap conductance.
155	LHLVR	HLVR	NCRZ	Interfacial HTC.
156	LRDHLR	RDHLR	NCRZ	Liquid HTC.
157	LRDHLH	RDHLH	NCRZ	Liquid HTC (HR).
158	LRDHVR	RDHVR	NCRZ	Vapor HTC.
159	LRDHVH	RDHVH	NCRZ	Vapor HTC (HR).
160	LHRFL	HRFL	NCRAZ	Liquid HTC fine mesh.
161	LHRFLH	HRFLH	NCRAZ	Liquid HTC fine mesh (HR).

Word	Name	Array	Dimension	Description
162	LHRFV	HRFV	NCRAZ	Vapor HTC fine mesh.
163	LHRFVH	HRFVH	NCRAZ	Vapor HTC fine mesh (HR).
164	LIDRGR	IDRGR	NCRZ	Flow regime flag.
165	LIHTC	IHTC	NCRZ	Heat transfer regime flag.
166	LIHTCH	IHTCH	NCRZ	Heat transfer regime flag (HR).
167	LIHTF	IHTF	NCRAZ	Heat transfer regime flag fine mesh.
168	LIHTFH	IHTFH	NCRAZ	Heat transfer regime flag fine mesh (HR).
169	LNFLM	NFLM	NCRAZ	Film location flag.
170	LNFLMH	NFLMH	NCRAZ	Film location flag (HR).
171	LPR	PR	NCRZ	Coolant pressure.
172	LPGAP	PGAP	NCRZ	Local gap gas pressure.
173	LPINT	PINT	NCRZ	Pellet clad contact pressure.
174	LPLDV	PLDV	NCRZ	Pellet dish volume.
175	LQAX	QAX	NCRAZ	Axial conduction heat source.
176	LQAXH	QAXH	NCRAZ	Axial conduction heat source (HR).
177	LQWRX	QWRX	NCRZ	Metal water reaction heat source.
178	LQWRXH	QWRXH	NCRZ	Metal water reaction heat source (HR).
179	LRDTLR	RDTLR	NCRZ	Average rod wall temperature to liquid.
180	LRDTVR	RDTVR	NCRZ	Average rod wall temperature to vapor.
181	LRND	RND	NDM1*NCRZ	Rod density.
182	LRNDH	RNDH	NDM1*NCRZ	Rod density (HR).
183	LROLR	ROLR	NCRZ	Liquid density.

Word	Name	Array	Dimension	Description
184	LROVR	ROVR	NCRZ	Vapor density.
185	LROMR	ROMR	NCRZ	Mixture density.
186	LRPOWF	RPOWF	NDM1*NCRZ	Rod power density.
187	LSIGR	SIGR	NCRZ	Surface tension.
188	LTCHFR	TCHFR	NCRZ	Wall temperature at CHF point.
189	LTCHFF	TCHFF	NCRAZ	Wall temperature at CHF point fine mesh.
190	LTCFH	TCFH	NCRZ	Wall temperature at CHF point (HR).
191	LTCFFH	TCFFH	NCRAZ	Wall temperature at CHF point mesh (HR).
192	LTLEID	TLEID	NCRAZ	Leidenfrost temperature.
193	LTLR	TLR	NCRZ	Liquid temperature.
194	LTSATR	TSATR	NCRZ	Saturation temperature.
195	LTVR	TVR	NCRZ	Vapor temperature.
196	LVISLR	VISLR	NCRZ	Liquid viscosity.
197	LVISVR	VISVR	NCRZ	Vapor viscosity.
198	LVLCR	VLCR	NCRZ	Liquid cross-flow velocity.
199	LVLZR	VLZR	NCRZ	Axial liquid velocity.
200	LVVCR	VVCR	NCRZ	Vapor cross-flow velocity.
201	LVVZR	VVZR	NCRZ	Axial vapor velocity.
202	LVMZR	VMZR	NCRZ	Axial mixture velocity.
203	LDRZ	DRZ	NCRZ	Old ZrO_2 reaction depth.
204	LDRZH	DRZH	NCRZ	Old ZrO_2 reaction depth (HR).
205	LRADR	RADR	NODES*NCRZ	Old radial node positions.
206	LRDT	RDT	NODES*NCRZ	Old rod temperature.
207	LRDTH	RDTH	NODES*NCRZ	Old rod temperature (HR).

Word	Name	Array	Dimension	Description
208	LRFT	RFT	NODES*NCRAZ	Old fine-mesh rod temperatures.
209	LRFTH	RFTH	NODES*NCRAZ	Old fine-mesh rod temperatures.
210	LDRZN	DRZN	NCRZ	New ZrO_2 reaction depth.
211	LDRZNH	DRZNH	NCRZ	New ZrO_2 reaction depth (HR).
212	LRADRN	RADRN	NODES*NCRZ	New radial node positions.
213	LRDTN	RDTN	NODES*NCRZ	New rod temperature.
214	LRDTNH	RDTNH	NODES*NCRZ	New rod temperature (HR).
215	LRFTN	RFTN	NODES*NCRAZ	New fine-mesh rod temperatures.
216	LRFTNH	RFTNH	NODES*NCRAZ	New fine-mesh rod temperatures (HR).

☆ U.S. GOVERNMENT PRINTING OFFICE: 1978—777-089/99